The role of the innate immune system in a murine gammaherpesvirus infection

Rona C Thomson

2007

Doctor of Philosophy

University of Edinburgh

Declaration

I declare that all work included in this thesis is my own except where otherwise stated. No part of this work has been, or will be, submitted for any other degree or professional qualification.

Acknowledgements

I would like to thank my supervisors Dr Bernadette Dutia, Professor Tony Nash and Dr Juraj Petrik for their advice and technical assistance throughout this project. I would particularly like to thank Bernadette who has given me a lot of support and advice during my PhD and Tony who has been a source of inspiration throughout. Thanks to members of the MHV-68/MDV group and PhD students, past and present, for various bits and pieces of help over the years. A big thank you to Yvonne Ligertwood and Deborah Allen for their technical support, in particular their help in tissue culture. I would also like to thank Shonna Johnston for her assistance with FACS.

I would like to thank my family and friends for providing both support and distraction from various stresses throughout my studies. Finally, I would like to say a big thank you to Douglas for his help and encouragement and for being a good listener to my rants during the last three years.

Abstract

Members of the *Gammaherpesvirinae* are characterised by their ability to establish latency within lymphoid cells. Gammaherpesviruses include the human pathogens Epstein-Barr virus and Kaposi's sarcoma-associated herpesvirus. Symptomatic disease and long-term persistence has been widely studied both *in vivo* and *in vitro*. However, as primary infection is largely asymptomatic, it has not been possible to determine virus-host interactions prior to the onset of symptoms. This has been further complicated by the narrow host range of the *gammaherpesvirinae*. Murine gammaherpesvirus-68 (MHV-68) is able to replicate in a number of cell lines *in vitro* and readily infects laboratory mice. It is therefore an important and flexible small animal model which provides a unique system for studying host-virus interactions at early time points post-infection.

The aim of this project was to determine the role of the innate immune system in the control of gammaherpesvirus infections. It has previously been shown that type I interferons (IFN) are critical for host survival. RT-PCR analysis confirmed that MHV-68 infection leads to induction of type I IFN at early time points post-infection. In addition, *in vitro* studies indicated that type I IFNs play a role in the inhibition of the exit of viral particles from the cell. A strong trend towards higher titres of cell-free virus from cells lacking type I IFN receptor compared to titres of cell-free virus from wt cells was observed. IFNβ knockout mice were utilised to show that IFNβ is important at early time points but does not play a role in long term control of infection. MHV-76 is a deletion mutant of MHV-68, lacking four genes (M1-M4) and eight vtRNAs unique to MHV-68 and present at the left hand end of the genome. This study found no difference in the type I IFN response following infection with either MHV-68 or MHV-76. These results suggest that M1-M4 and the 8 vtRNAs do not play an extensive role in the regulation of the type I IFN response. IFN stimulated genes (ISGs) are important for establishing an anti-viral response. Mice lacking ISG12a were utilised to show that ISG12a plays a role in the early stages of the establishment of latency following MHV-68 infection. *In vivo* studies showed that virus titres and the degree of splenomegaly were increased in the

spleens of ISG12a knockout mice resulting in an elevated latent infection compared to wt spleens. However, the mechanism by which ISG12a affects latency is not clear. No difference in viral titres was observed in the lungs or mediastinal lymph nodes between ISG12a knockout and wt mice. The role of NK cells was investigated by *in vivo* depletion of NK cells and by monitoring NK activation following infection. The NK cell population is expanded and activated at day 2 compared to day 4 post-infection and is capable of cytotoxic killing following infection with MHV-68. However, a lack of NK cells *in vivo* did not result in significantly elevated virus titres suggesting that NK cells are not essential for the control of MHV-68 infection. No difference was observed between MHV-68 or MHV-76 infection in the presence or absence of NK cells, nor in the expansion or activation of NK cells post-infection. It was therefore concluded that the genes M1-M4 and the 8 vtRNAs do not play a role in the regulation of NK cells.

Contents

List of Figures

List of Tables

Abbreviations

ADCC	antibody-dependent cellular cytotoxicity
BHK	baby hamster kidney
bp	base pair
BSA	bovine serum albumin
CD	cluster of differentiation
cDNA	complementary DNA
CHX	cycloheximide
CMV	cytomegalovirus
CPE	cytopathic effect
CpG	cytidine-phosphate-guanosine
dATP	deoxyadenosine triphosphate
DC	dendritic cell
dCTP	deoxycytidine triphosphate
dGTP	deoxyguanosine triphosphate
dH_2O	distilled water
$DIOC_{18}$	3,3'-dioctadecyloxacarbocyanine perchlorate
DMEM	Dulbecco's modified Eagle's medium
DNA	deoxyribonucleic acid
ds	double stranded
DTT	dithiothreitol
dTTP	deoxythymidine triphosphate
EBV	Epstein-Barr virus
EDTA	ethylenediaminetetra-acetic acid
eGFP	enhanced green fluorescent protein

eIF2α	eukaryotic initiation factor 2 α
FACS	fluorescence activated cell sorting
FADD	Fas associated death domain
FCS	foetal calf serum
FITC	fluorescein-isothiocyanate
GFP	green fluorescent protein
GM-CSF	granulocyte-macrophage colony stimulating factor
HEPES	N'-[2-hydroxyethyl]piperazine-N'-[2-ethanesulphonic acid]
HLA	human leukocyte antigen
HIV	human immunodeficiency virus
HSV	herpes simplex virus
IFN	interferon
IFNAR	interferon α/β receptor
ICP	infected cell protein
Ig	immunoglobulin
IKK	IκB kinase
IL	interleukin
IM	infectious mononucleosis
i.n.	intranasal
IRF	interferon regulatory gene
ISG	interferon stimulated gene
ISGF3	interferon stimulated gene factor 3
ISRE	interferon stimulated response element
ITAM	immunoreceptor tyrosine-based activation motif
ITIM	immunoreceptor tyrosine-based inhibitory motif

kb	kilobase
KIR	killer immunoglobulin-like receptors
KSHV	Kaposi's sarcoma-associated virus
LCMV	lymphocytic choriomeningitis virus
MACS	magnetic cell sorting
MEF	mouse embryonic fibroblast
MHC	major histocompatibility complex
MHV	murine gammaherpesvirus
MLN	mediastinal lymph node
MOI	multiplicity of infection
mRNA	messenger RNA
NCR	natural cytotoxicity receptors
NDV	Newcastle disease virus
NFkB	nuclear factor kappa B
NK	natural killer
NPC	nuclear pore complex
OAS	oligoadenylate synthetases
OD	optical density
ORF	open reading frame
PAMP	pathogen-associated molecular patterns
PBS	phosphate buffered saline
PCR	polymerase chain reaction
PE	phycoerythrin
PFA	paraformaldehyde
PFU	plaque forming units

p.i.	post-infection
PI	propidium iodide
PIAS	protein inhibitor of activated STAT
PKR	protein kinase R
Poly I:C	poly inosinic: poly cytidylic acid
PRD	positive regulatory domain
RNA	ribonucleic acid
RNase L	endoribonuclease L
RPMI	rosewell memorial park institiute
RT	room temperature
RTA	replication and transcription activator
RT-PCR	reverse transcription PCR
SDS	sodium dodecyl sulphate
SEM	standard error of the mean
SFV	semliki forest virus
SOCS	suppressor of cytokine signalling
ss	single stranded
STAT	signal transducer and activator of transcription
TAE	tris acetate EDTA
Taq	*Thermus aquaticus*
TGFβ	transforming growth factor β
TLR	Toll-like receptor
TNF	tumour necrosis factor
TRAIL	TNF-related apoptosis-inducing ligand
U	units

v	viral prefix
VSV	vesicular stomatitis virus
VZV	varicella zoster virus
wt	wild type
w/v	weight per volume

Chapter 1: Introduction

1. Introduction

1.1. The innate antiviral immune response

The innate immune system provides a first line of defence against disease, providing a primary non-specific response to an invading pathogen. The innate immune recognition of a virus leads to a variety of antiviral immune responses. Host cell receptors recognise pathogen-associated molecular patterns (PAMP) present on virus-associated molecules such as viral DNA or dsRNA. For example, Toll-like receptor (TLR) 3 recognises dsRNA, a common replication intermediate of RNA viruses (Alexopoulou *et al.*, 2001). Following recognition of viral components, the type I interferon (IFN) response is initiated and results in the induction of hundreds of genes involved in antiviral responses, immunomodulation, and the cell-cycle. Natural killer (NK) cells are also important for defence against viral infection. NK cells can kill virally infected cells through non-specific signals such as poor expression of MHC class I molecules. Other innate immune components involved in antiviral responses include phagocytes, complement, various chemokines and cytokines. Dendritic cells (DCs) are also involved in the innate immune system as they express TLRs and have reciprocal activation functions with NK cells (Gerosa *et al.*, 2005).

1.2. Type I IFNs

The type I IFNs were discovered by Isaacs and Lindenmann (Isaacs and Lindenmann 1957) as cytokines that interfered with virus replication. They are the first cytokines produced in infected cells in response to viruses and can act in an autocrine and paracrine manner; antiviral responses are induced in infected cells and the neighbouring uninfected cells. Type I IFNs are highly pleiotropic as signalling through their receptor leads to the expression of hundreds of genes. As well as direct antiviral actions, they can modulate downstream immune components, for example activation of NK cells (Biron *et al.*, 1999), and can control apoptosis of infected cells

(Tanaka *et al.*, 1998). This family of cytokines can be divided into various subtypes which are summarised in table 1.1.

IFN subclass	Details	Species	Expression pattern	Activity level*	Receptor
IFNα	Multiple subtypes	Human and mouse	Ubiquitously expressed	Variable between subtypes	IFNAR
IFNβ		Human and mouse	Ubiquitously expressed	High	IFNAR
IFNε		Placental mammals	Cells of the placenta		IFNAR
IFNκ		Human and mouse	Keratinocytes		IFNAR
IFNω		Human	Leukocytes		IFNAR
IFNδ		Pig	Trophoblasts		IFNAR
IFNτ		Ruminant ungulates	Trophoblasts		IFNAR
IFNξ	Limitin	Mouse		High	IFNAR

Table 1.1. Summary of type I IFN subtypes. * Activity levels for murine subtypes taken from (Van Pesch *et al.*, 2004).

The type I IFNs are an intronless family of genes clustered on chromosome 4 in mice and chromosome 9 in humans. The roles of IFNα and β have been widely studied and are the main focus of interest. Multiple IFNα genes have been found in the human and murine genomes. 14 genes encoding 13 functional IFNα subtypes (IFNα1 and IFNα13 encode the same protein) are found in the human genome and 14 genes (plus 3 pseudogenes) encoding functional IFNα subtypes are found in the murine genome (Van Pesch *et al.*, 2004). IFNα can be secreted by most cell types although production is mainly associated with plasmacytoid dendritic cells (pDCs) that can produce up to 1000 times more IFNα following virus infection than other cell types (Asselin-Paturel *et al.*, 2001; Siegal *et al.*, 1999). Studies of murine IFNαs showed that they differ in their antiviral and antiproliferative activities. For example,

IFNα4 and IFNα12 demonstrated higher activity than IFNα1 (Van Pesch *et al.*, 2004). It has been suggested that these differences may be related to differences in receptor binding affinity (Meister *et al.*, 1986). IFNβ is only encoded by a single gene locus and is traditionally known as fibroblast IFN although it can be expressed by most cell types. The type I IFNs share the same receptor known as the IFNα receptor (IFNAR). The receptor is ubiquitously expressed and consists of IFNAR1 and IFNAR2 subunits. IFN binding results in signalling cascades leading to the expression of the downstream interferon stimulated genes (ISGs). IFNγ is a type II IFN. It is produced indirectly during virus infection from NK cells, $CD8^+$ T cells and $CD4^+$ Th1 T cells in response to antigens presented on MHC class I and II molecules (Goodbourn *et al.*, 2000). IFNγ signals through the IFNγ receptor but functional overlap exists between the type I and II IFNs as many components of the IFNγ-induced antiviral response are also induced by the type I IFNs. A further group of IFNs related to type I IFN family has been discovered, the IFNλ family (also termed interleukin (IL)-28A, IL-28B and IL-29) (Sheppard *et al.*, 2003). Members are homologous to type I IFN, are induced in response to viral infection and induce an anti-viral state. However, they are a distinct group (termed type III IFNs) as they utilise a heterodimeric receptor consisting of the IL-10R2 and IFNλR1, are clustered on chromosome 19 and contain several introns (Kotenko *et al.*, 2003; Meager *et al.*, 2005). Why are there multiple type I IFN subtypes? It is possible that the different subtypes induce different gene sets. For example, hypoxia-inducible factor 1 gene is induced by IFNβ but not IFNα (Der *et al.*, 1998). Alternatively, multiple IFN subtypes may be important at different times throughout an infection. IFNβ and IFNα4 are produced initially, followed by other IFNα subtypes for further control if virus is still present within the cell. Different viruses may influence the type I IFN subtypes induced. Interferon regulatory factor (IRF) 5 induced different IFNα subtypes to those induced by IRF7 and was specific to Newcastle disease virus infection (NDV) (Barnes *et al.*, 2001). However, this remains controversial as other studies could not reproduce the activation of IRF5 by NDV (Cheng *et al.*, 2006).

1.2.1. IFN Signalling

The early expressed type I IFNs, IFNα4 and IFNβ, can signal through the IFNAR receptor on the infected cell as well as uninfected neighbouring cells. The binding of IFN to the receptor results in the activation of a Jak/STAT signalling pathway. The cytoplasmic domains of the two receptor subunits, IFNAR1 and IFNAR2, are associated with 'Janus' tyrosine kinases. IFNAR1 is associated with Tyk2 (Colamonici *et al.*, 1994) and IFNAR2 is associated with Jak1 (Novick *et al.*, 1994). IFN receptor binding leads to conformational changes allowing dimerisation of the two subunits and thus autophosphorylation and activation of Tyk2 and Jak1 (Novick *et al.*, 1994). Phosphorylation of a tyrosine residue on the IFNAR1 subunit by Tyk2 creates a binding site for the 'signal transducer and activator of transcription' (STAT) 2. Tyk2 is then responsible for the phosphorylation of STAT2. Phosphorylated STAT2 recruits STAT1 to form STAT1/STAT2 heterodimers that dissociate from the IFNAR and are translocated to the nucleus. The heterodimers then associate with the DNA binding protein IRF9. A heterotrimeric complex is formed which is known as the interferon stimulated gene factor 3 (ISGF3, reviewed in (Goodbourn *et al.*, 2000). ISGF3 can bind to the interferon stimulated response element (ISRE) contained in the promoters of ISGs via the DNA binding domain of the IRF9 component (Veals *et al.*, 1992). The pathway is summarised in figure 1.1. The importance of IFNAR signalling is demonstrated in mice that lack the IFNAR receptor. A lack of functional type I IFN signalling makes mice more susceptible to viral infections and often results in subclinical infections becoming lethal (Dutia *et al.*, 1999; Van Den Broek *et al.*, 1995).

1.2.2. Interferon Regulatory factors

Interferon regulatory factors (IRFs) are characterised by the presence of a DNA-binding domain in the N-terminus which mediates binding to the ISRE. IRFs (except IRF6) also contain an IRF-association domain which enables dimerisation between family members (Lohoff and Mak 2005). IRF3, 5, 7 and 9 are involved in the induction of type I IFNs. IRF5 is upregulated in macrophages and DCs following

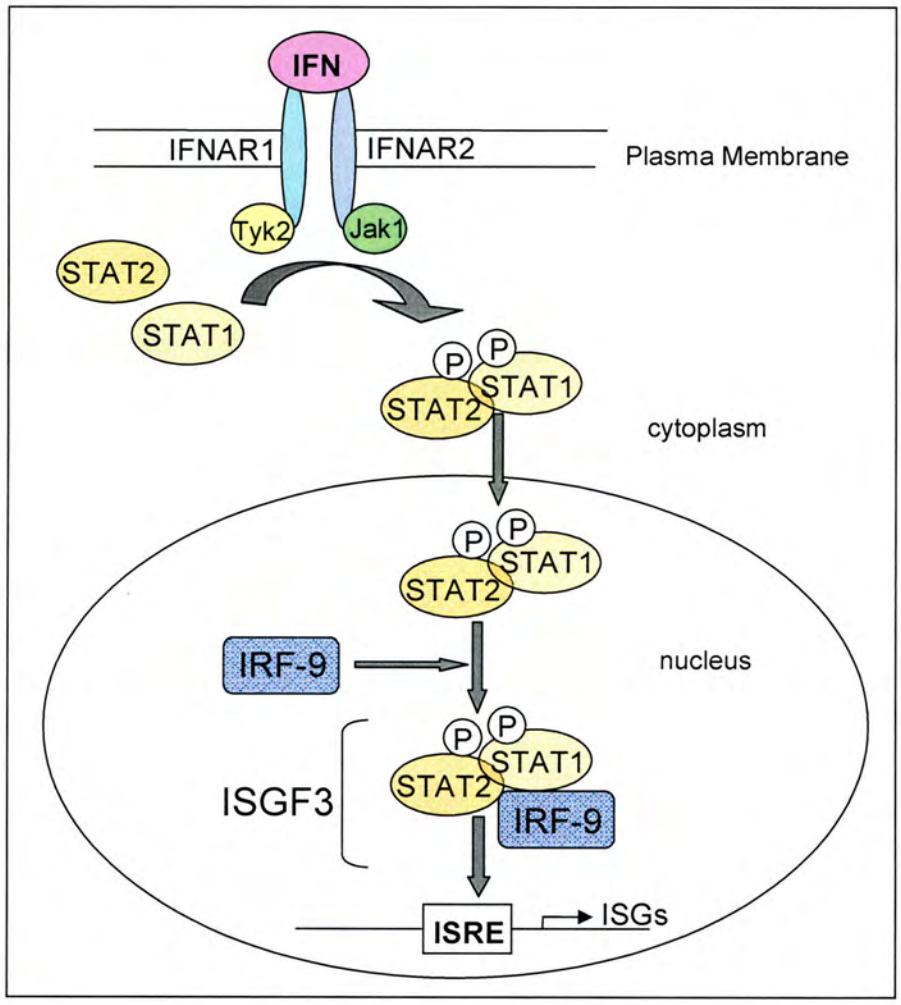

Figure 1.1. Type I IFN Jak/STAT signalling. IFN binding to the IFNAR results in the activation of a Jak/STAT signalling pathway. Binding of the ISGF3 complex to the ISRE of target genes and brings about activation of ISGs such as PKR, OAS and the Mx proteins. Figure adapted from Goodbourn *et al.*, 2000.

TLR signalling but it is unclear whether it can be induced by viral infection (Barnes *et al.*, 2001; Cheng *et al.*, 2006; Takaoka *et al.*, 2005). IRF9 is a component of the ISGF3 complex, stimulating expression of ISGs through the ISRE and resulting in induction of IRF7. IRF3 is constitutively expressed and is located in the cytoplasm. It is phosphorylated upon viral infection and then translocates to the nucleus where it can form homodimers or heterodimers with IRF7 that associate with CREB-binding protein (CBP) or p300 as part of the enhanceosome (see figure 1.3). IRF7 is constitutively expressed in small amounts but is strongly induced in response to type I IFN signalling. It also undergoes nuclear translocation following phosphorylation in response to viral infection. IRF3 efficiently activates the IFNβ gene whereas IRF7 strongly activates IFNβ and IFNα genes (Honda and Taniguchi 2006).

IFN induction is thought to occur through a positive feedback loop. Following viral infection, IRF3 becomes phosphorylated and thus activated by the kinases, TANK-binding kinase 1 (TBK1) and IκB kinase ε (IKKε) (Fitzgerald *et al.*, 2003). Activated IRF3 can then induce expression of the IFNα4 subtype and IFNβ. Expression of other IFNα subtypes rely on the expression of IRF7, upregulated in response to the early IFN subtypes produced. IRF7, again activated through phosphorylation by TBK1 and IKKε, binds to the promoters of the 'delayed' IFNαs such as IFNα2, 6 and 8 and induces their expression (Marie *et al.*, 1998). Recently this model of IFN induction has been shown to be over-simplified. A study by Prakash *et al.* (2005) showed that type I IFN induction after infection with influenza virus was reliant on IRF7 production, and thus positive feedback, in most tissues including the respiratory tract. However, pDCs were found to constitutively express high levels of IRF7 and could rapidly produce high levels of multiple IFNα subtypes in response to infection without positive feedback (Prakash *et al.*, 2005). Therefore, there appears to be cell type-specific differences in the induction of IRF7 and therefore the expression of the type I IFNs. Differential induction of the type I IFNs provides some degree of control over the IFN response, preventing over-expression of anti-viral genes.

1.2.3. Signalling through Toll-like receptors

Toll-like receptors (TLRs) are transmembrane receptors which are encoded by 10 genes in humans and 12 genes in mice. They function as pattern-recognition receptors that sense a variety of PAMPs on pathogens. Most cells express at least some of the TLRs although phagocytic cells such as DCs and macrophages appear to express the greatest levels of TLRs (Zarember and Godowski 2002). All TLRs encode a Toll/IL-1 receptor (TIR) domain which recruits TIR-containing adaptor proteins for downstream signalling (Honda and Taniguchi 2006). TLR3, 7, 8 and 9 are important for sensing viral products. TLR3 recognises dsRNA, TLR7 and 8 recognise ssRNA and TLR9 recognises unmethylated cytidine-phosphate-guanosine (CpG) DNA motifs which are present in viral DNA. Therefore, TLR9 becomes activated in response to infection with DNA viruses such as herpesviruses. Mice lacking functional TLR9 are more susceptible to MCMV infection and have impaired type I IFN production and NK cell activation (Tabeta *et al.*, 2004). TLR9 is located in the endosome and senses viral nucleic acid released following cell entry.

In particular, pDCs express TLR7 and TLR9 which signal through the adaptor protein, myeloid differentiation primary response protein 88 (MyD88). All TLRs except TLR3 signal through the MyD88-dependent pathway. Induction of type I IFN occurs through the association of MyD88 to IL-1R associated kinases (IRAK) 1, IRAK4 and TNF receptor-associated factor 6 (TRAF6). TRAF6 activates TGFβ activating kinase 1 (TAK1) which phosphorylates the kinases IKKα and IKKβ leading to phosphorylation and degradation of IκB and then translocation of NFκB to the nucleus. TAK1 additionally activates ATF-2/c-Jun via activation of mitogen-activated protein (MAP) kinases. MyD88 also associates with IRAK1 and IRF7. These pathways stimulate the expression of type I IFNs as well as the expression of other cytokines such as IL-12 and IL-6. Along with TRAF6-mediated ubiquitination, IRAK1 phosphorylates IRF7 allowing its activation and translocation to the nucleus leading to type I IFN production (Kawai and Akira 2006). The signalling pathways following activation of TLR9 are shown in figure 1.2. It is thought that the high basal

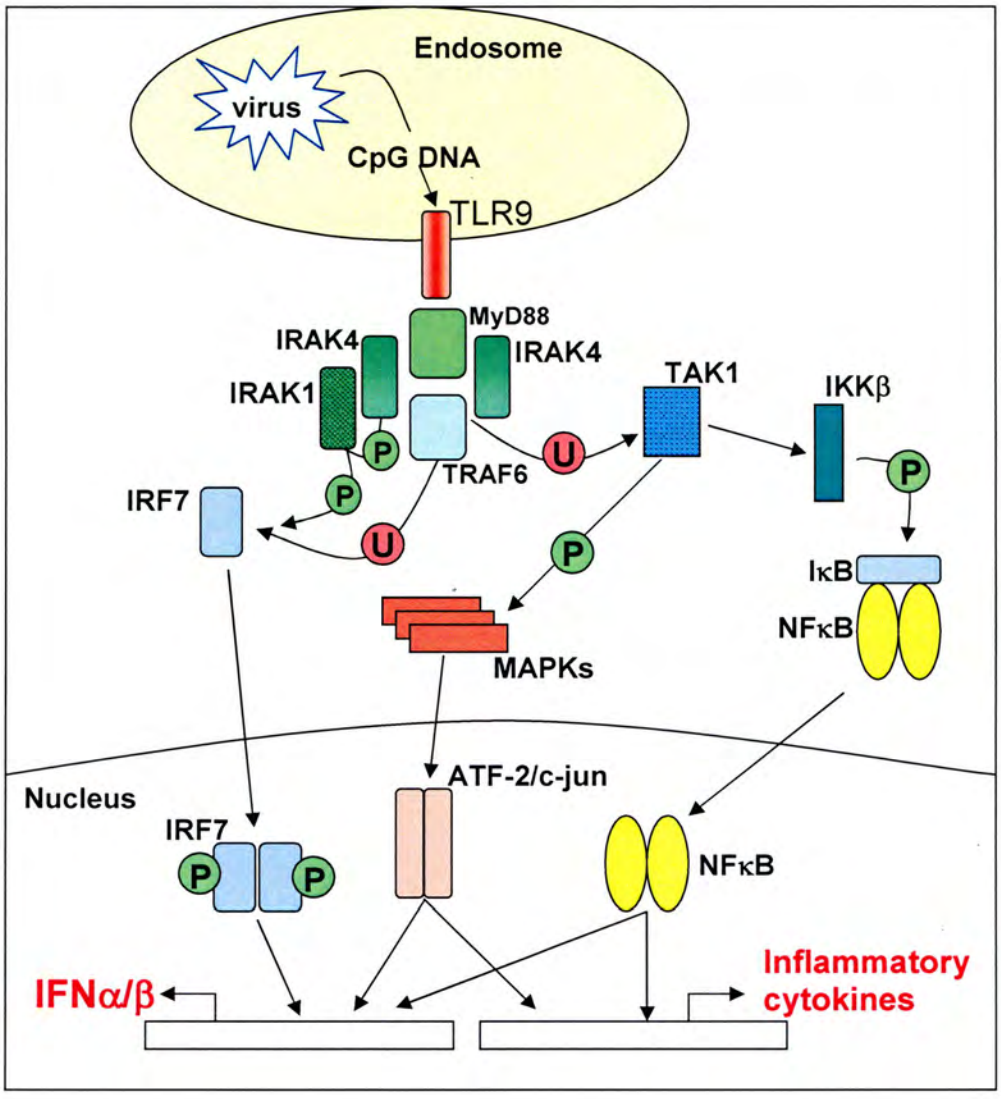

Figure 1.2. Recognition of viral DNA by TLR9. Recognition of viral DNA leads to recruitment of the adaptor protein MyD88. MyD88 interacts with IRAK 4 and TRAF6 which leads to activation of TAK1 by an ubiquitination (U)-dependent mechanism. TAK1 activates NFκB and ATF-2/c-jun via IKK-mediated IκB degradation and MAP kinase (MAPK) activation respectively. MyD88 can also associate with IRAK1 and IRF7. IRF7 is phosphorylated (P) by IRAK1 and translocates to the nucleus. Activation of IRF7 also requires TRAF6-mediated ubiquitination (U). Type I IFN is induced as a consequence of TLR9 signalling. Adapted from Kawai and Akira (2006).

levels of IRF-7, IRAK4 and TRAF6 present in pDCs allows for the rapid and significant expression of IFN upon detection of viral DNA (Izaguirre *et al.*, 2003; Uematsu *et al.*, 2005).

1.2.4. TLR-independent signalling

Retinoic acid inducible gene I (RIG-I) and melanoma differentiation associated gene 5 (mda5) are dsRNA receptors in the cytoplasm and are therefore important detectors of certain virus infections e.g. NDV and vesicular stomatitis virus (VSV). They have a RNA-binding helicase domain and 2 caspase recruitment domains (CARDs) (Yoneyama *et al.*, 2004). RIG-I recruits IFNβ promoter stimulator protein (IPS) -1 leading to downstream signalling. The IRF kinases, TBK1 and IKKε become activated and in turn activate IRF3 and IRF7 which can then bind the promoter region of IFNβ (Kawai and Akira 2006). IPS-1 knockout mice can still produce type I IFN in response to synthetic DNA or vaccinia virus (Kumar *et al.*, 2006). Furthermore, herpes simplex virus (HSV)-1 can stimulate type I IFN production from non-pDC cells in a TLR9 independent manner (Hochrein *et al.*, 2004). Upon cell entry HSV-1 can induce an efficient antiviral response in an IRF3-dependent manner which is independent of either the TLR or RIG-I pathways (Paladino *et al.*, 2006). However, a cytosolic receptor for dsDNA has not yet been identified.

1.2.5. IFNβ enhanceosome

Expression of IFNβ does not rely on *de novo* protein synthesis but requires multiple interactions between transcription factors that result in highly specific gene expression following viral infection. The IFNβ enhanceosome is located between 110 and 45bp upstream of the transcriptional start site (Merika and Thanos 2001). It consists of specific positive regulatory domains (PRD) IV, III-I and II that are recognised by the ATF-2/c-Jun heterodimer, IRF3 and 7, and the NF-κB p50 and p65 heterodimer respectively (figure 1.3) (Falvo *et al.*, 2000; Wathelet *et al.*, 1998). Two copies of the architectural proteins, the high mobility group I (Y) proteins (HMGI(Y)), are required for the assembly of the enhanceosome. One is situated

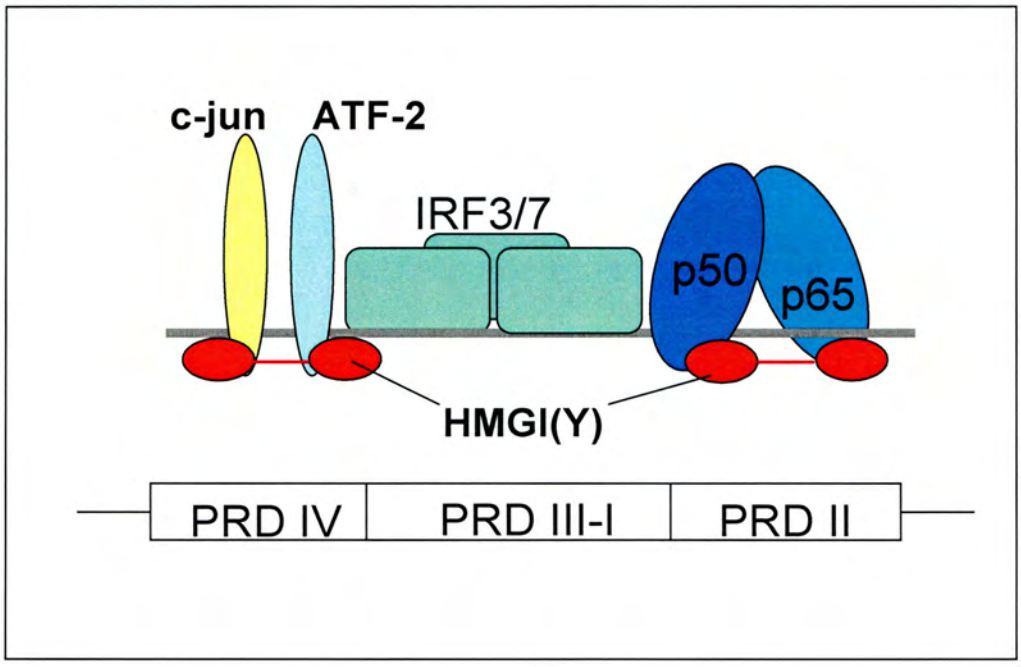

Figure 1.3. The IFNβ enhanceosome. Transcription factors associate to form the IFNβ enhanceosome. The components of AP-1 (c-jun and ATF-2) bind to positive regulatory domain (PRD) IV in association with HMGI(Y) molecules. IRF3 or IRF7 interact with PRD III and I. The NFκB subunits, p50 and p65, bind to PRD I with HMGI(Y) molecules. Adapted from Falvo *et al.*, 2000.

within PRD IV in association with ATF-2/c-Jun and the other situated within PRD II in association with NF-κB, aiding the stability of the nucleoprotein complex (Yie *et al.*, 1999). The co-activators CBP or p300 are also associated with the complex and are thought to interact with multiple components (Wathelet *et al.*, 1998). The enhanceosome is much more effective at inducing IFNβ expression than any of the individual components binding the promoter.

1.2.6. Cellular negative regulators of IFN signalling

As well as IRF-mediated control of IFN expression, the Jak-STAT signalling pathway can be suppressed by a number of other cellular proteins. Suppressors of cytokine signalling (SOCS) inhibit signalling by binding to the kinase domain in the cytoplasmic domains of Jaks suppressing their activation (Endo *et al.*, 1997; Fenner *et al.*, 2006). SOCS1 is induced by type I IFN. It is thought that SOCS1 associates with and regulates the IFNAR1 subunit leading to attenuated activation of STAT1 and thus reducing the extent of IFN signalling (Fenner *et al.*, 2006). The protein inhibitor of activated STAT (PIAS) 1 associates directly with STAT1 to prevent binding to DNA therefore inhibiting the induction of downstream effector genes (Liu *et al.*, 2004a).

1.3. Interferon stimulated genes

There are hundreds of interferon stimulated genes (ISGs) induced by type I IFNs that contribute to the anti-viral response, as well as the induction of the adaptive immune response. The ISGs encode a wide range of proteins including enzymes, cytokines, chemokines and transcription factors. Many such proteins are uncharacterised. A few of the best studied antiviral proteins are discussed below.

1.3.1. Protein kinase R

Protein kinase R (PKR) is constitutively expressed in the cytoplasm in an inactive form. It is a serine/threonine kinase that binds dsRNA present in the cytoplasm of infected cells and is upregulated by IFN signalling. Upon binding dsRNA, PKR undergoes a conformational change which allows it to dimerise and become activated as the catalytic domain is unveiled (Katze *et al.*, 1991). The optimal length of dsRNA for activation is approximately 80bp (Samuel 2001). Active PKR shuts down host protein synthesis by phosphorylating the eukaryotic translation initiation factor 2α (eIF2α) (Meurs *et al.*, 1992). At translation initiation, Met-tRNA is recruited to the 40S ribosomal subunit via eIF2 bound to GTP. This complex associates with mRNA and other initiation factors and bound GTP is hydrolysed to GDP. In order for translation initiation to continue GDP must be exchanged for GTP via eIF2B (a guanine exchange factor). However, once eIF2α is phosphorylated it interacts strongly with eIF2B. Subsequently, the recycling of GDP to GTP is prevented stopping translation initiation and thus viral replication (Ramaiah *et al.*, 1994).

PKR has other functions in the infected cell. NF-κB is essential for IFNβ induction and can be activated by PKR in response to dsRNA. This function is through activation of IKK, leading to the degradation of the inhibitors IκBα and IκBβ and resulting in activation of NFκB. IKK is not activated in response to dsRNA in PKR-deficient cell lines but the responses could be restored by co-transfection of PKR with dsRNA (Kumar *et al.*, 1997; Zamanian-Daryoush *et al.*, 2000). PKR has also been implicated in the regulation of apoptosis. PKR over-expression leads to cells undergoing apoptosis in response to dsRNA whereas PKR-null cells are resistant. PKR has been shown to upregulate Fas which interacts with the Fas associated death domain (FADD), part of the apoptosis pathway (Balachandran *et al.*, 1998).

1.3.2. 2'-5' Oligoadenylate synthetase system

The 2'-5' oligoadenylate synthetases (OAS) catalyse the synthesis of oligomers of adenosine linked by phosphodiester bonds in a 2' to 5' conformation. The product of OAS, 2'-5'A, binds to endoribonuclease L (RNase L) which is then activated via dimerisation. Activated RNase L catalyses cleavage of cellular and viral ssRNAs which leads to inhibition of protein synthesis. The 2'-5' molecules are highly labile so the activation of RNase L occurs in the vicinity of the viral transcripts that activated the 2'-5' OAS (Goodbourn *et al.*, 2000). This helps to ensure that viral transcripts are degraded preferentially over cellular transcripts. RNase L can also cleave 28S ribosomal RNA and thus is another effector of translational inhibition (Iordanov *et al.*, 2000).

1.3.3. Other ISGs

Mx proteins: The Mx proteins are large GTPases that are particularly effective against RNA viruses. Human MxA localises to the cytoplasm where it targets nucleocapsids. Mouse Mx1 protein localises to the nucleus and can inhibit transcription of influenza virus. The concentrations of the primary transcripts encoding the three polymerase proteins of influenza virus PB1, PB2, and PA were significantly reduced in the presence of Mx1 (Pavlovic *et al.*, 1992).

ISG15: ISG15 is an ubiquitin-like protein which covalently conjugates to target proteins in a process called ISGylation. Evidence suggests that ISG15 functions as an important antiviral molecule for a broad variety of viruses. ISG15-deficient mice were shown to be more susceptible to influenza virus, HSV-1, murine gammaherpesvirus-68 (MHV-68) and Sindbis virus infections (Lenschow *et al.*, 2007). It has antiviral activity against human immunodeficiency virus (HIV)-1 by inhibiting virus release *in vitro* but is not thought be important for the control of lymphocytic choriomeningitis virus (LCMV) (Okumura *et al.*, 2006; Osiak *et al.*, 2005). ISG15 can also be detected in the sera of mice after viral infection indicating

possible cytokine function as it has also been reported to induce NK cell proliferation, IFNγ production and maturation of DCs (Lenschow *et al.*, 2007).

ISG12: ISG12 was originally discovered by Rasmussen and colleagues in MCF7 human breast carcinoma cells in 1993. Found to be preferentially induced by type I IFN, it was designated a novel ISG (Rasmussen *et al.*, 1993). ISG12 was first termed p27 but due to potential confusion with p27kip it was later re-named ISG12 because of its molecular weight of 11.5 kDa. ISG12 is also known as IFNα-induced gene 27 (IFI27) and IFN-induced 11.5kDa protein. The ISG12 gene encodes a hydrophobic protein of 122 amino acids which shares 36% amino acid identity with the human 6-16 gene (Parker and Porter 2004) which is also highly induced in response to type I IFN. Sequence analysis shows that the promoter region of ISG12 containp putative ISRE, IRF1/IRF2 and STAT elements correlating with the ability of IFNα to upregulate ISG12 expression (Martensen *et al.*, 2001). ISG12 status as an IFNα-inducible protein was confirmed by analysis of ISG12 mRNA expression in various human cell lines. ISG12 gene expression was highly induced by IFNα, but not IL-2, IL-6 or TNF-α (Gjermandsen *et al.*, 2000). ISG12 expression has also been observed to be specifically highly up-regulated in mature and activated DCs but not in immature DCs or lipopolysaccharide-stimulated monocytes (Hashimoto *et al.*, 2000).

For the first time, an ISG has been found to be localised to the nuclear envelope. Cell fractionation was carried out on cells infected with a baculovirus expressing ISG12. ISG12 was detectable in the nuclear fraction of ISG12-expressing cells but not in cells infected with a control baculovirus. However, no nuclear localisation signal has been detected in the ISG12 sequence (Martensen *et al.*, 2001). Due to the localisation pattern, it has been speculated that ISG12 could be an inducible part of the nuclear pore complex (NPC) or interact with a protein of the NPC but this remains to be determined.

In silico analysis showed that the original ISG12 is part of a family of ISG12 genes that consists of 46 members so far in 25 different species. BLAST searches have found ISG12 genes in organisms including amoeba, fish, mammals and humans. All members of the family contain an 80 amino acid ISG12 motif. Four ISG12 family members have been found in humans, designated hISG12(a), (b) and (c) on chromosome 14q32, plus the 6-16 gene on chromosome 1p35, as grouped through phylogenetic analysis. Homologues to the ISG12 genes, but not 6-16, have been found in mice and these are termed mISG12(a), (b1) and (b2) and are found on chromosome 12F1 (Parker and Porter 2004). As the BLAST analysis of multiple ISG12 genes was only carried out in 2004, discussion of studies previous to that point only refer to a general ISG12 protein.

Sindbis infection of 4-week old mice led to increased expression of ISG12(b1) compared to 1-day old infected mice. This correlated with asymptomatic disease in the 4-week old mice compared to 1 day old mice where death occurred rapidly. In addition, enforced neuronal expression of murine ISG12(b1) in the 1 day old mouse brain led to significantly delayed mortality in the neonatal mice. These data suggest that upregulation of ISG12(b1) has a protective effect against Sindbis infection (Labrada *et al.*, 2002).

There are a great many other ISG products that have not been mentioned here and/or have yet to be fully characterised. There is likely a degree of redundancy between different ISGs. For example, although individually important components, mice triply deficient in PKR, RNase L and MxA can still mount an antiviral response to encephalomyocarditis virus (EMCV) (Zhou *et al.*, 1999).

1.4. Natural Killer cells

Natural killer (NK) cells are a fundamental component of the innate immune system. They were originally discovered because of their ability to 'naturally kill' tumour cells without prior sensitisation. Depletion of NK cells in an *in vivo* mouse model led to enhanced tumour formation showing that NK cells are important for suppression of tumour growth (Kim *et al.*, 2000). NK cells originate in the bone marrow and comprise approximately 5-10% of the lymphocyte population in the peripheral blood, spleen and liver (Lodoen and Lanier 2005). Although NK cells have been shown to be important for innate immune responses against transformed cells, this review concentrates on the antiviral activities of NK cells. They are important for the control of virus infections; targeting virus-infected cells via a number of mechanisms including cellular cytotoxicity, production of cytokines and shaping of the downstream adaptive immune response.

1.4.1. NK cell Receptors

Unlike B or T cells which express a rearranged receptor specific for a single ligand, NK cells express multiple cell surface receptors that do not undergo rearrangement and can recognise multiple ligands on a target cell. Such NK cell receptors can be inhibitory or activatory and can be triggered independently or in combination. Rather than considering NK cells to be non-specific, increased understanding of the NK cell receptor repertoire has led to NK cells being thought of as having a degree of specificity. Examples of inhibitory and activatory NK cell receptors are summarised in table 1.2 and some are discussed below in more detail. NK cell recognition of target cells is divided into three areas including recognition of pathogen-encoded molecules, 'missing-self' recognition of host proteins downregulated in infected cells (providing inhibitory signals from normal cells) and 'altered self' recognition of host molecules upregulated in infected cells.

1.4.1.1.Activatory receptors:

The mechanism of NK cell activation has not been fully determined. It likely results through the combined actions of cytokine receptors, adhesion molecules and activatory receptors recognising ligands on the infected target cell surface. NK cells express many activatory receptors including CD16, activatory killer immunoglobulin-like receptors (KIRs), NKG2D, natural cytotoxicity receptors (NCRs) and TLRs. In general, NK cell activatory receptors are transmembrane proteins that lack signalling activity. Such receptors associate with signal transducing adaptor proteins via residues in the transmembrane region and induce signalling through immunoreceptor tyrosine-based activation motifs (ITAM) in the cytoplasmic tails of the adaptors (Lanier 2001). The signalling adaptor proteins include DAP12, DAP10, FcεRIγ and CD3ζ. Signalling through the adaptor proteins lead to NK cell effector functions such as cytotoxicity and the release of cytokines.

Activation through the NK cell receptor CD16 leads to antibody-dependent cellular cytotoxicity (ADCC) in human and murine NK cells. However, the adaptor proteins differ between the two species. Human CD16 associates with homodimers and heterodimers of FcεRIγ and CD3ζ whereas murine CD16 only associates with homodimers of FcεRIγ. Signalling is thought to occur via a protein tyrosine kinase cascade leading to the recruitment and activation of Syk and ZAP70 if ITAM-containing adaptor proteins such as DAP12, FcεRIγ and CD3ζ are used by the NK cell receptor (DAP10 does not contain an ITAM, joining the cascade downstream of ZAP10/Syk) (Djeu *et al.*, 2002). Downstream effector molecules include phosphatidylinositol 3-kinase (PI3K), extracellular signal regulated kinase (ERK), Vav family guanine nucleotide exchange factor and Rho-Rac GTP binding proteins (Colucci *et al.*, 2002).

The NCRs are a family of immunoglobulin-like proteins and include NKp30, NKp46 and NKp44. Their expression is limited to NK cells only. These receptors appear to be the main receptors for activation of NK cells and along with NKG2D induce

Receptor	Ligand	Function	Species
CD16	IgG	activatory	Human, mouse
CD40	CD40L	activatory	Human, mouse
CD94/NKG2A	HLA-E (hu) Qa1 (mu)	inhibitory	Human Mouse
CD94/NKG2C	HLA-E (hu), Qa1 (mu)	activatory	Human Mouse
CD244 (2B4)	CD48	activatory	Human Mouse
DNAM-1	CD112, CD155	activatory	Human
KIR2DL1	HLA-C	inhibitory	Human
Ly49 (except D and H)	H-2K, H-2D	inhibitory	Mouse
Ly49D	H-2D	activatory	Mouse
Ly49H	MCMV (m157), others?	activatory	Mouse
NKG2D	MIC, ULBP(hu) RAE-1, H60, MULT-1 (mu)	activatory	Human Mouse
NKp30	Tumour ligands?	activatory	Human
NKp44	Viral proteins? influenza HA, Vaccinia virus	activatory	Human
NKp46	Viral proteins? influenza HA, Vaccinia virus	activatory	Human, mouse

Table 1.2. NK cell Receptors. Adapted from (Cerwenka and Lanier 2001; Colucci *et al.*, 2002). CD, cluster of differentiation; HA, haemagglutinin; HLA, human leucocyte antigen; hu, human; IgG, immunoglobulin G; KIR, killer immunoglobulin-like receptor; Ly49, lymphocyte antigen 49 complex; MIC, MHC class I related molecules; MCMV, murine cytomegalovirus; MULT-1, murine UL16-binding protein like transcript-1; mu, murine; RAE-1, retinoic acid early inducible 1; ULBP, UL16-binding protein.

virtually all cytotoxic activity (O'connor *et al.*, 2006). The extent of cytotoxic activity against susceptible target cells correlated with an increased surface intensity of the NCRs (Sivori *et al.*, 2000). NKp30 and NKp46 associate with the FcεRIγ and CD3ζ adaptor proteins and are expressed by all NK cells (Pende *et al.*, 1999; Sivori *et al.*, 1999) while NKp44 associates with DAP12 and is only expressed on activated NK cells (Cantoni *et al.*, 1999). At present little is known of the ligands for the NCR family. It has been shown that NKp44 and NKp46, but not NKp30, can bind the HA

of influenza virus and the HA-neuraminidase of Sendai virus and a subset of those NK cells require recognition by NKp46 in order to lyse cells expressing the viral glycoproteins (Arnon *et al.*, 2001; Mandelboim *et al.*, 2001). Furthermore, infection of cells with vaccinia virus resulted in a significant increase in their susceptibility to NK cell-mediated lysis. This effect is dependent on the NCRs which are thought to be activated by viral gene products expressed early in the virus life cycle (Chisholm and Reyburn 2006).

The NKG2D receptor is a member of the C-type lectin-like family and is encoded in the NK gene complex in murine chromosome 6 and human chromosome 12 along with the other NKG2 genes (Raulet 2003). It is expressed by all NK cells as well as $CD8^+$ T cells, NKT cells and activated macrophages. NKG2D associates with the DAP10 adaptor molecule which instead of an ITAM motif, contains a different tyrosine based motif (YINM) which recruits PI3K for downstream signalling (Wu *et al.*, 1999). The human NKG2D receptor was found to recognise MICA by means of a monoclonal antibody which blocked the interaction (Bauer *et al.*, 1999). MICB was also found to be recognised by NKG2D. MIC proteins are encoded by genes within the human MHC but they do not bind peptide or β_2-microglobulin. The MIC proteins are upregulated on stressed or tumourigenic cells but have a minimal expression on normal cells (Lanier 2001). Interestingly, the binding of the NKG2D/DAP10 complex provided an activatory signal that could override inhibitory signalling through the KIR/MHC class I complex (Cosman *et al.*, 2001). UL16 binding proteins (ULBPs) were also discovered to be ligands for human NKG2D, stimulating cytokine production from NK cells following binding. UL16 is an early CMV gene that can bind ULBP1, ULBP2 and MICB. The addition of soluble UL16 blocked these three ligands from binding the NKG2D receptor. Furthermore, addition of ULBPs to NK cell resistant target cells resulted in susceptibility to NK cell cytotoxicity (Cosman *et al.*, 2001). The ligands, retinoic acid early inducible 1 (RAE-1), H60 and mouse UL16 binding protein-like transcript 1 (MULT-1), for murine NKG2D have homology to the ULBPs. The importance of such ligands for NK cell responses to viral infection are highlighted by the evasion strategies employed by

murine cytomegalovirus (MCMV). The MCMV genes m152 and m155 downregulate expression of RAE-1 and H60 respectively to avoid NK cell activation (Hasan *et al.*, 2005).

The C57BL/6 mouse strain is relatively resistant to MCMV infection whereas BALB/c mice succumb to the infection. Studies using selective depletion of the $Ly49^+$ NK cell subset showed that the murine NK cell receptor Ly49H is involved and required for protection against MCMV in C57BL/6 mice (Brown *et al.*, 2001; Daniels *et al.*, 2001). Ly49H is encoded in the NK gene complex, *Cmv-1* in C57BL/6 mice but is lacking in BALB/c mice (Arase *et al.*, 2002). The Ly49 group are found in mice and are C-type lectin-like receptors and can be either activatory or inhibitory in function. The expression of Ly49 molecules is stably maintained in the clonal progeny of a NK cell. Ly49H is an activatory receptor which associates with DAP12 to signal the initiation of cytokine production and cytotoxicity. The ligand for Ly49H is a MHC class I-like MCMV glycoprotein, m157 which is expressed on the surface of infected cells. Site-directed mutagenesis studies have suggested that homodimerisation of Ly49H is central to recognising m157, but not MHC class I. This result links Ly49 dimer structure-variation to the potential recognition of various viral products (Kielczewska *et al.*, 2007).

1.4.1.2. Inhibitory receptors

It is important that NK cell activation is closely monitored in order to avoid autoimmune responses on normal host cells. The missing self hypothesis (NK cells recognise cells with downregulated MHC class I molecules) has been updated to state that 'NK cells recognise abnormal cells which lack sufficient MHC class I molecules or overexpress ligands for activatory receptors'. For example, erythrocytes do not express any MHC class I molecules yet are not targeted by NK cells and this may be attributed to the lack of activatory ligands on the erythrocyte surface (Lanier 2005). Therefore, the inhibitory receptors on NK cells can be considered as

regulatory receptors which reduce, rather than terminate, signalling from the activatory receptors.

The best characterised inhibitory receptors are members of the KIR family and CD94/NKG2A. KIRs are present on overlapping NK cell subsets as well as memory $CD8^+$ T cells and recognise different allelic groups of HLA-A, HLA-B and HLA-C molecules. For example, KIR2DL2 recognises HLA-C S77/N80 and KIR3DL1 recognises HLA-Bw4 (Lanier 2005). The inhibitory KIRs have an immunoreceptor tyrosine-based inhibitory motif (ITIM) in their cytoplasmic region. Binding of an inhibitory KIR to a MHC class I molecules suppresses NK cell cytotoxicity and cytokine release by means of SHP-1 and SHP-2 phosphatases which antagonise the activatory signalling cascade. Most members of the Ly49 family in mice contain an ITIM in their cytoplasmic domain (Ravetch and Lanier 2000). Ly49D and H are activatory receptors and thus lack an ITIM. The ligand for Ly49H, m157, is also recognised by the inhibitory receptor Ly49I in some strains of MCMV susceptible mice, dampening the NK cell response and thus contributing to susceptibility to the virus (Arase *et al.*, 2002). Ly49A and Ly49G have also been shown to be inhibitory receptors on NK cells and a subset of T cells. Addition of antibodies to both receptors led to enhanced lysis of target cells by T cells as well as increased production of TNFα and granulocyte-macrophage colony stimulating factor (GM-CSF) (Ortaldo *et al.*, 1998). Such studies demonstrate the similar functions of the Ly49 family to regulate both NK and T cell functions. CD94/NKG2A heterodimers are present as inhibitory receptors on human and murine NK cells. They recognise non-classical MHC class I molecules; HLA-E in humans (Brooks *et al.*, 1999) and Qa1 in mice (Vance *et al.*, 1998). The expression of CD94/NKG2A is not stable like the Ly49 receptors but is influenced by the cytokine environment. For example, TGF-β and IL-2 can induce upregulation of CD94/NKG2A on T cells *in vitro* (Bertone *et al.*, 1999; Derre *et al.*, 2002).

The role of certain NK cell receptors in the control of herpesviruses has been investigated. For herpesviruses to establish a persistent infection, MHC class I molecules are downregulated from the cell surface to avoid recognition by $CD8^+$ T cells. However, this results in infected cells being more susceptible to NK cell killing. Human cytomegalovirus (HCMV) has evolved many mechanisms to avoid NK cell recognition. For example, the UL18 glycoprotein is a MHC class I heavy chain homologue which can bind inhibitory NK cell receptors and therefore inhibit NK cell activation (discussed in more detail in section 1.5). In contrast to HCMV, Epstein-Barr virus (EBV) does not appear to encode a MHC molecule homologue. EBV infects and becomes latent in B cells. During latent infection there is limited gene expression which aids evasion from NK cell recognition. EBV downregulates MHC class I molecules from the cell surface during the early stages of lytic infection in order to evade T cell responses directed to lytic antigens. Consequently, EBV-infected cells are then more susceptible to NK cell recognition and induction of lytic replication results in increased NK cell lysis of EBV-infected B cells (Pappworth *et al.*, 2007). Susceptibility to NK cell cytotoxicity was a result of downregulation of ligands for the inhibitory NK cell receptors, HLA-A, -B and -C (binding to inhibitory KIR receptors) and HLA-E (binding to CD94/NKG2A). Additionally, ULBP-1 and CD112, ligands for the activatory receptors NKG2D and DNAM-1 respectively, were upregulated (Pappworth *et al.*, 2007). This study has highlighted the important balance of inhibitory/activatory NK cell receptors for the continued surveillance for virally infected cells.

1.4.2. Cytokines and NK cells

1.4.2.1. Cytokine regulation of NK cell function

As well as target recognition via cell surface receptors, NK cells can be activated via cytokine stimulation. A number of cytokines have been shown to influence NK cell activation and function. IFNα/β, produced from cells such as activated macrophages and DCs, can induce cytotoxicity and proliferation of NK cells during viral infection by signalling through the activatory IFNAR receptor (Biron *et al.*, 1999). IFNAR

knockout mice displayed inhibited cytotoxicity following infection with MCMV. STAT1 was shown to be required for IFNα/β-mediated NK cell cytotoxicity as there was a 70-fold reduction in cytotoxicity in STAT1-deficient mice despite sufficient IFNα/β serum levels (Nguyen *et al.*, 2002). IL-15 is important for the survival, homeostasis and accumulation of NK cells (Lodolce *et al.*, 1998) and IL-15 knockout mice lack NK cells (Kennedy *et al.*, 2000). It has been demonstrated that IFNα/β is important for the induction of IL-15 expression and thus the proliferation of the NK cell pool during MCMV infection (Nguyen *et al.*, 2002). IL-12 p70 is produced from DCs, macrophages and neutrophils and is critical for the efficient induction of IFNγ expression from NK cells during some, but not all viral infections. LCMV infection does not result in IL-12 induced IFNγ production from NK cells (Orange and Biron 1996). IL-12-dependent induction of IFNγ occurs during MCMV infection (Nguyen *et al.*, 2002). The regulation of IL-12 responses is important. IFNα/β inhibits IL-12, consequently inhibiting IFNγ expression (Cousens *et al.*, 1997). STAT1-deficient mice express higher levels of IFNγ, suggesting an important role for STAT1 in limiting IFNγ levels and thus inhibiting cytokine-mediated immunopathology. IL-18 is produced by activated macrophages as an inactive precursor which is then cleaved to the active form by caspase 1. IL-18 has been shown to enhance NK cell cytotoxic activity at early time points following infection with influenza virus (Liu *et al.*, 2004b). IL-18, TNFα and IL-1α/β can all synergise with IL-12 for the production of IFNγ from NK cells (Biron *et al.*, 1999). IL-10 and TGFβ negatively regulate NK cell function by inhibiting IL-12 induction (IL-10 and TGFβ) or by inhibiting IFNγ production and cytotoxicity (TGFβ) (Biron *et al.*, 1999). Macrophage inflammatory protein-1 α (MIP-1α) is induced during viral infection to induce NK cell chemoattraction and migration. During MCMV infection MIP-1α is required for the migration of NK cells into the liver (Salazar-Mather *et al.*, 1998).

1.4.2.2. Cytokine production

Binding of NK cell activatory receptors can lead to the production of cytokines, such as IFNγ, GM-CSF and TNFα, which augment the antiviral response. The role of NK cell production of IFNγ has been well documented. Levels of NK cell-derived IFNγ typically peak within hours to the first few days of infection, after which the primary source of IFNγ is T cells. NK cell IFNγ production is important during some but not all viral infections. For example, control of MCMV infection requires IFNγ production from NK cells whereas no IFNγ production is detectable during LCMV infection (Orange and Biron 1996). Studies in T cell-deficient mice (so removing T cells as an alternative source of IFNγ) showed that IFNγ was detectable at early time points post-MCMV infection and this was due to NK cells as depletion of NK cells resulted in significantly reduced IFNγ levels (Orange *et al.*, 1995). IL-12 is a potent inducer of IFNγ and the NK cell IFNγ response is reliant on the production of the biologically active IL-12 p70 heterodimer during MCMV infection. Antibody neutralisation of IL-12 inhibited NK cell IFNγ production and consequently, control of MCMV infection. Administration of even low doses of IL-12 led to a two-fold increase in NK cell cytotoxicity and IFNγ production in MCMV-infected mice. In contrast, LCMV replication is not affected by the absence of IL-12 and this correlates with the lack of IFNγ production during infection (Orange and Biron 1996; Orange *et al.*, 1995). It has been shown that NK cell recruitment into draining lymph nodes provides a primary source of IFNγ to stimulate Th1 polarisation of T cells (Martin-Fontecha *et al.*, 2004). TNFα can lead to DC maturation and therefore helps to initiate an efficient adaptive immune response. TNFα is also produced by NK cells upon MCMV infection although NK cells are not the only source of this cytokine and are not necessary for its production (Orange *et al.*, 1995). IL-2 activated NK cells can control HCMV infection *in vitro* by means of TNFα and TNFβ secretion leading to IFNβ production in infected cells (Iversen *et al.*, 2005). NK cells also produce certain chemokines such as MIP-1α and lymphotactin which have important chemoattractant properties (Bluman *et al.*, 1996).

1.4.3. Cytotoxicity

The primary pathway of NK cell-mediated cytotoxicity is through granule exocytosis (see figure 1.4). The directional release of perforin and granzymes towards an infected cell results in lysis. Perforin causes disruption of the target cell membrane, allowing entry of granzymes and induction of apoptosis. The granules are stored in the cytoplasm allowing rapid release when the NK cell is stimulated via activatory receptors on its surface. A common pathway of activation is induced following binding and cross-linking of activatory receptors to ligands on the target cell surface. For example, the CD16 receptor undergoes clustering upon binding of the Fc fragment of Ig (immunoglobulin) G-opsonised targets. This leads to coupling of the receptor with its adaptor proteins, induction of the signalling cascade and consequently ADCC. It has been shown that activation of ERK, a common downstream effector of the activatory receptor-induced signalling pathways results in mobilisation of lytic granules towards the target cell (Djeu *et al.*, 2002; Wei *et al.*, 1998). Rapid reorganisation of microtubules occurs followed by polarisation and secretion of the cytolytic granule content. Intracellular staining shows that upon binding of a tumour target, both perforin and granzyme B are redirected towards the tumour contact zone within five minutes (Wei *et al.*, 1998).

Perforin is a membrane disrupting protein which was traditionally thought of as a pore forming protein for the passive delivery of granzymes to the target cell. However, this idea has been discounted recently as there is no firm evidence for the formation of transmembrane pore complexes *in vivo*. Perforin is expressed in both $CD8^+$ T cells and NK cells. Infection of perforin-deficient mice with MCMV results in higher viral titres and increased mortality compared to infection of wild-type mice (Van Dommelen *et al.*, 2006). Furthermore, NK cells were shown to be an important source of perforin during MCMV infection as NK cell depletion of IFNγ knockout mice resulted in higher viral titres in the spleen and liver (Loh *et al.*, 2005). This demonstrates an important IFNγ-independent mechanism of MCMV control by NK cells. In contrast, perforin was shown to be dispensable for the control of MHV-68 as

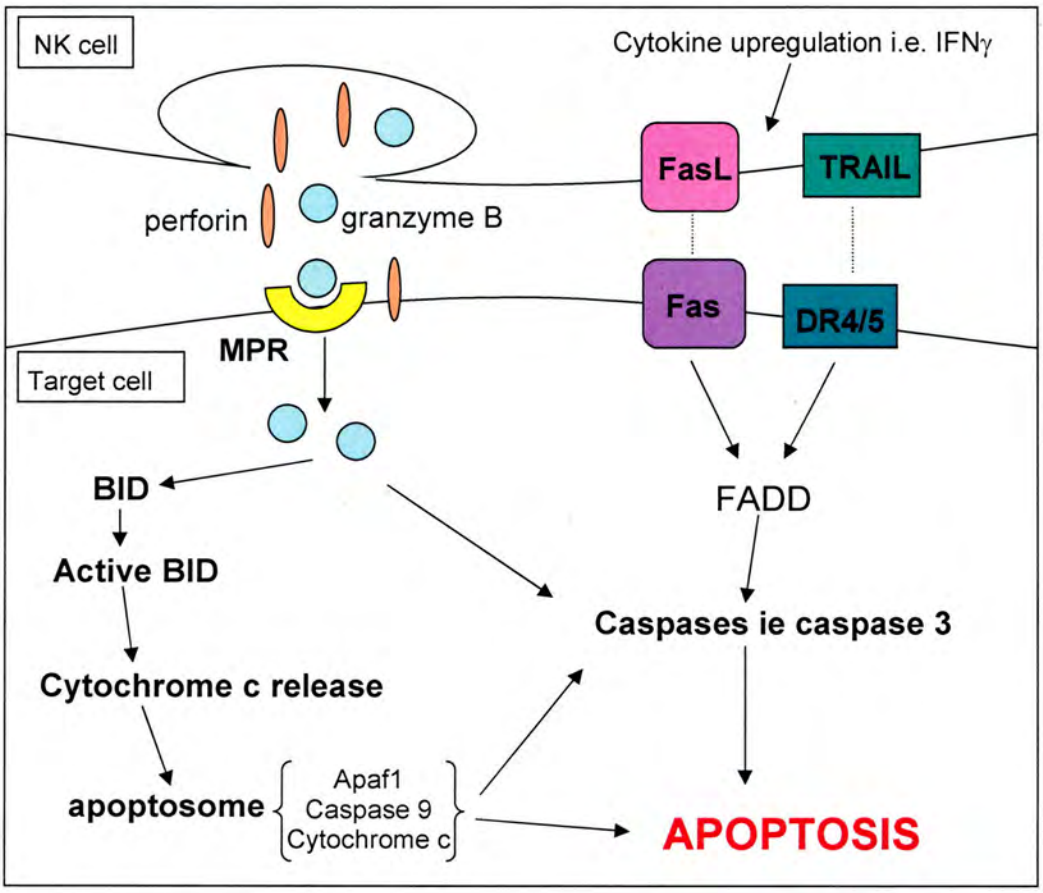

Figure 1.4. Pathways of NK cell cytotoxicity. The granule exocytosis pathway involves the release of cytotoxic granule contents (perforin, granzymes, serglycin) into the intercellular space. The uptake of granzyme B into target cells can occur rapidly by receptor-mediated endocytosis via the mannose 6-phosphate receptor (MPR). Granzyme B and perforin may bind to the target-cell surface as part of a single macromolecular complex associated with serglycin. Granzymes can then trigger apoptotic cell death via caspase-dependent or -independent pathways. Members of the TNF family, FasL and TRAIL, are regulated by cytokines such as IFN-γ. These ligands induce caspase -dependent target cell apoptosis via Fas-associated death domains (FADD) in the cytoplasmic domains of their corresponding receptors Fas and DR4/DR5, respectively.

viral titres did not differ between wild type and perforin deficient mice (Usherwood *et al.*, 1997). Also, there was no difference in MHV-68 titres following infection of NK cell-depleted and wild-type mice (Usherwood *et al.*, 2005). Although perforin is important for granzyme-mediated apoptosis, studies have shown that purified granzyme B can enter cells without perforin although this is unlikely to be sufficient for function at physiological levels (Trapani and Smyth 2002). Granzyme B can enter cells via the mannose-6-phosphate receptor (Trapani and Smyth 2002). The presence of a target cell receptor suggests that granzyme B entry may, in part, be mediated by receptor-mediated endocytosis. It has also been suggested that delivery of granzymes to a target cell may occur via a complex with perforin and serglycin (a chondroitin sulphate proteoglycan) which act as translocator and scaffold respectively (Metkar *et al.*, 2002). However, the mechanism of delivery remains to be fully determined.

NK and T cells avoid lysis through the perforin they secrete by the action of cathepsin B. Cathepsin B is a protease present in the cytolytic granules. It is rapidly sequestered on the surface of the T or NK cell following granule exocytosis and can cleave perforin molecules that diffuse back to the effector cell. In the presence of cathepsin B-specific protease inhibitors cytotoxic cells that release granules die rapidly via perforin-dependent suicide (Balaji *et al.*, 2002).

The granzymes are a family of serine proteases (enzymes which cleave peptide bonds and have a serine residue in the active site). Ten granzymes are expressed in mice (A-K, M and N) and five in humans (A, B, H, K and M). Members cleave at different residues. For example, A and K are tryptases whereas H is a chymase, cleaving after hydrophobic residues such as phenylalanine. B is the best studied member of the granzyme family. Granzyme B induces apoptosis by both caspase-dependent and -independent pathways, cleaving target cell proteins at specific aspartate residues. Granzyme B has been shown to interact directly with certain procaspases. For example, procaspase 3 is cleaved to caspase 3 by granzyme B thus activating it and leading to apoptosis of the cell. Indirect caspase activation is also

mediated by granzyme B. It can activate members of the Bcl-2 family directly such as BH3-interacting domain death agonist (BID). BID interacts with receptors on mitochondria to cause cytochrome c release which then activates procaspase 9 in the cytoplasm to result in apoptosis (Russell and Ley 2002). Granzyme A is thought to act through a distinct pathway from granzyme B as it does not activate caspases but induces apoptosis through the induction of single-stranded DNA breaks (Beresford *et al.*, 1999).

The second pathway of NK cell-mediated cell cytotoxicity is termed as death-receptor mediated and can either be through stimulation of FasL or TNF-related apoptosis-inducing ligand (TRAIL). The pathways are summarised in figure 1.4. Such molecules are expressed by NK cells as important mediators of apoptosis. TRAIL, also known as Apo2 ligand, binds to the human receptors DR4 (TRAILR1) and DR5 (TRAILR2) to induce apoptosis through death domains in their cytoplasmic domains (Degli-Esposti 1999). Activation by IL-2, type I IFN, IFNγ or IL-15 results in high TRAIL expression in human and murine NK cells. NK cell cytotoxicity is enhanced by type I IFN through upregulation of TRAIL due to the presence of an ISRE in the murine TRAIL promoter (Sato *et al.*, 2001). The importance of TRAIL-mediated cytotoxicity for control of viral infection is demonstrated by the requirement for control of EMCV infection and the fact that TRAIL receptor expression was increased on CMV infected cells (Smyth *et al.*, 2005). Fas expression on the surface of target cells is upregulated by IFNγ secreted by NK cells. NK cells can then induce apoptosis of tumour cells in a Fas-dependent manner (Screpanti *et al.*, 2005).

1.4.4. NK cell proliferation in response to viral infection

NK cells proliferate rapidly during viral infection, significantly expanding the NK cell pool. NK cell numbers were found to be significantly elevated in patients with infectious mononucleosis (IM), the acute phase of infection with EBV (Williams *et al.*, 2005). Similarly, NK cell numbers increase during early MCMV infection. This

initial phase of proliferation is non-specific, regardless of cell surface receptor expression, and is thought to be due to the action of proproliferative cytokines such as IL-15 (Dokun *et al.*, 2001). It is thought that IFNα/β can induce IL-15 expression, in a STAT-1-dependent manner, to induce NK cell proliferation. In STAT-1- or IFNα/β-deficient mice, the degree of NK cell proliferation was drastically reduced and the reduction was associated with a lack of IL-15 induction (Nguyen *et al.*, 2002). Furthermore, blocking of IL-15 function by antibodies to the IL-15 receptor resulted in vastly reduced numbers of NK cells accumulating in response to MCMV infection compared to control mice (Nguyen *et al.*, 2002). Although IL-18 alone is not sufficient to promote NK cell proliferation and survival, it can augment the action of IL-15 *in vitro* (French *et al.*, 2006). This effect remains to be determined *in vivo* but the production of IL-18 from activated macrophages and DCs may act synergistically with IL-15 during viral infection to induce an efficient NK cell response early in infection.

Following non-specific proliferation, a specific phase of proliferation occurs during MCMV infection. Specific proliferation of NK cells during MCMV infection has been shown to be due to Ly49H activation through recognition of infected cells and results in a pool of $Ly49H^+$ NK cells, peaking between 4 to 6 days post-infection (Dokun *et al.*, 2001). This viral-induced specific expansion resembles the clonal expansion of antigen-specific T cells. $Ly49H^-$ NK cells expressing other activatory receptors proliferated during the initial non-specific phase but did not undergo expansion during the later specific phase. As the adaptive immune response develops the NK cell pool contracts and returns to steady-state levels. The contraction phase is not well understood but may be a result of declining proproliferative cytokine levels or increasing levels of antiproliferative cytokines.

1.4.5. NK cells and human herpesvirus infection

The importance of the NK cell response against virus infection was demonstrated in a patient with defective NK cell responses with other immune responses at normal or

near normal. Studies showed that the patient lacked NK cells as no lymphocytes expressing CD56 or CD16 could be found. The patient first presented with a disseminated, life threatening varicella zoster virus (VZV) infection and varicella pneumonia and went on to develop severe HCMV and HSV infections (Biron *et al.*, 1989). Studies in the mouse model have shown a role for NK cells in clearance of HSV-1. NK cell numbers increased in the lung following intranasal infection. These cells were activated, had enhanced cytotoxic activity and NK cell-depletion led to higher virus titres during the early stages of infection (Reading *et al.*, 2006). Studies of the NK cell response to MCMV have shown that depletion or deficiency leads to severe disseminating infections and the $Ly49H^+$ activatory receptor is associated with the ability to control infection in mouse strains that are relatively resistant to MCMV infection (Daniels *et al.*, 2001; Orange *et al.*, 1995). Severe CMV infections are also observed in humans with defective/no NK cells. In addition, low NK cell cytotoxicity was associated with increased mortality to HCMV infection in patients following bone marrow transplants (Quinnan *et al.*, 1982).

The importance of NK cells for EBV control has been demonstrated in a number of rare genetic disorders. For example, patients with Chediak-Higashi syndrome are susceptible to disseminating EBV infection (Merino *et al.*, 1983). They have defective NK cell cytotoxicity due to mutations in the lysosomal trafficking regulator (LYST) gene. It is thought that this mutation results in defective vesicle attachment to microtubules therefore inhibiting granule exocytosis (Orange 2002). Patients with X-linked lymphoproliferative disease (XLP) have a severe immunodeficiency characterized by mutations in the signalling lymphocytic activation molecule (SLAM)-associated protein (SAP) and by the inability to control EBV infections (Benoit *et al.*, 2000). A fatal infectious mononucleosis occurs following acute infection with EBV. SAP is an important intracellular adaptor protein for the activatory NK cell receptor 2B4 (CD244). NK cells from XLP patients fail to kill EBV^+ B lymphoblastoid cell lines even though the 2B4 ligand, CD48 is highly expressed on such cells (Parolini *et al.*, 2000). The CD48:2B4 interaction is a possible mechanism for the recognition of EBV-infected cells and thus a lack of

downstream signalling contributes to the failure of NK cells to control EBV infection.

1.5. Virus Evasion of the Innate Immune system

At early times post-infection viruses encounter various components of the innate immune system which are important for mounting an antiviral response. The potency of the antiviral response has led to virus families evolving mechanisms to counteract these responses. Examples of mechanisms to evade type I IFN and NK cells are discussed in the following section. Given the volume of evasion mechanisms described this section will concentrate mainly on those employed by the *Herpesviridae*.

1.5.1. Evasion of the type I IFN System

Viruses have evolved means to block almost all components of the type I IFN system. Mechanisms include inhibition of IFN synthesis, inhibition of IFN signalling and inhibition of ISG expression and effector functions (reviewed in (Goodbourn *et al.*, 2000; Weber *et al.*, 2004).

The *Herpesviridae* encode a number of genes to limit type I IFN induction and escape the downstream responses. For example, the immediate-early gene, ICP0, of HSV-1 can block the activation of IRF3 and IRF7. The ICP0-mediated inhibition of IRF3 was shown to be through blocking nuclear accumulation of activated IRF3 (Lin *et al.*, 2004; Melroe *et al.*, 2004). The HCMV structural protein p65 acts in a similar manner, by inhibiting nuclear translocation and phosphorylation of IRF3 (Abate *et al.*, 2004). Kaposi's sarcoma-associated herpesvirus (KSHV) encodes a number of IRF homologues which compete with their cellular counterparts and consequently inhibit IRF functions. vIRF1, encoded by the K9 gene, is expressed during lytic replication. It inhibits transcriptional responses to IFN by suppressing the activity of IRF1 and IRF3. Inhibition occurs directly or through competition for the

transcriptional enhancers CBP/p300, therefore inhibiting the formation of transcriptionally competent IRF3-CBP/p300 complexes (Burysek *et al.*, 1999; Lin *et al.*, 2001). vIRF2 can be detected from 2 to 24 hours post-infection *in vitro* (Krishnan *et al.*, 2004). It was shown to inhibit IFNα-driven activation of an ISRE-containing promoter as well as inhibiting activation of the IFNβ promoter by IRF3 (Fuld *et al.*, 2006). vIRF3 is suggested to downregulate NFκB activity by inhibiting nuclear translocation thus lowering the level of type I IFN induction (Seo *et al.*, 2004). A fourth vIRF has been identified but this protein is still to be characterised. The ORF45 tegument-associated protein of KSHV interacts with IRF7, inhibiting its phosphorylation and blocking its accumulation in the nucleus (Zhu *et al.*, 2002). ORF45 may act to complement the vIRFs as its presence within the virion ensures its presence at the earliest stages of infection.

Herpesviruses can interfere with IFNAR signalling and thus the induction of antiviral responses. HSV-1 expresses a virion host shutoff protein (vhs) which functions as an RNase to degrade cellular transcripts. Proteins such as IRF7, that require transcriptional activation, would be sensitive to vhs-mediated transcript degradation (Weber *et al.*, 2004). Vhs also led to the rapid downregulation of Jak1 and STAT2 from infected cells (Chee and Roizman 2004). HSV-1 also induces expression of SOCS3 leading to the prevention of Jak and STAT phosphorylation (Yokota *et al.*, 2004). The MCMV pM27 protein binds and downregulates STAT2. Mutant MCMV lacking pM27 was susceptible to type I IFNs and this effect was reversed in IFNAR-deficient mice (Zimmermann *et al.*, 2005).

Herpesviruses employ mechanisms for escaping the IFN-induced antiviral proteins. The HCMV protein TRS1 encodes a dsRNA binding domain at the amino terminus to sequester dsRNA, whereas the carboxy-terminal domain is necessary for preventing the phosphorylation of eIF2α (Hakki and Geballe 2005). The vIRF2 protein of KSHV can also block phosphorylation of eIF2α through the binding of PKR (Burysek and Pitha 2001). The HSV-1 protein Us11 can directly bind PKR

preventing its activation. Us11 RNA binding domain is necessary to inhibit the PKR-mediated protein synthesis inhibition in infected cells suggesting that the RNA binding function may be required to prevent PKR activation (Poppers *et al.*, 2000). Us11 also is thought to inhibit the activation of 2'-5' OAS through binding available dsRNA (Sanchez and Mohr 2007). Another HSV-1 protein, ICP34.5 recruits cellular phosphatase 1 to dephosphorylate eIF2α and therefore reverses the translational block induced by PKR (He *et al.*, 1997). The importance of ICP34.5 is demonstrated by HSV-1 lacking ICP34.5 which are attenuated in wt mice but exhibit wt virulence in PKR-deficient mice (Leib *et al.*, 2000). EBV encodes small RNA molecules known as EBERs which can bind PKR so compete with dsRNA to prevent activation of PKR (Elia *et al.*, 1996).

1.5.2. Evasion of NK cells

Viral mechanisms for the avoidance/inhibition of NK cell responses can be divided into five categories: expression of virally encoded MHC class I homologues, modulation of MHC class I protein expression by viral proteins, inhibition of activatory receptor function, virus encoded cytokine-binding proteins or cytokine receptor antagonists and direct inhibition of NK cell function.

Many viruses avoid T cell responses by downregulating MHC class I molecules from the host cell surface. However, this renders infected cells more susceptible to NK cell killing due to less opportunity for NK cell inhibitory receptors to bind class I molecules such as HLA-C. CMV encodes MHC class I homologues, UL18 (HCMV) and m144 (MCMV). A m144-deletion mutant virus was attenuated *in vivo* and depletion of NK cells restored virulence to wild-type levels (Farrell *et al.*, 1997). The exact mechanisms of these proteins remain to be elucidated but rather than being a decoy ligand, UL18 can bind the inhibitory receptor, leukocyte Ig-like receptor 1(LIR-1), expressed on B, monocytes and a subset of NK cells (Cosman *et al.*, 1997). m157 from MCMV is a class I homologue which can bind the inhibitory receptor

Ly49I and thus inhibit NK cell function in susceptible strains of mice (Arase *et al.*, 2002).

HCMV UL40 functions to inhibit NK cell cytotoxicity by maintaining HLA-E expression on the cell surface, even in the absence of other class I molecules. HLA-E binds a peptide derived from the leader segment of MHC class I molecules and binds the CD94/NKG2A inhibitory receptors. UL40 contains the same peptide and can therefore upregulate HLA-E expression and prevent lysis (Tomasec *et al.*, 2000). Viral proteins can also target the MHC class I synthesis pathway. The HCMV US2 and US11 gene products can induce the relocation of class I molecules from the endoplasmic reticulum (ER) to the cytoplasm where they are degraded by the proteasome. It has been shown that US2 targets HLA-A, -B and -G but not HLA-C or -E. US3 binds and retains MHC class I molecules in the ER whereas US6 inhibits MHC class I expression by blocking translocation of peptides through the transporters associated with antigen processing molecules into the ER (Lodoen and Lanier 2005). The KSHV proteins K3 and K5 increase endocytosis of surface class I molecules for degradation. K3 downregulates HLA-A, -B, -C, and -E, whereas K5 only downregulates HLA-A and HLA-B2 (Coscoy and Ganem 2000).

Interference with activation receptors and their ligands is another mechanism of NK cell evasion. K5 ensures inhibition of NK cell-mediated cytotoxicity by downregulating and ubiquitinating the target cell ligands ICAM-1 and CD86 (B7-2) (Ishido *et al.*, 2000). MCMV encoded proteins downregulate surface expression of ligands for the activatory receptor NKG2D. m155 downregulates H60, m152 downregulates RAE-1 and m145 downregulates MULT-1 (Hasan *et al.*, 2005; Lodoen *et al.*, 2004). Deletion of the m138 gene, which encodes an FcγR, resulted in viral attenuation even in the absence of antibodies and therefore demonstrated an additional function to IgG Fc binding. m138 was shown to promote rapid downregulation of MULT-1 and H60 and thus provides an alternate mechanism for blocking NK cell activation (Lenac *et al.*, 2006).

Viruses may indirectly dampen NK cell responses through modulation of cytokines or chemokines. For example, viral encoded IL-10 homologues such as the BCRF-1 gene of EBV can result in general NK cell inhibition. The M3 gene of MHV-68 encodes a broad spectrum chemokine binding protein which blocks the activity of several NK cell chemoattractants such as MIP-1α and RANTES (Parry *et al.*, 2000).

Viruses may exert direct effects on NK cells, possibly through infection of the NK cells themselves or by direct contact. The hepatitis C virus envelope protein E2 binds to CD81 on the NK cell surface resulting in inhibition of NK cell cytotoxicity. It also resulted in inhibition of IFNγ production even after exposure to IL-12, -15 or CD16 cross-linking (Tseng and Klimpel 2002). Thus E2 can inhibit NK cells by directly binding an inhibitory receptor.

1.6. Herpesviruses

Herpesviruses comprise a large group of at least 130 viruses that can infect a wide variety of hosts including oysters, fish, birds and humans. Through a long co-evolution, herpesviruses are well adapted to their hosts. In immunocompetent individuals they can persist for a lifetime without overt signs of disease. However, serious disease can result when an alternative host species or immunocompromised host becomes infected.

The herpesviruses are double stranded DNA viruses, varying in length from 120 to 250kb. The genetic material is contained in an icosadeltahedral capsid made up from 162 capsomeres. The tegument layer is a complex, proteinaceous layer containing a number of virus proteins. It appears to have an ordered structure, linking the capsid to the outer envelope and maintaining virion integrity. Surrounding the tegument is the viral envelope. Derived from cellular membranes, it encompasses viral proteins and glycoproteins. The overall size of virions can vary between 120 to 300nm

(Roizman and Pellet 2001). Members of the family *Herpesviridae* share four biologic properties:

1. The genome encodes a large range of enzymes involved in nucleic acid metabolism (e.g. thymidine kinase), DNA synthesis (e.g. DNA polymerase) and protein processing (e.g. protein kinase).
2. Viral DNA synthesis and capsid assembly occurs in the nucleus.
3. Production of infectious progeny results in destruction of the host cell.
4. They can maintain a latent infection in their natural host, where a limited subset of viral genes is expressed from a circular genome.

The capacity to become latent, with minimal gene expression, allows some avoidance from the host immune system, and allows persistence for the lifetime of the host. Periodic reactivation from latency leads to production of infectious progeny for transmission to new hosts (Roizman and Pellet 2001).

1.6.1. Herpesvirus Life Cycle

The process of herpesvirus assembly and maturation is complex and the following is only a brief overview of key stages. The majority of research has focused on the replication cycle of HSV-1 so the majority of examples are concerning this virus. Initial attachment to a host cell usually occurs via binding of viral glycoproteins to cell surface glycosaminoglycans. The gB and/or gC ligands of HSV-1 bind to heparin sulphate on the cell surface. Heparan sulphate is also used as a tether in other members of the herpesvirus family, such as KSHV (Akula *et al.*, 2001). However, this is not always the case as EBV attaches to target B cells by binding of CD21 (complement receptor 2) via gp350. The various cell receptors used help to explain the differences in cell and tissue tropisms of herpesviruses. Co-receptor binding allows for entry into the cell by fusion of the virion envelope with the plasma membrane. For example, gp42 of EBV binds HLA class II and is critical for entry into B cells (Spear and Longnecker 2003).

Following fusion with the plasma membrane, the de-enveloped virus is released into the cytoplasm where certain tegument proteins such as the virus host shutoff protein of HSV-1 remain in the cytoplasm to make the cellular environment more favourable to virus replication. Capsids are transported along microtubules to the nucleus where viral DNA is released and assumes a circular conformation. Transcription of the viral genome results in a regulatory cascade comprised of immediate-early (IE), early (E) and late (L) mRNAs. The IE genes require no *de novo* protein synthesis for their expression. The predominant role of this group appears to be transactivation of later viral gene expression and modulation of the host cell. E-gene expression requires viral protein synthesis for their expression. These genes are mainly required for viral nucleic acid metabolism such as the thymidine kinase (TK) gene (Roizman and Knipe Dm 2001). L-genes are dependent on protein and viral gene synthesis and can be further subdivided into two groups: the leaky-late, where expression is enhanced by viral DNA synthesis; and the true late genes, which are not expressed in the absence of DNA synthesis. The L-genes primarily encode the structural components of the virion, including gC and gB. DNA replication occurs in a rolling-circle fashion. The concatameric DNA is cleaved during encapsidation into empty capsids.

Capsids exit the nucleus by budding into the perinuclear space, obtaining a primary envelope (Mettenleiter 2004). Free capsids are transported to the cytoplasm following fusion of the primary envelope to the outer nuclear membrane. Tegumentation occurs within the cytoplasm, through a complex series of protein-protein interactions that have yet to be fully defined. Final envelopment occurs through budding into trans-golgi vesicles after which mature virions are secreted from the cell via the vesicular route (Mettenleiter 2004).

1.6.2. Herpesvirus Classification

The *Herpesviridae* family can be classified into three subfamilies: the *Alphaherpesvirinae*, the *Betaherpesvirinae* and the *Gammaherpesvirinae*. Historically, this classification was based on their biologic properties such as host range, sites of latent infection and length of the replication cycle. Recently, DNA

sequencing has become the main approach to classification (McGeoch et al., 2006). Examples of murine and human herpesviruses from each subfamily are shown in table 1.3.

Alphaherpesvirinae

The *alphaherpesvirinae*, including the genera *Simplexvirus* and *Varicellovirus*, have the capacity to establish latent infections mainly within sensory ganglia. They are also characterised by a variable host range, rapid spread *in vitro* and a relatively short replication cycle. The diseases associated with herpesvirus infections can be wide

Subfamily	Genus	Virus	Abbreviation	Major Host
Alphaherpesvirinae	*Simplexvirus*	Herpes simplex virus-1	HSV-1	Human
		Herpes simplex virus-1	HSV-2	Human
	Varicellovirus	Varicella zoster virus	VZV	Human
		Bovine herpesvirus-1	BHV-1	Cattle
	Mardivirus	Marek's disease virus 1	MDV-1	Chicken
		Herpesvirus of turkey	HVT	Turkey
Betaherpesvirinae	*Cytomegalovirus*	Human cytomegalovirus	HCMV	Human
		Rhesus monkey cytomegalovirus	RhCMV	Rhesus macaque
	Muromegalovirus	Murine cytomegalovirus	MCMV	Mouse
		Rat cytomegalovirus	RCMV	Rat
	Roseolovirus	Human herpesvirus-6	HHV-6	Human
		Human herpesvirus-7	HHV-7	Human
Gammaherpesvirinae	*Lymphocrytovirus*	Epstein-Barr virus	EBV	Human
		Marmoset lymphocryptovirus	marLCV	Marmoset
	Rhadinovirus	Kaposi's sarcoma-associated herpesvirus	KSHV	Human
		Murine gammaherpesvirus-68	MHV-68	Mouse
		Herpesvirus saimiri	HVS	Squirrel Monkey

Table 1.3. Examples of known herpesviruses from each subfamily and their natural hosts. Adapted from McGeoch *et al.*, 2006.

ranging, even within the same genus. HSV-1 is associated with cold sores whereas HSV-2 is associated with genital lesions. VZV can cause chicken pox, shingles and post-herpetic neuralgia.

Betaherpesvirinae

Betaherpesviruses can be characterised by their establishment of latency primarily within cells of the myeloid lineage but virus can also be detected in cells of the salivary glands and kidneys (Reddehase *et al.*, 2002). They share a set of 80 ORFs that are common to all betaherpesviruses (Mocarski and Courcelle 2001). Infected cells often become enlarged in a process known as cytomegalia. In culture the replication cycle is relatively long with a slow progressing infection. Members of the cytomegalovirus genus are associated with mononucleosis and HCMV can cause congenital deformities. HHV-6 and -7 are associated with roseola (exanthema subitum), characterised by fever and rash which is common in children.

Gammaherpesvirinae

The gammaherpesviruses have a very narrow host range with infection often restricted to the family or order to which the host belongs. *In vivo* latent virus is often found in lymphoid tissue. Latency is maintained primarily within B- and T-lymphocytes but can also be established in other cell types. *In vitro* all gammaherpesviruses can replicate in lymphoblastoid cells with some also being able to cause lytic infections in epithelial and fibroblast cell lines. EBV is the causal agent of IM and is also associated with a range of tumours including Burkitt's lymphoma, nasopharyngeal carcinoma and post-transplant lymphoproliferative disease (PTLD). KSHV is the most recently discovered tumourigenic herpesvirus. It is associated with Kaposi's sarcoma (KS), primary effusion lymphoma and some plasma cell forms of multicentric Castleman's disease (MCD).

1.6.3. Animal models of gammaherpesvirus infection

Primary infection with gammaherpesviruses is largely asymptomatic. Therefore, the majority of information regarding infection has been determined by studies of long-term persistence and symptomatic disease such as PTLD, KS and IM. In these studies it has not been possible to determine virus-host interactions prior to the onset of symptoms. The narrow host range of the *gammaherpesvirinae* has also impeded studies. A suitable animal model of gammaherpesvirus infection is required to thoroughly investigate virus-host interactions and illuminate possible therapeutic approaches.

Initially, non-human primates were chosen as an animal model system for the study of EBV and KSHV pathogenesis. EBV infection of cotton-top tamarins (*Saguinus oedipus*) leads to B cell proliferation and thus provides a useful model for the study of PTLD. However, animals surviving lymphoproliferative disease do not become latently or persistently infected (Epstein *et al.*, 1985). Therefore the cotton-top tamarin is not a useful model for all areas of EBV pathogenesis. Lymphocryptoviruses (LCV), closely related to EBV, can infect Old World primates. Similar to EBV, LCV-infected cell lines produce virus able to immortalise B cells (Wang *et al.*, 2001). Oral inoculation of rhesus macaques with a rhesus LCV mimics EBV infection leading to lymphoadenopathy, persistent virus shedding from the oral mucosa and an asymptomatic latent infection in the peripheral blood (Moghaddam *et al.*, 1997).

Simian KSHV homologues can be found within the New World primates, for example, herpesvirus saimiri (HVS) infection of squirrel monkeys, as well as in the Old World primates, such as rhesus rhadinovirus (RV2mac) infection of macaques (*Macaca mulatta*) (Damania and Desrosiers 2001). RV2mac was found to contain a viral IL-6 gene homologue analogous to that of KSHV suggesting similar host-virus interactions (Mansfield *et al.*, 1999). KSHV and RV2mac have extensive homology and similar transcription profiles but RV2mac does lack genes present in KSHV such

as the immune evasion genes K3 and K5 (Dittmer *et al.*, 2005). Nonetheless, co-infection of rhesus macaques with simian immunodeficiency virus and RV2mac can result in lymphoproliferative disease resembling MCD and arteriopathy resembling KS vascular lesions (Mansfield *et al.*, 1999) thus providing a model for human co-infection with HIV and KSHV.

Although non-human primate models are useful for the investigation of gammaherpesvirus infections, study is often limited by mandatory high security, high expense and strict government regulations. A murine model of disease is advantageous for a number of reasons; they are smaller, cheaper, easier to keep and development of transgenic animals is more straightforward. Furthermore, the murine immune system has been studied in greater depth than that of non-human primates. There are numerous in-bred and transgenic mouse strains with which to study virus-host interactions *in vivo*. For example, severe combined immunodeficient (SCID) mice inoculated with peripheral blood mononuclear cells from EBV-seropositive individuals develop disease resembling PTLD (Johannessen and Crawford 1999). MHV-68 provides an amenable small animal model for studying gammaherpesvirus infection as productive and latent infections, analogous to EBV infection, are observed in inbred strains of mice (Sunil-Chandra *et al.*, 1992). MHV-68's gene organisation and homology to other gammaherpesviruses are shown in figure 1.5. Recombinant MHV-68 viruses, with deletion of endogenous genes or addition of foreign genes, allow the study of virus-host interactions and gene function with MHV-68 as well as EBV and KSHV genes.

1.6.4. Course of MHV-68 infection

MHV-68 (also known as murid herpesvirus-4) was originally isolated in 1980 from bank voles (*Clethrionomys glareolus*) in Slovakia (Blaskovic *et al.*, 1980). The genome consists of an 118kbp unique region flanked by 1239bp of terminal repeats which vary in number. The genome encodes 73 ORFs as well as 8 vtRNAs and 9 possible microRNAs (Efstathiou *et al.*, 1990; Pfeffer *et al.*, 2005).

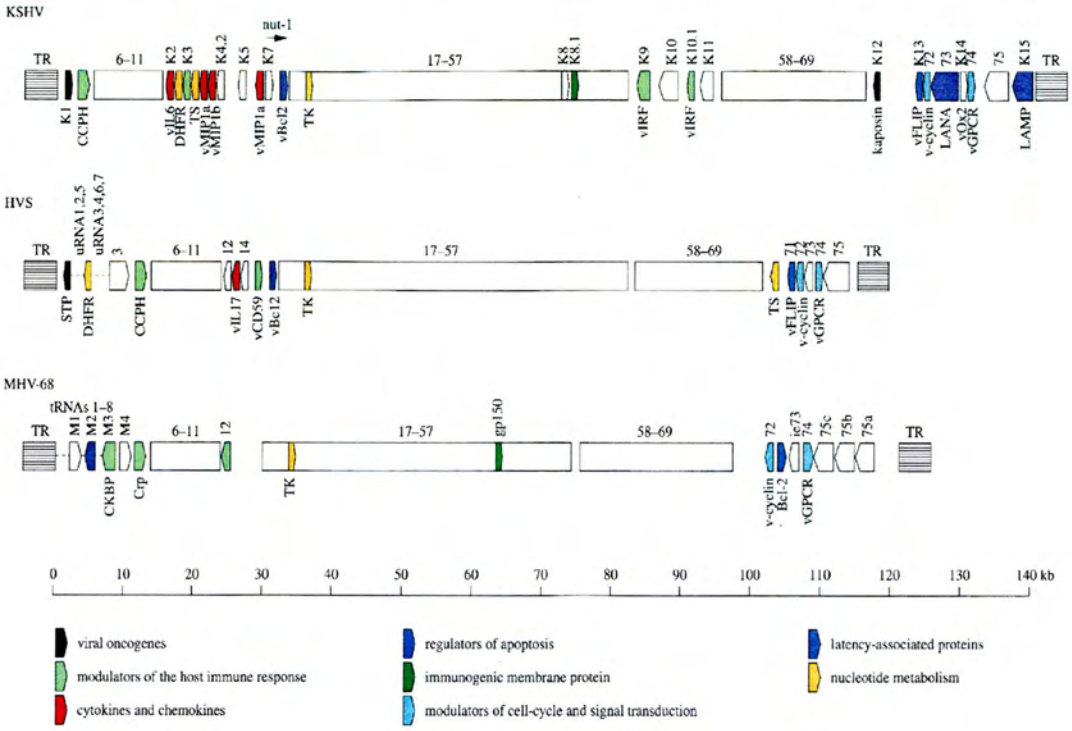

Figure 1.5. Diagrammatic representation of the MHV-68 genome aligned with the genomes of KSHV and HVS. Open boxes represent blocks of conserved genes. Adapted from Nash *et al.*, 2001.

Initial studies by Sunil-Chandra *et al.* showed that MHV-68 could infect the inbred mouse strain BALB/c, and give rise to disease similar to that of EBV infection (Sunil-Chandra *et al.*, 1992). The natural route of infection is uncertain. Infection of laboratory mice is usually carried out via the intranasal or intraperitoneal route. Given that MHV-68 is more often detected in the respiratory tract than the spleen in free living wood mice (Blasdell *et al.*, 2003) it appears likely that the intranasal route of inoculation is the most accurate reflection of natural infection. However, the digestive route may also be a possibility as productive infection could be detected in intestinal epithelia following gastric instillation (Peacock and Bost 2000).

Following intranasal inoculation of BALB/c mice, a lytic infection occurs predominantly in the alveolar epithelial cells although some mononuclear cells in the lung are also virus-positive (Sunil-Chandra *et al.*, 1992). Viral titres rise to a peak at day 5-7 post-infection which is accompanied by bronchiolitis. The virus induces an inflammatory infiltrate in the lungs, which was characterised by bronchoalveolar lavage. The infiltrate consists mainly of macrophages (peaking at day 3), monocytes and $CD8^+$ T cells (peaking at day 7) (Nash *et al.*, 2001; Sarawar *et al.*, 2002). Acute infection in the lung resolves after 7-10 days, primarily due to the action of $CD8^+$ T cells (Ehtisham *et al.*, 1993). MHV-68 cannot be detected by plaque assay after 10 days although inflammation resolves later in the second week of infection and foci of mononuclear cells can still be detected up to 30 days post-infection (Sunil-Chandra *et al.*, 1992).

MHV-68 is trafficked to the mediastinal lymph node (MLN) from the lung where lymphoadenopathy occurs due a transient expansion of B cells driven by $CD4^+$ T cells (Usherwood *et al.*, 1996a). Virus trafficking to the MLN is likely to be mediated by DCs. Virus can be detected in $CD11c^+$ DCs regardless of the presence or absence of B cells. In the absence of B cells, virus still reaches the MLN and infects macrophages and DCs but fails to spread to other lymphoid compartments.

This suggests B cells are primarily infected in the MLN and are the principal cell type required for trafficking of the virus to other organs (Nash *et al.*, 2001).

From the MLN, virus traffics to the spleen where a latent infection is established within germinal centre B cells, macrophages and DCs (Flano *et al.*, 2000). Acute-phase latency is associated with splenomegaly which peaks during the second week of infection due to rapid proliferation of B cells and T cells (Usherwood *et al.*, 1996b). The elevated numbers of latently infected cells are located in enlarged and more numerous germinal centres. Splenomegaly and thus the number of latently infected cells is controlled by $CD4^+$ T cells as mice in which $CD4^+$ T cells are depleted do not develop splenomegaly and have reduced levels of latent virus (Usherwood *et al.*, 1996a). Surprisingly, the virus can still establish a latent infection even in the absence of $CD4^+$ T cell-driven B cell expansion. The number of long-term latently infected cells remains constant whether $CD4^+$ T cells are present in the host or not (Nash *et al.*, 2001).

A peripheral mononucleosis, resembling IM caused by EBV, occurs during MHV-68 infection, peaking at around 35 days post-infection. It is characterised by a skewed expansion of circulating $CD8^+$ T cells expressing the Vβ4 T cell receptor (Tripp *et al.*, 1997). It is thought that this phenomenon is MHC-independent and the $V\beta4^+$ $CD8^+$ T cells are recognising an as yet uncharacterised viral ligand. These cells persist long-term, probably due to continued ligand expression (Flano *et al.*, 2004).

Following the transient peak of latent infection, the numbers of latently infected cells fall to levels around the limit of infection (Sunil-Chandra *et al.*, 1992). Long term latency is maintained mainly in germinal centre and memory B cells. Willer and Speck showed that latency was largely found within the surface IgD^- subset of splenic B cells, which resemble memory B cells, at 6 months post-infection (Willer and Speck 2003). Furthermore, maintenance of latency is dependent on the development of memory B cells as latency was lost in $CD40^-$ B cells. CD40 is

required for the survival of memory B cells (Kim *et al.*, 2003). Latent virus can also be detected in macrophages and DCs (Flano *et al.*, 2000). The maintenance of latency in non-B cells is confirmed in the spleens of μMT (B cell deficient) mice where persistent virus could be detected 6 weeks post-infection (Weck *et al.*, 1996).

Viral persistence also occurs in sites other than the spleen. Virus genomes were detectable in bone marrow, nasopharyngeal-associated lymphoreticular tissue, lung and spleen at 3 months post-infection although the higher viral frequencies in the lung and spleen indicated these as major reservoirs for long-term latency of MHV-68 (Flano *et al.*, 2003). MHV-68 was shown to persist in the lungs of wt and μMT mice. Latent virus was determined by in situ hybridisation for the vtRNAs (as markers of latent infection) within lung sections of both μMT and wt mice suggesting that persistence was occurring independently of B cells. Further investigation determined that latency was occurring in epithelial cells (Stewart *et al.*, 1998). In contrast Flano *et al.* (2003), showed that B cells, macrophages, DCs and "null" (predominantly stromal and epithelial) cells in the lung were MHV-68 genome-positive at 14 days post-infection (after clearance of lytic virus). However, by 3 months post-infection B cells were the only substantial population of latently infected cells. This discrepancy may due to the techniques employed and remains to be resolved.

1.6.5. Immune response to MHV-68

1.6.5.1. Natural Killer cells

Little is known about the impact of NK cells during gammaherpesvirus infections. A paper published during this study suggested that control of MHV-68 infection is independent of NK cells. A lack of NK cells did not have any effect on the control of acute or latent infection, nor did it appear to affect $CD8^+$ T cell responses (Usherwood *et al.*, 2005). In support of these findings, perforin-deficient mice were able to control MHV-68 infection with similar kinetics to wt mice even though NK

cell cytotoxic activity was shown to be impaired (Kagi *et al.*, 1994; Usherwood *et al.*, 1997).

1.6.5.2. Type I IFN

The type I IFN system is crucial in controlling the initial stages of MHV-68 infection. Whilst wt mice are resistant to MHV-68 infection, infection of IFNα/β $R^{-/-}$ mice (mice with a targeted disruption of the type I IFN receptor) led to higher viral titres, systemic dissemination and 80-90% mortality. Mice deficient in STAT1 have a 100% mortality rate by day 21 post-infection whereas 50% of IFNα/β $R^{-/-}$ mice survive beyond this point. This suggests that STAT1-dependent pathways can protect IFNα/β $R^{-/-}$ mice during the second week of infection (Barton *et al.*, 2005). The number of latently infected cells was increased 10-fold in IFNα/β $R^{-/-}$ compared to wt spleens during acute-phase latency and this difference was resolved by 3 weeks post-infection (Dutia *et al.*, 1999). Type I IFN is also suggested to play a role in inhibiting viral reactivation during latency as latent virus from IFNα/β $R^{-/-}$ splenocytes reactivated with 5-fold increased efficiency compared to wt splenocytes (Barton *et al.*, 2005).

1.6.5.3. Cytokines and Chemokines

The cytokines and chemokines induced following viral infection are important for limiting spread and influencing other arms of the immune response. Cells from the spleen, MLN and cervical lymph node produce high levels of IL-6 and IFNγ and lower levels of IL-2 and IL-10 following MHV-68 infection. Cytokines were induced from day 3 but peaked around day 10 post-infection, correlating with the clearance of virus from the lung (Sarawar *et al.*, 1996). Little or no IL-4 or IL-5 (Th2 cytokines) was detected, possibly due to high IFNγ levels skewing cellular responses towards a Th1 environment or lack of IL-4 inducing a Th2 response. It is thought that IL-6 and IL-10 may have a role in maintenance of persistent gammaherpesvirus infections (Sarawar *et al.*, 1996). IL-6-does not appear to play a significant role *in vivo* as there

was no effect on lytic MHV-68 infection, nor the establishment or maintenance of latent infection in IL-6 deficient mice (Sarawar *et al.*, 1998). A recent study has shown that viral persistence results in significant upregulation of IL-10 production from antigen presenting cells (primarily DCs but also B cells) resulting in diminished T cell effector responses (Brooks *et al.*, 2006). IL-12 production from macrophages and DCs is important for the development and activation of $CD8^+$ T cells and NK cells. MHV-68 infection of IL-12p40 $^{-/-}$ mice led to lower IFNγ levels suggesting that IFNγ production is partly dependent on the presence of IL-12 (Elsawa and Bost 2004). Chemokine levels peak around day 7 post-infection and are important for the infiltration of T cells and monocytes. For example, the chemokine IP-10 and its receptor CXCR3 are upregulated during MHV-68 infection. Mice deficient in CXCR3 have delayed virus clearance from the lung accompanied by delayed T cell recruitment (Lee *et al.*, 2005). The importance of the chemokine family is highlighted by the immune evasion mechanisms employed by MHV-68 to evade them. MHV-68 encodes a chemokine-binding protein (M3; discussed further in section 1.6.7.) as well as a CXCR2 chemokine receptor homologue (Virgin *et al.*, 1997).

1.6.5.4. B cells

B cells are important for the establishment of MHV-68 latency. General IgG2a and IgG2b levels rise quickly following infection, to far higher levels than virus-specific antibody production, and remaining high for at least 70 days post-infection (Sangster *et al.*, 2000). Virus-specific IgG remains low for the first 2 weeks of infection then increases progressively over at least 70 days (Stevenson and Doherty 1998). However, no significant difference in virus titres in the lung was observed in μMT compared to wt mice, suggesting little role for virus-specific antibody during acute infection (Usherwood *et al.*, 1996b).

1.6.5.5. $CD8^+$ T cells

The importance of $CD8^+$ T cells during MHV-68 infection has been demonstrated in mice depleted of $CD8^+$ T cells. A lack of $CD8^+$ T cell responses led to greatly elevated infectious virus titres in the lung and spleen and eventual death (Ehtisham *et al.*, 1993). $CD8^+$ T cells are critical for clearance of virus from the lung. They have also been shown to regulate the number of latently infected cells in the spleen. This may be due to the actions of granzymes A and B which have been shown to be important for control of acute phase latency although there is functional redundancy between the two (Loh *et al.*, 2004). Perforin/granzyme exocytosis is a major mechanism of cytotoxic T cell killing. The function and activation of $CD8^+$ T cells during MHV-68 infection is not dependent on the co-stimulatory molecule CD28 (binds B7.1 [CD80] and B7.2 [CD86] on the surface of antigen presenting cells leading to further activation events), as CD28-deficient mice could clear virus from the lung with similar kinetics to wt mice and there was no significant difference in cytotoxic T cell activity between CD28-deficient and wt mice (Lee *et al.*, 2002). MHV-68 encodes a $CD8^+$ T cell evasion protein, K3. K3 ubiquitinates MHC class I heavy chains in the ER, therefore targeting them for proteasome-dependent degradation. A K3 mutant virus was attenuated in the establishment of latency in the spleen and was accompanied by an increased frequency of virus-specific $CD8^+$ T cells. Depletion of $CD8^+$ T cells reversed the attenuation observed in the spleen thus illustrating the importance of $CD8^+$ T cell control of MHV-68 infection (Stevenson *et al.*, 2002).

1.6.5.6. $CD4^+$ T cells and IFNγ

$CD4^+$ T cells do not play a major role in controlling MHV-68 infection in the lung but are required for the development of splenomegaly and are responsible for aiding the maturation and proliferation of B cells that lead to development of the antibody response (Sangster *et al.*, 2000). IFNγ is required for $CD4^+$ T cell-mediated control of MHV-68 as demonstrated via depleting antibodies or in IFNγ-deficient mice (Sparks-Thissen *et al.*, 2005). Short-term depletion of the $CD4^+$ T cell subset made little

difference to virus titres in the lung (Ehtisham *et al.*, 1993). However, mice lacking functional $CD4^+$ T cells fail to control MHV-68 infection in the long term. Infection of MHC class II-deficient mice led to increasing levels of latently infected splenocytes and resulted in death by approximately day 120 post-infection (Cardin *et al.*, 1996).

IFNγ alone is not sufficient to fully control MHV-68 infection even though it is produced to high levels in infected tissues. There was little difference in lung virus titres, cytotoxic T cell activity or cytokine environments between mice lacking functional IFNγ and wt mice, thus indicating a non-essential role for IFNγ in the control of acute infection (Dutia *et al.*, 1997; Sarawar *et al.*, 1997). However, IFNγ does aid control of chronic MHV-68 infection as a lack of IFNγ leads to increased reactivation from latency, increased persistent replication and severe vascular arteritis (Steed *et al.*, 2006). There is an increase of latently infected cells in IFNγ $R^{-/-}$ mice at 14-17 days post-infection as well as an infiltration of granulocytes during the second week of infection. Fibrosis of the spleen develops accompanied by a loss of B- and T-cells. It is thought that the splenic changes are mediated by $CD8^+$ T cells and, to a certain extent, $CD4^+$ T cells as depletion of each subset reversed the changes (Dutia *et al.*, 1997).

1.6.6. The immune response to EBV and KSHV

EBV-positive immunocompromised individuals can develop uncontrolled virus-driven proliferation of B cells leading to a range of malignancies such as B-cell lymphoproliferative disease. The EBV-disease associations for immunocompromised individuals highlight the importance of the immune system in controlling EBV infection. NK cell upregulation and activation has been shown to occur during EBV infection and EBV-infected cells that enter the lytic cycle become susceptible to NK cell killing (Pappworth *et al.*, 2007; Williams *et al.*, 2005). During IM, the NK cell population is elevated at the time of diagnosis. This expansion lasted at least one month post-diagnosis and the NK cells exhibited enhanced levels of cytotoxicity.

The elevated NK cell numbers correlated with significantly lower EBV titres in the peripheral blood (Williams *et al.*, 2005).

An antibody response results in high IgM and developing IgG responses to lytic and late antigens. Antibody responses to the gp350 antigen (on the viral envelope) prevent binding to CD21 and therefore limit EBV spread (Crawford 2001). $CD8^+$ T cells are critical for the control of acute infection with the majority of cells during lymphocytosis being activated $CD8^+$ T cells. During IM, $CD8^+$ T cell responses are predominantly towards lytic viral antigens and certain individuals may have up to 44% of their $CD8^+$ T cells specific for one epitope from a lytic cycle protein (Callan *et al.*, 1998). $CD8^+$ T cells specific for lytic (predominantly) and latent epitopes remain detectable during persistent infection, comprising 0.1-1% of peripheral $CD8^+$ T cells (Tan *et al.*, 1999). $CD4^+$ T cells do not become expanded to the same extent as the $CD8^+$ T cells. A study showed only 1.4% of $CD4^+$ T cells were EBV-specific during IM and this fell to 0.22% during persistent infection (Amyes *et al.*, 2003). Less is known of the immune responses to KSHV. However, there has been a great deal of investigation of the immune evasion genes encoded by the virus. 22/86 KSHV genes have putative immunoregulatory function. For example, K3 and K5 increase endocytosis of MHC class I molecules from the cell surface for degradation in the lysosome (Coscoy and Ganem 2000) and thus lower viral antigen presentation to $CD8^+$ T cells. K5 also lowers surface expression of CD86 and thus reduces binding to the co-stimulatory molecule CD28 on T cells. The result of this is reduced T cell activation by the infected, antigen presenting B cells (Rezaee *et al.*, 2006). KSHV has developed a number of other immune evasion genes. Three chemokine homologues are encoded by K6, K4 and K4.1 and are called vCCL-1, -2 and -3 respectively. They preferentially induce a Th2 skewed response through binding of the chemokine receptors CCR4 and CCR8 and thus reducing the efficiency of the antiviral response (Rezaee *et al.*, 2006). KSHV modulates apoptosis to facilitate persistent infection and survival of lytically infected cells to aid viral replication. For example, vFLIP inhibits Fas-mediated apoptosis by preventing activation of caspases

3, 8 and 9 (Djerbi *et al.*, 1999). Genes involved in innate immune evasion are discussed in more detail in section 1.5.

1.6.7. MHV-76 and the role of the left-end of MHV-68

MHV-76 and MHV-68 were isolated at the same time; MHV-68 from the bank vole (*Clethrionomys glareolus*) and MHV-76 from the yellow-necked mouse (*Apodemus flavicollis*) (Blaskovic *et al.*, 1980). The MHV-76 genome is identical to that of MHV-68 except for a deletion of 9538 bp at the left end of the unique region resulting in a lack of the genes M1, M2, M3 and M4 and all the vtRNAs. It is thought that MHV-76 is a deletion mutant of MHV-68, derived either through *in vitro* passage or in nature (Macrae *et al.*, 2001). MHV-76 replication *in vitro* occurs with identical kinetics to MHV-68. However, MHV-76 is attenuated *in vivo* as it is cleared more rapidly from the lungs of BALB/c mice during acute infection. This is accompanied by a greater inflammatory response. A lower number of latently infected cells in the spleen and a significantly reduced degree of splenomegaly were also observed in comparison to MHV-68 infection. Nonetheless, MHV-76 can still establish a long-term latent infection (Macrae *et al.*, 2001). This study suggests that the left end of the MHV-68 genome contains components important for viral pathogenesis, possibly via the evasion of the host immune system.

The genes M1-M4 and the vtRNAs are present at the left end of MHV-68 and are unique to the virus. The M1 gene exhibits sequence homology to poxvirus serine protease inhibitors (serpins) and the M3 gene of MHV-68. However, deletion of M1 does not appear to affect acute infection of the lung or establishment of latency in the spleen although it is suggested to suppress viral reactivation (Clambey *et al.*, 2000; Simas *et al.*, 1998).

M3 is an abundant protein, detectable during productive and latent infection (Simas *et al.*, 1999). It is a secreted, broad spectrum chemokine binding protein, binding all chemokine classes, CC, CXC, C and CX3C but with no homology to known

chemokine receptors, binding proteins or chemokines (Parry *et al.*, 2000; Van Berkel *et al.*, 2000). This suggests a role as a novel immune evasion gene. Infection with an M3-deletion virus did not affect the course of infection in either the lung or spleen. However, the study did suggest that M3 is important during acute infection of the CNS. The titre of an M3-deficient virus was 10-fold lower than wt MHV-68 after intracerebral inoculation (Van Berkel *et al.*, 2002). Chemokines are induced in the CNS following MHV-68 infection suggesting that M3 may block chemokine-mediated functions in a tissue-specific manner. It has been suggested that M3 may be involved in reducing the inflammatory infiltrate and thus decreasing morbidity and mortality in response to MHV-68 infection (Townsley 2004). It is possible that M3 plays a more important role in the natural host for MHV-68, the wood mouse (Blasdell *et al.*, 2003).

M4 is expressed as an I-E transcript and is detectable during lytic replication in the lung and acute-phase latency in the spleen. When M4 was inserted into MHV-76 (MHV76inM4), it led to higher viral titres compared to MHV-76 at early time points post-infection (Townsley *et al.*, 2004). These findings suggest a possible immunoregulatory role for M4 during the innate immune response. M4 has also been shown to be important for the establishment of latency. Studies using a M4-disrupted virus showed that there was a rapid decline in the numbers of latently infected splenocytes from day 10 onwards, resulting in 100-fold less latent virus compared to wt spleens by day 14 post-infection (Geere *et al.*, 2006).

M2 is a latency-associated transcript, expressed only in B cells in the spleen, with no discernible homology to other viral or cellular proteins (Husain *et al.*, 1999; Macrae *et al.*, 2003). It contains an epitope recognised by $CD8^+$ T cells so provides a target for the cytotoxic T cell response to control latent infection (Husain *et al.*, 1999). Studies with a M2-deletion virus have suggested a role for M2 in the reactivation from latency in splenic B cells and/or establishment acute-phase latency (Herskowitz *et al.*, 2005; Macrae *et al.*, 2003). *In vitro* studies have suggested that the M2 protein

may have a type I IFN evasion function. ISG15 expression was upregulated in the presence of IFNα but not in the presence of IFNα and M2 (Liang *et al.*, 2004). M2 expression was upregulated in IFNα/β $R^{-/-}$ splenocytes, suggesting its regulation by type I IFN during latent infection *in vivo* (Barton *et al.*, 2005). It has recently been discovered that M2 can interact with Vav1 and Vav2 (Madureira *et al.*, 2005). Vav proteins promote GDP/GTP exchange on Rho/Rac proteins, facilitating rapid transition of those GTPases from their inactive (GDP-bound) to active (GTP-bound) states during signal transduction. Activation of Rho/Rac proteins leads to cytoskeletal change, mitogenesis, and cell survival. These findings suggest a role for M2 in B cell proliferation and survival during latent infection via signal transduction through Vav1 and Vav2 (Rodrigues *et al.*, 2006). The 8 vtRNAs have been found to be expressed during lytic and latent infection and can be detected in long-term latency in the spleen but their function remains to be determined (Bowden *et al.*, 1997). Similarly, the nine predicted microRNAs of the left-end region of MHV-68 remain to be characterised.

1.7. Project outline

The role of the innate immune response in the control of gammaherpesvirus infections has not been extensively characterised. The aim of this study was to investigate the role of three innate immune components during MHV-68 infection. Firstly, virus growth in various IFN knockout cell lines and type I IFN induction was investigated during *in vitro* infection. The role of IFNβ was further studied *in vivo* by means of an IFNβ$^{-/-}$ mouse model. The second aim was to investigate the role of ISG12a following MHV-68 infection. Finally, the role of NK cells was investigated by *in vivo* depletion of NK cells and by monitoring NK activation and cytotoxic activity following infection.

Chapter 2: Materials and Methods

2. Materials & Methods

2.1. Cell Culture

2.1.1. Harvesting and Counting of Cells

Cells were maintained at 37°C (5% CO_2) and were allowed to reach approximately 70% confluence before sub-culture. Firstly, growth medium was removed and the cell monolayer washed with 0.02% (w/v) versene. Adherent cells were removed from the culture flasks by the addition of 0.25% (w/v) trypsin (Invitrogen, UK) followed by mild shaking. Trypsinisation was stopped by the addition of an equal volume of fresh growth medium. Cells were centrifuged at 450 x g for 5 minutes and the pellet resuspended in 10 mls of fresh growth medium. A 40 µl aliquot of cells were added to 0.1% (w/v) trypan blue in a 1:1 dilution for counting. The viable cell count was determined using the following calculation:

cells/ml = unstained cell count x dilution factor x 10^{-4} cm^3

Sterile plastic cell culture T175 flasks (Nunc) were seeded with an appropriate number of cells in 40 mls of fresh growth medium.

2.1.2. Growth Media

Glasgow's Modified Eagles medium (GMEM) – supplemented with 10% (v/v) tryptose phosphate broth (Invitrogen, UK), 10% new born calf serum (Invitrogen, UK), 2 mM L-glutamine (Merck, BDH), 100 U/ml penicillin (Merck, BDH) and 100 U/ml streptomycin (Merck, BDH).

Roxwell Park Memorial Institute (RPMI) medium - supplemented with 10% foetal calf serum, 2 mM L-glutamine, 100 U penicillin, 100 U/ml streptomycin, 50 μM 2-mercaptoethanol and 25 mM HEPES.

Dulbecco's Modified Eagles Medium (DMEM) – supplemented with 10% foetal calf serum (Invitrogen, UK), 2 mM L-glutamine, 100 U/ml penicillin and 100 U/ml streptomycin.

2.1.3. Cell lines Used

Baby Hamster Kidney fibroblast cells (BHK-21) are an immortal fibroblastoid cell line, originally derived from kidneys of one day old hamsters and were grown in Glasgow's medium (Macpherson and Stoker 1962).

Yac-1 cells are murine T-lymphocyte leukaemia cell line originally derived from inoculation of murine Moloney leukaemia virus into newborn A/Sn mice (Kiessling *et al.*, 1975). These cells were grown in suspension in RPMI medium.

L929 cells are a fibroblastoid cell line from subcutaneous areolar and adipose tissue of a 100 day old C3H/ An mouse. These cells were grown in DMEM.

2.2. Virus stocks

MHV-68, clone g.4, was grown in BHK-21 cells. BHK-21 cells were harvested and counted as previously described. Cells were infected at MOI of 0.001 and incubated at 37°C with shaking for 1.5 hours to enhance infection. Cells were subsequently transferred to T175 flasks and incubated for 5-6 days until they reached 100% cytopathic effect. Once this stage was reached, cells were removed from the flask with a cell scraper (Nunc) and centrifuged 2000 x g for 20 minutes. The cell pellet

was resuspended in a minimal volume of chilled, sterile PBS before homogenisation with approximately 30 strokes of a chilled Dounce homogeniser. The homogenate was transferred to a glass universal tube and sonicated in a sonicating ice bath for 15 minutes. The homogenate was centrifuged at 2000 x g for 20 minutes at 4°C. The supernatant obtained following centrifugation was placed in a fresh universal tube and kept on ice. The pellet was resuspended in 1 ml of sterile PBS, re-homogenised and centrifuged at 2000 x g for 20 minutes at 4°C. The supernatants were pooled, aliquoted and stored at -70°C. Virus titre was determined using a similar procedure to the infectious virus assay (as described below), except a 20 µl aliquot was added to 180 µl of Glasgow's growth medium to create the initial 1:10 dilution. 100µl of 1:10 dilution was added to 900 µl growth medium to create a 1:100 dilution. A ten-fold dilution series was then created by addition of 440 µl of the previous dilution into 4 mls growth medium.

2.3. Mice

2.3.1. Mouse Stocks

Wild-type C57BL/6 mice were bought from Harlan UK Ltd. IFNβ knockout (ko) mice on a C57BL/6 background were obtained from A. C. G. Porter, Imperial College School of Medicine, London (Deonarain et al., 2000). np27 ko mice were also obtained from A. C. G Porter. wt 129/Sv/Ev and wt 129/ola mice were obtained from departmental stocks. Mice were housed under specific pathogen-free conditions in HEPA filtered cages treated under the authority of a UK Home Office Animal License.

2.3.2. Animal Infections

Mice were infected intranasally (i.n.) with $4x10^3$ or $4x10^5$ pfu of virus (in 40 µl of sterile PBS) at 4-6 weeks of age. Mice were anaesthetised with halothane and

euthanized via CO_2 asphyxiation. At specific times post infection, various organs were harvested for further analysis.

2.4. Genotyping

2.4.1. IFNβ$^{-/-}$ mice

Stocks of IFNβ$^{-/-}$ mice were backcrossed with wt 129/Sv/Ev mice in order to obtain appropriately matched control mice. Offspring were genotyped by PCR amplification of the transgenic region to establish if (1) the green fluorescent protein (GFP) gene was present and (2) the IFNβ gene was absent. DNA was extracted from ear clip samples by incubation in 50 µl 25 mM NaOH, 0.2 mM EDTA (pH12) at 95°C for 25 minutes with periodic vortexing to break up the tissue. The reaction was neutralised by the addition of 50 µl of 40 mM Tris-HCl (pH5). 2 µl of DNA solution was used in subsequent PCR reactions. Extracted DNA was stored at -20°C.

2.4.2. np27$^{-/-}$ mice

DNA was extracted from ear clip samples as described for IFNβ$^{-/-}$ mice. 2 µl of extracted DNA was used for PCR analysis using a GC-RICH PCR System Kit (Roche).

2.5. Generation of MEFS

Mouse embryonic fibroblasts (MEFs) were isolated from IFNβ$^{-/-}$ and np27$^{-/-}$ embryos at 13.5 days gestation. Neural and haematopoietic areas were removed and embryonic tissue was minced and digested in two trypsination steps at 37°C for 10 minutes. After washing, MEFs were maintained in supplemented DMEM. IFN type I receptor $^{-/-}$ and wild type MEFs were obtained from B. M. Dutia's stocks.

2.6. *In vitro* Assays

2.6.1. Infectious virus assay

In order to determine the virus titre within samples, tissues were homogenised in 1.8 mls of Glasgow's medium and subjected to one freeze-thaw cycle in order to disrupt cellular membranes. Upon thawing, homogenates were centrifuged (1300 x g, 5 minutes, 4°C) to get rid of any particulate matter. 440 µl supernatant was added to 3.96 ml of fresh Glasgow's medium to create a 1:10 dilution. A ten-fold dilution series was created to which $2x10^6$ BHK-21 cells were added and shaken for 1 hour (250 rpm, 37°C). 2mls of each dilution was added in duplicate to a 60 mm Petri dish (Nunc) along with 3 mls of Glasgow's medium. As a negative control, BHK-21 cells were plated without the addition of supernatant. The plates were incubated for four days at 37°C, 5% CO_2. Cell monolayers were fixed with 4% neutral buffered formalin and stained with 0.1% toluidine blue. Plaques were counted and the titre determined by:

Viral titre (pfu/ml) = (average plaque count x dilution) / 2

2.6.2. Infective centre assay (*ex vivo* reactivation assay)

Determination of the *ex vivo* reactivation frequency from latently infected splenocytes was carried out using the infective centre assay. Briefly, spleen cells were teased out of the capsule with a scalpel blade into complete RPMI. The suspension was transferred to a universal pre-rinsed with RPMI and was centrifuged at 450 x g for 5 minutes. The supernatant was removed and the pellet was resuspended in the remaining liquid. Erythrocytes were lysed with the addition of 1ml sterile distilled water and osmolarity was corrected by the addition of 9mls of sterile PBS. Excess cell debris was discarded and the remaining liquid was transferred to a new pre-rinsed universal. The sample was then centrifuged at 450 x g for 5 minutes. The supernatant was discarded and the pellet resuspended in 5mls RPMI. Viable splenocytes were counted using trypan blue. Ten-fold dilutions of cells were added to 1 x 10^6 BHK cells (in 5mls RPMI medium) in duplicate 60mm petri

dishes and incubated at 37°C (5% CO_2) for 5 days. Cell monolayers were fixed and stained as described for the infectious virus assay.

The quantity of pre-formed infectious virus present in samples was determined by subjecting splenocytes to one freeze-thaw cycle before titration according to the infectious virus assay.

2.6.3. One step growth curve

A one step growth curve was carried out to compare the growth of MHV-68 *in vitro* in IFNβ$^{-/-}$, IFN type I receptor$^{-/-}$, np27$^{-/-}$ and wild type MEFs. MEFs were infected in suspension at an MOI of 5 for 1 hour at 37°C. Cells were pelleted by centrifugation at 450 x g for 5 minutes and resuspended in 40mls of fresh DMEM three times to remove unbound virus. 5 x 10^4 MEFs were seeded into each well of a 24 well plate and at specific times post-infection, cell supernatants were removed and stored separately, and fresh media added to the monolayer. Cells and supernatants were harvested and subjected to three freeze-thaw cycles. Infectious virus was titrated on BHK cells according to the infectious virus assay. All infections were carried out in duplicate with each well titrated in duplicate.

2.6.4. Expression of GFP in IFNβ$^{-/-}$ MEFs

2 x 10^6 IFNβ$^{-/-}$ MEFs were added to each well of a 6-well plate in 2 mls of DMEM. Cells were allowed to settle into a monolayer for 1-2 hours before being infected with MHV-68 at MOI of 5 pfu/cell. Cells were incubated at 37°C, 5% CO_2. Wells were investigated for the presence of GFP by examination under an inverted fluorescence microscope at various intervals from 3 to 48 hours post-infection.

2.6.5. Expression of eGFP in np27$^{-/-}$ MEFs

1 x 10^6 np27$^{-/-}$ MEFs were added to each well in 6-well plates in 2 mls of DMEM. Cells were allowed to settle into a monolayer for 1-2 hours before being treated as detailed below:

Untreated

MHV-68 infected – MOI of 5 and 0.5

MHV-76 infected – MOI of 0.5

SFV (A774) infected – MOI of 0.5

Poly inosinic: poly cytidylic acid (poly I:C) treated – 100 μg/ml

IFNα in DMEM – either 200 or 1000 U

Cells were incubated at 37°C, 5% CO_2. Wells were investigated for the presence of eGFP by fluorescence microscopy at various intervals from 3 hours to 3 days post-treatment.

2.7. Cryostat sectioning

Rapid freezing: Lungs were dissected out and reinflated via the trachea with 50% water: 50% Tissue-Tek OCT (Sakura Finetek, USA). Tissues were frozen immediately on dry ice/isopentane. Samples were stored at –70°C until required.

Slow freezing: Lungs were dissected out and the tissues fixed for 3 hours in 4% paraformaldehyde (PFA) at room temperature (RT). PFA was removed and the lungs reinflated with 50% water: 50% Tissue-Tek OCT. Embedded tissues were kept in the dark for 24 hours at 4°C and then slowly frozen at –70°C in a box covered with cotton wool.

Tissue sections were cut at various thicknesses (6, 10, 15 and 25 μm) using a cryostat chilled to -30°C before being transferred onto polylysine coated slides. Slides were stored at –20°C until examination by fluorescence microscopy.

2.8. DNA Extraction

2.8.1. DNA extraction from lymphocytes

DNA was extracted from lymphocytes using a DNeasy Tissue Kit (QIAGEN, UK). Approximately 1 x 10^7 cultured splenocytes or MLN-derived lymphocytes were centrifuged for 5 minutes at 300 x g and the pellet resuspended in 200 μl PBS. 40 μl proteinase K and 400 μl buffer AL were added before incubation overnight at 56°C. Digestion was complete when no cell debris was visible in the sample. Following digestion, 400 μl of ethanol was added before transfer of the sample to a DNeasy mini spin column. The mixture was centrifuged at 6000 x g for 1 minute to bind the DNA to the DNeasy membrane. Bound DNA was washed with 500 μl each of buffers AW1 (6000 x g, 1 minute) and AW2 (20000 x g, 3 minutes) and subsequently eluted in 150 μl of buffer AE (6000 x g, 1 minute).

2.8.2. DNA extraction from tissues

DNA was extracted from tissue samples using a DNeasy Tissue Kit (QIAGEN Ltd., UK) according to manufacturer's instructions. The amount of starting material varied according to tissue type.

Whole lungs were homogenised in 2 mls lysis buffer (10 mM Tris-Cl [pH 8], 0.1M EDTA [pH 8], 0.5% [w/v] SDS). 20 μl of proteinase K was added before samples were incubated overnight at 56°C with occasional vortexing to help break up tissue. 200 μl aliquots were used in the DNeasy kit. Briefly, 200 μl buffer AL was added to the samples and incubated for 10 minutes at 70°C. 200 μl ethanol was added and

mixed thoroughly. The mixture was then applied to a DNeasy mini spin column where DNA binding, washing and elution was carried out using the same procedure as described for splenocytes. Extracted DNA was stored at -20°C.

2.8.3. Quantification of DNA

DNA concentration was determined by spectrophotometry (CE 2041, Cecil Instruments). Samples were diluted 1 in 10 or 1 in 100 in dH_2O. The spectrophotometer was zeroed against water alone before sample readings were taken at wavelengths of 260nm and 280nm. DNA concentration in unknown samples was calculated by the following calculation:

concentration (ng/µl) = OD_{260} x dilution factor x 50

The absorbance ratio at 260 and 280nm was used to estimate the purity of the DNA in samples.

2.9. Polymerase Chain Reaction (PCR)

2.9.1. Standard PCR

PCR amplifies a region of DNA between two oligonucleotide primers. During each reaction cycle primers and template were denatured at a temperature of 94°C before primers were allowed to anneal to the template sequence at a primer-pair specific temperature. Sequence extension occurred at 72°C for approximately one minute per kilobase of product length. The product synthesised in the first round can act as a template in subsequent rounds, doubling the product with each round of amplification. Standard PCR was carried out in a final volume of 50 µl in 0.5 ml PCR tubes (Thermohybaid). Each PCR mix contained the following reagents: 100-500 ng of sample DNA, 3 µl of 3 mM $MgCl_2$ (Invitrogen, UK), 5 µl of 10x PCR

buffer (20 mM Tris-HCl (pH8.4), 50 mM KCl, Invitrogen, UK), 50 pmol of each primer (MWG Biotech, Germany), 100 μM of each of the deoxynucleotide triphosphate bases (dNTPs [dATP, dCTP, dGTP and dTTP], Roche, UK) and 2 U of Taq recombinant DNA polymerase (Invitrogen, UK). Typically master mix per reaction was made up as follows.

10x buffer 5 μl

$MgCl_2$ 3 μl

dNTP 1 μl

primer 1 μl each

Taq 1 μl of a 1 in 3 dilution of stock

ddH_2O 37 μl

DNA 2 μl

The volume was adjusted to 50 μl with water (RNase, DNase-free, Fluka, UK) in each case. Reactions were overlaid with mineral oil (Sigma, UK). All reactions were carried out in an Omnigene thermal cycler (Hybaid) using a hot start protocol. Tubes were heated to 95°C for 3 minutes and held at 80°C prior to the addition of Taq in order to ensure high specificity amplification of the product. Negative control reactions lacking template DNA were included in each run. Cycling conditions and primers used are listed in table 2.1.

2.9.2. Agarose Gel Electrophoresis

PCR products were electrophoresed on 0.5–2% (w/v) agarose (SeaKem, Flowgen, UK) in TAE containing ethidium bromide (Sigma, UK). 3 μl of loading buffer (0.25% [w/v] orange G, 15% [w/v] ficoll, Sigma, UK) was added to 10 μl of each PCR sample before loading into the gel. 1 kb plus ladder (Invitrogen, UK) was

included in each run to provide known molecular weight standards, allowing estimation of DNA fragment size. Electrophoresis was performed at 70-90 V in horizontal gel tanks containing TAE. Gels were viewed using a UV transilluminator.

2.9.3. Isolation of DNA fragments from Agarose

DNA fragments of interest were isolated from agarose using a QIAquick gel extraction kit (QIAGEN, UK). Viewed under long-wave UV light, the correct sized band of DNA was cut out using a sterile scalpel blade in as small a volume of agarose as possible. The excised band was weighed and, assuming that 1 mg of gel was equal to 1 µl, added to three volumes of QG buffer. The mixture was incubated at 50°C for 10 minutes until the gel was completely dissolved. One volume of isopropanol was added before the mixture was transferred to a QIAquick column and centrifuged (1 minute, 20000 x g) to bind the DNA to the column membrane. Two washing steps were performed with 500 µl of buffer QG and 750 µl of buffer PE. To elute the DNA, 50 µl of buffer EB (10 mM Tris-Cl [pH8.5]) was applied to the membrane and incubated for 1 minute at RT before centrifugation at 20000 x g for 1 minute. Eluted DNA was stored at -20°C.

2.10. RNA Extraction and Manipulation

2.10.1. RNA Extraction using a RNeasy Mini Kit (QIAGEN, UK)

4 x 10^6 cultured cells were washed in PBS to remove medium and pelleted at 300 x g for 5 minutes. 350 µl of buffer RLT+β-mercaptoethanol was added and the sample loaded onto a QIAshredder spin column (QIAGEN, UK) in order to homogenise the cells. 350 µl of 70% ethanol was added to the lysate. The mixture was then added to a RNeasy mini column and centrifuged for 15 seconds at >10000 x g to bind total RNA to the column membrane. The column was then washed with 700 µl Buffer RW1 once (spun 15 seconds at >10000 x g), then washed twice with 500 µl of Buffer RPE (spun 15 seconds at >10000 x g then >10000 x g for 3 minutes). RNA was

eluted from the column by centrifugation (>10000 x g, 1 minute) with 40 µl of RNase-free water. RNA integrity was checked by gel electrophoresis and quantified via spectrophotometry (CE 2041, Cecil Instruments). RNA was stored at -80°C.

2.10.2. DNase treatment of RNA

Contaminating DNA was removed from RNA preparations by the addition of recombinant DNase I using DNA-free™ (Ambion, UK). 4 units of DNase I and 1 µl of 10X DNase I buffer (100 mM Tris-HCl, pH 7.5, 25 mM $MgCl_2$, 5 mM $CaCl_2$) were added to 10-15 µg RNA in a total volume of 13 µl. The mixture was incubated at 37°C for 30 minutes. 2 µl of DNase inactivation reagent (Ambion, UK) was added and the samples incubated for 2 minutes at RT. The inactivation reagent was pelleted by centrifugation to avoid carryover into downstream reactions. 2-5 µg of DNased-RNA was transferred into a fresh RNase-free tube for reverse transcription.

2.10.3. Reverse Transcription of RNA

cDNA was generated from RNA using Superscript™ II RNase H- Reverse Transcriptase (Invitrogen). 2-5 µg of DNased-RNA was incubated for 5 minutes at 65°C in the presence of 200 ng of random primers (Amersham Biosciences, UK) and 100 µM of dATP, dTTP, dGTP and dCTP (Roche, UK) in a total volume of 12 µl. The mixture was chilled on ice and incubated for 10 minutes at RT. 4 µl of 5X first strand buffer (250 mM Tris-HCl, pH 8.3, 375 mM KCl, 15 mM $MgCl_2$), 2 µl 0.1M dithiothreitol and 40 U of RNaseOUT™ (Invitrogen) were added, mixed gently and incubated for 5 minutes at room temperature followed by incubation at 42°C for 2 minutes. 200 U of Superscript™ II was added and the mixture was incubated at 42°C for 50 minutes. The reaction was inactivated by incubation at 70°C for 15 minutes. For reverse transcriptase-PCR, 2 µl of cDNA was used per PCR reaction in a PCR mix as previously described. cDNA synthesis reactions without addition of reverse transcriptase and PCR without the addition of template were included as control

reactions. PCR products were run on 1% (w/v) agarose gels and visualised by ethidium bromide staining.

2.11. Time course assay of IFN stimulation

Briefly, $4x10^6$ L929 cells were infected in suspension with either MHV-68 (MOI of 10), MHV-76 (MOI of 10), poly I:C (100 μg/ml), 100 μg cycloheximide (Sigma) or were left untreated. Cells were shaken for 1 hour (37°C) to allow virus to adsorb to the cells before being transferred to tissue culture flasks and incubated at 37°C (5% CO_2). Cells were harvested at various times post-infection. When the effect of cycloheximide treatment was investigated, cycloheximide was added to cells 30 minutes prior to the addition of virus. Mock-infected controls were included with the addition of sterile PBS in place of virus after cycloheximide treatment. Poly I:C was included as a positive control and was harvested at 5 hours post-infection. Monolayers were removed and pelleted in DMEM, followed by two washes in ice cold sterile PBS to remove any unadsorbed poly I:C or virus. RNA was extracted from cell pellets and cDNA prepared as described above. RT-PCR was carried out using primers specific for various groups of Type I IFNs. The cycling conditions are shown in table 2.1.

2.12. Real-time PCR Analysis

2.12.1. Real-time PCR

Real-time PCR analysis was used to quantify viral genome load following DNA extraction. Reactions contained 100 ng DNA. Levels of dsDNA product were determined using the intercalating dye, SYBR green (Biogene, UK). Reaction mix (total of 20 μl) was made up as follows:

10.75 µl ddH_2O

2 µl PCR Reaction Buffer (50 mM Tris-HCl, 10 mM KCl, 5 mM $(NH_4)_2SO_4$, 20 mM $MgCl_2$, pH8.8)

1 µl Primers (100 nM)

0.4 µl dNTPs (40 µM each of dATP, dTTP, dGTP, dCTP)

0.15 µl FastStart taq DNA polymerase (0.15 U) (Roche)

0.7 µl SYBR green

5 µl DNA

In all reactions, samples were initially denatured at 95°C for 10 minutes before 40 cycles of amplification were carried out. Cycling details are presented in table 2.1. A 10-fold serial dilution of a standard (either cloned template or a PCR amplified fragment of a gene) was amplified in parallel during each run to generate a standard curve. At the end of each PCR a melt curve analysis was performed during an increase of temperature from 65°C to 94°C in order to determine the specificity of the reaction. All runs were performed on a Rotorgene (Corbett Research, Australia) and each sample or standard was run in triplicate. Genome copy number was calculated from the cycle number at which the SYBR green signal crossed the threshold of the standard curve. In addition to quantifying the viral genome, levels of the housekeeping gene, β-actin, were quantified in order to normalise the levels of DNA present within individual samples. The ratio of the β-actin content in relation to the 75th percentile of β-actin levels of all samples was calculated, giving a measure of each sample's difference in relation to the 75th percentile. This ratio was then used to normalise the viral gene of interest. This method was used for normalisation as outliers do little to affect the 75th percentile value and therefore minimise the risk of results being skewed in a particular direction.

2.12.2. Generation of DNA standards for real-time PCR

β-actin

A DNA template was generated by taking the PCR product generated from outer primers (1F & 1R) and purifying it from agarose using a QIAquick gel extraction kit (QIAGEN, UK) as described previously. The purified product's copy number was quantified and 10-fold serial dilutions generated. Each dilution was used as a template for real-time PCR using inner primers (2F & 2R) for amplification. The copy number of the β-actin standard was calculated as shown below:

Concentration of DNA = absorbance at 260nm x dilution factor x 50

$= 0.016 \times 100 \times 50$

$= 80$ ng/μl

$= 80 \times 10^{-9}$ g/μl

Molecular weight of dsDNA β-actin fragment = no. base pairs x 660 Da

$= 400 \times 660$

$= 2.64 \times 10^{5}$ Da

1 mol $= 2.64 \times 10^{5}$g

$$\text{Copy number} = \frac{\text{Avogadro's constant x DNA concentration}}{\text{Molecular weight}}$$

$$= \frac{6.02 \times 10^{23} \times 80 \times 10^{-9}}{2.64 \times 10^{5}}$$

$= 1.82 \times 10^{11}$ copies/μl

Viral Gene Standards

M4 plasmid DNA (pCR2.1 Topo Cloning Kit, Invitrogen, plus a 1169bp insert from the M4 gene) was prepared using an Endofree Plasmid Maxi Kit (QIAGEN, UK). The resultant plasmid preparation was cut with *Eco RI* (New England Biolabs) and quantified as described above. M3 and RTA standards were obtained from Kerra Templeton.

2.12.3. Two Step PCR

At early time points in MLN tissue, viral load was low and thus close to or below the limit of detection. To resolve this problem a two step PCR protocol was performed. Briefly, 2µl of DNA was amplified in a standard PCR reaction with RTA (ORF50) primers for 12 cycles of 94°C for 30 seconds, 66°C for 30 seconds and 72°C for 1 minute. The resulting PCR product was diluted 1 in 10 in ddH_2O. 5 µl of diluted product was used for 40 rounds of real-time PCR using the same primers.

2.13. *In vivo* Cell Depletions

2.13.1. Isolation of immunoglobulin from mouse serum

Blood samples were obtained from non-infected mice and allowed to clot for 1-2 hours at RT. Samples were centrifuged for 5 minutes at 3000 x g before serum was aspirated off the blood clot. The volume of serum was measured and an equal volume of saturated ammonium sulphate was added drop-wise whilst undergoing continuous stirring for 30 minutes. The mixture was centrifuged for 10 minutes at 3000 x g. The pellet was resuspended in one volume of sterile PBS and added to dialysis tubing before subsequent dialysis against PBS for 4 hours at 4°C. Immunoglobulin was stored at -70°C.

2.13.2. Quantification of serum Ig

The concentration of immunoglobulin in the resultant solution was quantified using the BCA protein assay reagent kit (Pierce). Briefly, the presence of protein in the alkaline medium results in reduction of Cu^{2+} to Cu^{1+}. Cu^{1+} is detected by bicinchoninic acid (BCA) and results in a colourimetric change (green to purple) which exhibits a strong absorbance at 562 nm. Buffer WR was prepared using 50 parts of reagent A (Na_2CO_3, $NaHCO_3$, BCA and sodium tartrate in 0.1M NaOH) to 1 part reagent B (4% cupric sulphate). 25 µl of unknown sample was added to 200 µl buffer WR. The mixture was incubated at 37°C for 30 minutes before absorbance was measured. The absorbance value was compared to a standard curve prepared from a series of dilutions of known concentration (bovine serum albumin) in order to quantify the immunoglobulin concentration in the samples.

2.13.3. Biotinylation of monoclonal antibody

Immunoglobulin (clone PK136 (NK1.1)) was prepared by Dr B.M. Dutia and Y. Ligerwood by growing hybridoma cells in protein-free medium, then concentrating the medium. SDS PAGE analysis showed the concentrate was over 90% immunoglobulin. The immunoglobulin concentration was quantified using the BCA protein assay reagent kit (Pierce) as described above. PK136 was added to 0.1 M $NaHCO_3$ buffer (pH8.5) at a concentration of 1 mg/ml along with biotin (biotinamidocaproate N-hydroxysuccinimide ester, Sigma, UK) at 75 µg/ml. The solution was mixed on a rotating mixer for 5 hours at RT before the reaction was stopped with 500 µl of 5% (w/v) sodium azide. The mixture was dialysed overnight at 4°C against 0.9% PBS, 0.01% azide before dialysis against PBS/20% glycerol for 4 hours. During each dialysis the buffer was replaced with fresh solution at regular intervals. The biotinylated antibody was stored at 4°C until use.

2.13.4. *In vivo* depletion of NK cells

To deplete NK cells, C57Bl/6 mice were injected intraperitoneally with 200-500 μg of NK1.1 antibody (PK136 - unbiotinylated) in 200 μl of sterile PBS. Antibody doses were given on days -2, -1 and +2 relative to infection (day 0). When investigating the role of NK cells at later time points, for example, day 12 post infection (p.i.), an additional dose of PK136 was administered at day 9. Control mice were given comparable doses of control immunoglobulin isolated from non-infected mouse serum as described above. The efficiency of NK cell depletion was confirmed by FACS analysis of both depleted and non-depleted splenocytes.

2.14. Fluorescence Activated Cell Sorting Analysis

2.14.1. FACS analysis of NK cell Depletion

During dissection, whole MLNs or a portion of the spleen were reserved for FACS analysis in order to ensure the NK cell depletions were effective. Cells were teased out of the MLN or splenic capsule into FACS buffer (0.1% sodium azide, 1% bovine serum albumin in PBS) to create a single cell suspension. Erythrocytes were lysed by the addition of 1 ml sterile distilled H_2O followed by immediate addition of 9 mls PBS. Cells were washed twice by being spun at 300 x g for 5 minutes then resuspended in 2 mls FACS buffer. The pellet was resuspended before being counted using white blood cell (wbc) counting fluid (5% glacial acetic acid, 2% ethanol (v/v) in distilled H_2O plus 1-2 drops of 2% methylene blue). For each mouse analysed, approximately 5 x 10^6 lymphocytes were stained with the following antibodies 1. fluorescein-isothiocyanate (FITC) - labelled anti-CD3 + biotin labelled PK136 + phycoerythrin (PE) – labelled streptavidin (Pharmingen). 2. FITC – labelled anti-CD3 + biotin labelled CD49b + PE – labelled streptavidin. Additional controls were included for gating. These included unstained wbc and wbc stained with 1. PE-labelled CD19 alone and 2. FITC-labelled CD3 alone. Antibody suppliers are detailed in table 2.2. Staining was carried out in a series of 20 minute incubations for each antibody followed by two washing steps in FACS buffer and each incubation

was carried out in the dark at RT. Prior to FACS analysis, virally infected cells were fixed in 400µl FACS buffer + 2% formal saline. Non-virally infected samples were stored in FACS buffer alone. Flow cytometry was performed on a FACScan using CellQuest software (BD Biosciences). For each sample a minimum of 10000 events was counted. Further analysis was carried out on WinMDI software.

2.14.2. Intracellular IFNγ staining

MLNs were dissected from C57Bl/6 mice at day 2 and 4 p.i. and placed in 2 ml RPMI (without 2-mercaptoethanol) in the presence of 10 µg/ml Brefeldin A (BFA, Sigma, UK). Cells were teased out of MLNs and erythrocytes lysed by the addition of 1ml sterile distilled H_2O followed by immediate addition of 9 mls PBS. Lymphocytes were washed in staining wash buffer (SWB) (1x PBS, 2% FCS, 0.1% NaN_3) + BFA three times to ensure removal of media. $1x10^6$ cells were stained per sample. FcR receptors were blocked by incubation with an antiCD16/CD32 antibody (Pharmingen) for 15 minutes at 4°C before being washed once in SWB + BFA. NK cell surface marker antibody, FITC-labelled CD49b (Serotec), was added and incubated for 20 minutes at RT. Cells were washed in PBS + BFA before being fixed in 2% neutral buffered formalin then placed in permeabilisation buffer (SWB + 0.5% saponin). Cells were permeabilised for 10 minutes at RT before the addition of PE-labelled IFN-γ antibody (Pharmingen). Samples were incubated for 30 minutes on ice, washed in PBS and resuspended in SWB for analysis. For a positive control, 1 x 10^6 cells were incubated in RPMI+BFA with phorbol 12-myristate 13-acetate (PMA) (50 ng/ml) and ionomycin (500 ng/ml) (both Sigma, UK) for 4 hours at 37°C, 5% CO_2 before being stained as described above. An isotype control antibody was also included. Flow cytometry was performed on a FACScan using CellQuest software (BD Biosciences). For each sample a minimum of 50000 events was counted. Further analysis was carried out using WinMDI software.

2.15. Chromium Release Assay

2.15.1. Complement Depletion and preparation of effector cells

$CD4^+$ and $CD8^+$ T lymphocytes or NK cells were removed from a mixed lymphocyte population using a complement depletion method. Briefly, 4-8 MLNs were pooled and the lymphocytes pelleted by centrifugation at 450 x g for 5 minutes. During this spin, 500 µl of Low-Tox®-H rabbit complement (Cedarlane Labs) was added to 1500 µl of ice-cold RPMI and the mixture sterilised through a 0.2 µm sterilising filter. Appropriate antibodies were added to give a final antibody concentration of 100 µg/ml. These included an anti-CD4 and anti-CD8 or an anti-NK1.1 antibody as detailed in table 2.2. 1 ml of the complement/antibody mixture was used to resuspend the pelleted lymphocytes and incubated for 1 hour at 37°C on a shaker. After incubation the cells were washed 3 times in fresh RPMI to remove any unused complement then counted, pelleted and resuspended in RPMI for use in a cytotoxicity assay. To confirm that complement depletion was successful, an aliquot of 1 x 10^6 cells were removed for FACS analysis. A range of lymphocyte concentrations were prepared from the complement depleted suspension to correspond to various lymphocyte: target ratios in a total volume of 200 µl in the appropriate wells of a 96-well tissue culture plate.

2.15.2. Preparation of target cells:

Yac-1 is a mouse lymphoma cell line that is particularly susceptible to NK cell killing due to low expression of MHC class I molecules on the cell surface. This cell line was therefore chosen as target cells for cytotoxicity assays to measure NK cell killing. On the day of the assay Yac-1 cells were pelleted and counted and 5 x 10^5 were aliquoted into a 15 ml tube per sample. If T lymphocyte killing was included in the assay, Yac-1 cells were infected with MHV-68 (MOI of 5) overnight before use. The aliquoted cells were pelleted and resuspended in the smallest volume of medium possible prior to labelling. 50 µCi (1850 Bq) of the radioisotope ^{51}Cr (Amersham Biosciences) were added and the mixture incubated in a lead box at 37°C for 1 hour.

Cells were then washed in RPMI medium for 5 minutes at 300 x g to remove excess extracellular ^{51}Cr. This was repeated 3 times. 100 µl aliquots (1 x 10^4 cells) were added to the wells of a 96 well round-bottomed tissue culture plate containing the effector cells. To measure the spontaneous and maximum release of ^{51}Cr from target cells, 1 x 10^4 labelled cells were added to wells containing 100 µl of RPMI only or 100 µl of 5% Triton X-100 (in PBS) respectively.

Target and effector cells were incubated together for 4-8 hours at 37°C in 5% CO_2. Each sample was run in triplicate. Post-incubation, the plate was centrifuged at 300 x g for 5 minutes to pellet the cells at the bottom of each well. 100 µl of supernatant was removed and transferred to a tube to be counted in an automatic gamma-counter. The percentage of specific lysis was calculated using the following formula:

$$\text{Specific percentage lysis} = \frac{(\text{test } ^{51}Cr \text{ release} - \text{spontaneous } ^{51}Cr \text{ release})}{(\text{maximum } ^{51}Cr \text{ release} - \text{spontaneous release})} \times 100$$

2.16. Fluorescence-based Cytotoxicity Assay

2.16.1. Magnetic Cell Sorting (MACS)

A NK Cell Isolation Kit (Miltenyi Biotech) was used to separate NK cells from suspensions of MLN cells via an indirect magnetic labeling system. Non-NK cells such as T cells, B cells, dendritic cells, granulocytes, macrophages and red blood cells were removed from the suspension via a mixture of biotin-conjugated antibodies against CD4 (L3T4), CD8a (Ly-2), CD5 (Ly-1), CD19, Ly-6G (Gr-1) and Ter-119. NK cells were left untouched to avoid antibody cross-linking of cell surface proteins and thus non-specific activation of the cytotoxic response. Microbeads conjugated to anti-biotin monoclonal antibodies were added to allow non-NK cells to be retained on the MACS MS column while non-magnetically labeled NK cells were

washed through using 2 mls MACS buffer (PBS pH7.2, 0.5% bovine serum albumin, 2 mM EDTA).

Aliquots of pre-separation lymphocytes, the post-separation NK-cell enriched fraction and the post-separation non-NK cell fraction were labeled with an anti-NK cell antibody (DX5 conjugated to FITC, Serotec) to assess the purity of the NK cell enriched fraction by FACS analysis.

2.16.2. Cytotoxicity Assay

Preparation of effector lymphocytes: 4-8 female C57Bl/6 mice of 4-6 weeks of age were infected i.n. with 4 x 10^5 pfu MHV-68. Mice were sacrificed via CO_2 asphyxiation at day 2 or 3 p.i. MLNs were harvested and pooled together in order to get sufficient numbers to carry out the assay. A spleen was also harvested at the same time point to provide additional lymphocytes for control samples when required.

Splenic lymphocytes were separated from erythrocytes by Ficoll-Hypaque 1077 density gradient centrifugation (Sigma). Due to small cell numbers and the presence of an anti-erythrocyte antibody in the MACS kit, erythrocytes and lymphocytes from the MLN were left as a mixed population. NK cells were isolated from a mixed lymphocyte population by either complement depletion or MACS isolation as described above. NK cells were counted in trypan blue to ensure viability.

Effector NK cells were pelleted at 300 x g for 5 minutes at room temperature before being resuspended in 300 µl PBS. The green fluorescent dye, $DIOC_{18}$ (3,3'-dioctadecyloxacarbocyanine perchlorate) (Sigma, UK) was used to stain the membrane of the effector cells. 20 µl of $DIOC_{18}$ at 200 µg/ml in DMSO was added to the cell suspension and incubated in the dark at 37°C for 30 minutes. Cells were washed three times in PBS. Cells were transferred to fresh tubes between washes to minimise carry-over of unbound $DIOC_{18}$ and thus non-specific staining.

A range of NK cell concentrations were prepared to correspond to various lymphocyte to target ratios. 100 µl of each concentration was added to the appropriate wells of a 96-well tissue culture plate.

Preparation of target cells: Yac-1 cells in the log phase of growth were pelleted and counted using trypan blue to ensure exclusion of dead cells. Cells were resuspended at 5 x 10^5 per ml in complete RPMI. 5 x 10^4 cells in a volume of 100 µl were added to 100 µl of NK cells in each well.

Target and effector cells were incubated together for 4 hours at 37°C in 5% CO_2. Each sample was run in triplicate. Post-incubation, the contents of each well were transferred to a 5 ml FACS tube. Each sample was washed twice in PBS before being resuspended in 1 ml of FACS buffer. Samples were kept in the dark on ice until analysis.

To detect the presence of dead cells, 2 µl of a 50 µg/ml solution of the red fluorescent dye, propidium iodide (PI) (Sigma, UK) was added to each sample immediately prior to analysis on a FACScan machine using Cell Quest software (BD Biosciences). Each sample was run until at least 5000 unlabelled target events had been acquired. Specific lysis (percentage of the target population killed) was calculated by subtracting lysis in the absence of NK cells (spontaneous lysis) from lysis in their presence. The average of three repeats was calculated for each sample.

Controls: To measure the spontaneous and maximum killing of target cells, 5 x 10^4 Yac-1 cells in 100 µl RPMI were added to wells containing 100 µl of RPMI only or 100 µl of 5% Triton X-100 (in PBS) respectively. As a positive control, 100 µg/ml of poly I:C was added to an aliquot of NK cells in 1 ml of RPMI. The mixture was incubated at 37°C, 5% CO_2 overnight. Post-incubation, cells were stained with $DIOC_{18}$, mixed with Yac-1 cells and incubated together in the well of a 96-well plate

as described above. All control samples were run in triplicate and were stained with PI to measure the proportion of dead cells. The percentage of specific lysis was calculated using the following formula:

Specific % lysis = (release in presence of NK cells – spontaneous lysis) X 100

2.17. Statistical analysis

Data was analysed with the non-parametric Mann-Whitney test unless otherwise described.

Name	Primer Sequence 1. 5'-3'	Primer sequence 2. 5'-3'	Cycling condition (°C/sec)	PCR Product
IFNβgeno	TGGGAAATTCCTCTG AGGCAG	CACTCATTCTGAGGCA TCAACTGAC	94/30 60/30 72/30 (X 35)	Murine IFNβ gene 717bp
GFPgeno	GGTGAAGGTGATGCA ACATACGG	TGTGGACAGGTAATGG TTGTCTGG	94/30 60/30 72/30 (X 35)	GFP gene 513bp
TARG 1 & 2	CCGTGCTTGATTGAA GTTAGGC	TTCTCGTTGGGGTCTTT GCTC	94/30 58/30 66/120 (X 35)	Targeting construct in np27 ko mice 3.5kb
KO 1 & 2	GGCTTCCATTGTCTC CAAGATG	TGAGGTCAGGATGCTA CATGCTC	94/30 58/30 66/180 (X 35)	Exon 2 within np27 gene. 169bp in wt mice. 3kb in ko mice
IFNα4	CTGGTCAGCCTGTTC TCTAGGATG	TCAGAGGAGGTTCCTG CATCAC	94/30 57/30 72/30 (X 40)	Murine IFNα4 314bp
Non IFNα4	ARSYTGTSTGATGCA RCAGGT	GGWACACAGTGATCCT GTGG	94/40 55/30 72/30 (X 40)	Murine IFNα's except IFNα4 104bp
UIFNα	ATGGCTAGGCYGTGT GCTTTC	TCTGAYCACCTCCCAG GCACA	94/60 50/90 72/120 (X 40)	All IFNα subtypes 500bp
IFNβmod	CTATCCAAGAGATGC TCCAG	GTGGAGAGCAGTTGAG GACA	94/40 62/60 72/60 (X 40)	Murine IFNβ 150bp
RTA qRT	GGCACATTTGCTGCA GAACCCAG	GAACGGCGCCTGTGTA CTCAAAGG	95/20 66/20 72/25 (X 45)	MHV-68 ORF 50 357bp
M3 qRT	TGGCACTCAAACTTG GTTGTGG	TAACAGGCAGATTGCC ATTCCC	95/20 65/20 72/25 (X45)	MHV-68 M3 gene
Bactin inner	CGTTGACATCCGTAA AGACC	CTGGAAGGTGGACAGT GA	94/30 62/20 72/20 (X45)	Murine β-actin 202bp
Bactin outer	GTGGCATCCATGAAA CTACA	GTACTCCTGCTTGCTGA TCC	94/45 55/45 72/60 (X 40)	Murine β-actin 272bp

Table 2.1 (previous page). Primers Utilised in this Study. Cycling conditions: 1st line indicates denaturing stage, 2nd line indicates annealing stage, 3rd line indicates elongation stage and 4th line indicates number of cycles.

Table 2.2. Antibodies Utilised in this Study

Cell Surface Marker	**Clone**	**Isotype**	**Label**	**Supplier**
CD3	KT3	Rat IgG2a	FITC	Serotec
CD4	YTS 191.1	Rat IgG2b	unlabelled	In house
CD8	YTS 169	Rat IgG2b	unlabelled	In house
CD16/CD32	2.4G2	Rat IgG2b	unlabelled	Pharmingen
CD19	6D5	Rat IgG2a	PE	Caltag
CD49b	DX5	Rat IgM	Biotin	Serotec
CD49b	DX5	Rat IgM	FITC	Serotec
NK1.1	PK136	Rabbit IgG2a	Biotin	In house
IFNγ	XMG1.2	Rat IgG1	PE	Pharmingen

Chapter 3: Role of the type I IFNs in the control of a MHV-68 infection

3. Role of the Type I IFNs in the Control of MHV-68 infection

3.1. Introduction

Type I IFNs are expressed almost immediately in response to virus infection. One IFNβ and 14 IFNα genes have been found in the mouse genome, all of which share a common dimeric receptor. Mice with a targeted disruption in an essential chain of the type I IFN receptor gene (IFNα/β $R^{-/-}$) have been used to study the role of type I IFNs during virus infection. Using this system, type I IFN was shown to be important during both RNA and DNA virus infections including lymphocytic choriomeningitis virus, Semliki Forest virus and vaccinia virus (Van Den Broek *et al.*, 1995).

The role of type I IFNs in gammaherpesvirus infections was highlighted by the infection of IFNα/β $R^{-/-}$ mice with MHV-68. Virus titres in the lungs of IFNα/β $R^{-/-}$ mice were 100- to 1000-fold higher than in wt mice and 90% of IFNα/β $R^{-/-}$ mice infected with 4×10^5 pfu of MHV-68 died by day 10 post-infection. In the spleens of IFNα/β $R^{-/-}$ mice there was an increased incidence of latently infected cells compared to wt (Dutia *et al.*, 1999). In addition, Barton *et al.* (2005) showed that infectious virus was detectable in the spleens of IFNα/β $R^{-/-}$ mice by day 7 post-infection whereas infectious virus can only be detected in the lungs of wt mice. These studies show that type I IFN is critical for the control of MHV-68 infection. The importance of the type I IFN response to gammaherpesvirus infection is also highlighted by the immune evasion strategies that have evolved to counteract its actions (see section 1.5).

In this study, the characteristics of the type I IFN response to MHV-68 have been examined *in vitro* in order to further understanding of the control of gammaherpesvirus infections. The left end of the MHV-68 genome has been implicated as important for pathogenesis due to the attenuation of MHV-76 replication at early time points post-infection. It has been suggested that the M2

protein may have a type I IFN evasion function. *In vitro*, ISG15 was upregulated 10-fold in response to IFNα in the absence of M2. Conversely, minimal ISG15 induction was observed following IFNα stimulation when M2 was expressed in cells (Liang *et al.*, 2004). MHV-76 infection was investigated in order to determine if the genes M1-M4 and the vtRNAs have an immune evasion function during the type I IFN response.

It was of interest to further characterise the type I IFN response by specifically investigating the role of IFNβ during both *in vitro* and *in vivo* infection. Previous studies have utilised IFNα/β $R^{-/-}$ mice. This approach results in the whole type I IFN system being disrupted but is convenient due to the difficulty of knocking out each of the multiple IFNα genes present. Only a single IFNβ gene is present and has thus made the generation of an IFNβ null strain of mice more straightforward. Mice that lack the IFNβ gene have been shown to be more susceptible to vaccinia virus infection, succumbing to doses that are sub-lethal to wt mice (Deonarain *et al.*, 2000).

The aims of this study were to (1) investigate type I IFN responses to a gammaherpesvirus infection *in vitro*, (2) elucidate the role for IFNβ specifically during *in vitro* and *in vivo* infection and (3) examine and compare type I IFN responses to MHV-68 and MHV-76 infection to elucidate a role for the left end of the genome in immune evasion.

3.2. Role of Type I IFNs in the control of MHV-68 in vitro

3.2.1. *In vitro* stimulation of type I IFNs by MHV-68 or MHV-76

The kinetics of induction of type I IFNs differ in response to virus infection. In general, IFNα4 can be produced rapidly post-infection, without the need for *de novo* protein synthesis but other IFNα subtypes such as IFNα5 have delayed induction and rely on the synthesis of IRF-7 produced in response to early IFN production. This results in the establishment of a positive feedback loop (Harle *et al.*, 2002; Marie *et al.*, 1998). The ability of MHV-68 to induce type I IFN and thus the kinetics of induction following MHV-68 infection were examined *in vitro*. It was also of interest to investigate IFN induction by MHV-76 infection. Would the lack of the genes M1-M4 and the vtRNAs in MHV-76 lead to altered kinetics of IFN production in comparison to MHV-68? To address this question, the induction of type I IFNs following infection was examined in a time course assay. L929 cells were infected with either MHV-68 or MHV-76 (MOI of 10) before being allowed to settle into a monolayer. Cells were harvested at 0.5, 1, 2, 3 and 5 hours post-infection, then RNA extracted and cDNA prepared. The synthetic double-stranded RNA poly I:C was added to cells in order to act as a positive control due to its ability to strongly induce type I IFN responses. It was found that 100μg/ml of poly I:C was sufficient to stimulate IFN responses in this assay. Primer pairs designed to detect various IFN transcripts were designed by Deonarain *et al.* (Deonarain *et al.*, 2000) and purchased from MWG: one specific for IFNβ, another specific for IFNα4, one to detect all IFNα transcripts apart from IFNα4 (IFNnonα4) and one to detect all IFNα subtypes (universal IFNα). Optimisation of the cycling conditions for each primer pair was carried out using cDNA extracted from poly I:C stimulated cells. The optimal cycling conditions are shown in table 2.1. Unfortunately, optimisation failed to avoid non-specific binding and band smearing when using the universal IFNα primer pair. As all IFNα transcripts could be detected by either the IFNα4 or IFNnonα4 primers a decision was made to not use the universal IFNα primers further. Results from the RT-PCR analysis are shown in figure 3.1. β-actin was readily detectable for each sample ensuring that cDNA was present and of suitable quality. Band intensity

indicated that there were similar amounts of cDNA in each sample. For each PCR, IFN could be readily detected in samples stimulated with poly I:C demonstrating that each PCR resulted in a band of the expected size. These data show that both MHV-68 and MHV-76 readily induced type I IFN within hours of infection. After infection with MHV-68 a band for IFNβ could be detected by 1 hour post-infection. Following infection with MHV-76, IFNβ transcripts could be detected by 2 hours post-infection in two separate experiments. IFNα4 was detectable from 1 hour post-infection onwards in both the MHV-68 and MHV-76 samples in two separate experiments. Although the assay is not quantitative, the induction of IFNα4 appeared to be stronger than the induction of other transcripts examined. The stimulation of the other IFNα subtypes was investigated using the IFNnonα4 primers. In the MHV-68 infected samples IFNnonα4 transcripts were detectable by 3 hours post-infection whereas transcripts were detectable at 2 hours post-infection in the MHV-76 infected samples in the PCR shown in figure 3.1. However, these differences were not consistently repeated as detection varied between 2 and 3 hours in a further repeat of this assay indicating that the results of these experiments were dependent on sample to sample variability. It was concluded that no consistent difference in the induction of IFN transcripts between viruses could be observed by this technique. However, the later detection of IFNnonα4 does agree with previous findings that IFNα4 is a rapidly expressed transcript whereas other IFNα subtypes have a delayed induction.

Cycloheximide (CHX) is a protein synthesis inhibitor that acts specifically on the 60S subunit of eukaryotic ribosomes. Cells were treated with 100μg of CHX for 30 minutes prior to the addition of either MHV-68 or MHV-76. Cells treated with CHX, but not virus, were included as controls for any IFN induction due to CHX treatment alone. Cells were harvested at 5 hours post-infection in order to investigate the ability of the virus to induce IFN transcripts in the absence of viral protein synthesis. However, the results obtained with either CHX alone or CHX plus virus were

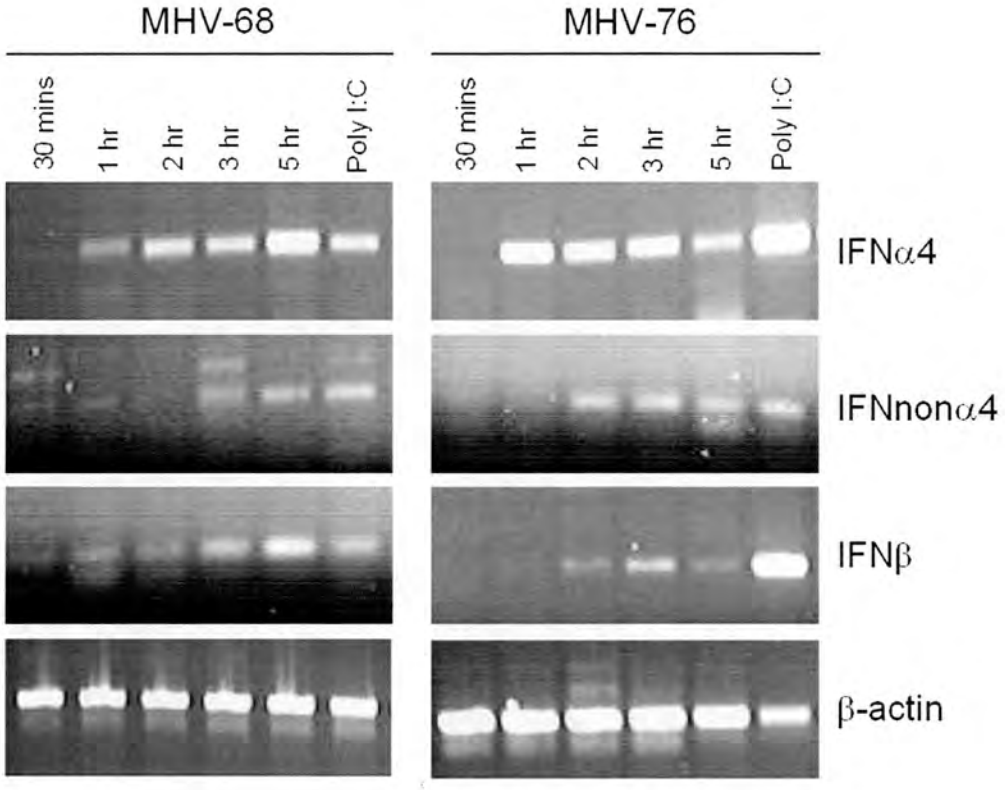

Figure 3.1. RT-PCR analysis of IFN induction post-infection. Cells were infected with either MHV-68 or MHV-76. cDNA was prepared from RNA extracted from L929 cells at specific times post-infection. RT-PCR was performed using primers specific for various type I IFNs in addition to murine β-actin. In each PCR, Poly I:C was included as a positive control and was harvested at 5 hours p.i. A sample containing no cDNA was included as a negative control and a RNA sample was included without the addition of reverse transcriptase to control for the carryover of DNA in the reaction (data not shown).

inconsistent. IFN was detectable in some assay repeats, but not others and was evident even when no virus was present and thus no conclusions could be drawn.

This technique could have been pursued further but as no particularly fruitful results were obtained it was decided to explore other aspects of the type I IFN response to MHV-68 infection.

3.2.2. Genotyping of mice

IFNβ$^{-/-}$ mice were generated by Deonarain *et al.*, (2001), whereby a targeting construct was used to replace the IFNβ gene with a green fluorescent protein (GFP) reporter gene as shown in figure 3.2. HM-1 embryonic stem cells transfected with the GFP construct were injected into C57BL/6 blastocysts and the chimeras showing efficient germ-line transmission were crossed with C57Bl/6 mice to generate a IFNβ$^{+/-}$ F1 generation (Deonarain *et al.*, 2000). The heterozygous littermates were crossed to generate IFNβ$^{+/+}$, IFNβ$^{+/-}$ and IFNβ$^{-/-}$ mice. We obtained IFNβ$^{-/-}$ mice to study the role of IFNβ during MHV-68 infection. PCR analysis using DNA extracted from ear biopsy tissue confirmed the presence of the GFP gene (513bp product) and absence of the IFNβ gene (717bp product) in the IFNβ$^{-/-}$ mice (figure 3.2).

3.2.3. MHV-68 replication in IFN knockout cell lines

Single step growth curves were carried out in order to assess the involvement of type I IFNs during MHV-68 replication *in vitro*. It was hypothesised that MHV-68 infection of cells lacking IFNβ and IFNα would result in lesser control of virus replication and thus higher viral titres than a wt cell line. Correspondingly, a cell line lacking only IFNβ would result in MHV-68 titres that were intermediate to the IFNα/β R$^{-/-}$ and wt cell lines. The single replication cycle of MHV-68 was assessed

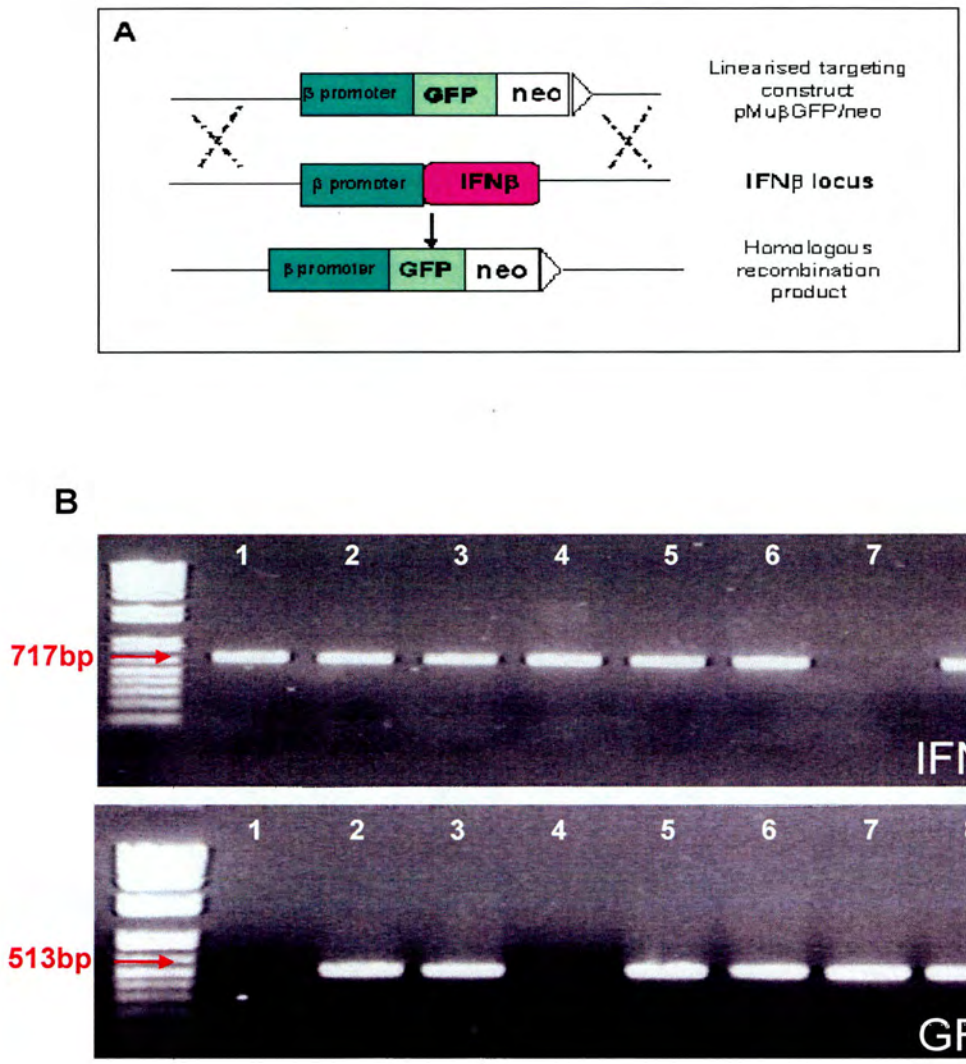

Figure 3.2. Genotypic analysis of IFNβ$^{-/-}$ mice. (A) Schematic diagram of the generation of IFNβ ko mice. (B) Representative PCR for the genotyping of IFNβ$^{-/-}$ x wt 129/Sv/Ev crosses. DNA was extracted from mouse ear biopsy tissue at 3 weeks of age. PCR was performed using primers specific for IFNβ (717bp product) and GFP (513bp product). Lane 7 shows the result from an IFNβ$^{-/-}$ mouse, lanes 1 and 4 show wt mice and 2, 3, 5, 6 and 8 show heterozygous mice. A reaction containing no DNA template was included to control for cross-contamination of samples (data not shown).

in three mouse embryonic fibroblast (MEF) cell lines. The first lacked all type I IFN responses (IFNα/β $R^{-/-}$) due to disruption of the shared type 1 IFN receptor. The second lacked IFNβ (generated from 13.5 day old $IFN\beta^{-/-}$ embryos) and the third was a wt cell line. Cells were infected with MHV-68 at MOI of 5 pfu/cell and duplicate samples taken at intervals from 0 to 72 hours post-infection. At each time point, media was removed from the well and titrated separately from the cell monolayer to examine both cell-associated and cell-free virus. No supernatant sample was taken at 0 hours post-infection as cells had not settled into a monolayer and therefore cell associated and cell free virus could not be separated. Samples were titrated in duplicate on BHK-21 cells. When cell-associated virus and cell-free virus were examined together, it appeared that MHV-68 replicated with similar kinetics in all three cell types (figure 3.3). However, when cell-associated virus was examined independently there were increased levels of cell-associated virus in the wt MEFs in comparison to the $IFN\beta^{-/-}$ and IFNα/β $R^{-/-}$ MEFs from 12 hours post-infection onwards. Conversely, it was evident that from 12 hours post-infection onwards there were increased levels of cell-free virus in the IFNα/β $R^{-/-}$ MEFs than in either the $IFN\beta^{-/-}$ or wt MEFs. It was decided to repeat the 12 and 24 hour time points on two further occasions to determine if this effect was reproducible. Cell-free viral titres at 12 and 24 hours post-infection are shown in figure 3.4 and cell-associated viral titres at 12 and 24 hours post-infection are shown in figure 3.5. In each figure, panels A and D show results obtained during the full growth curve analysis whereas the other panels represent data from the two individual repeat experiments focusing on 12 and 24 hours post-infection. These data show that the titres of MHV-68 tend to be higher overall in IFNα/β $R^{-/-}$ MEFs in comparison to $IFN\beta^{-/-}$ and wt MEFs. The majority of virus in the $IFN\beta^{-/-}$ and wt MEFs is cell-associated rather than cell-free, whereas a higher proportion of virus was detected in the supernatant of the IFNα/β $R^{-/-}$ MEFs compared to the other cell types. The titres of cell-free virus in the $IFN\beta^{-/-}$ and wt cell lines were small in comparison to the viral titres from the IFNα/β $R^{-/-}$ MEFs. The difference in viral titre between the $IFN\beta^{-/-}$ and wt MEFs was not as striking as for the IFNα/β $R^{-/-}$ MEFs. However, in 2/3 cases at both 12 and 24 hours post-infection, the titre of cell-associated virus in the wt MEFs was higher than in the $IFN\beta^{-/-}$ MEFs.

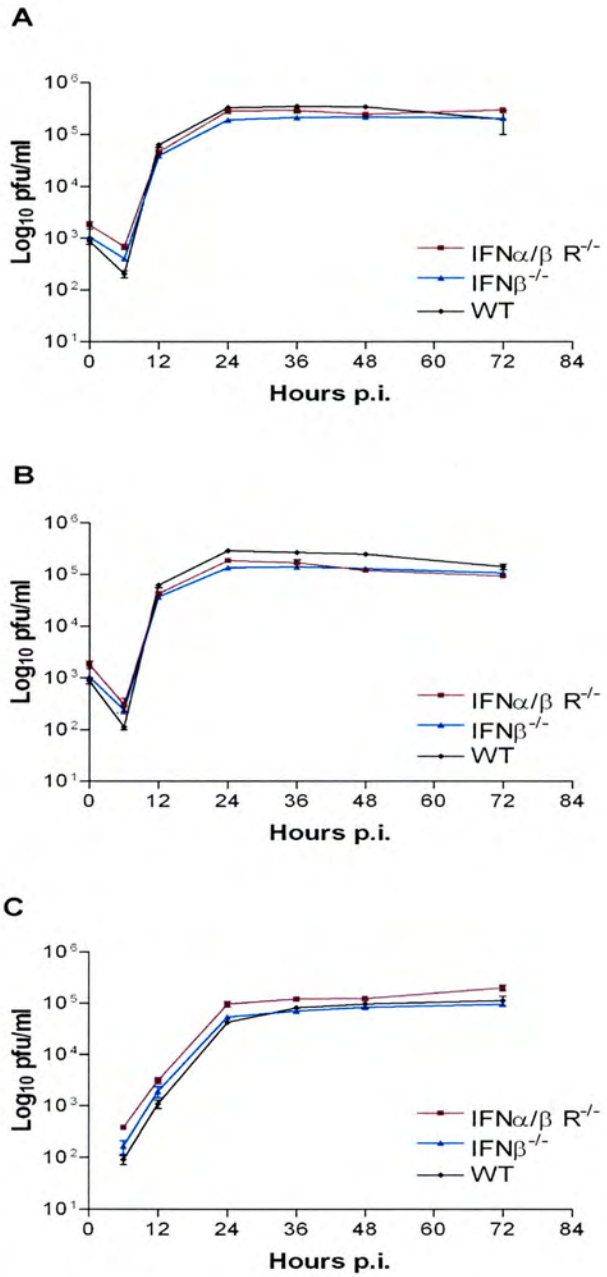

Figure 3.3. Single-step replication of MHV-68 in IFNα/β $R^{-/-}$, $IFN\beta^{-/-}$ and wt MEFs *in vitro*. Cells were infected with an MOI of 5 and harvested at various times p.i. Values represent two separate experiments with each sample titrated in duplicate. Data points represent the $\log_{10}$ of the virus titre ± standard error of the mean (SEM). The combined viral titres from both the cells and the cell supernatant are shown in panel A. B represents cell associated virus only and C represents cell-free virus only.

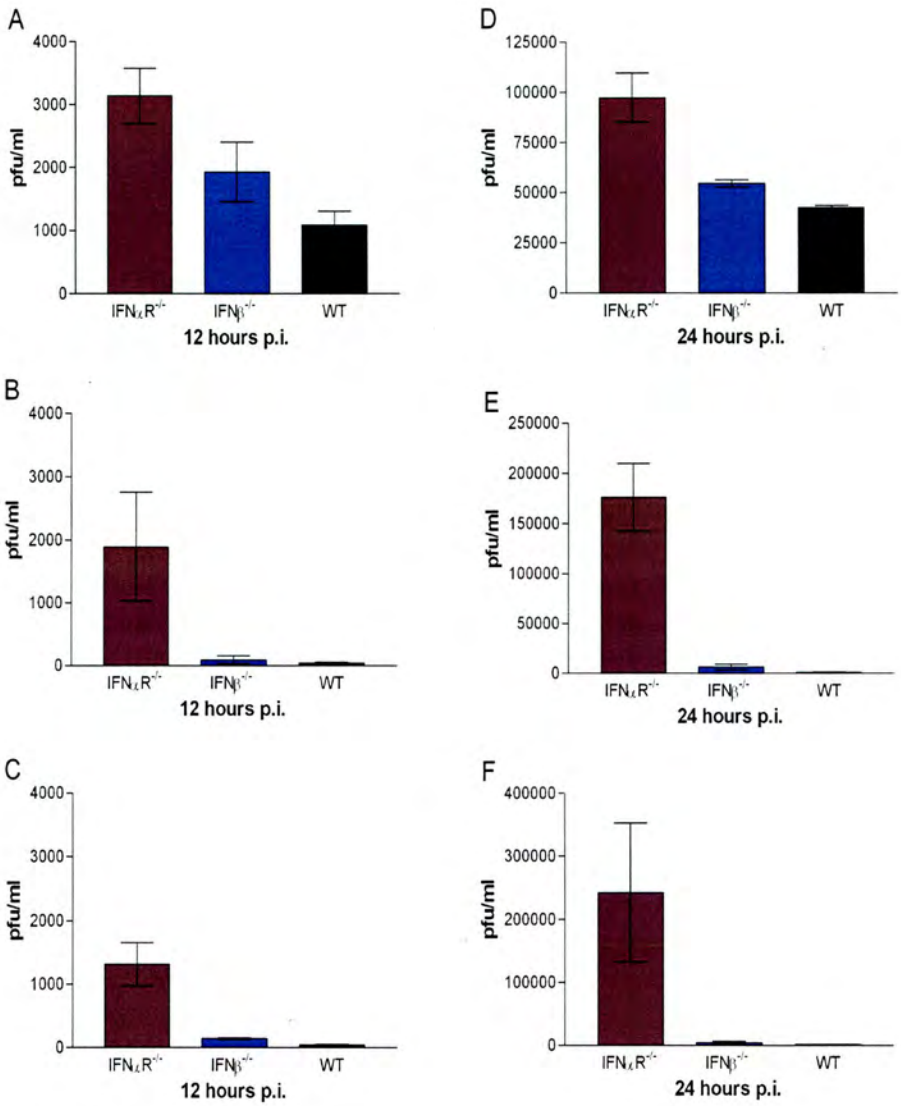

Figure 3.4. Titres of cell-free virus in the supernatant of IFNα/β $R^{-/-}$, $IFN\beta^{-/-}$ and wt MEFs at 12 and 24 hours p.i. MEFs were infected with MHV-68 at an MOI of 5 and harvested after 12 (A-C) or 24 (D-F) hours p.i. Each time point was assayed independently on three occasions and each experiment is shown as a separate graph. Cells were removed and assayed separately (see figure 3.5). Values represent the virus titre ± standard error of the mean (SEM) from two independent experiments with each sample titrated in duplicate. Red bars denote IFNα/β $^{-/-}$ MEFs, blue bars denote $IFN\beta^{-/-}$ MEFs and black bars denote wt MEFs.

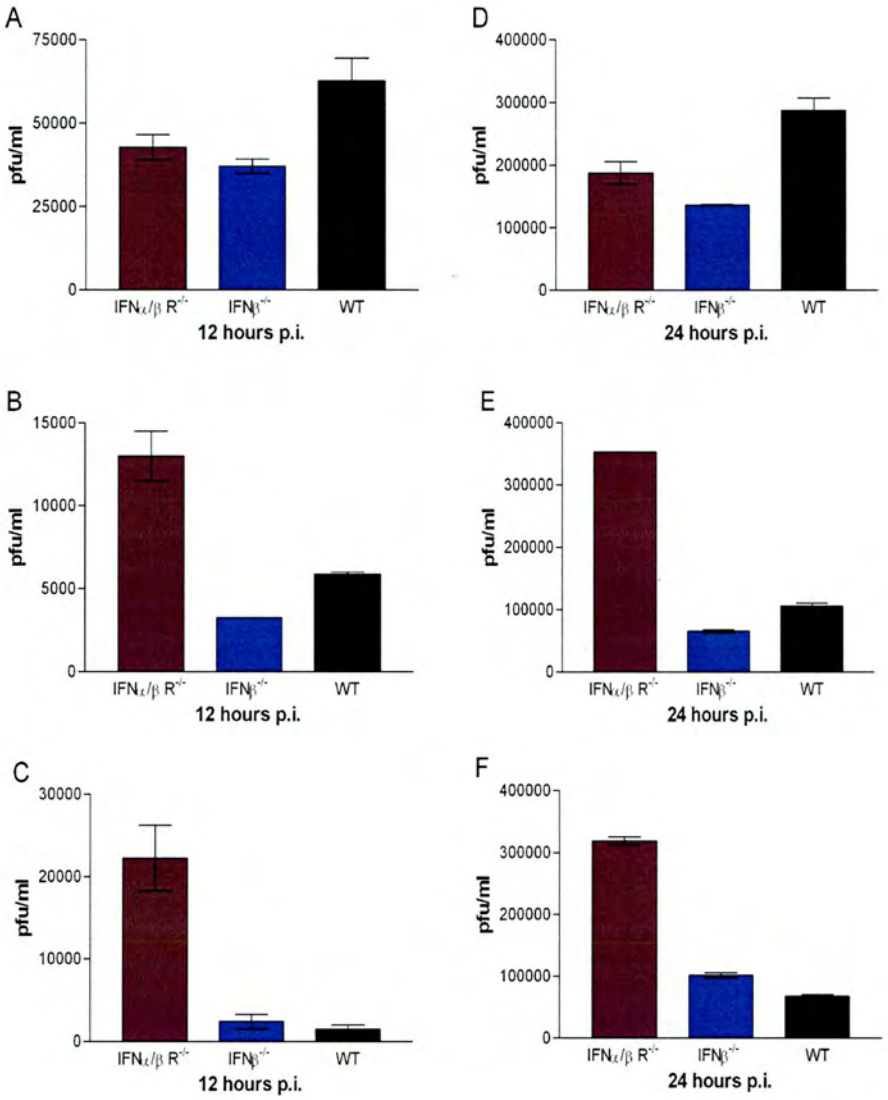

Figure 3.5. Titres of cell-associated virus in IFNα/β $R^{-/-}$, IFNβ$^{-/-}$ and wt MEFs at 12 and 24 hours p.i. MEFs were infected with MHV-68 at an MOI of 5 and harvested after 12 (A-C) or 24 (D-F) hours p.i. Each time point was assayed independently on three occasions and each experiment is shown as a separate graph. Cell supernatant was removed and assayed separately (see figure 3.4). Values represent the virus titre ± standard error of the mean (SEM) from two independent experiments with each sample titrated in duplicate. Red bars denote IFNα/β $^{-/-}$ MEFs, blue bars denote IFNβ$^{-/-}$ MEFs and black bars denote wt MEFs.

Conversely, in 3/3 cases at both 12 and 24 hours post-infection, the titre of cell-free virus in the IFNβ$^{-/-}$ MEFs was higher than in the wt MEFs. These data suggest that the viral titres in the IFNβ$^{-/-}$ MEFs are reflecting the increased proportion of cell-free virus observed in the IFNα/β R$^{-/-}$ MEFs but to a lesser extent. No statistical analysis was carried out on these data as there was too much variation in titres between the first experiment and the further two repeats, hampering reliable interpretation.

3.3. Role of IFNβ in the control of MHV-68 in vivo

Studies using mice that lack a functional IFNα/β receptor have highlighted the importance of the Type I IFNs during MHV-68 infection. IFNβ$^{-/-}$ mice were used in this study in order to investigate specifically the role of IFNβ during MHV-68 infection. It was hypothesised that a lack of IFNβ would result in an intermediate pathology between that observed in IFNα/β R$^{-/-}$ and wt mice. As the IFNβ$^{-/-}$ mice were derived from a HM-1/C57Bl/6 mixed background, and there was no HM-1/C57Bl/6 wt mice with which to obtain littermate controls, C57Bl/6 mice were chosen to act as controls during initial *in vivo* studies.

IFNβ$^{-/-}$ and C57BL/6 mice were infected intranasally with 4 x 10^5 pfu of MHV-68 and tissues were harvested at day 3, 5, 7 and 10 post-infection. Lytic replication in the lung was investigated by infectious virus assay and the results are shown in figure 3.6. At 3 days post-infection, the titre of MHV-68 was similar in the IFNβ$^{-/-}$ and wt lungs but by day 5 post-infection there was significantly more virus in the IFNβ$^{-/-}$ lung compared to the wt lung ($p=0.0286$). By day 7 post-infection the difference between the two groups was resolved and virus in the wt and IFNβ$^{-/-}$ lung was cleared by day 10 post-infection. Establishment of latency in the spleen was determined by *ex vivo* reactivation assay and the results are shown in figure 3.7. Infective centres could be detected in both the IFNβ$^{-/-}$ and wt spleen by day 5 post-infection with a peak of latency observed between 10 and 14 days post-infection.

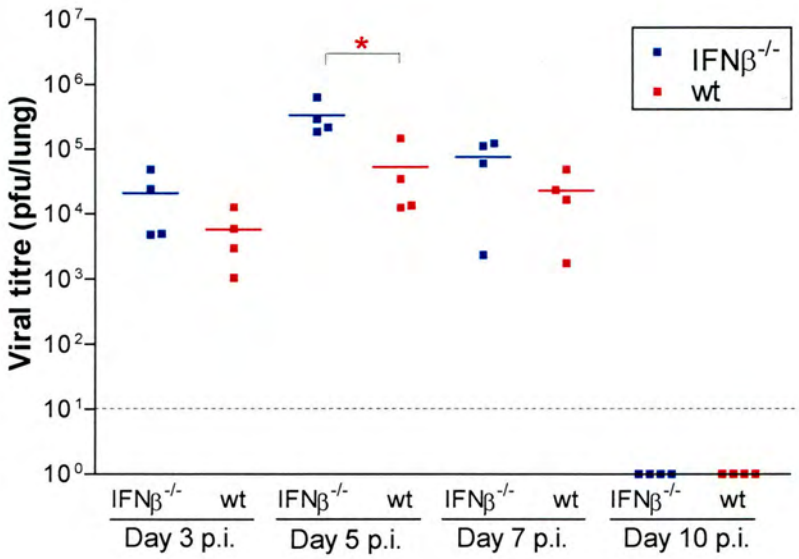

Figure 3.6. Viral titre in the lungs of IFNβ ko or wt mice. Mice were infected intranasally with 4 x 10^5 pfu of MHV-68. Lungs were harvested at days 3, 5, 7 and 10 post-infection and virus titre was determined by infectious virus assay. Each data point represents the virus titre from individual mice and the solid line represents the mean virus titre for each group. The dashed line represents the limit of detection (10 pfu) for this assay. Groups that have mean values that vary significantly ($p \leq 0.05$) by Mann Whitney test are indicated by *.

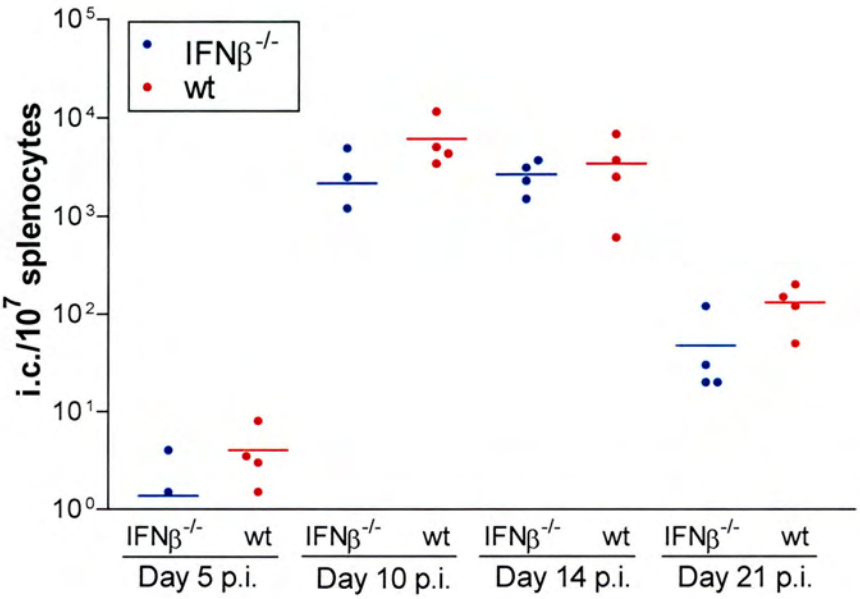

Figure 3.7. Latent virus in the spleens of IFNβ ko and wt mice. Mice were infected intranasally with 4 x 10^5 pfu of MHV-68 and spleens were harvested at days 5, 10, 14 and 21 post-infection. Latent virus titre was determined by infective centre assay. Each data point represents individual mice and the solid line represents mean latent virus for each group.

There was no significant difference in viral titres between the wt and IFNβ$^{-/-}$ mice at any time point investigated. Similarly, there was no notable difference in the degree of splenomegaly between both groups (figure 3.8) as measured by whole spleen weight.

Given the encouraging results obtained in the initial experiment it was decided that it might be beneficial to cross the IFNβ$^{-/-}$ strain onto a wt 129/Sv/Ev background to obtain age-matched wt littermates as the most appropriate controls and ensure a more accurate background match between the wt and IFNβ$^{-/-}$ mice. Genotypes of the resultant litters from the IFNβ$^{-/-}$ x wt 129/Sv/Ev crosses were determined by PCR analysis using DNA extracted from ear biopsy tissue. The presence of the GFP gene was confirmed with a 513bp product and the presence of the IFNβ gene was confirmed by a 717bp product. An example of PCR analysis of littermate genotypes is shown in figure 3.2.

It was decided to repeat the *in vivo* analysis using IFNβ$^{-/-}$ and wt littermates derived from crossing the F1 heterozygotes. These mice were thus a better match than the mice used in the initial experiment. The experiment was carried out using a lower dose of virus to further elucidate subtle differences in MHV-68 pathogenesis between the IFNβ$^{-/-}$ and wt mice which may have been obscured during infection with a higher dose of virus. IFNβ$^{-/-}$ and wt mice were infected intranasally with $4x10^3$ pfu of MHV-68. Tissues were harvested at days 5, 7, 10 and 14 post-infection. The level of lytic replication in the lung was determined by infectious virus assay and the results are shown in figure 3.9. The viral titres in the lungs of the IFNβ$^{-/-}$ mice rose more quickly, peaking at day 7 post-infection, whereas viral titres in the wt lungs peaked at day 10 post-infection. At day 7 post-infection, the titre of virus in the IFNβ$^{-/-}$ lung was significantly higher than in the wt lung ($p=0.0286$). By day 10 the difference had resolved and the infection had cleared from the lungs of both groups by day 14 post-infection. Real-time PCR was used to confirm the difference in virus titre between the IFNβ$^{-/-}$ and wt lungs at day 7 post-infection (figure 3.10). DNA was

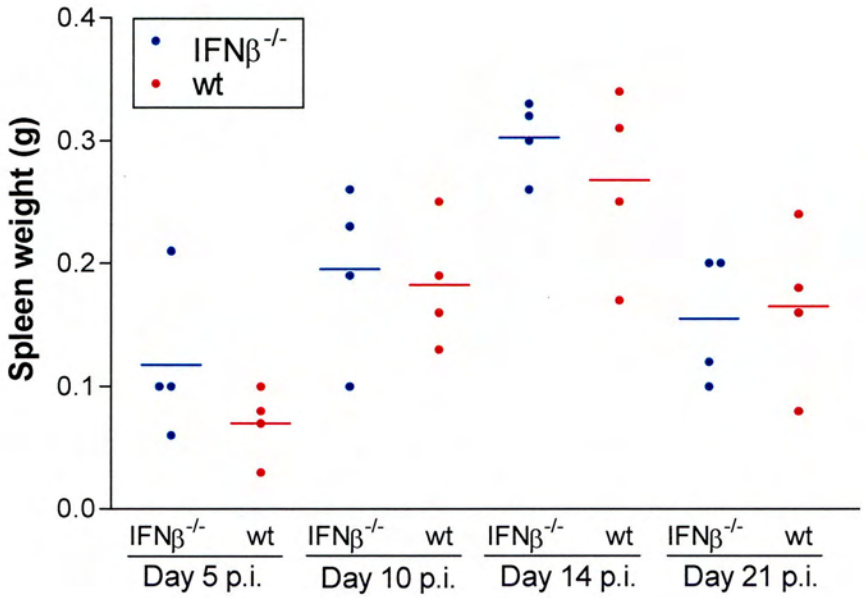

Figure 3.8. Whole spleen weights in IFNβ and wt mice. Mice were infected intranasally with 4 x 10^5 pfu of MHV-68. Spleens were harvested at days 5, 10, 14 and 21 post-infection. Data points represent the whole spleen weights of individual mice and the solid line represents the mean spleen weight for each group.

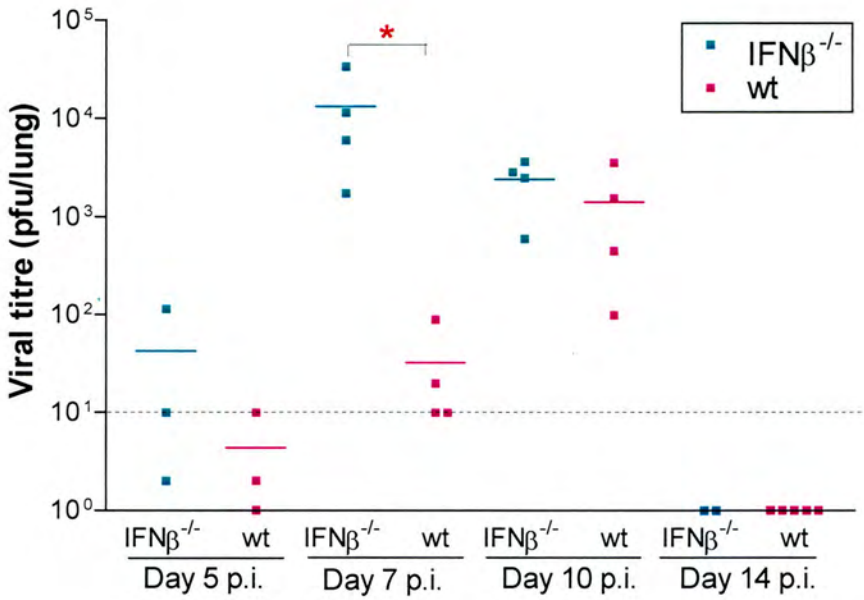

Figure 3.9. Viral titre in the lungs of IFNβ ko or wt mice. Mice were infected intranasally with 4 x 10^3 pfu of MHV-68. Lungs were harvested at days 5, 7, 10 and 14 post-infection. Virus titre was determined by infectious virus assay. Each data point represents the virus titre from individual mice and the solid line represents the mean virus titre for each group. The dashed line represents the limit of detection (10 pfu) for this assay. Groups that have mean values that vary significantly ($p \leq 0.05$) by Mann Whitney test are indicated by *.

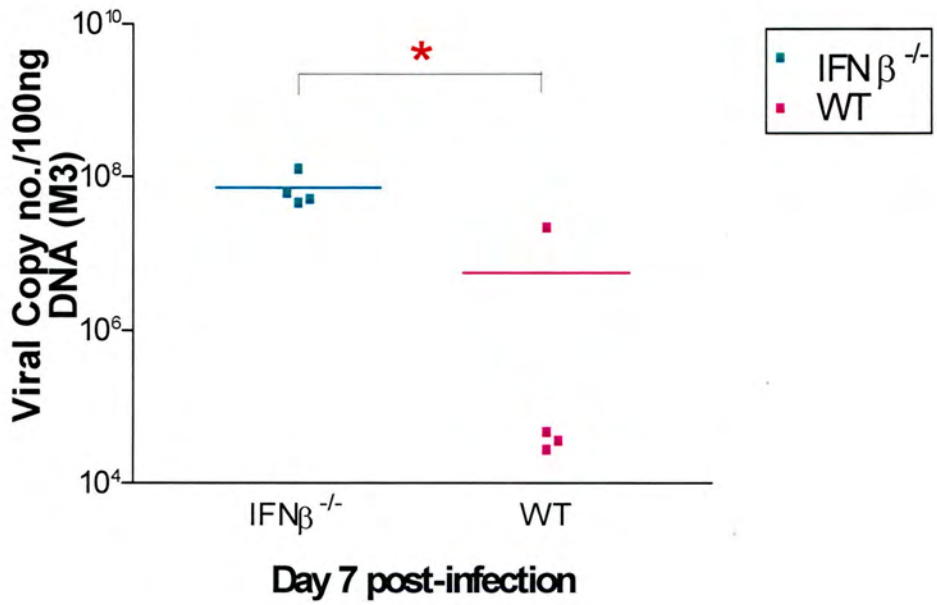

Figure 3.10. Viral load in the lungs of IFNβ ko or wt mice at day 7 post-infection. Mice were infected intranasally with 4 x 10^3 pfu of MHV-68. Viral load was determined by real time PCR using primers specific for the viral gene, M3 and normalised as determined by the level of β-actin within each sample. Each data point represents the viral load from individual mice and the solid line represents the mean viral load for each group. Groups that have mean values that vary significantly ($p \leq 0.05$) by Mann Whitney test are indicated by *.

extracted from lung tissue and the viral load was determined using primers specific for the viral gene, M3. The data were normalised as determined by the level of β-actin within each sample. The groups were found to be significantly different ($p=0.0286$), thus agreeing with both infectious virus assays carried out on the groups infected with either the low or high doses of virus. Latent virus in the spleen was assessed by *ex vivo* reactivation assay and the results shown in figure 3.11. Virus was detectable in both groups by day 10 post-infection. From day 10 onwards there was a trend towards higher levels of latent virus in the IFNβ$^{-/-}$ spleens compared to the wt spleens. However, this was not significant at any time point investigated. Although at day 14 post-infection the viral titres in the IFNβ$^{-/-}$ group appeared higher than the wt group, there were only two members in the IFNβ$^{-/-}$ group so no statistics could be performed. Likewise, there was a trend towards a higher degree of splenomegaly in the IFNβ$^{-/-}$ spleen compared to the wt spleen at day 14 and 21 post-infection (figure 3.12). Again, no statistics could be performed at day 14 post-infection as there were only 2 mice in the IFNβ$^{-/-}$ spleen group. At day 21 post-infection, the difference in spleen weight between the IFNβ$^{-/-}$ and wt groups was almost at significance ($p=0.0571$).

3.4. Infection of IFNβ$^{-/-}$ mice with MHV-68 and MHV-76

MHV-76 replication is attenuated during *in vivo* infection, being cleared more rapidly from the lung than MHV-68. Previous studies in BALB/c mice have shown that MHV-76 viral titres in the lungs are approximately 1 log lower than MHV-68 titres at day 7 post-infection (Macrae *et al.*, 2001). It was hypothesised that if a component of the left end of MHV-68 was involved in regulation of the IFNβ response, a lack of IFNβ would confer an advantage to MHV-76 and it would be cleared from the lung with similar kinetics to MHV-68. To address this hypothesis, IFNβ$^{-/-}$ mice were infected intranasally with 4×10^5 pfu of either MHV-68 or MHV-76. Lungs were harvested at days 3, 5, 7 and 10 post-infection. Infectious virus

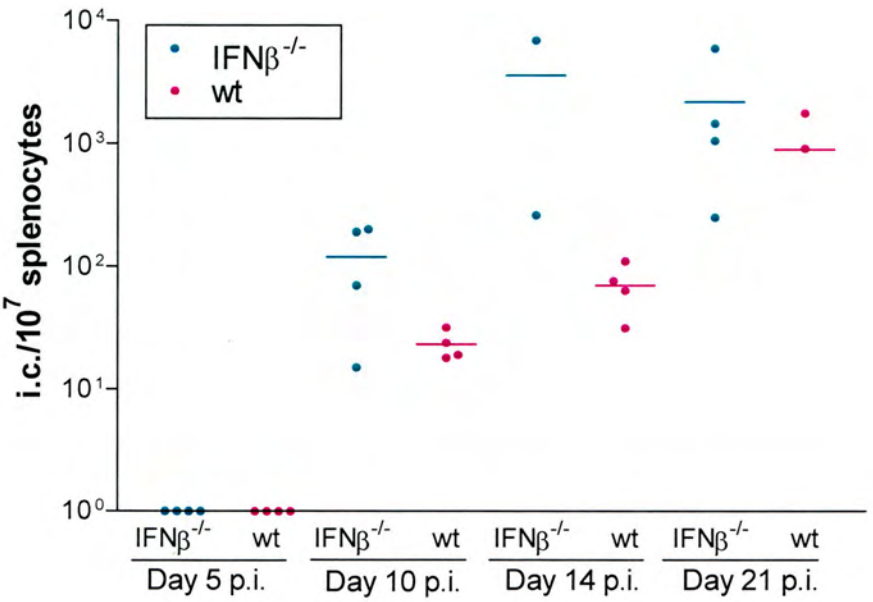

Figure 3.11. Latent virus in the spleens of IFNβ ko and wt mice. Mice were infected intranasally with 4 x 10^3 pfu of MHV-68. Spleens were harvested at days 5, 10, 14 and 21 post-infection and latent virus was determined by infective centre (i.c.) assay. Each data point represents individual mice and the solid line represents mean latent virus for each group.

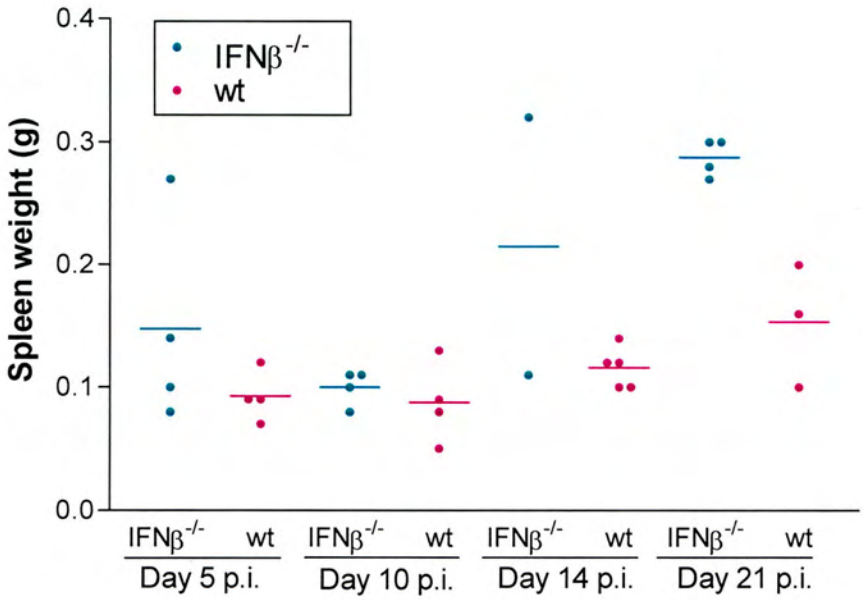

Figure 3.12. Whole spleen weights in IFNβ and wt mice. Mice were infected intranasally with 4×10^3 pfu of MHV-68. Spleens were harvested at days 5, 10, 14 and 21 post-infection. Data points represent the whole spleen weights of individual mice and the solid line represents the mean spleen weight for each group.

assays were carried out to assess the productive infection in the lungs (figure 3.13). There was no difference between the MHV-68 and MHV-76 titres at day 3 and 5 post-infection and the titres of both groups reached a peak around day 5 post-infection. At day 7 post-infection, the mean viral titre (6625 pfu/lung) of the MHV-68 group was significantly higher than the mean (712.5 pfu/lung) of the MHV-76 group ($p=0.0286$). In agreement with previous findings in wt mice (Macrae *et al.*, 2001), these data show an approximate log difference between the two groups at day 7 post-infection. Both viruses were cleared from the lung by day 10 post-infection. These data show that even in the absence of IFNβ MHV-76 is cleared from the lung faster than MHV-68, therefore suggesting that components of the left end of the MHV-68 genome do not interfere greatly with the IFNβ response.

3.5. Further Studies

The wt and IFNβ$^{-/-}$ mice littermates used for investigating MHV-68 infection continued the results of the first experiment and suggested that virus might be trafficking to the spleen faster in the IFNβ$^{-/-}$ mice. To confirm these results more mice were required. One problem that has arisen during the breeding of the matched littermates was that although the expected ratio of mice was 2:1:1 for heterozygous: wt: ko, more heterozygotes were usually obtained than expected and thus it was difficult to obtain sufficient numbers of wt or ko mice. It was therefore decided to backcross the IFNβ$^{-/-}$ mice onto wt129 to produce IFNβ$^{-/-}$ mice on the 129/Sv/Ev background. After two years of crossing, backcrossed homozygous IFNβ$^{-/-}$ and wt mice were obtained following approximately seven generations. Unfortunately, there was an outbreak of mouse hepatitis virus in the animal unit in which they were being housed. Neonatal IFNβ$^{-/-}$ mice appeared weak and the majority died before they could be weaned. Prior to the MHV infection there was no problem with the health of these mice and it is possible that the pups were succumbing to MHV infection. A decision was made to re-derive the IFNβ$^{-/-}$ mice from heterozygotes in order to

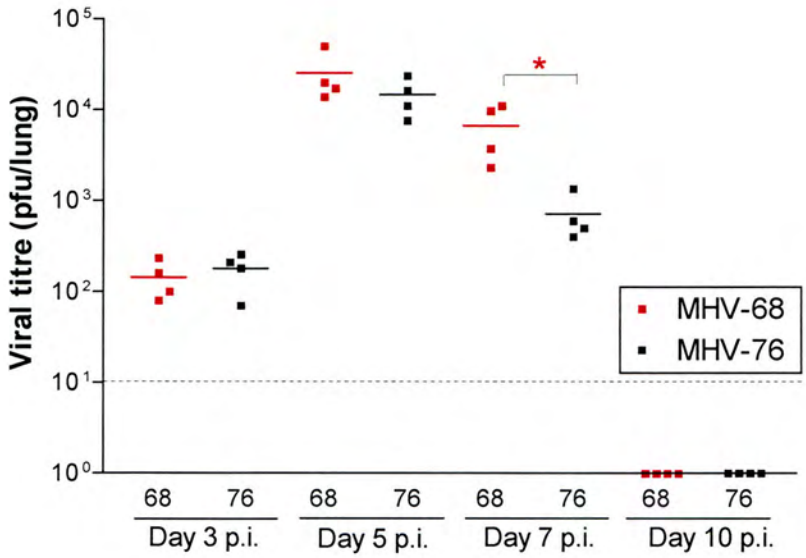

Figure 3.13. Viral titre in the lungs of IFNβ ko mice. Mice were infected intranasally with 4 x 10^5 pfu of either MHV-68 or MHV-76. Lungs were harvested at days 3, 5, 7 and 10 post-infection. Virus titre was determined by infectious virus assay. Each data point represents the virus titre from individual mice and the solid line represents the mean virus titre for each group. The dashed line represents the limit of detection (10 pfu) for this assay. Groups that have mean values that vary significantly ($p \leq 0.05$) by Mann Whitney test are indicated by *.

produce 'clean' mice. Therefore it was not possible to carry out further experiments in the available time.

3.6. Analysis of MHV-68 cell tropism

IFNβ is expressed at early time points following viral infection and is secreted from infected cells to protect neighbouring cells in a paracrine fashion. In IFNβ$^{-/-}$ mice, the IFNβ promoter drives expression of GFP and therefore, GFP should be expressed in and around MHV-68 infected cells. It was decided to utilise this system to investigate the extent of MHV-68 infection in the lung and proceed to determine the MHV-68 cell tropism. IFNβ$^{-/-}$ and wt 129/Sv/Ev mice were infected intranasally with 4 x 10^5 pfu of MHV-68. Lungs were harvested at day 5 post-infection, re-inflated and frozen before cryostat sections were prepared. Sections were examined under a fluorescent microscope for the presence of GFP-expressing cells, signalling the induction of IFNβ following infection. Unfortunately, no GFP-expressing cells could be detected and it was postulated that this may have been due to high background fluorescence. It was suggested that paraformaldehyde used for fixation may have been contributing to background fluorescence via binding to elastin in the lung tissue. However, when unfixed sections were examined background fluorescence remained high. It was decided to try a slow freezing protocol designed to better preserve the structure of the fluorescent protein (Shariatmadari *et al.*, 2001). When sections were examined, the background fluorescence was reduced but no GFP expression could be detected. Similarly, infection of IFNβ$^{-/-}$ MEF monolayers with MHV-68 (MOI of 5 pfu/cell) failed to generate detectable GFP by examination under a fluorescence microscope. As GFP could not be detected the cell tropism of MHV-68 was not investigated further.

3.7. Discussion

This study has used *in vitro* assays and transgenic mice to further understanding of the type I IFN response to MHV-68 infection. The kinetics of IFN expression following MHV-68 and MHV-76 infection were investigated by RT-PCR analysis. To the best of my knowledge, this is the first study to show definitively that MHV-68 leads to the induction of type I IFN at early time points post-infection. As expected, IFNα4 and IFNβ transcripts were detected early post-infection, followed by the expression of the other IFNα subtypes (IFNnonα4). This supports previous studies in which IFNβ and IFNα4 were found to be expressed almost immediately, amplifying their expression through induction of IRF-7 which subsequently leads to the expression of other IFNα subtypes (Marie *et al.*, 1998; Prakash *et al.*, 2005). A recent study has shown that there are cell-type specific differences in the mechanism of type I IFN production. IFN production was determined to be IRF-7 dependent in most tissues, including the lungs, of influenza virus-infected mice, consistent with the requirement of a positive feedback loop. However, plasmacytoid dendritic cells (pDCs) in the spleen constitutively expressed high levels of IRF-7 and thus produced high levels of type I IFN rapidly in response to virus infection (Prakash *et al.*, 2005). It is likely that positive feedback is the mechanism of type I IFN induction in the tissue culture cell lines employed in this *in vitro* assay. Some viruses such as lymphocytic choriomeningitis virus induce IFN only by positive feedback as they do not stimulate IFN production from pDCs (Dalod *et al.*, 2002). This study has shown that MHV-68 can induce type I IFN during *in vitro* infection. However, given the difference in host responses between viruses *in vivo*, it would be of interest to further investigate mechanisms of type I IFN induction in various cell types and tissues in response to gammaherpesvirus infection *in vivo*. Previous studies investigating the ISGF3 and ISG54 responses to HSV-1 did not observe their induction following CHX treatment alone (Nicholl *et al.*, 2000; Preston *et al.*, 2001). However, the experiments in this study to investigate the effect of CHX treatment were unsuccessful as inconsistent detection of IFN was obtained following treatment with CHX alone and CHX + MHV-68. Further optimisation of the duration of CHX pre-treatment and concentrations used may help to resolve these problems.

There did not appear to be a considerable difference in the kinetics of IFN induction following infection with MHV-68 compared to MHV-76. The later detection of IFNnonα4 after infection with MHV-76, as shown in figure 3.2, is likely due to the sample to sample variation of the assay as the detection of transcripts during both MHV-68 and MHV-76 infection varied between 2 and 3 hours in both repeats of this assay. IFNβ can be detected by 1 hour post-infection with MHV-68 but following infection with MHV-76, IFNβ transcripts could only be detected by 2 hours post-infection. It is possible that a gene present in MHV-68, but not MHV-76, might be responsible for the difference. For example, M4 is an immediate-early gene of MHV-68 that could result in induction of an earlier IFNβ response. Alternatively, it may be that the level of IFNβ is at or around the limit of detection of this assay at around 1 to 2 hours post-infection and there is no difference between MHV-68 and MHV-76's ability to induce IFNβ. Further analysis and experimental repeats are required before firm conclusions can be drawn about the induction of IFNβ following infection with MHV-68 compared to MHV-76. Real-time PCR analysis may help to elucidate whether there is a quantitative difference in the induction of IFNβ following infection with either MHV-68 or MHV-76. These data suggest that there is no down-regulation of IFN expression by components of the left end of MHV-68. However, M2, present in MHV-68 but absent from MHV-76, has been implicated in inhibition of type I IFN responses when expressed by means of a vector system (Liang *et al.*, 2004). It may be that the system used to express M2 alone does not accurately reflect conditions during infection where M2 may not be expressed to such high levels and thus would not have such an antagonistic effect on IFN responses. Furthermore, M2 is a latency-associated transcript which is inconsistent with a role for evasion of type I IFN.

Analysis of MHV-68 replication *in vitro* was carried out in cell lines deficient in IFNα/β, IFNβ or wt. MEFs deficient in the type I IFN receptor showed a trend towards higher viral titres than the $IFN\beta^{-/-}$ or wt MEFs. In addition, a higher proportion of virus in the IFNα/β $R^{-/-}$ MEFs appeared to be found in the cell

supernatant. In comparison, more virus appeared to be cell-associated rather than cell-free in the IFNβ$^{-/-}$ and wt MEFs. There did appear to be slightly more virus in the supernatant of the IFNβ$^{-/-}$ MEFs compared to wt MEFs, suggesting that a lack of IFNβ did allow increased virus exit into the cell supernatant. This effect was not as pronounced as for the IFNα/β R$^{-/-}$ MEFs, most likely as relatively efficient control of virus release was maintained through the presence and action of IFNα. These data suggest that the exit of virus particles is inhibited by type I IFNs. Following replication in the nucleus, viral capsids bud through the inner nuclear membrane, forming primary enveloped virions in the perinuclear space. After fusion of the primary envelope with the outer nuclear envelope, capsids are released into the cytoplasm before acquisition of tegument and envelope proteins through secondary envelopment into trans-golgi vesicles. Mature virions are released from the cell through binding of the vesicle membrane with the plasma membrane of the cell (Mettenleiter 2004). Following activation by type I IFNs, various ISGs are likely to interact with MHV-68 components throughout the process of viral egress, therefore inhibiting the exit of virions from the cell. Perhaps a lack of type I IFN leads to an overall lack of ISG induction in various sub-cellular compartments and therefore more MHV-68 virions exit from the cell. There are hundreds of identified ISGs but the functions and cellular locations of many are unknown. There is increasing evidence that many are important for control of virus infections. ISG60 is a type I IFN inducible protein and is upregulated 42-fold after HCMV infection of human foreskin fibroblasts. It has been shown to be clustered in the perinuclear space (Defilippis *et al.*, 2006; Yu *et al.*, 1997). Activation of murine ISG60 could lead to inhibition of MHV-68 virions budding through the perinuclear space and consequently limit viral titres. Similarly, ISG17 (IFN induced transmembrane protein 1) has a murine homologue and is upregulated >20-fold in response to both IFNα and IFNβ (Der *et al.*, 1998). Located in plasma membrane, it might play a role in inhibition of virus release from the cell (Tanaka *et al.*, 2005). ISG15 is an ubiquitin-like protein, activated by type I IFN, but also upregulated following herpesvirus infection. *In vitro,* HCMV infection leads to 13-fold up-regulation at 8 hours post-infection (Defilippis *et al.*, 2006). ISG15 inhibits the assembly and release of HIV-1

virions by interfering with the ubiquitin-dependent pathway used by the virus to exit the cell (Okumura *et al.*, 2006). Its importance during infection is further highlighted by the immune evasion strategy developed by influenza B virus whereby the NS1 protein blocks covalent linkage and thus ISG15 function (Yuan and Krug 2001). The importance of individual ISGs during MHV-68 infection could be determined by transgenic mouse or siRNA knockdown studies. Given the number of ISGs upregulated in response to type I IFN it is likely that there is a certain degree of redundancy, with many involved in MHV-68 control.

No statistical analysis was carried out on these data as the variation in titre range between the first experiment and further two repeats was too large to allow reliable interpretation. It is possible that the variation observed was due to the different passage numbers of the MEFs between experiments or the cells being in different states of health after thawing from liquid nitrogen.

The ability of the IFNβ$^{-/-}$ mice to control MHV-68 infection was assessed by infectious virus and *ex vivo* reactivation assays. Virus titres in the lungs of IFNβ$^{-/-}$ mice infected with both higher and lower doses of MHV-68 were significantly higher at the peak of acute infection (day 5 and 7 post-infection respectively) than in the wt groups. These data reflect those observed in IFNα/β R$^{-/-}$ mice where lung titres are significantly higher than in wt mice during acute infection (Dutia *et al.*, 1999). However, at time points other than the peak of acute infection, MHV-68 was controlled and cleared from the lung to a similar degree in both IFNβ$^{-/-}$ and wt mice. It is likely that the presence of other immune components, such as IFNα, results in compensation for the lack of IFNβ, allowing development of an efficient adaptive immune response and thus the relative control of MHV-68 infection in IFNβ$^{-/-}$ mice. As shown in the *in vitro* stimulation study, IFNα4 is expressed early after MHV-68 infection so may allow the host to mount an efficient immune response at early time points post-infection, even in the absence of IFNβ. Ideally these experiments would have been carried out with backcrossed mice. However, as encouraging results were

obtained with both the C57BL/6 and littermate control mice, and with two different virus doses, there is strong evidence that the data obtained in the lung reflects a difference of physiological significance and is not strain-dependent.

There was no significant difference in the ability of either group to control latent infection in the spleen after infection with 4 x 10^5 pfu of MHV-68. In the IFNα/β $R^{-/-}$ mice, latent virus is detected earlier in the spleen and reaches a peak approximately 10-fold higher than in wt mice (Dutia *et al.*, 1999). Mice lacking both IFNβ and IFNα lose control of virus replication to a greater extent as the immune response is not able to compensate as efficiently for the loss of both IFNα and IFNβ. It is possible that by the time latency is established, the lack of IFNβ is not important as the remaining IFNα is present to aid development of the adaptive immune response to MHV-68 infection. The use of a lower dose of virus (4 x 10^3 pfu) to expose subtle differences suggested that there may an increased latent viral load in the spleens of the $IFN\beta^{-/-}$ mice in comparison to the wt mice. At day 14 post-infection, the mean latent virus load in the $IFN\beta^{-/-}$ spleen was considerably higher than the mean load in the wt spleen but as there were only two mice in the $IFN\beta^{-/-}$ group, no statistical analysis could be carried out and no conclusions could be drawn from these data. The use of a lower virus dose did appear to aid detection of subtle pathogenic differences between the two groups. These experiments would have been repeated with larger group sizes in the backcrossed $IFN\beta^{-/-}$ mice but due to the presence of mouse hepatitis virus within the small animal facility this was not possible.

It would be of interest to further investigate the development of the immune response in the absence of IFNβ. Quantitative analysis of IFNα levels in the lung would elucidate whether IFNα was up-regulated to compensate for the absence of IFNβ or was lower due to a less efficient response to MHV-68 infection. Furthermore, analysis of other cytokines and cell subsets, such as IFNγ and NK cells, in the tissues

of wt, IFNα/β $R^{-/-}$ and $IFN\beta^{-/-}$ mice would help to elucidate the contribution of the type I IFNs to the development of downstream responses to MHV-68.

MHV-68 and MHV-76 infection was compared in the $IFN\beta^{-/-}$ lung. It was postulated that if a component of the left end of MHV-68 was involved in regulation of the IFNβ response, a lack of IFNβ would confer an advantage to MHV-76 and clearance from the lung would be similar to that of MHV-68. However, this was not the case as clearance from the $IFN\beta^{-/-}$ lung occurred with the same kinetics as observed in the wt lung: MHV-76 was cleared faster than MHV-68. Previous studies have shown that MHV-76 infection resulted in higher morbidity and mortality in IFNα/β $R^{-/-}$ mice, postulated to be due to an excessive inflammatory response to MHV-76 infection in comparison to MHV-68 infection. However, MHV-76 titres in the lung remained lower than the titres of MHV-68 at day 9 post-infection (Townsley 2004) showing that the lack of functional type I IFN did not result in enhanced lytic replication of MHV-76 over MHV-68. These findings are in support of the results obtained in the $IFN\beta^{-/-}$ lung. The MHV-76 lung titres were lower than MHV-68's leading to the suggestion that the morbidity and mortality was a result of a greater immune response due to the lack of immunomodulatory molecules in MHV-76 such as M3 (Townsley 2004). Unlike the IFNα/β $R^{-/-}$ mice, no increased morbidity or mortality was observed in the $IFN\beta^{-/-}$ mice. The most probable explanation for this is that the remaining IFNα species present during MHV-76 infection aided the control of virus replication to a higher extent than the IFNα/β $R^{-/-}$ mice and therefore the $IFN\beta^{-/-}$ mice do not develop an excessive inflammatory response. MHV-76 does not obtain a replication advantage in either the $IFN\beta^{-/-}$ or IFNα/β $R^{-/-}$ lung and this reflects observations in wt mice. These data suggest that components of the left end of the MHV-68 genome do not interfere greatly with the type I IFNs. Moreover, these data are supported by the results from the *in vitro* IFN induction assays where there was no evidence of MHV-68-mediated down-regulation of type I IFN induction compared to MHV-76 infection.

As the IFNβ$^{-/-}$ mice expressed GFP under the control of the IFNβ promoter it was of interest to examine the cell types expressing GFP (in place of IFNβ) following infection with MHV-68. However, no visible GFP could be detected in either cryostat sections of infected tissues or MEFs infected *in vitro* although genotype analysis proved that the GFP gene was present in the mice and cell lines used. In support of these findings, (Deonarain *et al.*, 2000) showed that GFP transcripts could be detected in MEFs by RT-PCR but GFP fluorescence in the tissues of IFNβ$^{-/-}$ mice could not be detected by FACS analysis. One reason for this problem might be that the IFNβ promoter is too weak to result in suitable levels of GFP to be detected by fluorescence microscopy. The use of a stronger form of GFP, such as enhanced GFP, would possibly aid detection and thus allow further analysis of the cell tropism of MHV-68.

Chapter 4: Investigating the function of ISG12 during MHV-68 infection

4. Investigating the function of ISG12 during MHV-68 infection

4.1. Introduction

The downstream effects of the Type I IFNs are important for the control of many herpesvirus infections and an antiviral state is mainly achieved through the activation of ISGs such as PKR and 2'-5' OAS (reviewed in section 1.5). ISG induction can be IFN-dependent but can also be stimulated directly in response to viral infection. Fibroblasts infected with HCMV show rapid expression of ISGs even in the presence of protein synthesis inhibitors and this IFN-independent regulation of ISG responses is thought to be due to the activation of IRF3 (Browne *et al.*, 2001; Defilippis *et al.*, 2006).

There are several ISGs for which there are no known cellular or biochemical functions. ISG12 is one such protein. Originally known as p27, it was later termed ISG12 to avoid confusion with other non-related genes such as p27kip and as it has a molecular weight of 12kDa. ISG12 was found to be preferentially upregulated in response to IFNα in a wide variety of cell types (Gjermandsen *et al.*, 2000) and sequence analysis showed that the promoter region contained putative ISRE, IRF1/IRF2 and STAT binding elements (Martensen *et al.*, 2001). ISG12 homologues can be found within a number of species including hamster, rat and mouse. It has also been shown to localise to the nuclear envelope in HeLa cells although its function in this location remains unknown (Martensen *et al.*, 2001). *In silico* analysis has suggested that there are three members of the murine ISG12 family: ISG12(a), (b1) and (b2) (Parker and Porter 2004). A study showed that during Sindbis infection, ISG12(b1) expression was expressed to a higher extent in 4 week old mouse brains, resulting in asymptomatic disease compared to 1 day old mouse brains where death occurred rapidly. Moreover, enforced expression of murine ISG12(b1) in 1 day old mice delayed mortality. These data suggest that up-regulation of ISG12(b1) has a protective effect against Sindbis infection (Labrada *et al.*, 2002).

Type I IFN is important for the control of gammaherpesvirus infections and ISGs are essential components of that innate immune response. It was hypothesised that mice lacking ISG12 would be unable to control MHV-68 infection as efficiently as wt mice. This study has utilised a strain of mice, termed np27$^{-/-}$, that lack ISG12(a), to investigate this hypothesis. The aims of this study were to (1) examine the function of ISG12(a) during MHV-68 infection *in vitro* and (2) elucidate the role for ISG12(a) during *in vivo* infection.

4.2. Genotyping of mice

Np27$^{-/-}$ mice were generated by Porter *et al.*, through disruption of the ISG12(a) gene by insertion of a construct containing eGFP (Porter, A., personal communication). Chimeras showing efficient germ-line transmission of the targeted gene were bred onto a wt 129/ola background. The genotypes of the np27$^{-/-}$ mice were checked by PCR analysis of DNA extracted from ear biopsy samples. A schematic diagram of the disrupted ISG12(a) gene is shown in figure 4.1 along with a representative example of the PCR analysis carried out on wt and np27$^{-/-}$ mice. The analysis proved that the np27$^{-/-}$ mice carried the targeting construct containing an eGFP gene and were negative for the ISG12(a) gene whereas wt control mice were positive for the presence of the ISG12(a) gene and negative for the eGFP targeting construct.

4.3. Characterisation of ISG12 *in vitro*

4.3.1. GFP expression *in vitro*

The np27$^{-/-}$ mice have an eGFP gene under the control of the ISG12 promoter so any cells responding to IFNα, and thus expressing ISG12(a), should be green following infection. It was of interest to investigate the ability of MHV-68 to stimulate ISG12(a) *in vitro* through examination of the eGFP expression. Mouse embryonic fibroblasts were generated from np27$^{-/-}$ embryos at 13.5 days gestation. Cells were left to settle in 6 well plates for 1 hour before the addition of various stimulants or

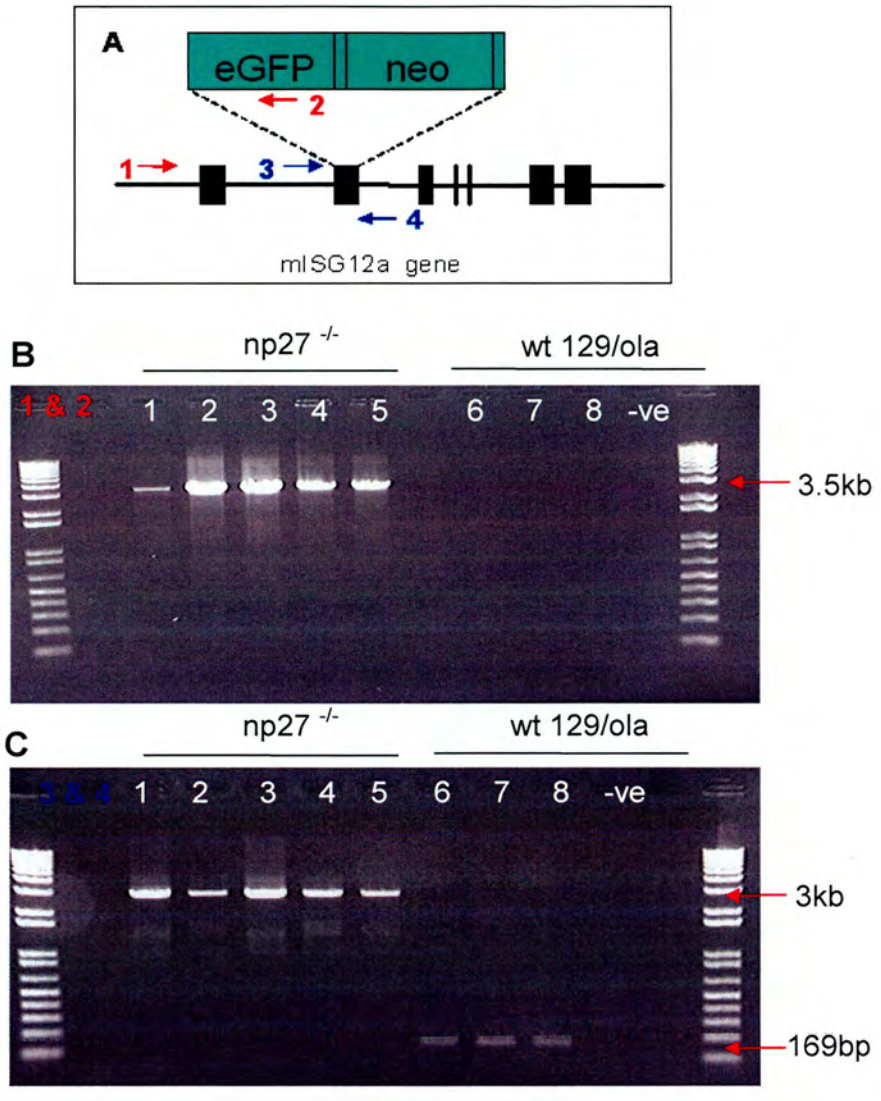

Figure 4.1. Genotypic analysis of np27$^{-/-}$ mice. (A) Schematic diagram of primer location within the ISG12(a) gene. eGFP denotes enhanced GFP and neo denotes neomycin. Primers 1 and 2 (TARG 1 and 2) are shown in red. TARG 1 is specific for the region out with the construct and TARG 2 is construct specific. Primers 3 and 4 (KO 3 and 4) are shown in blue. KO 3 & 4 amplify across exon 2 of the ISG12(a) gene. DNA was extracted from ear biopsy tissue. Panel B shows a representative PCR for the genotyping of np27$^{-/-}$ mice using primer set TARG 1 & 2. ko mice give a fragment of 3.5 kb whereas wt mice do not. Panel C shows a representative PCR using primer set KO 3 and 4. ko mice give a 3kb product from the targeted gene and wt mice give a 169bp product. For both B and C, numbers 1-5 show the results from np27$^{-/-}$ mice and 6-8 show the results from wt mice. A reaction containing no DNA template (-ve, negative) was included to control for cross-contamination of samples.

virus to induce activation of the ISG12 promoter and thus the eGFP reporter gene. MEFs were infected with MHV-68 or MHV-76 with a MOI of 5 or 0.5 pfu per cell and examined under an inverted fluorescent microscope at various intervals from 3 hours to 3 days post-infection. No fluorescence could be detected throughout the period of observation. It was postulated that the lack of visible fluorescence could be a MHV-68 specific effect. It was therefore decided to use other agents that are known to stimulate IFN responses to act as positive controls. Cells were stimulated with recombinant murine IFNα, poly I:C (a synthetic dsRNA), and Semliki Forest virus. Semliki Forest virus is a RNA virus known to stimulate readily detectable type I IFN responses *in vitro* (Baigent *et al.*, 2002). Nonetheless, no eGFP expression could be detected by examination under a fluorescent microscope at any time point post-infection, with any agent used. It was concluded that the lack of visible eGFP was not a virus-specific effect and was due to the cell line itself. Therefore, this investigative approach was not pursued further.

4.3.2. MHV-68 replication in a np27$^{-/-}$ cell line

Single step growth curves were carried out in order to assess the involvement of ISG12(a) during MHV-68 infection *in vitro*. As ISG12 is thought to be localised to the nuclear envelope, it was postulated that it might play a role in regulating the budding of MHV-68 particles from the nuclear envelope to the cytoplasm during replication. It was hypothesised that if ISG12 was interfering with the release of virus particles from the nucleus, virus titres would be increased in the np27$^{-/-}$ cell line where ISG12-mediated regulation was lost. The single replication cycle was assessed within mouse embryonic fibroblasts either with (wt) or without (np27$^{-/-}$) the ISG12(a) gene. Cells were infected with MHV-68 at an MOI of 5 pfu/cell and duplicate samples taken at intervals from 0 to 72 hours post-infection. At each time point, media was removed from the well and titrated separately from the cell monolayer to examine both cell-associated and cell-free virus. No supernatant sample was taken at 0 hours post-infection as cells had not settled into a monolayer so cell associated and cell free virus could not be separated. Samples were titrated in duplicate on BHK-21 cells. When cell-associated virus and cell-free virus were

examined in combination, it was evident that MHV-68 replicated with very similar kinetics in both cell types (figure 4.2). When examined individually, the titre of cell-associated virus appeared similar for both groups. However, the titre of cell-free virus in the np27$^{-/-}$ MEFS appeared to be slightly lower in comparison to the titre in wt MEFs at 12 and 24 hours post-infection. It was decided to repeat these two time points on two further occasions, to determine if the effect was reproducible. Cell-associated viral titres at 12 and 24 hours post-infection are shown in figure 4.3 and cell-free viral titres at 12 and 24 hours post-infection are shown in figure 4.4. From the repeat experiments it was evident that there was no difference in the ability of MHV-68 to replicate in wt or np27$^{-/-}$ MEFs. There was no difference in the titres of cell-associated, cell-free or combined virus between the np27$^{-/-}$ and wt MEFs. As the variation in titre range between the first experiment and the further two repeats was too large to allow reliable interpretation, no statistical analysis was carried out on these data.

4.4. Characterisation of ISG12 *in vivo*

4.4.1.Preliminary infection of np27$^{-/-}$ mice

The type I IFNs have been shown to be important for the control of gammaherpesvirus infections. As mentioned previously, knockout of the type I IFNs (by knockout of the shared receptor) causes mice to be more susceptible to MHV-68 infection (Dutia *et al.*, 1999). It was postulated that as ISG12 is a downstream effector of IFNα, mice in which ISG12 is absent may be less able to control infection due a less efficient innate response. In order to assess the contribution of ISG12(a) during *in vivo* infection, np27$^{-/-}$ and wt 129/Sv/Ev mice were infected intranasally with 4 x 10^5 pfu of MHV-68. No wt 129/ola mice were available for use at the time the experiment was set-up so wt 129/Sv/Ev were used as the closest available matched controls for the preliminary experiment. Tissues were harvested at 5 and 7 days post-infection with four mice per group per time point. This experiment was termed experiment I. Real-time PCR was carried out on DNA extracted from lung, MLN and spleen in order to examine the viral load in these tissues. The level of virus

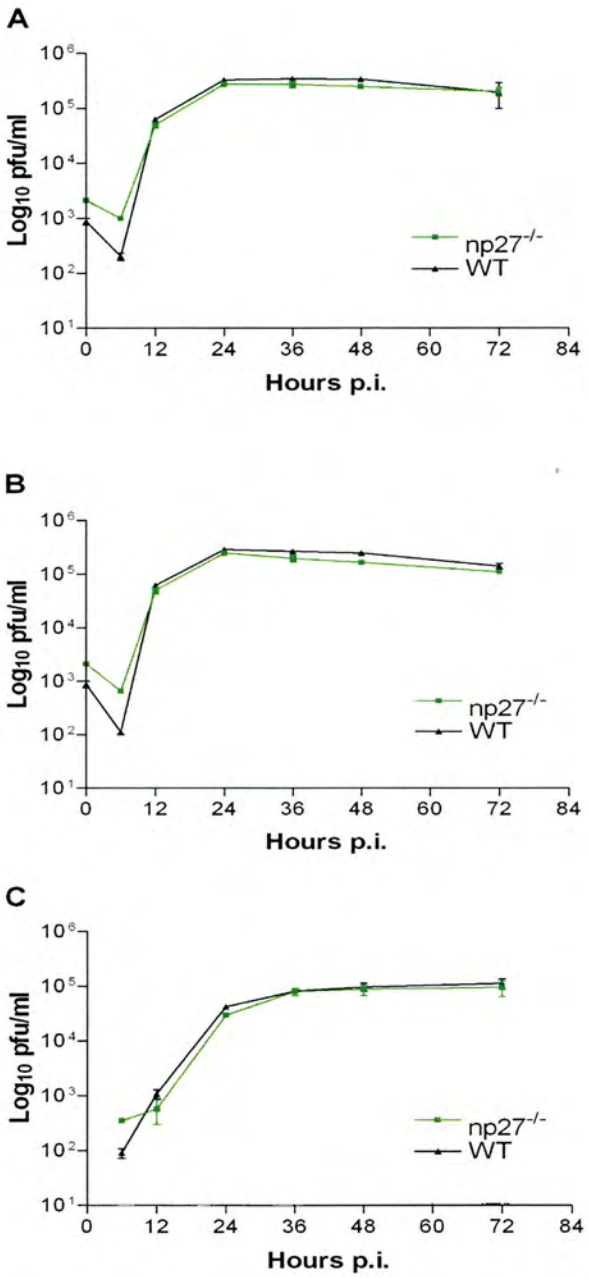

Figure 4.2. Single-step replication of MHV-68 in np27$^{-/-}$ and wt MEFs *in vitro*. Cells were infected with an MOI of 5 pfu/cell and harvested at various times p.i. Values represent two separate experiments with each sample titrated in duplicate. Data points represent the $\log_{10}$ of the virus titre ± standard error of the mean (SEM). The combined viral titres from both the cells and the cell supernatant are shown in panel A. B represents cell associated virus only and C represents virus within the supernatant only.

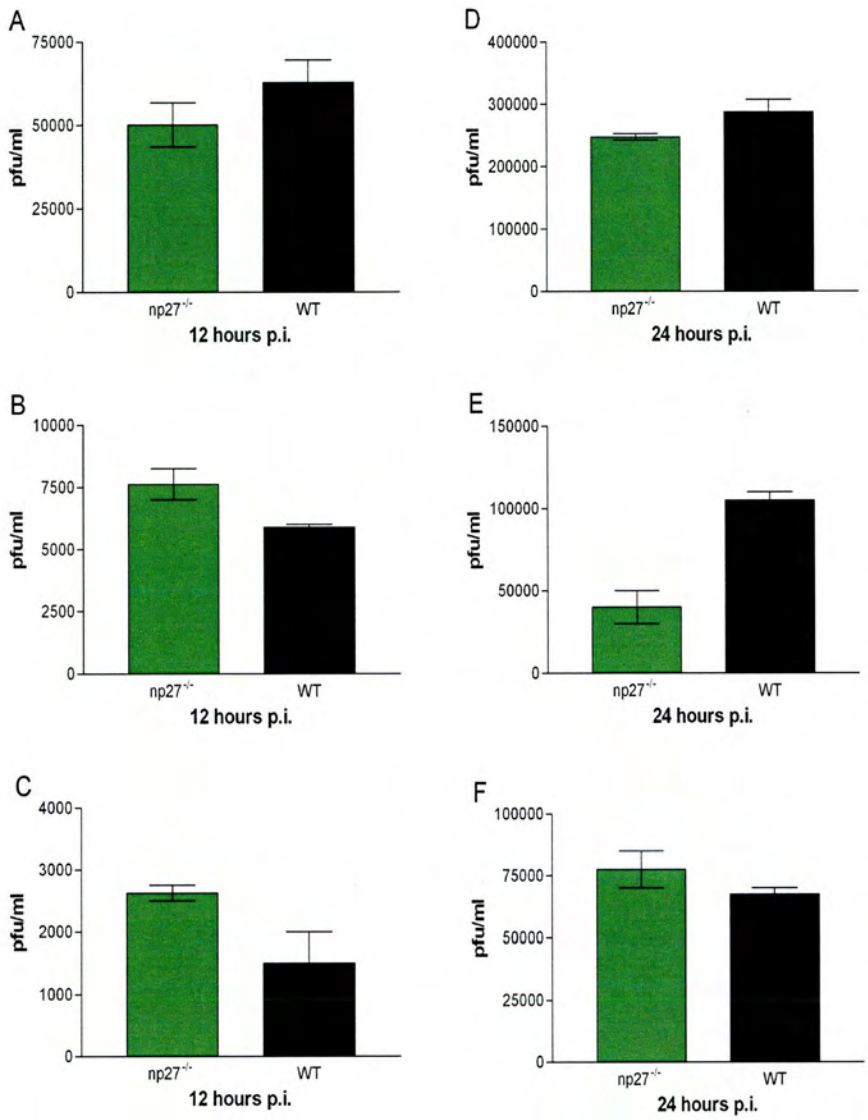

Figure 4.3. Titres of cell-associated virus in np27$^{-/-}$ and wt MEFs at 12 and 24 hours p.i. MEFs were infected with MHV-68 at an MOI of 5 pfu/cell and harvested after 12 (A-C) or 24 (D-F) hours p.i. Each time point was assayed independently on three occasions and each experiment is shown as a separate graph. Cell supernatant was removed and assayed separately (see figure 4.4). Values represent the virus titre ± standard error of the mean (SEM) from two independent experiments with each sample titrated in duplicate. Green bars denote np27$^{-/-}$ MEFs and black bars denote wt MEFs.

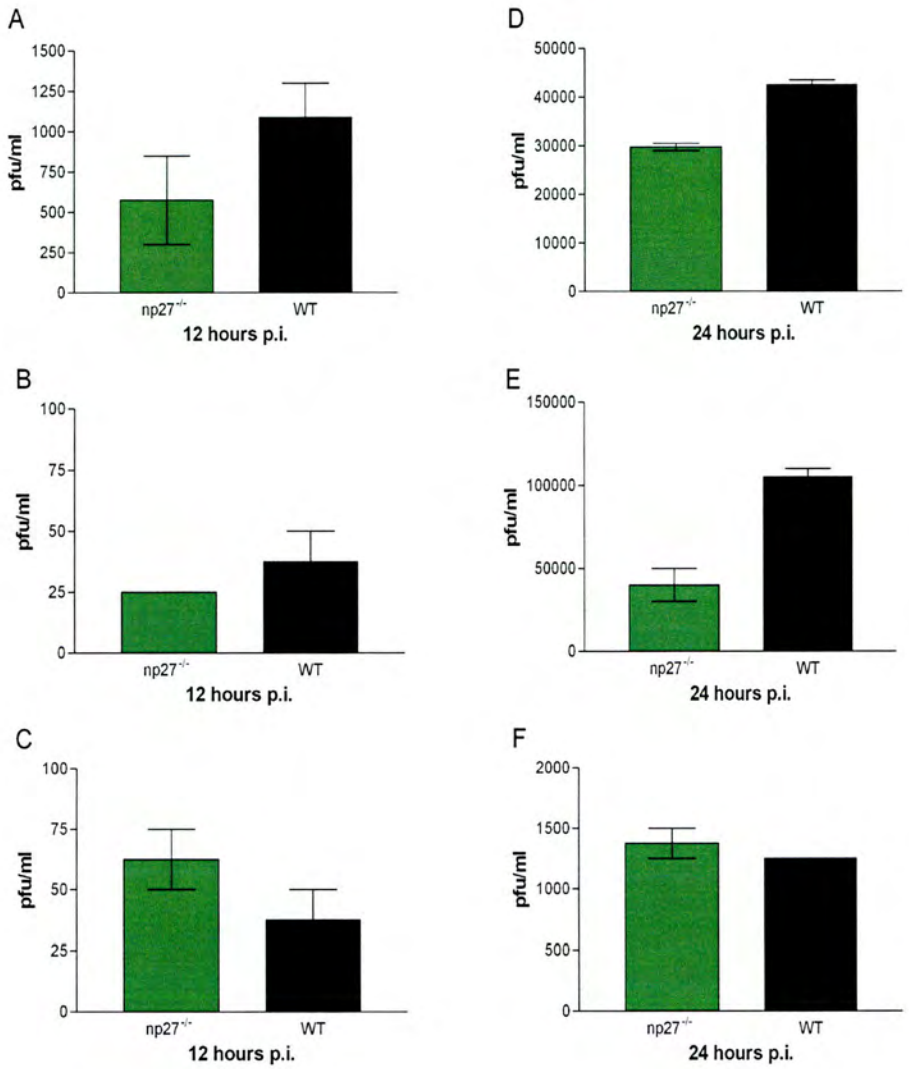

Figure 4.4. Titres of cell-free virus from np27$^{-/-}$ and wt MEFs at 12 and 24 hours p.i. MEFs were infected with MHV-68 at an MOI of 5 pfu/cell and harvested after 12 (A-C) or 24 (D-F) hours p.i. Each time point was assayed independently on three occasions and each experiment is shown as a separate graph. Cells were removed and assayed separately (see figure 4.3). Values represent the virus titre ± standard error of the mean (SEM) from two independent experiments with each sample titrated in duplicate. Green bars denote np27$^{-/-}$ MEFs and black bars denote wt MEFs.

DNA was measured by amplification of M3 and normalised to the level of β-actin within each sample. At day 5 and 7 post-infection there was no difference in viral load in the lung or MLN (figure 4.5). However, there did appear to be a trend towards higher viral loads in the spleens of $np27^{-/-}$ mice compared to wt mice at both time points investigated (figure 4.6). At day 5 post-infection, 100% (4/4) of $np27^{-/-}$ spleens contained detectable virus compared to only 25% (1/4) of the wt spleens although this was not significant by Mann Whitney test (p=0.0571). Similarly, there appeared to be an increased degree of splenomegaly in the $np27^{-/-}$ spleens at day 7 post-infection compared to the wt spleens but again, this was not significant (p=0.0571).

4.4.2. Acute infection within the lung and MLN

Previous experiments using the $IFN\beta^{-/-}$ mice showed that infecting with a low dose of virus can help to elucidate subtle pathogenic differences that may be masked when using a higher dose of virus. As there appeared to be a subtle difference between the $np27^{-/-}$ and wt groups it was decided to repeat the experiment using 4×10^3 pfu of MHV-68 instead of 4×10^5 pfu to further investigate the role of ISG12(a). Wt 129/ola mice were used as strain-matched controls. $np27^{-/-}$ and wt 129/ola mice were infected intranasally with 4×10^3 pfu of MHV-68 and tissues harvested at 4, 8, 12 and 16 days post-infection. Due to a limited number of wt 129/ola mice at the time of infection, no control group was investigated at day 4 post-infection. As in the previous experiment, real-time PCR was carried out to investigate the viral load within the lungs, MLNs and spleens of $np27^{-/-}$ and wt 129/ola mice. This experiment was termed experiment II. There was no significant difference in viral load in the lungs between the $np27^{-/-}$ and wt groups at any time point investigated (figure 4.7). Similarly, the MLNs of the $np27^{-/-}$ and wt mice contained viral loads that did not differ significantly at any time point investigated (figure 4.8).

The experiment was repeated with the lower dose of virus. Again, $np27^{-/-}$ and wt 129/ola mice were infected intranasally with 4×10^3 pfu of MHV-68 and tissues

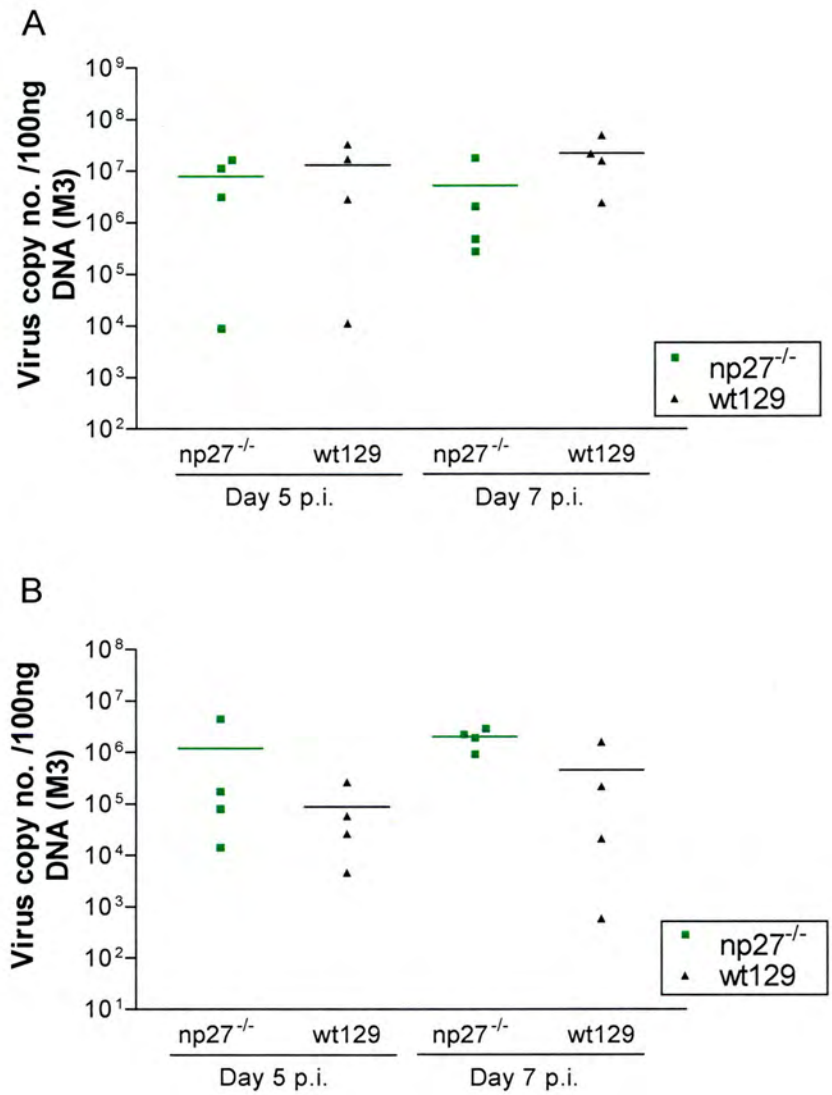

Figure 4.5. Experiment I. Viral load in the lungs (A) and MLNs (B) of np27$^{-/-}$ or wt 129/Sv/Ev mice. Mice were infected intranasally with 4 x 10^5 pfu of MHV-68. Tissues were harvested at day 5 and day 7 post-infection with 4 mice per group per time point. Viral load was determined by real time PCR using primers specific for the viral gene, M3 and normalised as determined by the level of β-actin within each sample. Each data point represents the viral load from individual mice and the solid line represents the mean viral load.

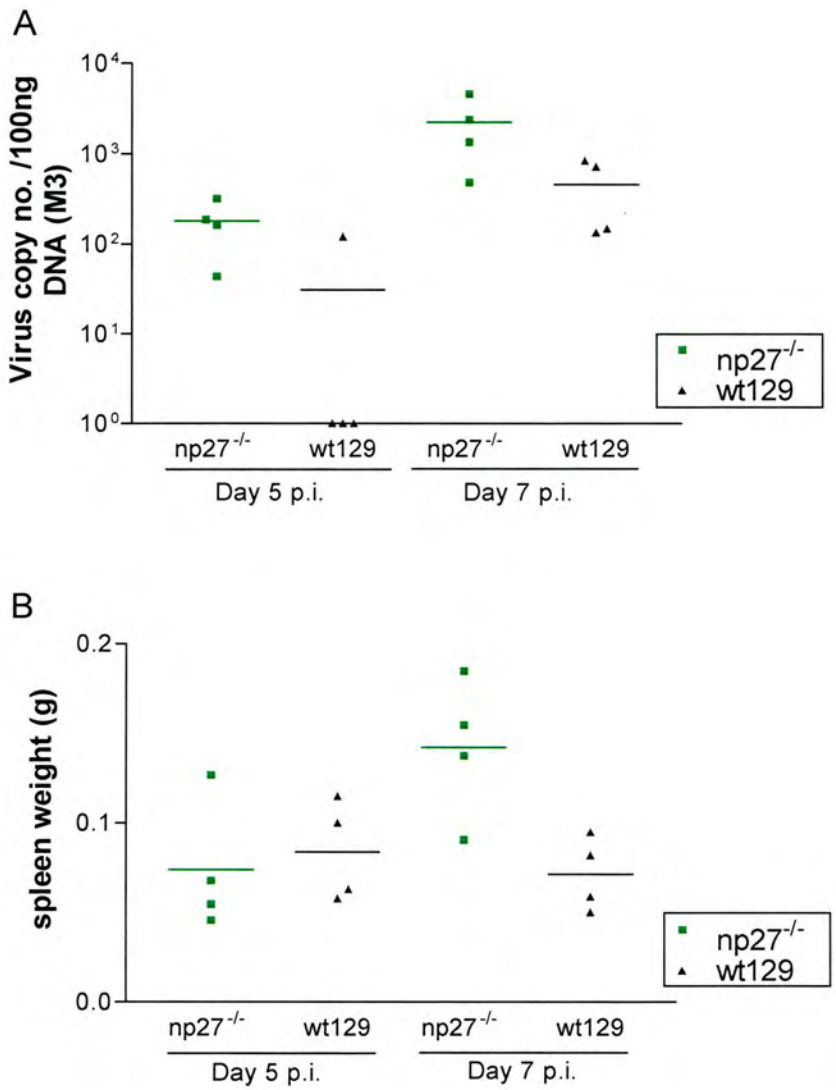

Figure 4.6. Experiment I. Viral load in the spleen (A) and spleen weight (B) in $np27^{-/-}$ and wt 129/Sv/Ev mice. Mice were infected intranasally with 4 x 10^5 pfu of MHV-68. Tissues were harvested at day 5 and day 7 post-infection with 4 mice per group per time point. Viral load (A) was determined by real time PCR using primers specific for the viral gene, M3 and normalised as determined by the level of β-actin within each sample. Each data point represents the viral load from individual mice and the solid line represents the mean viral load. In panel B, each data point represents the whole spleen weight from individual mice and the solid line represents mean spleen weight.

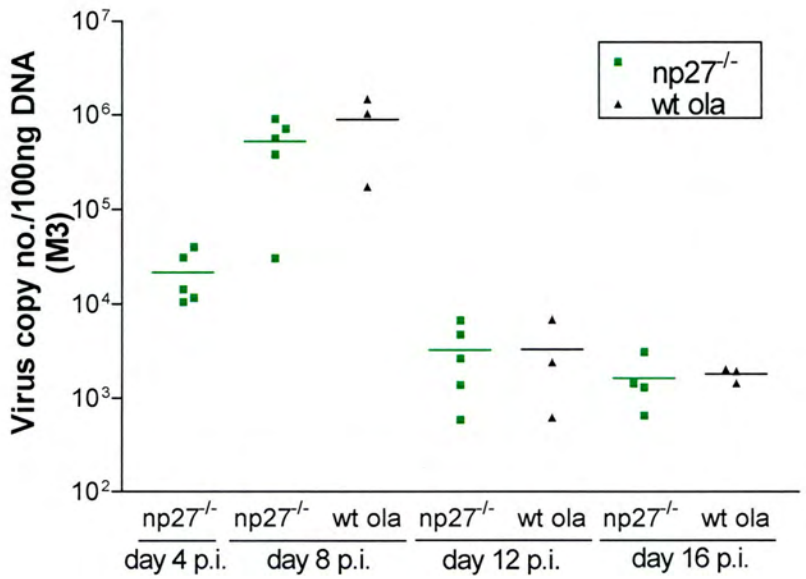

Figure 4.7. Experiment II. Viral load in the lungs of np27$^{-/-}$ or wt 129/ola mice. Mice were infected intranasally with 4 x 10^3 pfu of MHV-68. Tissues were harvested at days 4, 8, 12 and 16 post-infection. Viral load was determined by real time PCR using primers specific for the viral gene, M3 and normalised as determined by the level of β-actin within each sample. Each data point represents the viral load from individual mice and the solid line represents the mean viral load.

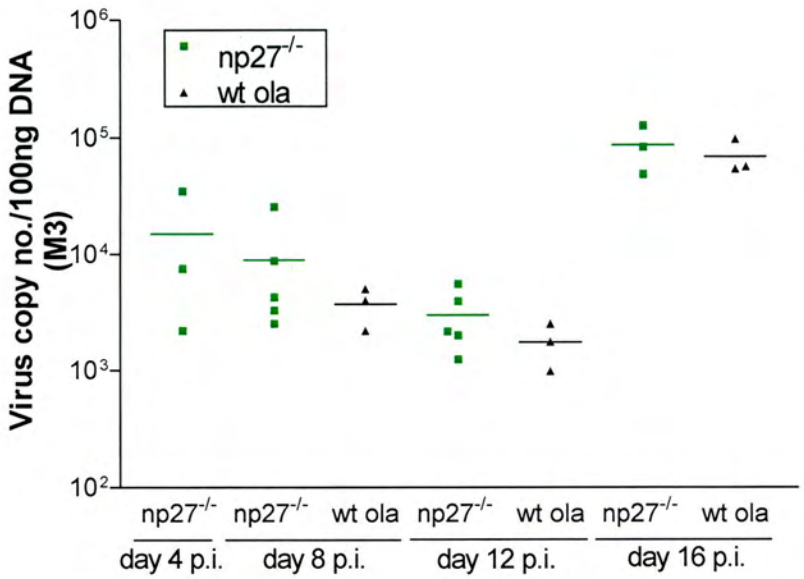

Figure 4.8. Experiment II. Viral load in the MLNs of np27$^{-/-}$ or wt 129/ola mice. Mice were infected intranasally with 4 x 10^3 pfu of MHV-68. MLNs were harvested at days 4, 8, 12 and 16 post-infection. Viral load was determined by real time PCR using primers specific for the vIral gene, M3 and normalised as determined by the level of β-actin within each sample. Each data point represents the viral load from individual mice and the solid line represents the mean viral load.

harvested at 4, 8, 12 and 16 days post-infection. In this case, viral load was investigated by infectious virus assay as well as real-time PCR to determine if the titre of replicating infectious virus differed with respect to viral load. This experiment is referred to as experiment III. There was no significant difference in viral load in the lungs between the np27$^{-/-}$ and wt groups at any time point investigated (figure 4.9). Figure 4.9 also shows that there was no significant difference in the titre of infectious virus in the lungs of either group. Similarly, the viral load in the MLNs of the np27$^{-/-}$ and wt mice (figure 4.10) was equivalent at all time points investigated. Due to the relatively small cell numbers within the MLNs post-infection it was decided to analyse viral load by quantitative PCR only. These data are in agreement with the findings in both the lungs and MLNs from experiment II. These data suggest that ISG12(a) does not play an important role for the control of lytic MHV-68 replication in the lung and nor does it influence the trafficking of virus from the lung to the MLN.

4.4.3. Establishment of latency within the spleen

During MHV-68 infection, virus is detectable in the spleen by approximately day 3 post-infection. From this point there is a rapid increase in the number of latently infected splenocytes and an accompanying splenomegaly. The viral load in the spleen following MHV-68 infection of np27$^{-/-}$ and wt 129/ola mice was determined by real-time PCR (experiment II). As shown in figure 4.11, virus was detectable in both groups by day 8 post-infection. The viral load in the np27$^{-/-}$ spleens was significantly higher ($p=0.0357$) than in the wt spleens at day 8 post-infection. By day 12 post-infection, the viral load was no longer significantly different between the np27$^{-/-}$ and wt groups and this remained the case at day 16 post-infection. The degree of splenomegaly was assessed by whole spleen weight. The np27$^{-/-}$ group exhibited a significantly higher degree of splenomegaly at day 8 post-infection than the wt group ($p=0.0357$) (figure 4.11, experiment II). The later time points investigated were not significantly different but there was a trend at day 12 and 16 post-infection for the np27$^{-/-}$ spleens to display a higher degree of splenomegaly than the wt spleens.

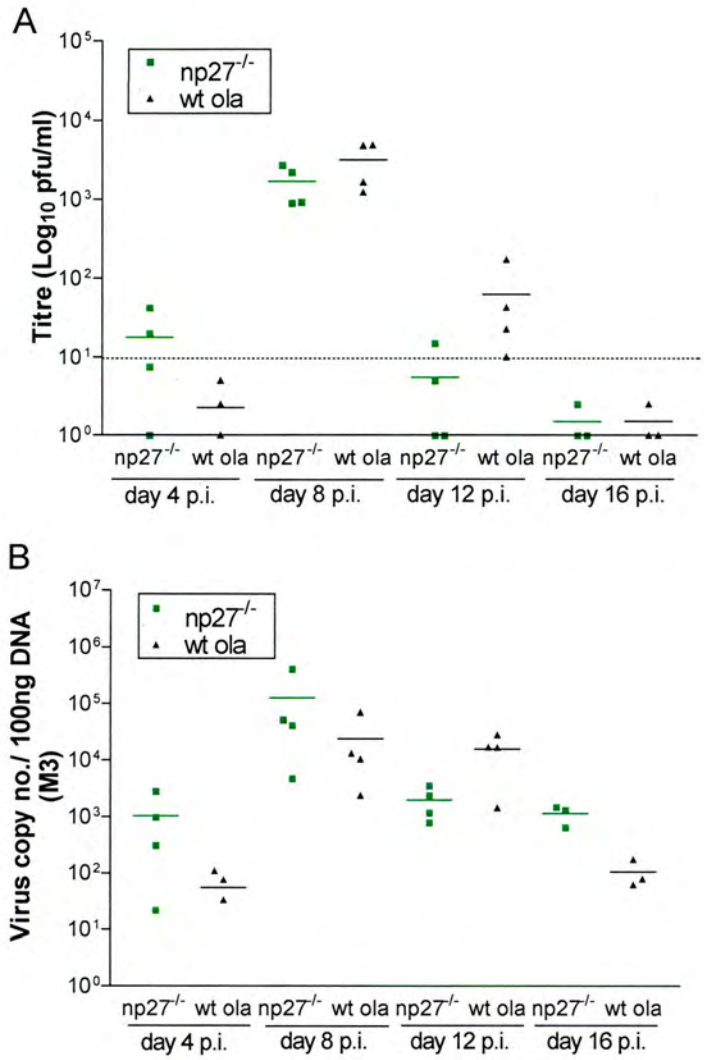

Figure 4.9. Experiment III. Virus titre (A) and viral load (B) in the lungs of np27$^{-/-}$ or wt 129/ola mice. Mice were infected intranasally with 4 x 10^3 pfu of MHV-68. Tissues were harvested at days 4, 8, 12 and 16 post-infection. Virus titre was determined by infectious virus assay and viral load was determined by real time PCR using primers specific for the viral gene, M3 and normalised as determined by the level of β-actin within each sample. Each data point represents either the virus titre (A) or viral load (B) from individual mice and the solid line represents the mean virus titre or viral load. The dashed line represents the limit of detection (10 pfu) for this assay.

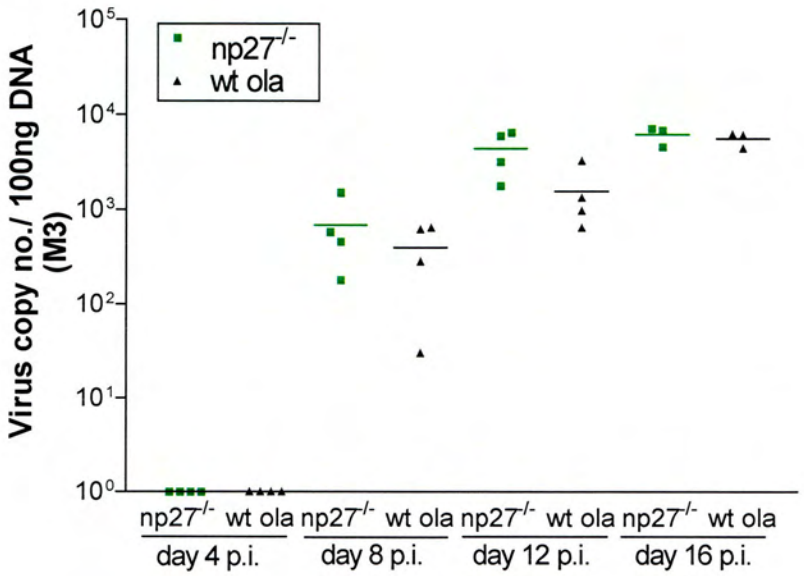

Figure 4.10. Experiment III. Viral load in the MLNs of np27$^{-/-}$ or wt 129/ola mice. Mice were infected intranasally with 4 x 10^3 pfu of MHV-68. MLNs were harvested at days 4, 8, 12 and 16 post-infection. Viral load was determined by real time PCR using primers specific for the viral gene, M3 and normalised as determined by the level of β-actin within each sample. Each data point represents the viral load from individual mice and the solid line represents the mean viral load.

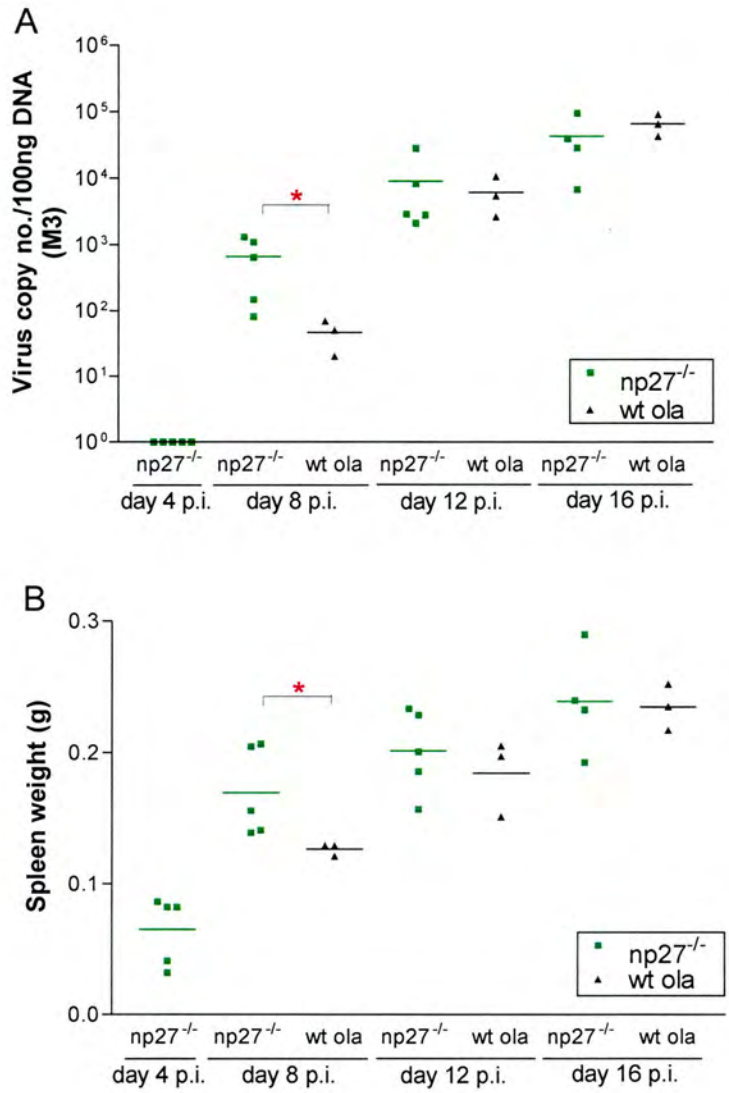

Figure 4.11. Experiment II. Spleen viral load (A) and spleen weight (B) in np27$^{-/-}$ and wt 129/ola mice. Mice were infected intranasally with 4 x 10^3 pfu of MHV-68. Tissues were harvested at days 4, 8, 12 and 16 post-infection. Viral load (A) was determined by real time PCR using primers specific for the viral gene, M3 and normalised as determined by the level of β-actin within each sample. Each data point represents the viral load from individual mice and the solid line represents the mean viral load. In panel B, each data point represents the whole spleen weight from individual mice and the solid line represents mean spleen weight. Groups that have mean values that vary significantly ($p \leq 0.05$) by Mann Whitney test are indicated by *.

The experiment was repeated (experiment III). MHV-68 infection was investigated by real-time PCR as well as *ex vivo* reactivation assay to determine if the viral load differed from the number of latently cells. Figure 4.12 shows that virus was detectable in 3/4 np27$^{-/-}$ samples and 2/4 wt samples by *ex vivo* reactivation assay, and virus was detectable in 4/4 samples of both groups by real-time PCR by day 8 post-infection. At day 12 post-infection, the viral load in the np27$^{-/-}$ spleen was significantly higher ($p=0.0286$) compared to the viral load in the wt mice. The difference was confirmed in an *ex vivo* reactivation assay (figure 4.12) as the titre of latent virus in the np27$^{-/-}$ spleen was significantly higher ($p=0.0286$) than the titre in the wt spleen. It was speculated that the apparently higher viral load in the np27$^{-/-}$ spleen may have been due to infectious virus in the spleen as opposed to a latent infection. An infectious virus assay was carried out on the same number of splenocytes as used for the latent virus assay (figure 4.13). A maximum of 1 plaque was detected in 3 of 32 samples and thus the vast majority of virus detected in the *ex vivo* reactivation assay was a result of a latent infection. Similarly to experiment II, experiment III displayed a trend for the np27$^{-/-}$ spleens to exhibit a higher degree of splenomegaly than the wt mice although this was not significant at any time point investigated.

4.5. Discussion

ISGs have been shown to be activated in response to a number of herpesvirus infections. ISG12 mRNA was found to be increased 7-fold in response to HCMV infection of human fibroblasts (Zhu *et al.*, 1998). In this study, the role of ISG12(a) during MHV-68 infection has been investigated *in vitro* and *in vivo*. MEFs that express eGFP following activation of the ISG12 promoter were infected with MHV-68 in order to investigate the kinetics of ISG12 induction. However, no eGFP expression was visible under a fluorescent microscope from 3 hours up to 3 days post-infection. It was hypothesised that the lack of eGFP could be due to MHV-68 mediated down-regulation of ISG12(a) expression in order to evade its function. The phenomenon of ISG down-regulation has been observed during other herpesvirus

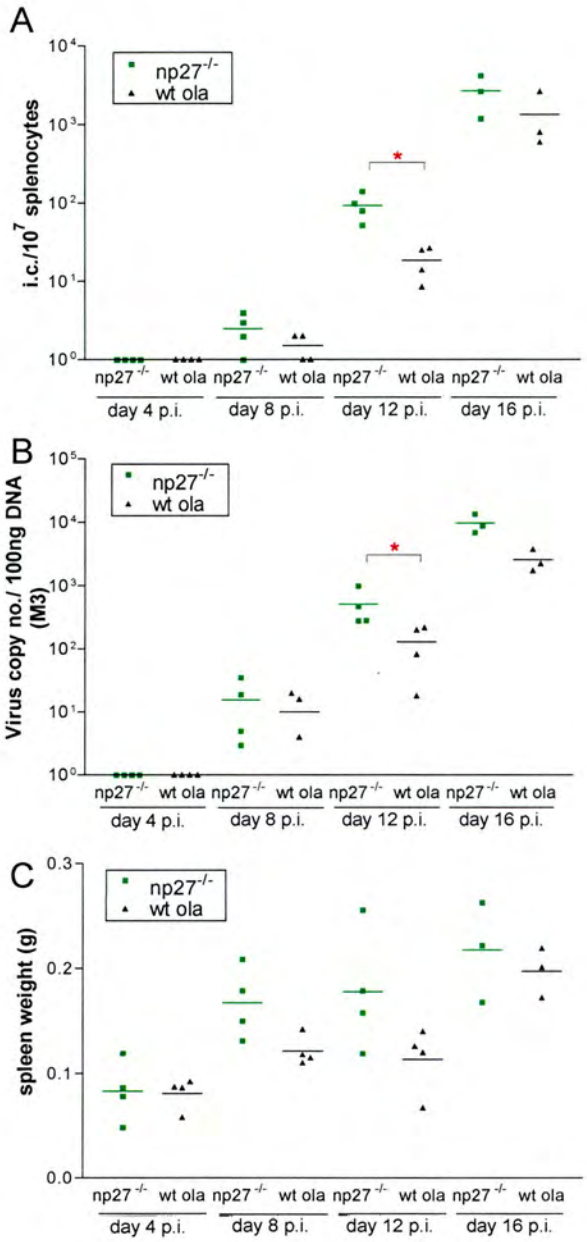

Figure 4.12. Experiment III. Spleen latent virus (A), viral load (B) and weight (C) in np27$^{-/-}$ and wt 129/ola mice. Mice were infected intranasally with 4 x 10^3 pfu of MHV-68. Spleens were harvested at days 4, 8, 12 and 16 post-infection. Latent virus was determined by infective centre assay, viral load was determined by real time PCR using primers specific for the viral gene, M3 and normalised as determined by the level of β-actin within each sample. Each data point represents individual mice and the solid line represents mean values. Groups that have mean values that vary significantly ($p \leq 0.05$) by Mann Whitney test are indicated by *.

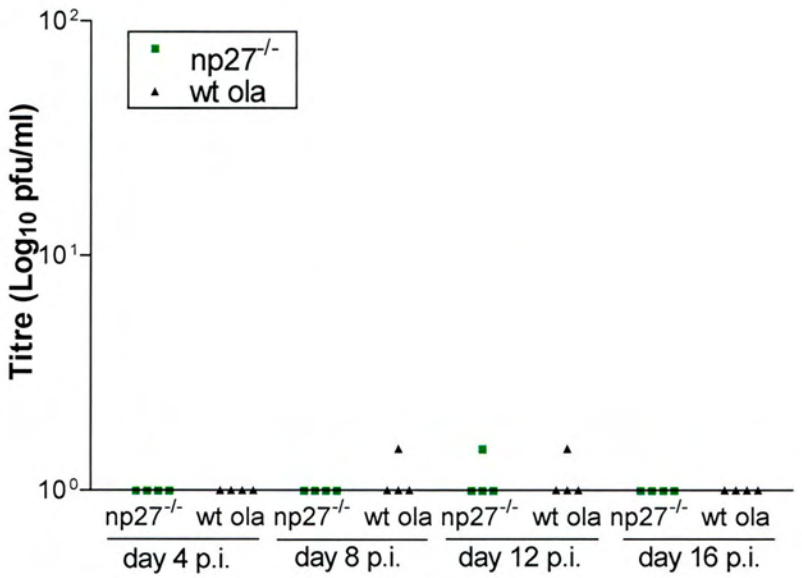

Figure 4.13. Experiment III. Infectious virus in the spleens of np27$^{-/-}$ or wt 129/ola mice. Mice were infected intranasally with 4 x 10^3 pfu of MHV-68. Tissues were harvested at days 4, 8, 12 and 16 post-infection. Virus titre was determined by infectious virus assay Each data point represents the virus titre from individual mice.

infections. ISG induction occurs upon HSV-1 entry to the cell, but only in the absence of viral protein synthesis, thus suggesting that a viral protein may disarm the response following the onset of HSV-1 gene expression (Mossman *et al.*, 2001). In order to determine if the lack of ISG12(a) activation was a MHV-68 specific effect, other agents known to be adequate inducers of IFNα and therefore ISGs were investigated for their ability to stimulate ISG12(a). However, no eGFP expression was detected after treatment with IFNα, poly I:C or SFV. These results suggest that the lack of eGFP expression was not a MHV-68-mediated effect and was due to the cell line itself. It has previously been shown that ISG12 expression is variable in different cell types. For example, in HeLa (epithelial) cells there was a 100-fold increase in the level of human ISG12 in response to IFNα and 14-fold increase in response to poly I:C. In contrast, there was only a 3-fold induction of ISG12 in response to IFNα and 2-fold induction in response to poly I:C in HT1080 (fibroblast) cells (Gjermandsen *et al.*, 2000). It is possible that the murine fibroblasts are inadequate inducers of ISG12(a) in response to MHV-68. The ISG12 promoter may not be strong enough to result in sufficient, visible levels of eGFP expression. The presence of eGFP transcripts should be verified by RT-PCR to ensure that the GFP construct is activated and expressing properly. However, such analysis was not carried out due to time constraints.

Certain ISGs have been shown to limit virus replication or release *in vitro*. For example, ISG15, a ubiquitin-like protein, has been shown to inhibit the assembly and release of HIV-1 virions by interfering with the ubiquitin-dependent pathway used by the virus to exit the cell (Okumura *et al.*, 2006). Interestingly, ISG12 is the first ISG found to be localised to the nuclear membrane and is hypothesised to interact with the nuclear pore complex, although this is yet to be determined (Martensen *et al.*, 2001). It was hypothesised that ISG12(a) may play a role in regulation of MHV-68 particle release from the nuclear envelope to the cytoplasm during replication. Subsequently, a lack of ISG12(a) would lead to increased release of virus particles and therefore elevated viral titres. Analysis of MHV-68 replication was carried out in np27$^{-/-}$ and wt MEFs *in vitro*. There was no difference in cell-free, cell-associated or

combined virus titres between np27$^{-/-}$ and wt MEFs at any time point investigated. When viral titres at 12 and 24 hours post-infection were investigated in two further repeat experiments, no consistent trend for either cell-free or cell-associated virus could be determined between the np27$^{-/-}$ and wt cell lines. The differences observed between experimental repeats are likely due to differences in assay set up rather than the presence or absence of ISG12(a). It is possible that the variation was due to different cell line passage numbers between experiments or the cells being in different states of health after thawing from liquid nitrogen. The results from this study indicate that ISG12(a) is not playing a major role in the regulation of MHV-68 release from the nuclear envelope into the cytoplasm, and is therefore not having a major effect on the resultant viral titres. Perhaps a degree of redundancy between ISGs allows for compensation and therefore there is no evident role for ISG12(a) *in vitro*. The high MOI used in this study may have made it difficult to observe the effect of the lack of ISG12(a) *in vitro*. A high MOI infection results in the infection of the majority of cells and therefore cell shut down rather than induction of ISGs and a protective state in non-infected cells. In future experiments a low MOI would help to elucidate a possible protective effect of ISG12(a) in neighbouring uninfected cells. To investigate ISG12's role in regulation of virus release in more detail it would be of interest to carry out electron microscopy in order to visualise the location of MHV-68 virions within compartments of the cell. This technique may help to elucidate whether the nuclear localisation of ISG12 is affecting the budding pathway of MHV-68. It may also be worth further investigating the nuclear localisation of ISG12 in MEFs by immunohistochemistry. Localisation to the nuclear envelope was confirmed in HeLa and 293 cells, both of human epithelial origin. There may be alternate localisations in other cell types such as fibroblasts, as well as differences between murine and human systems which should be confirmed to help elucidate protein function.

The ability of the np27$^{-/-}$ mice to control MHV-68 infection was assessed by quantitative PCR, infectious virus and *ex vivo* reactivation assays. The level of lytic replication in the lungs of np27$^{-/-}$ and wt mice was found to be similar by both

quantitative PCR and infectious virus assay at all time points investigated. Challenge with a lower dose of virus failed to elucidate any subtle differences in the lungs between the two groups. These data suggest that ISG12(a) does not play a central role in the control of lytic MHV-68 replication in the lung. This result was surprising as it was hypothesised that a lack of ISG12(a) would result in a less efficient innate immune response and thus a higher amount of viral replication at early times post-infection. In further study it would be of interest to assess if there was any difference in the extent of acute infection between np27$^{-/-}$ and wt mice at days 1 to 3 post-infection. This would elucidate whether the function of ISG12(a) is evident at earlier time points than were assayed in this study. Viral load in the MLNs of the np27$^{-/-}$ and wt mice were examined by quantitative PCR. Virus copy number did not differ significantly at any time point investigated. Virus did not appear to be cleared from the lung quicker, nor did it become detectable earlier or to a higher extent in the np27$^{-/-}$ MLN. These results suggest that ISG12(a) does not influence the trafficking of virus from the lung to the MLN.

These data show that a lack of ISG12(a) leads to higher latency load in the spleen and a trend for a higher degree of splenomegaly from 8 days post-infection onwards. This outcome was indicated during infection with 4 x 10^5 pfu of MHV-68 and was confirmed in the two experiments investigating infection with 4 x 10^3 pfu of MHV-68. These experiments show that the role of ISG12 can be better studied after lower dose challenges. It was hypothesised that viral load may not accurately reflect the level of virus that was able to establish a latent infection and perhaps the increased viral load in np27$^{-/-}$ mice was not entirely due to the presence of latent virus. Both the quantitative PCR and the *ex vivo* reactivation assays gave the same result. In each case the real-time data closely reflected the data from the infectious virus and *ex vivo* reactivation assays, although the real-time PCR assay did appear to be more sensitive. Importantly, the viral load equated to the level of *ex vivo* reactivation showing that there are higher numbers of latently infected cells in the np27$^{-/-}$ mice. Infectious virus can only be detected in the lungs of wt mice whereas it can be detected in other tissues of some immunodeficient strains such as the IFNα/β R$^{-/-}$

mice (Barton *et al.*, 2005). The increased level of virus in the np27$^{-/-}$ spleens was not due to infectious virus and the lack of ISG12(a) did not result in lytic infection outside of the lung. Therefore, the increased level of virus detected in the np27$^{-/-}$ spleen was due to the absence of ISG12(a), resulting in an elevated latent infection compared to the wt spleen. Overall, it can be concluded that ISG12(a) plays an important role in the early stages of the establishment of latency.

As shown previously, there was no difference in either clearance of virus from the lung or viral load in the MLN between the np27$^{-/-}$ and wt mice. These data suggest that ISG12(a) does not greatly influence the trafficking of virus to the MLN from the lung which is thought to be reliant on dendritic cells and macrophages (Selvarajah 2001). However, trafficking to the spleen is via B cells which are likely to become infected via dendritic cells in the lymph node. It may be that there is faster infection of B cells in the MLNs of np27$^{-/-}$ mice, leading to earlier virus dissemination to the spleen and establishment of a greater latent infection.

Infection in experiment III appeared to be progressing at a slower pace in comparison to experiment II. The mice in each experiment were of the same age at the time of infection. However, the difference observed between experiments may be due to mouse to mouse variation.

The question remains; what is the role of ISG12 during the establishment of latency in the spleen? The lack of a phenotype *in vitro* and its role *in vivo* strongly suggests that ISG12(a) is important for the immune response to viral infection. It is possible that expression of ISG12 is important for control of infection in a cell population specific to the spleen. There are four distinct populations of DCs found within the murine spleen. They mature in response to type I IFN leading to increased expression of co-stimulatory molecules such as CD80, CD86 and CD40 (Kawai and Akira 2006) and are heterogeneous in phenotype and function. One study has shown that ISG12 is specifically and highly expressed in mature, activated DCs developed *in vitro* from

myeloid precursors. ISG12 mRNA transcripts were found to be upregulated 40-fold in mature and activated DCs but were not up-regulated at all in immature DCs or monocytes (Hashimoto *et al.*, 2000). It can be hypothesised that during MHV-68 infection the lack of ISG12(a) leads to a less effective splenic DC response and thus increased MHV-68 replication and/or increased expansion of MHV-68 infected B cells in the spleen.

It is possible that ISG12 may be more highly expressed in more than one splenic DC population. One important DC population found in the spleen is the murine pDCs (characterised by markers: $Ly6G/C^{+}$ $CD8\alpha^{-}$ $CD11b^{-}$ $B220^{+}$). They are a major source of type I IFN and IL-12 and can develop from both myeloid and lymphoid progenitors (Shigematsu *et al.*, 2004). Stimulation with virus or IFNα leads to enhanced survival and T cell stimulatory activity (Asselin-Paturel *et al.*, 2001). The importance of splenic pDCs for the control of other herpesvirus infections has been shown previously. MCMV infection leads to maturation of splenic pDCs leading to substantial production of type I IFNs, IL-12 and the stimulation of NK cell responses, all of which are important for MCMV control (Dalod *et al.*, 2003). Furthermore, pDCs were suggested to be the major IFNα producers in the spleens of MCMV-infected mice (Asselin-Paturel *et al.*, 2001). A lack of ISG12(a) expression in a cell type, such as pDCs, that are important for control of herpesvirus infections, could help to explain the increased viral load in the spleens of $np27^{-/-}$ mice.

Although the exact function of ISG12 remains to be determined, a less efficient DC response in ISG12(a) ko mice may lead to indirect downstream effects such as decreased IFNα/β responses, lower IL-12 production and inefficient NK cell responses leading to a less efficient adaptive immune response. Immunostaining techniques would help to determine if there is a difference in cellular populations in the spleen of $np27^{-/-}$ compared to wt mice. A lower level of a particular cell type such as T cells, DCs or NK cells, either resident or migrating to the spleen during infection could lead to higher viral titres. It would be of interest to investigate the

phenotypes and effector functions of the DC populations in the np27$^{-/-}$ spleen in comparison to the wt spleen after infection with MHV-68. Furthermore, analysis of downstream responses would determine if the level of IL-12 and IFNα/β production in the spleen is down-regulated and/or if NK and T cell activation is less efficient.

ISG12(a) might have a role involving interaction with latency-associated viral antigens in the spleen during latent infection. One candidate is ORF73, a latency-associated gene (Martinez-Guzman *et al.*, 2003), expressed in nuclei (Kedes *et al.*, 1997) with homology to the latency-associated nuclear antigens (LANA) of KSHV. ORF73 of MHV-68 has been shown to be critical for the establishment of latency in the spleen but is not important for *in vitro* replication (Moorman *et al.*, 2003). This study has shown that ISG12(a) appears to be important for *in vivo*, but not *in vitro* infection. It is possible that ISG12(a) has a role to limit ORF73 function in the nucleus in some way, thus reducing latent virus load in wt mice. Clearly, further analysis of the interactions with ISG12 by latent genes, such as ORF73, are required to determine if this is the reason for increased virus titres within the np27$^{-/-}$ spleen. Infection of np27$^{-/-}$ mice with an ORF73-deletion mutant of MHV-68 would be useful for investigating this possibility. Analysis of the MHV-68 latent gene expression profile in np27$^{-/-}$ compared to wt mice would help to elucidate if there was an up-regulation of latent gene expression in the absence of ISG12(a).

The presence of more than one ISG12 gene, as indicated by *in silico* analysis, complicates investigation of ISG12 gene function. In this study, a clear phenotype has been elucidated for ISG12(a) *in vivo*. It is likely that all three share function as each are small hydrophobic proteins suggesting a transmembrane location and transcripts from each of the three genes were upregulated in response to type I IFN (Parker and Porter 2004). Although an obvious phenotype has been observed with ISG12(a) knockout alone there may be functional redundancy between family members. Clues to ISG12 function may become clearer if a multiple gene knockout model was utilised.

Chapter 5: The role of natural killer cells during MHV-68 infection

5. The role of natural killer cells during MHV-68 infection.

5.1. Introduction

NK cells are an important component of the innate immune response to many virus infections and have been shown to play a particular role in the control of herpesvirus infections. Low NK cell cytotoxicity in humans leads to increased susceptibility to severe disseminating herpesvirus infections such as CMV and VZV. These infections tend to be recurrent even when other immune components are at normal or near normal levels (Biron 1997). A critical role for NK cells can also be demonstrated in a mouse model. NK cell deficient mice, through either antibody depletion or genetic mutation, have been shown to be more susceptible to various herpesvirus infections.

The role of NK cells have been studied in detail in mice infected with MCMV. Increased viral titres and mortality is observed in susceptible mouse strains such as BALB/c when NK cells are depleted. Conversely, adoptive transfer of functional NK cells back into susceptible mice leads to protection against MCMV infection. C57Bl/6 mice are relatively resistant to MCMV infection in comparison to BALB/c mice. The loci associated with these strain differences and thus resistance to infection in C57Bl/6 mice have been mapped to the NK gene complex, *Cmv-1*, on chromosome 6 (Arase *et al.*, 2002). The *Cmv-1* locus was found to encode the activating NK cell receptor, Ly49H, which binds the MHC-like viral glycoprotein, m157. Ly49H is sufficient and required for protection against MCMV in C57BL/6 mice (Daniels *et al.*, 2001). Given the importance of the NK cell response during infection, MCMV has developed mechanisms to evade the NK cell response. The MCMV gene m152, down-regulates the expression of retinoic acid early inducible gene 1, an activatory ligand for the NKG2D receptor, in order to avoid NK cell recognition of infected cells. Although m157 acts as an activatory receptor for NK cells in MCMV-resistant mice it also binds to an inhibitory NK cell receptor, Ly49I, in MCMV-susceptible 129/J mice (that lack the Ly49H ligand) and thus reduces the

NK cell response (Arase *et al.*, 2002). The viral immune evasion strategies of MCMV are wide-ranging and are reviewed in more detail in section 1.5.

Far less is known about the role of NK cells in the control of gammaherpesvirus infection. Studies of primary EBV infection, infectious mononucleosis, have shown that during symptomatic disease there are elevated NK cell numbers in the peripheral blood and enhanced NK cell cytotoxicity. In addition, higher NK cell counts correlated with lower EBV titres in the peripheral blood (Williams *et al.*, 2005). It may be that the extent of the NK cell response determines the severity of the clinical disease. Furthermore, low NK cell activity has been linked to uncontrolled EBV infection in Chediak- Higashi syndrome (Merino *et al.*, 1983).

Are NK cells important in the control of gammaherpesvirus infections? Studies with EBV suggest that NK cells do play a role but how important are NK cells for the control of gammaherpesvirus infection? To answer these questions, MHV-68 was used as a model to investigate the NK cell response to a gammaherpesvirus at early time points post-infection. It was hypothesised that, given the important role of NK cells in other herpesvirus infections, NK cells would play a critical role in determining the outcome of MHV-68 infection. MHV-76 is identical to MHV-68 except it lacks the ORFs M1-M4 and the viral tRNAs. MHV-76 grows *in vitro* with same efficiency as MHV-68 but is attenuated during *in vivo* infection as it is cleared more rapidly from the lung and achieves a lower maximal titre in comparison to MHV-68 at early time points post-infection (Macrae *et al.*, 2001). These data indicate that the left end of the genome has a key role for pathogenesis. Furthermore, when M4 was replaced back into MHV-76 (MHV76inM4) it led to higher titres compared to MHV-76 at day 1 post-infection (Townsley *et al.*, 2004). These findings suggest a possible immunoregulatory role for the left end of the MHV-68 genome during the innate immune response and therefore a possible role in modulating the NK cell response.

The aims of this study were to (1) investigate the level of NK cell proliferation and activation post-infection, (2) examine cytotoxic activity and (3) elucidate the role for NK cells during *in vivo* infection. In addition, this study postulated that a component of the left end of the MHV-68 genome may be involved in the regulation of NK cell responses.

5.2. The NK cell population in the MLN

During MHV-68 infection lymphocyte expansion and accompanying lymphoadenopathy is observed in the MLN, the draining lymph node from the lung. C57Bl/6 mice were infected with 4 x 10^5 pfu of MHV-68 and the MLNs removed at early time points until day 12 post-infection. Total lymphocyte counts were performed for each tissue. The kinetics of lymphocyte expansion within the MLN is shown in figure 5.1. By day 2 post-infection the number of lymphocytes had continued to rise to a peak at day 5 post-infection. By day 12 post-infection lymphocyte numbers in the MLN had begun to return to the resting level, correlating with the clearance of virus from the lung during acute infection. It was speculated that a proportion of the expanded lymphocytes within the MLN would be NK cells activated in response to MHV-68 antigens.

Cell surface markers such as NK1.1, DX5 and the Ly49 group can be used to define NK cell populations. Expression can differ between mouse strains. For example, BALB/c mice express DX5 but not NK1.1 whereas C57Bl/6 mice express both markers. The Ly49 family exhibits heterogeneous expression and different expression patterns occur on overlapping NK cell subsets. NK1.1 and DX5 are the most commonly used due to their stable expression and the wide availability of monoclonal antibodies conjugated to various fluorophores. FACS analysis was carried out to investigate the NK cell population in the MLN post-infection. A major function of NK cells is IFNγ production post-activation, leading to the activation of other cell types such as T cells and macrophages. NK cells are induced to express

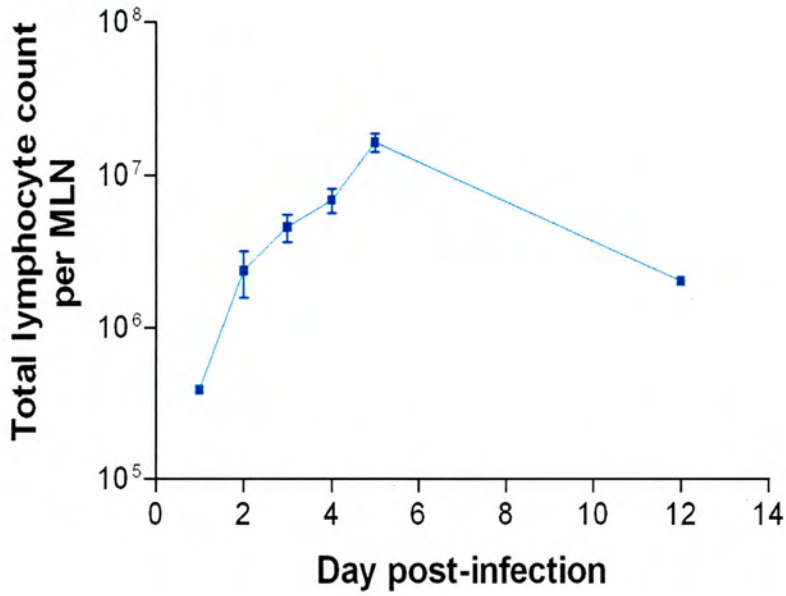

Figure 5.1. Total lymphocyte count in the MLNs of C57Bl/6 mice following infection with MHV-68. Mice were infected intranasally with 4 x 10^5 pfu of MHV-68. MLNs were harvested at various time points p.i. and total lymphocytes counted. Data points represent one count at days 1 and 12 p.i. and 7 counts at days 2-5 p.i. For days 2-5 p.i., values represent lymphocyte counts ± standard error of the mean (SEM).

IFNγ following infection with MCMV. This response has been shown to play a major role in NK cell-mediated protection against infection (Orange *et al.*, 1995). Given the importance of NK-cell secreted IFNγ during herpesvirus infection it was decided to use IFNγ as a measure of NK cell activation. MHV-76 was also included in the study in order to determine if there is a difference in the ability of the NK cell population to expand and become activated in response to MHV-76 compared to MHV-68. Mice were infected intranasally with 4 x 10^5 pfu of either MHV-68 or MHV-76 and MLNs were harvested at days 2 and 4 post-infection. The percentage of NK cells present and the percentage of cells expressing IFNγ were determined by FACS analysis. Cells were stained with an antibody to the NK cell marker, DX5 (CD49b), and intracellular staining carried out with an antibody to IFNγ. Figure 5.2 shows representative FACS stains from lymphocyte populations double stained with antibodies to DX5 and IFNγ. Four MLNs from uninfected mice were pooled together in order to obtain an average value for the percentage of NK cells and level of IFNγ in uninfected MLNs.

The percentage of NK cells in the MLN post-infection are shown in figure 5.3. The data suggest that the NK cell population is expanded at early time points post-infection. At day 2 post-infection the MHV-68 and MHV-76-infected samples had mean NK cell populations of 1.06% and 1.36% respectively in comparison to day 4 post-infection where the NK cell population had fallen to 0.67% and 0.74% for MHV-68 and MHV-76 infection respectively. The uninfected sample had a NK cell population of 0.34%. This suggests that the population was elevated by day 2 and was returning to resting levels by day 4. Alternatively, the percentage of NK cells may be reduced due to increased populations of other lymphocytes by day 4 post-infection. This would have to be determined by further FACS analysis of other cell populations within the MLN during MHV-68 and MHV-76 infection. There was no significant difference between the NK cell populations of MHV-68 and MHV-76 infected MLNs as determined by Mann-Whitney test at either day 2 or day 4.

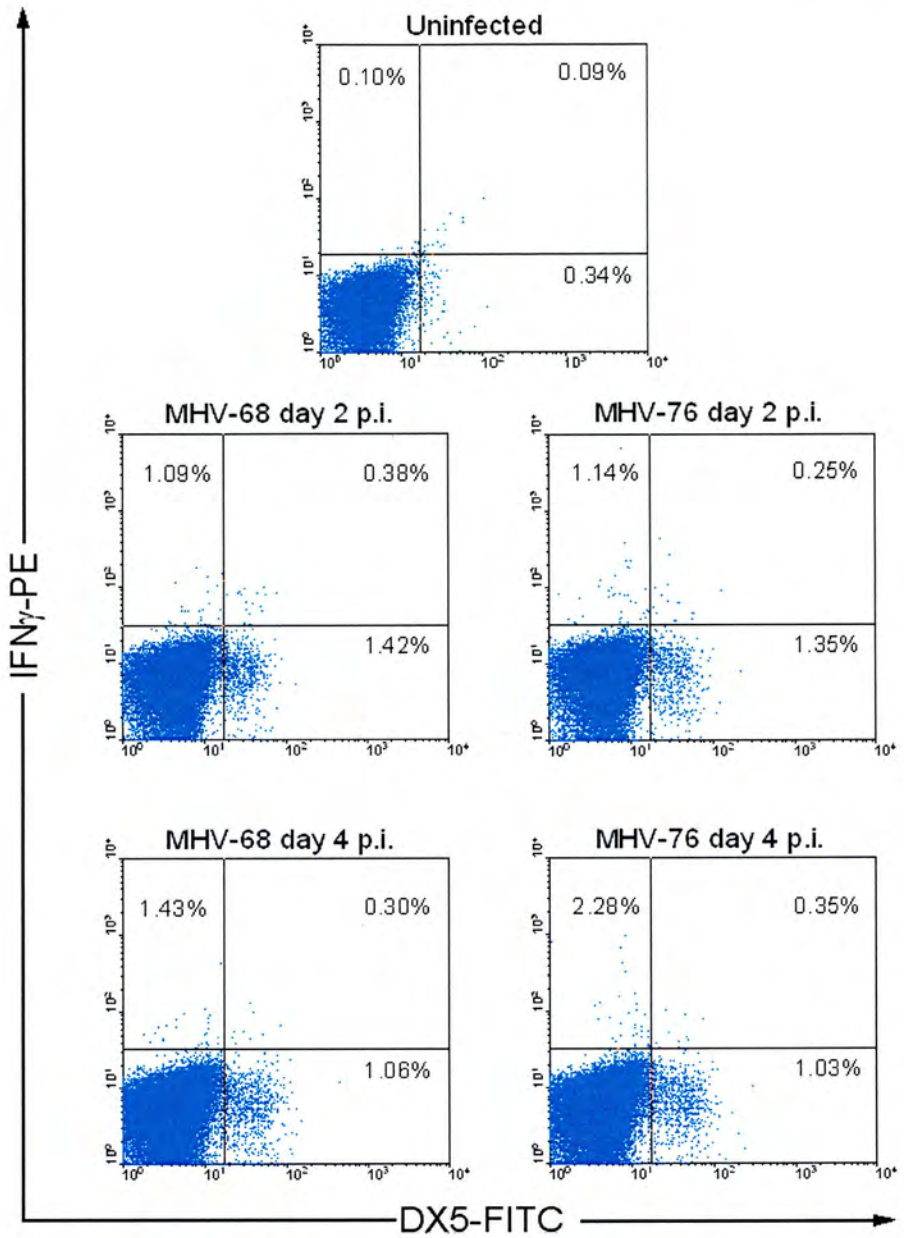

Figure 5.2. FACS analysis of NK populations in the MLN. Mice were infected with 4 x 10^5 pfu of either MHV-68 or MHV-76. MLNs were harvested at day 2 and 4 post-infection. Lymphocytes were extracted and intracellular staining carried out for IFNγ and surface staining carried out for the NK cell marker, DX5. One mouse was left uninfected to act as a control and establish resting levels of both NK cells and IFNγ.

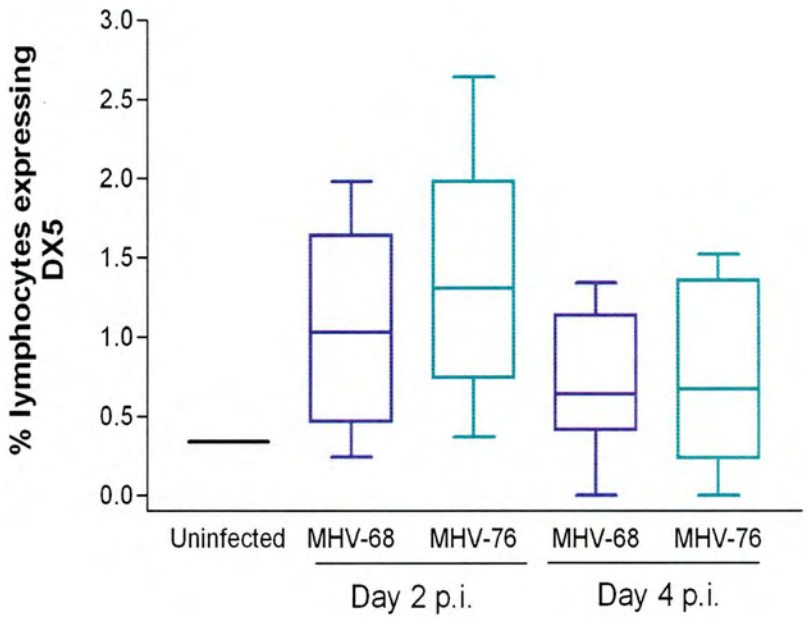

Figure 5.3. NK cell populations in the MLN following infection with MHV-68 or MHV-76. Mice were infected with 4 x 10^5 pfu of either MHV-68 or MHV-76. MLNs were harvested at day 2 and day 4 p.i. Lymphocytes were extracted and stained with an NK cell specific antibody (DX5). Each data set represents a combination of three individual experiments, each with nine to eleven data points per group, except the uninfected MLN data (represented by a black horizontal line) which was analysed once. The median for each dataset is indicated by the centre line. The first and third quartiles are shown by the edges of the box area. The extreme values are indicated by the whiskers extending from the box.

Intracellular IFNγ staining was used to determine if NK cells were activated following infection. The proportion of NK cells that were expressing IFNγ post-infection is shown in figure 5.4. At day 2, an average of 34.33% of NK cells were activated in response to MHV-68. At day 4, an average of 41.13% of NK cells were activated in response to MHV-68. Similarly, at day 2 post-infection, an average of 31.36% of NK cells were activated in response to MHV-76. At day 4, an average of 47.57% of NK cells were activated in response to MHV-76. These data suggest that NK cells are activated following infection with MHV-68 or MHV-76. Furthermore the proportion of activated NK cells appears to be slightly increased by day 4 post-infection in response to both MHV-68 and MHV-76. However, this is not significant as the range of activation had a relatively high level of variation for each group. There was no significant difference between the levels of activated NK cells of MHV-68 and MHV-76 infected MLNs as determined by Mann-Whitney test at either day 2 or day 4. Figure 5.5 shows the number of activated NK cells as a portion of IFNγ positive lymphocytes. At day 2 post-infection, activated NK cells in the MHV-68-infected MLN comprised a mean value of 0.57% and activated NK cells in the MHV-76-infected MLN comprised a mean value of 0.60% of the total $IFN\gamma^+$ population. At day 4 post-infection, activated NK cells in the MHV-68-infected MLN comprised a mean value of 0.49% and activated NK cells in the MHV-76-infected MLN comprised a mean value of 0.63% of the total $IFN\gamma^+$ population. There was no significant difference (by Mann-Whitney test) between MHV-68 and MHV-76 in the ability to stimulate NK cells to express IFNγ at either day 2 or day 4 post-infection. These data show that activated NK cells express IFNγ in response to MHV-68 and MHV-76 infection.

5.3. NK cell responses following MHV-68 infection

During infection NK cells can lyse target cells by release of cytotoxic granules containing perforin and granzymes and by binding to receptors to induce apoptosis.

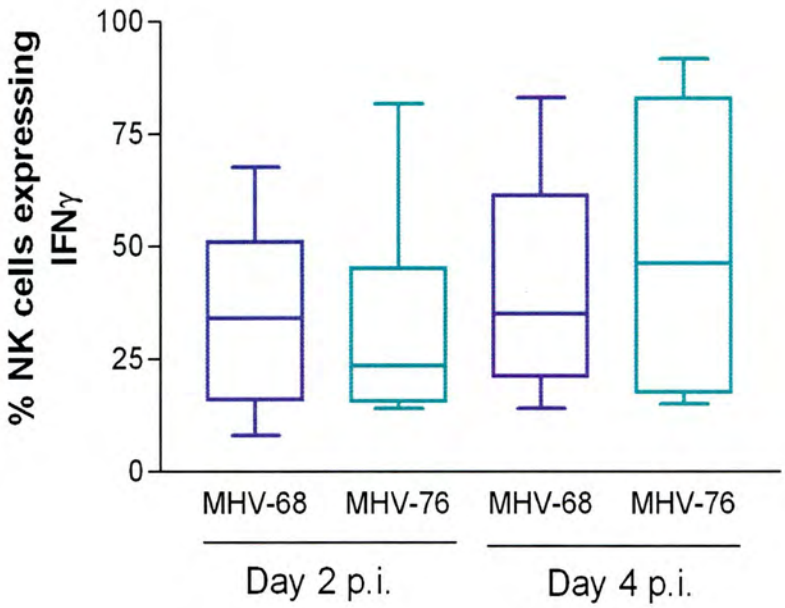

Figure 5.4. Percentage of activated NK cells in the MLN following infection with MHV-68 or MHV-76. Mice were infected with 4 x 10^5 pfu of either MHV-68 or MHV-76. MLNs were harvested at day 2 and day 4 p.i. Lymphocytes were extracted and intracellular staining carried out with an antibody to IFNγ and surface staining with a NK cell specific antibody (DX5). Each data set represents a combination of three individual experiments, each with nine to ten data points per group. The median for each dataset is indicated by the centre line. The first and third quartiles are shown by the edges of the box area. The extreme values are indicated by the whiskers extending from the box.

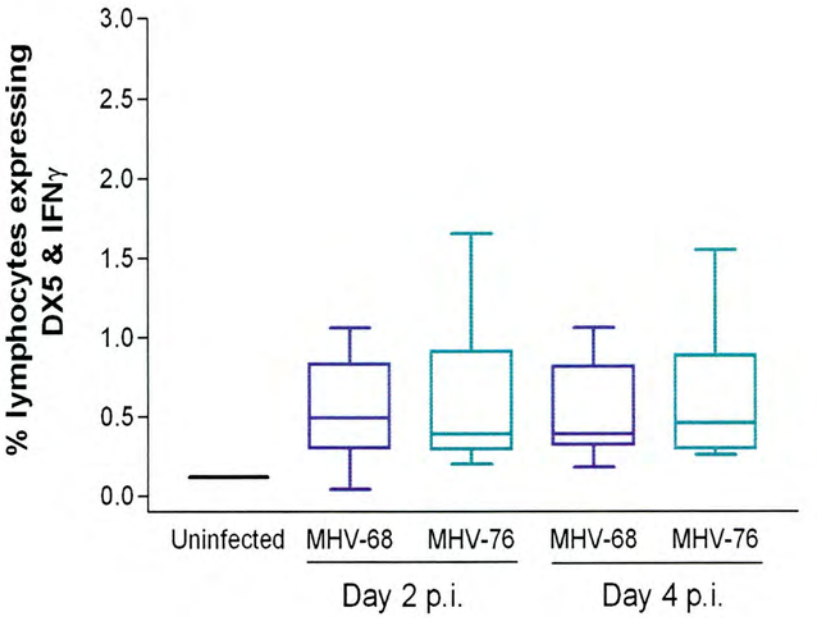

Figure 5.5. Activated NK cells in the MLN following infection with MHV-68 or MHV-76. Mice were infected with 4 x 10^5 pfu of either MHV-68 or MHV-76. MLNs were harvested at day 2 and day 4 p.i. Lymphocytes were extracted and intracellular staining carried out with an antibody to IFNγ and surface staining with a NK cell specific antibody (DX5). Each data set represents a combination of three individual repeat experiments, each with nine to eleven data points per group, except the uninfected MLN data (represented by a black horizontal line) which was analysed once. The median for each dataset is indicated by the centre line. The first and third quartiles are shown by the edges of the box area. The extreme values are indicated by the whiskers extending from the box.

Cytotoxicity assays were carried out in order to address the question; are NK cells, activated in response to MHV-68, capable of killing target cells? In the first instance, chromium release was chosen as an indicator of target cell killing. The murine T cell lymphoma cell line, Yac-1, was chosen as the target cells for these assays due to the low level of MHC class I on the cell surface and therefore their susceptibility to NK cell killing. C57BL/6 mice were infected intranasally with 4 x 10^5 pfu of MHV-68 and the MLNs harvested at day three post-infection. At least four MLNs were required, and pooled, per experiment in order to get sufficient numbers of lymphocytes for analysis. T-lymphocytes were removed from the lymphocyte suspension by complement depletion to increase the chance of cell-cell contact between NK cells and the Yac-1 target cells. FACS analysis was carried out on aliquots of cells from the T lymphocyte-depleted and non-depleted fractions to ensure elimination of $CD3^+$ cell populations. An example is shown in figure 5.6. For each cytotoxicity assay, each sample was analysed in triplicate including a spontaneous lysis control containing media only and a maximum lysis control containing 5% Triton X detergent solution. However, although killing was detected in the maximum lysis control samples, the data was not reproducible and there was little or no specific lysis obtained in the MHV-68 infected samples. Numerous attempts were made to increase the sensitivity and reproducibility of the assay. For example, cells were pelleted gently prior to incubation to maximise cell contact, the incubation period was increased from four to eight hours, cell numbers were increased to optimise the effector/target ratios and the amount of chromium added to cells was increased to aid uptake and thus sensitivity. Despite these measures, chromium release from targets incubated with T-cell depleted lymphocytes never rose above background levels. Similarly, a cytotoxicity assay was carried out to investigate if CTL-killing of MHV-68 infected targets could be detected with this assay. Lymphocytes from a MHV-68 infected (day 5 post-infection) mouse were depleted of NK cells by complement depletion. The Yac-1 target cells were infected overnight with a MOI of 5 pfu/cell. This assay also failed to show detectable cytotoxicity by CTLs. This correlates with observations from K. Robertson (Robertson 1999) where T lymphocytes failed to kill MHV-68 infected targets. It

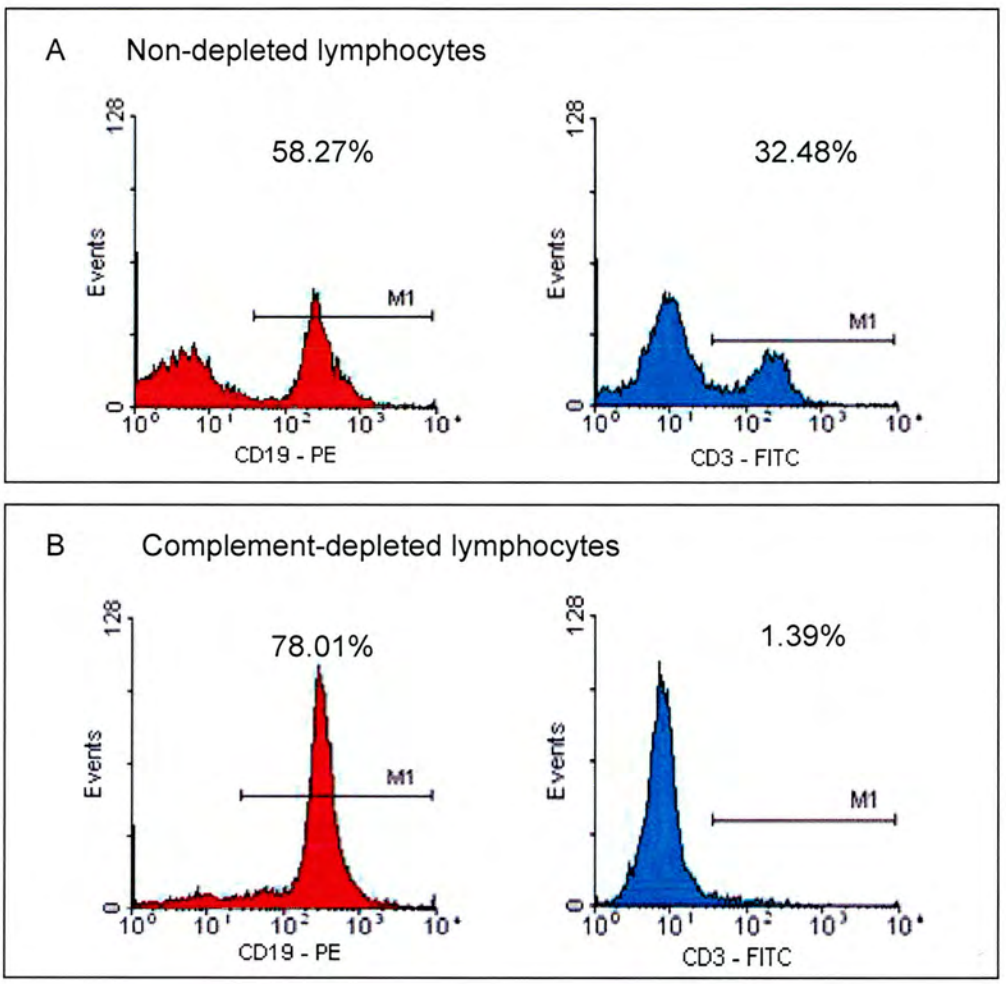

Figure 5.6. Complement depletion of T lymphocytes. $CD4^+$ and $CD8^+$ T lymphocytes were removed from a mixed lymphocyte population by incubation with complement and anti-CD4 (YTS 191) and anti-CD8 (YTS 169) antibodies for 1 hour. The efficiency of the depletions were analysed by FACS analysis of untreated (A) or complement-depleted (B) lymphocytes. The red histograms show B lymphocyte populations. The blue histograms show T lymphocyte populations.

may be that the Yac-1 cells were not infected properly, making them poor targets for CTL killing. Infection of Yac-1 cells with MHV-68 expressing GFP (LHΔGFP) failed to result in detectable GFP when examined under a fluorescent microscope thus suggesting that these cells are not readily infectable with MHV-68.

It was decided to change the detection method from chromium release to flow cytometric analysis of NK cell specific lysis in order to increase assay sensitivity. The principle of the flow-based assay is to label the effector cells with a non-toxic fluorescent dye before co-incubation with the target cells for four hours. The mixed cell population is then stained with a DNA dye such as propidium iodide to identify dead cells and the populations analysed by flow cytometry.

Eight C57BL/6 mice were infected intranasally with 4 x 10^5 pfu of MHV-68. MLNs were harvested at either day 2 or 3 post-infection and all eight pooled together per experiment to get sufficient numbers of lymphocytes for analysis. The NK cell population was enriched by MACS separation to raise the sensitivity of the assay and increase the proportion of NK cells contacting the Yac-1 target cells. The NK cell population was enriched from 3.18% in the unseparated lymphocytes to 87.35% in the MACS-separated population (figure 5.7). Controls for spontaneous and maximum lysis were included as per the chromium release assay and all samples were analysed in triplicate. Poly I:C has been shown to significantly upregulate NK cell killing of K562 target cells (Pisegna *et al.*, 2004). It was therefore decided to include poly I:C stimulated NK cells as a positive control for the assay. NK cells were isolated from a spleen taken from day 2 infected mice. Unfortunately, the stimulated NK cell control did not give suitably high levels of killing. Although unlikely, it is possible that NK cells could not be activated to a suitable level because of immune evasion strategies employed by MHV-68 during infection, resulting in NK cells remaining inactivated or activation being switched off. Perhaps a more likely explanation is that the stimulation of NK cells requires more optimisation of poly I:C concentration and incubation conditions. However, due to time restraints

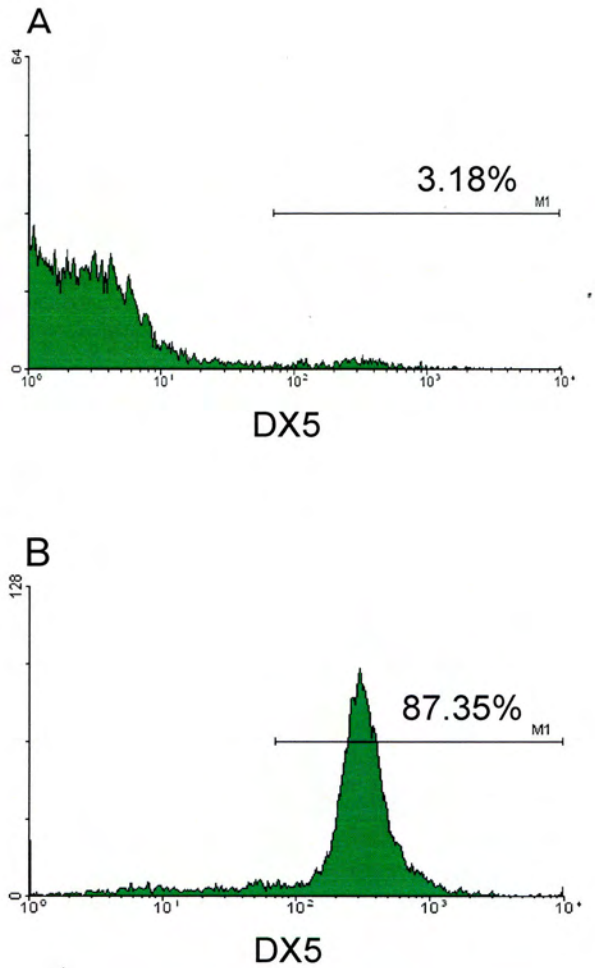

Figure 5.7. MACs enrichment of NK cells. Mice were infected with 4 x 10^5 pfu of MHV-68. MLNs were harvested at day 3 p.i., pooled and lymphocytes extracted. A MACS NK cell isolation kit was used to enrich the NK cell population for use in a cytotoxicity assay. An aliquot of lymphocytes were taken pre-isolation (A) and an aliquot taken post-isolation (B) for analysis by FACS. Cells were stained with a CD49b (DX5) antibody and analysed on a FACScan.

they were discarded as a positive control. The green fluorescent membrane dye, $DiOC_{18}$, was chosen to label the effector cells (the NK cells) as it has been shown to be stable and gives homogeneous staining (Piriou *et al.*, 2000). The red fluorescent DNA dye, propidium iodide, was used to detect dead cells. Each dye was titrated to ensure optimal staining for the separate populations. Following co-incubation of the effectors and targets, cells were analysed by flow cytometry. Single-stained aliquots of effector and target cells were included for FACS analysis of each experiment to ensure correct compensations and settings were being used. The gating strategy used is shown in figure 5.8. Figure 5.9 shows results obtained from the fluorescence-based cytotoxicity assay of Yac-1 cells by NK cells purified from MHV-68 infected MLNs. At an effector/target ratio of 2.5:1, there was mean specific lysis of 2.41%. This increased to 5.93% at a ratio of 5:1 and 12.8% at a ratio of 10:1. This assay demonstrates that NK cells activated during MHV-68 infection are capable of cytotoxic killing of susceptible targets.

5.4. *In vivo* depletion of NK cells

Following analysis of the NK cell population and cytotoxicity post-infection it was hypothesised that a lack of NK cells *in vivo* would render mice more susceptible to gammaherpesvirus infection. NK cells were depleted by administration of an anti-NK1.1 antibody in order to investigate their role during infection. This approach was taken over the use of knockout mice due to the lack of a suitable model in which NK cells were selectively and efficiently depleted. For example, beige mice carrying the bg mutation (beige lysosomal trafficking regulator, chromosome 13) have malfunctioning NK cell cytotoxicity but retain the ability to produce cytokines from their NK cells. The mutation also affects the granules of other cell types so is not selective or absolute and is therefore of limited use in this type of study (Kim *et al.*, 2000).

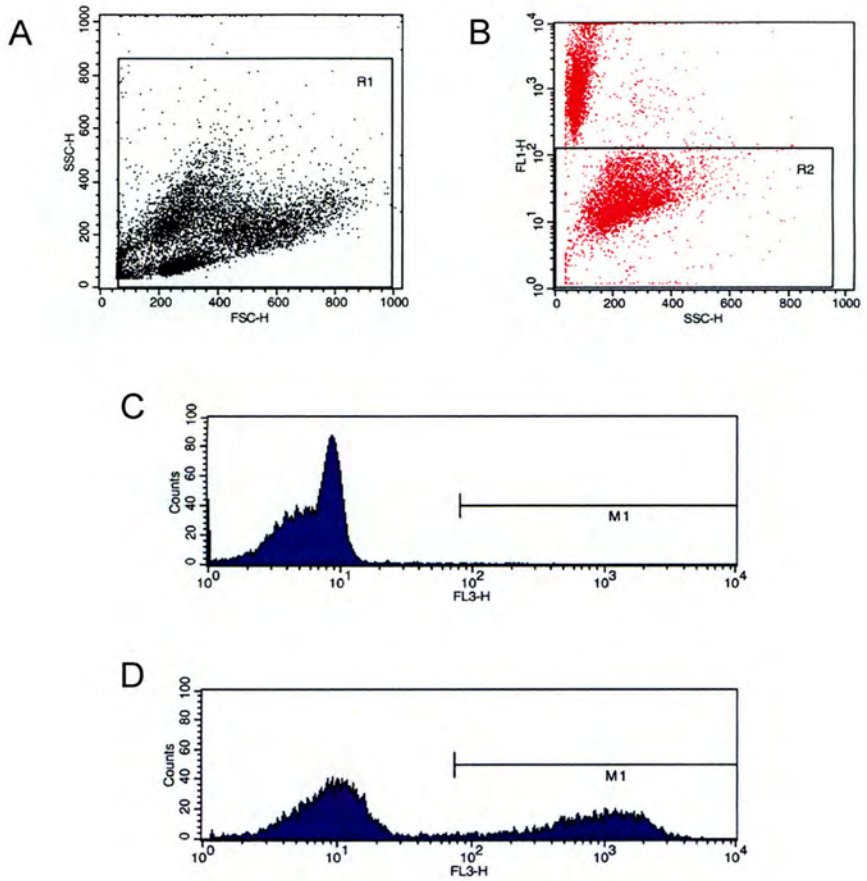

Figure 5.8. Gating strategy for assessing NK cell cytotoxicity. The combined Yac-1 and NK cells from the cytotoxicity assay plate were analysed by FACS analysis. Forward scatter (FSC) was plotted against side scatter (SSC) and debris gated out in gate 1 (R1) as shown in panel A. Gate 1 events were plotted on a SSC against $DiOC_{18}$ fluorescence (FL1) dot plot (B). Gate 2 (R2) was applied around the $DiOC_{18}$-negative events (target cells). All events corresponding to Gate 1 and 2 were displayed on a propidium iodide (FL3) histogram and the marker, M1, was applied to dead cells as shown in panels C and D. Histograms for spontaneous lysis (C) and maximum lysis (D) of Yac-1 cells are shown.

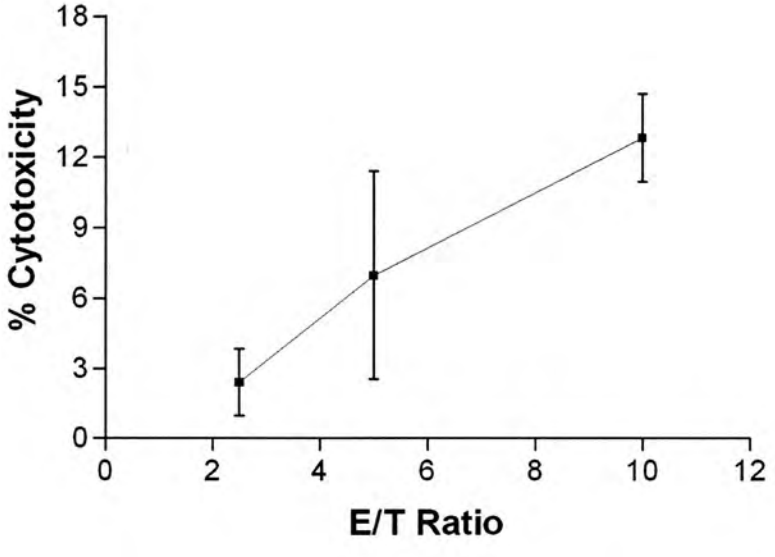

Figure 5.9. Specific lysis of Yac-1 cells by MHV-68 stimulated NK cells. NK cells were extracted from the MLNs of mice infected with 4 x 10^5 pfu of MHV-68 at day 3 p.i. NK cells were mixed and incubated with Yac-1 target cells for 4 hours before specific lysis was determined by FACS analysis. Data points represent the mean of three replicates and the bars represent the standard error of the mean.

An accepted method of NK cell depletion is via the administration of an anti-NK1.1 antibody (Seaman *et al.*, 1987). C57Bl/6 mice were depleted of NK cells by administration of PK136 on at least three occasions: day -2, -1 and +2 relative to the day of infection (day 0). A second group were given matching doses of control serum immunoglobulin. The efficiency of the NK cell depletions were examined by FACS analysis of splenocytes from both the depleted and non-depleted groups using both DX5 and biotinylated-PK136. This analysis was carried out at least twice each time the experiment was performed and a representative result is shown in figure 5.10. With each antibody investigated there was a small residual population that could not be reduced with either increased doses of antibody nor increased frequency of administration. As BALB/c mice do not express NK1.1 it was decided to use the PK136 antibody to stain BALB/c lymphocytes and therefore investigate if the residual PK136 staining was non-specific. Splenocytes from an untreated BALB/c mouse were stained with an antibody to CD3 and either DX5 or PK136. The result is shown in figure 5.11. These data show that 6.68% of splenocytes were $DX5^+$ while 1.93% of splenocytes stained positive for PK136. This suggests that there is a considerable degree of non-specific staining when using the PK136 antibody. Antibodies may lack specificity due to binding multiple cell types, binding a common epitope on several proteins, binding through the Fc portion of the antibody to non-specific receptors or by binding dead cells with disrupted membranes. As DX5 exhibited a similar residual population it is possible that non-specific staining was occurring through the binding of dead cells in lymphocyte preparations. Erythrocytes are removed from the lymphocyte population by the relatively harsh process of osmotic lysis which may also result in lysis of lymphocytes. This could be minimised by separating the cell types by density gradient centrifugation. The non-specific staining of dead cells can be eliminated by gating out cells stained with a DNA dye such as propidium iodide. The gentler treatment of cells and additional staining step are recommended for future experiments of this type.

As well as investigating MHV-68, it was decided to look at a number of different viruses to investigate the role of the left end of the viral genome and its interaction

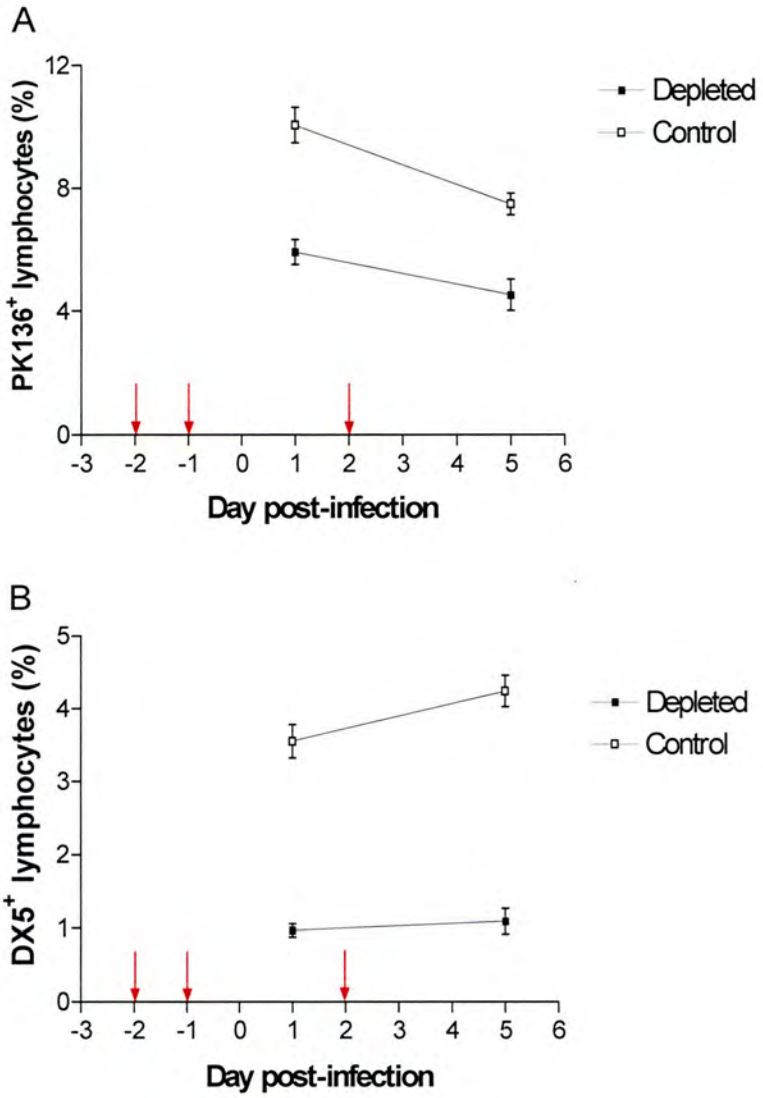

Figure 5.10. FACs analysis of *in vivo* NK cell depletions. In order to deplete NK cells *in vivo*, C57Bl/6 mice were treated with 200-500μg of NK1.1 antibody (PK136) (■). Control mice were given matching doses of serum immunoglobulin (□). Antibody was injected intraperitoneally on days -2, -1 and +2 relative to the day of infection (day 0) as denoted by the red arrows (→). Mice were infected intranasally with 4 x 10^5 pfu MHV-68 on day 0. The efficiency of the depletion was analysed by FACS analysis of $PK136^+$ (A) and $DX5^+$ (B) NK cells from both depleted and non-depleted mice at day 1 and 5 p.i. Data points represent the percentage of NK cells ± the standard error of the mean.

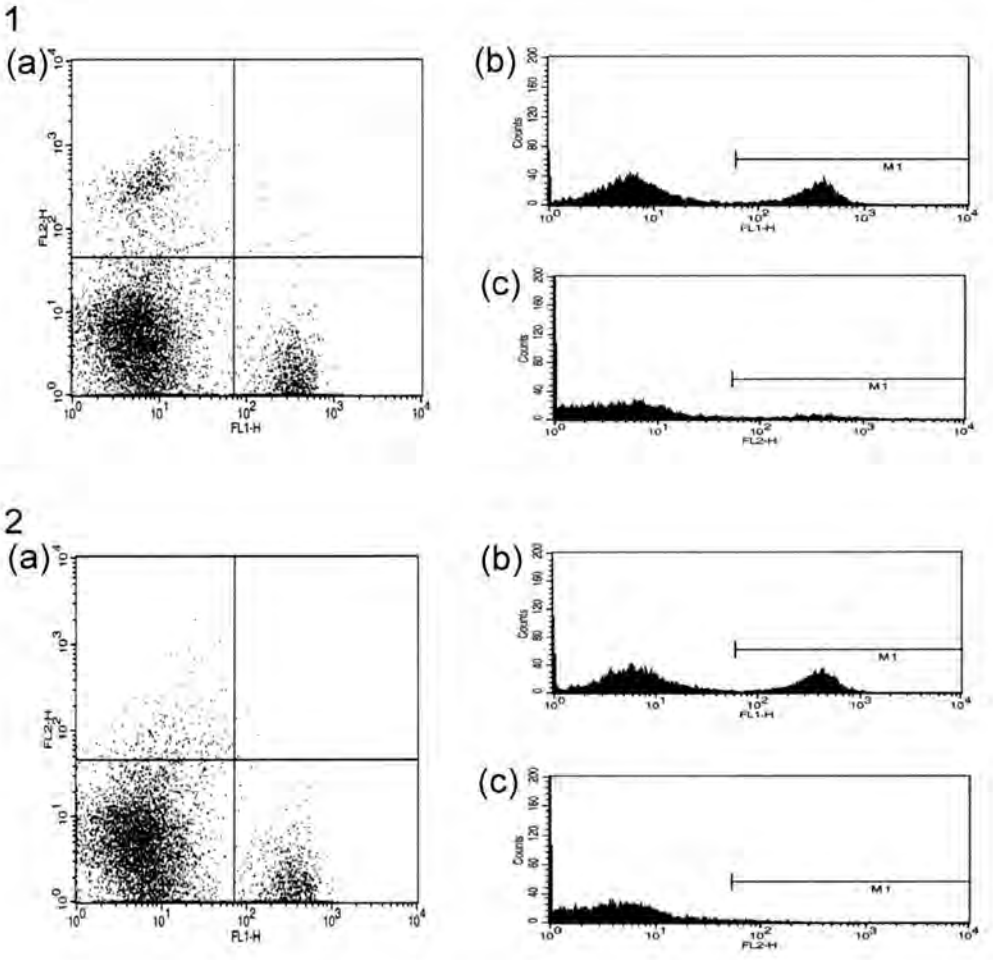

3

	FL1 %	FL2 %
CD3 & PK136	31.28	1.93
CD3 & DX5	30.95	6.68

Figure 5.11. Analysis of PK136 antibody specificity. Splenocytes were extracted from a Balb/c mouse and double stained with an antibody to CD3 (FL-1) and either an antibody to DX5 (1) or PK136 (2) (FL-2). In both 1 and 2, (a) shows a dot plot for the splenocyte population, (b) shows a FL-1 histogram for the proportion of $CD3^+$ T cells and (c) shows a FL-2 histogram for the proportion of $DX5^+$ (1) or $PK136^+$ (2) NK cells. Panel 3 shows a summary table for the percentages of positive cells post-staining.

with NK cells *in vivo*. The viruses used to study this in this system are shown in figure 5.12. MHV-68 is the wild-type virus. It was hypothesised that the depletion of NK cells may confer a replication advantage to MHV-76, thus compensating for the lack of the genes and vtRNAs at the left end of the genome. Furthermore, it has been postulated that the M4 gene may play a role in innate immune regulation as it is expressed as an immediate-early/early transcript associated with productive infection at early times post-infection and is not necessary for replication *in vitro*. M4.stop is a M4 knockout virus, constructed using the MHV-68 bacterial artificial chromosome (BAC), pHA3 (Adler *et al.*, 2000). It contains a nonsense mutation at 8672bp within the M4 region but retains the other genes and RNA species at the LHE. The wild-type virus PHA4 was included as both it and the M4.Stop virus were derived by the BAC system and contain a residual LoxP site left following Cre recombinase excision of the BAC sequences (Geere *et al.*, 2006).

NK cell depleted and non-depleted mice were infected intranasally with 4 x 10^5 pfu of MHV-68, MHV-76 or M4.Stop. The first virus to be investigated was MHV-68. Tissues were harvested at days 1, 2, 3 and 5 post-infection with four mice per group per time point. Viral load was determined by quantitative PCR using primers specific for sequences within the RTA gene. The results are shown in figure 5.13. There was no difference in the viral load in the lung between depleted and non-depleted animals at any time point investigated suggesting that NK cells do not influence acute infection in the lung. Similarly, there were no significant differences in viral load in the MLN between NK cell depleted and non-depleted mice. These data suggest that NK cells do not play a significant role in clearance of virus from the lung. Virus could be detected in the spleen by day 3 post-infection. There was no significant difference between the groups suggesting that replication in the lung, virus trafficking to the spleen or establishment of latency is not significantly controlled by NK cells.

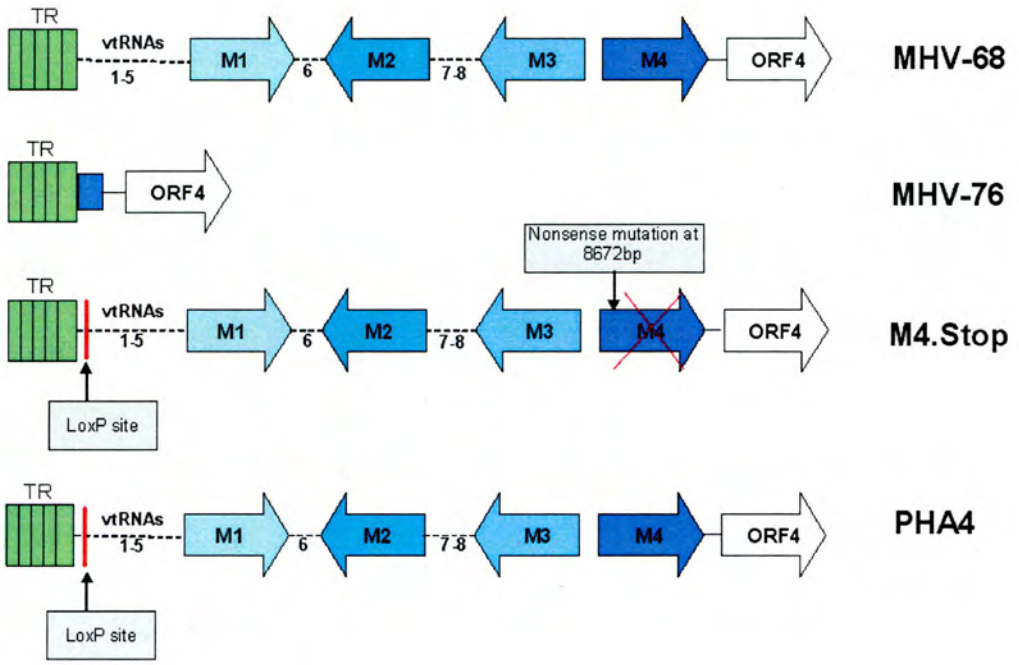

Figure 5.12. Schematic diagram of the left-termini of the viruses used in this study. The green rectangles denote the terminal repeats (TR). The unique genes, M1-M4, are labelled in blue and the 8 viral tRNAs are denoted by a dashed line. ORF4, with a number of homologues in several other herpesviruses, is shown in white. The remaining portion of the M4 sequence in MHV-76 is denoted by a blue rectangle.

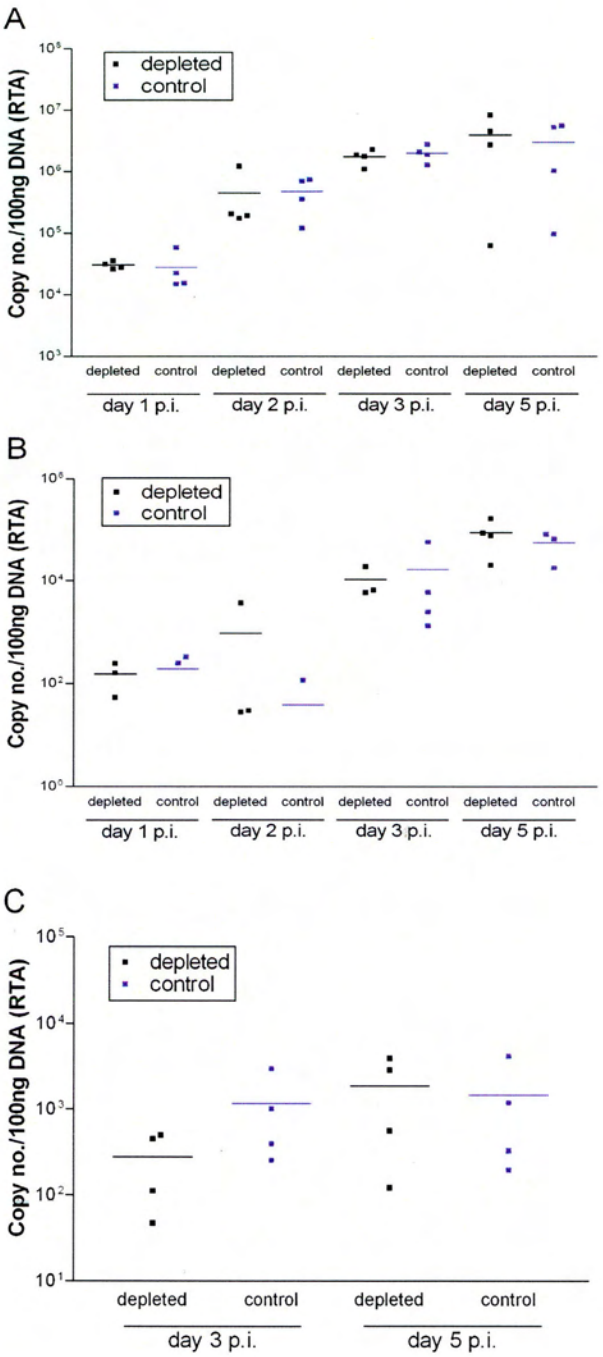
A
depleted
control
Copy no./100ng DNA (RTA)
depleted control depleted control depleted control depleted control
day 1 p.i.
day 2 p.i.
day 3 p.i.
day 5 p.i.
B
depleted
control
Copy no./100ng DNA (RTA)
depleted control depleted control depleted control depleted control
day 1 p.i.
day 2 p.i.
day 3 p.i.
day 5 p.i.
C
depleted
control
Copy no./100ng DNA (RTA)
depleted control depleted control
day 3 p.i.
day 5 p.i.

Figure 5.13. Infection of NK cell depleted mice with MHV-68. NK cells were depleted by administration of an anti-NK 1.1 antibody (PK136) on days -2, -1 and +2 relative to the day of infection. Mice were infected intranasally with 4 x 10^5 pfu of MHV-68 on day 0. NK cell depleted mice are denoted by black squares (■) and control (non-depleted) mice by purple squares (■). Tissues were harvested on days 1, 2, 3 & 5 p.i. using four mice per group per time point. Viral load was determined in lung (A), MLN (B) and spleen (C) by real-time PCR using primers specific for the viral gene, RTA. Viral DNA was quantified by amplification of the RTA gene and normalised as determined by the level of β-actin within each sample. The mean viral load of each group is shown by a horizontal line. These results are representative of two independent experiments for each tissue.

The role of NK cells in the control of MHV-76 was also investigated. It was expected that if a component of the left end of the virus genome was interacting with NK cells, then the depletion of NK cells would confer a replication advantage to MHV-76. Tissues were harvested at days 2, 3 and 4 post-infection with four mice per group per time point. The results are shown in figure 5.14. Again, there was no difference in the viral load in the lung between the depleted and non-depleted animals at any time point investigated. Likewise, there were no significant differences in viral load between the groups within the MLN or spleen. Figure 5.15 shows the data obtained when mice were infected with the M4.Stop virus or the PHA4 control virus. Tissues were harvested at days 2, 3 and 4 post-infection with four mice per group per time point. There was no significant difference in viral loads between depleted and non-depleted groups at any time point investigated, nor in any tissue. Also, there was no significant difference between the PHA4 control virus and the M4.Stop virus load. Taken together, the results for the MHV-76 and M4.Stop infected mice indicate that the left end of the MHV-68 genome does not play a role in regulation of NK cell function.

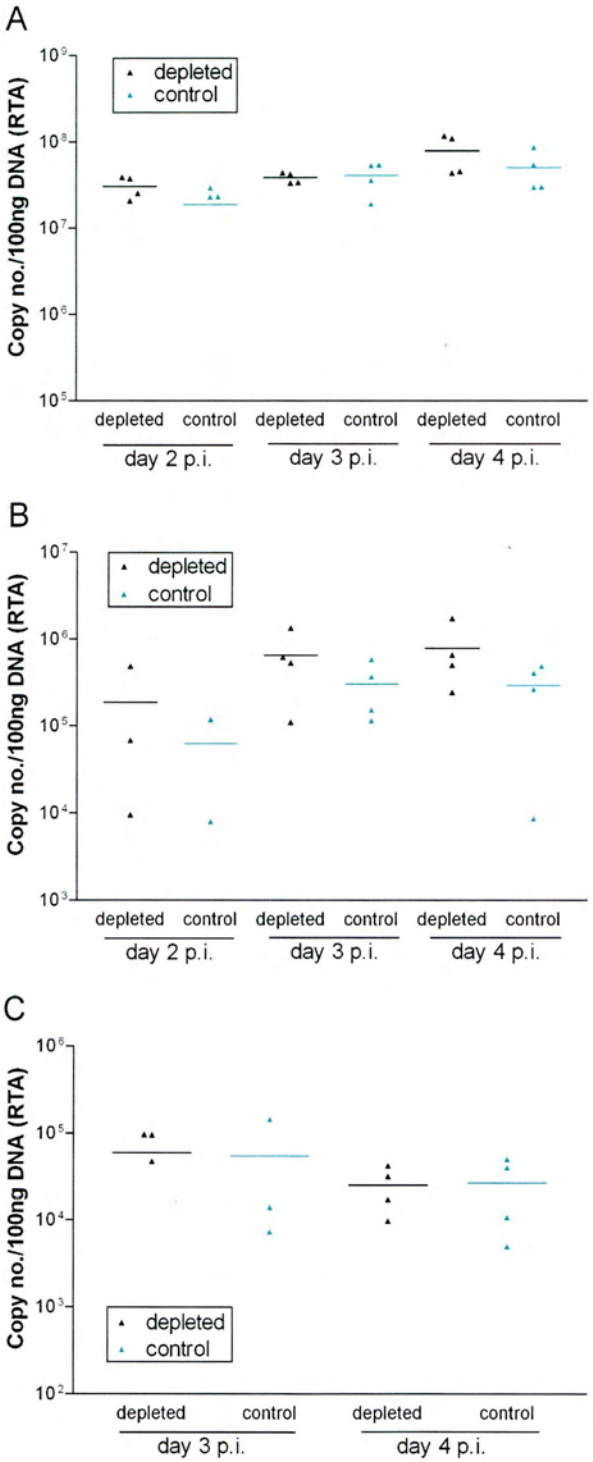
A
Copy no./100ng DNA (RTA)
depleted
control
depleted control depleted control depleted control
day 2 p.i.
day 3 p.i.
day 4 p.i.
B
Copy no./100ng DNA (RTA)
depleted
control
depleted control depleted control depleted control
day 2 p.i.
day 3 p.i.
day 4 p.i.
C
Copy no./100ng DNA (RTA)
depleted
control
depleted control depleted control
day 3 p.i.
day 4 p.i.

Figure 5.14. Infection of NK cell depleted mice with MHV-76. NK cells were depleted by administration of an anti-NK1.1 antibody (PK136) on days -2, -1 and +2 relative to the day of infection. Mice were infected intranasally with 4 x 10^5 pfu of MHV-76 on day 0. NK cell depleted mice are denoted by black triangles (▲) and control (non-depleted) mice by green triangles (▲). Tissues were harvested on days 2, 3 & 4 p.i. using four mice per group per time point. Viral load was determined in lung (A), MLN (B) and spleen (C) by real-time PCR using primers specific for the viral gene, RTA. Viral DNA was quantified by amplification of the RTA gene and normalised as determined by the level of β-actin within each sample. The mean viral load of each group is shown by a horizontal line. These results are representative of two independent experiments for each tissue.

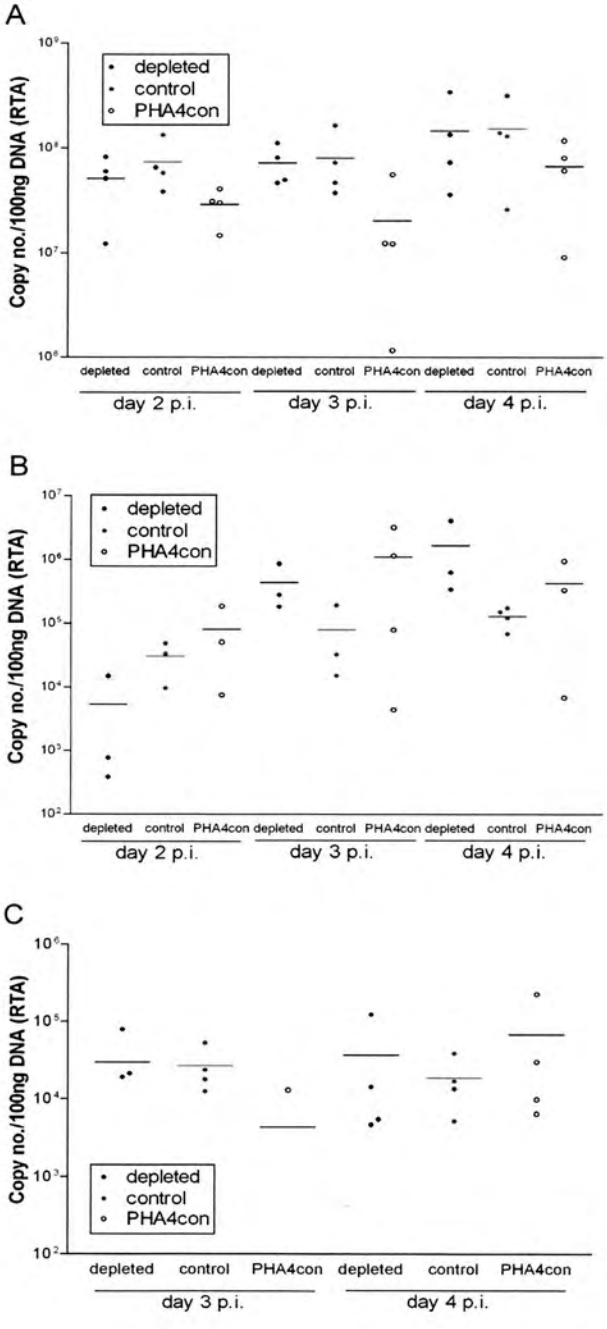
A
Copy no./100ng DNA (RTA)
depleted
control
PHA4con
depleted control PHA4con depleted control PHA4con depleted control PHA4con
day 2 p.i.
day 3 p.i.
day 4 p.i.
B
Copy no./100ng DNA (RTA)
depleted
control
PHA4con
depleted control PHA4con depleted control PHA4con depleted control PHA4con
day 2 p.i.
day 3 p.i.
day 4 p.i.
C
Copy no./100ng DNA (RTA)
depleted
control
PHA4con
depleted control PHA4con depleted control PHA4con
day 3 p.i.
day 4 p.i.

Figure 5.15. Infection of NK cell depleted mice with M4.Stop or PHA4. NK cells were depleted by administration of an anti-NK1.1 antibody (PK136) on days -2, -1 and +2 relative to the day of infection. Mice were infected intranasally with 4 x 10^5 pfu of M4.Stop or PHA4 on day 0. NK cell depleted mice, infected with M4.Stop, are denoted by black circles (●), control (non-depleted) mice, infected with M4.Stop, by orange circles (●) and control mice infected with PHA4 by empty circles (○). Tissues were harvested on days 2, 3 & 4 p.i. using four mice per group per time point. Viral load was determined in lung (A), MLN (B) and spleen (C) by real-time PCR using primers specific for the viral gene, RTA. Viral DNA was quantified by amplification of the RTA gene and normalised as determined by the level of β-actin within each sample. The mean viral load of each group is shown by a horizontal line.

5.5. Discussion

NK cells have been shown to be critical for the control of several herpesvirus infections where the presence of viral antigens results in their activation, proliferation and accumulation at sites of infection. This study has focused on the role of NK cells in the control of MHV-68 infection. An expansion of the NK cell population in the MLN was observed at early time points. At day 2 post-infection, NK cell levels had increased in response to MHV-68 in comparison to day 4 post-infection where levels had decreased. This could be due to decreasing numbers of NK cells as the adaptive immune response is established or a smaller percentage of NK cells in the MLN due to increased populations of other lymphocytes such as $CD8^+$ T cells. The expansion of NK cells observed could have been due to NK cell proliferation within the MLN, accumulation of NK cells at this site or by a combination of both. The level of NK cell activation was determined by means of intracellular IFNγ staining. These data show that a proportion of NK cells were activated post-infection and that this level stayed relatively constant from day 2 to day 4 post-infection. These data prove that the NK cell population was expanded and activated in response to MHV-68 infection. During each experiment the role of MHV-76 infection was investigated in parallel to MHV-68 to determine whether the left end of the genome was responsible for regulation of the NK cell response. In each case the results were similar for both viruses suggesting that there is no role for the unique genes, M1-M4, in NK cell expansion and activation in the MLN. Cytokines expressed early in infection such as IFNα/β and IL-12, are important in shaping the NK cell response to infection. A study by Nguyen *et al.* has shown that these cytokines take on quite separate roles during the NK cell response to MCMV. IL-12 promotes IFNγ production whereas IFNα/β stimulates proliferation and cytotoxicity (Nguyen *et al.*, 2002). It would be of interest to determine if the NK cell population expansion would still occur in IFNα/β receptor knockout mice and whether this effect was IFNα/β dependent.

The ability of activated NK cells from MHV-68 infected mice to kill target cells was assessed by cytotoxicity assay. Initially, chromium release assays were carried out but these assays did not prove to be sensitive enough to detect NK cell killing in the samples. It may be that there was not sufficient cell-cell contact between NK cells and their targets due to the presence of other lymphocyte populations in the effector cell fraction. This effect was not improved by complement depletion of T lymphocytes as the majority of remaining lymphocytes were B lymphocytes and contact inhibition could still hinder NK cell cytotoxicity. Other optimisation techniques also did not improve the sensitivity of the assay. It was decided to change the detection of cytotoxicity from chromium release to fluorescence. A number of studies have shown that fluorescence based cytotoxicity assays have a number of benefits including increased sensitivity, safety and reduced background levels. A fluorescence based cytotoxicity assay was developed to determine if the activated NK cells from the MLNs of MHV-68 infected mice were capable of cytotoxic killing. These results have shown that NK cells from the infected MLNs are capable of killing susceptible cell targets. However, the level of killing was relatively low. This was not unexpected as studies with perforin knockout mice show that a lack of perforin has little effect on MHV-68 infection, thus suggesting that the cytotoxic release by NK cells does not play a major role in the control of the virus (Usherwood *et al.*, 1997).

It would be interesting to further investigate the cytotoxic response by directly infecting the target cells with MHV-68. It is possible that this would result in higher killing of target cells due to the increased antigen available and down regulation of MHC class I molecules. For example, infection of human foreskin fibroblast cells with vaccinia virus results in increased susceptibility of targets to lysis by NK cells (Chisholm and Reyburn 2006). Increased recognition was determined to be due to changes in the target cell induced by the early gene products of vaccinia virus infection and was dependent on the human natural cytotoxicity receptors NKp30, NKp44 and NKp46. A similar outcome is possible for infection with MHV-68. Conversely, MHV-68 infection of targets may reduce the level of killing observed

through immune evasion strategies that are yet to be determined. MHV-68 may employ NK cell evasion mechanisms, encoding proteins with similar functions to those of MCMV as discussed earlier. For example, the proteins K3 and K5 of KSHV induce rapid down regulation of MHC class I molecules from the cell surface. This would render cells susceptible to NK cell killing. However, K5 also down regulates ICAM-1 and B7-2 which are ligands for NK cell activatory receptors. This results in strong inhibition of NK cell mediated killing (Ishido *et al.*, 2000).

Given the important role for NK cells in other herpesvirus infections such as CMV it was expected that NK cells would be important for the control of MHV-68 infection. However, these data show that NK cells do not play a major role in the control of MHV-68 infection *in vivo*. Loss of NK cells did not affect viral load in the lung, MLN or spleen at any time point investigated as there was no significant difference between NK cell depleted and non-depleted mice. These data support previous findings that NK cell-depletion had no effect on the control of MHV-68 during the acute or latent stages of infection (Usherwood *et al.*, 2005). This was surprising due to the correlation between high NK cell numbers and lower viral loads during acute EBV infection suggesting an important role during gammaherpesvirus infections. It may be that the MHV-68 model underestimates the role for NK cells during human infections with gammaherpesviruses. Similarly, it may be that NK cells contribute more to counter infection in MHV-68's natural host, the wood mouse, than in inbred laboratory strains of mice (Blasdell *et al.*, 2003). A subtle role for NK cells during MHV-68 infection can not be ruled out as the NK cells are expanded, activated and are capable of killing susceptible targets post-infection. There is a great deal of compensation within the immune system and it may be that a lack of NK cells is efficiently compensated for during MHV-68 infection. It was expected that K3, expressed by MHV-68 during infection to down regulate MHC class I from the cell surface, would lead infected cells to be more susceptible to NK cell killing. However, this did not appear to be the case, possibly due to further NK cell immune evasion strategies. These data suggest that NK cells do not greatly influence the outcome of MHV-68 infection *in vivo*.

The viruses MHV-76 and M4.Stop were investigated to determine if there was a role for the unique genes at the left end of the MHV-68 genome in the manipulation of the NK cell response. The M4 gene is an immediate early/early transcript, mainly expressed during acute infection *in vivo* and has no role for replication *in vitro*. A M4 knock-in virus, MHV-76inM4, replicated to higher titres than MHV-76 at day 1 post-infection suggesting a possible immunoregulatory role for M4 during the innate response (Townsley *et al.*, 2004). However, the results show that there was no difference in viral load between the NK cell depleted and non-depleted mice infected with either MHV-76 or M4.Stop. From these data it has been concluded that the left end of MHV-68, including M4, is not involved in regulation of the NK cell response *in vivo* as no difference in MHV-76 or M4.Stop viral load could be detected whether in the presence or absence of NK cells.

Overall, it can be concluded from these data that the NK cell population is expanded, activated and is capable of cytotoxic killing at early time points following infection with MHV-68. However, NK cells do not appear to be vital for control of infection *in vivo*.

Chapter 6: Conclusions

6. Conclusions

The role of the innate immune system during gammaherpesvirus infection remains relatively uncharacterised. Using MHV-68 as a useful small animal model, this study was undertaken to answer the following questions concerning the role of the innate immune system during a murine gammaherpesvirus infection:

1. What components of the type I IFN response are important in the innate immune response to MHV-68 infection?
2. Does murine ISG12a play a role in the control of MHV-68 infection?
3. Do natural killer cells contribute to MHV-68 control at early time points?
4. Do genes unique to MHV-68 (M1-M4) play a role in evasion of the innate immune response?

This study has used *in vitro* assays and transgenic mice to increase understanding of the type I IFN response to gammaherpesvirus infection. The induction of type I IFNs was investigated *in vitro* by RT-PCR analysis. This is the first study to show that MHV-68 infection leads to the induction of various type I IFN subtypes within the first few hours of infection. IFNα4 and IFNβ transcripts were detected first post-infection, followed by the expression of other IFNα subtypes (IFNnonα4). This result is supported by previous studies with other viruses in which IFNβ and IFNα4 were found to be expressed very early post-infection, leading to the expression of other IFNα subtypes by signalling through IRF7 (Marie *et al.*, 1998). The importance of this positive feedback loop during virus infection was demonstrated *in vivo* by Prakash *et al.* (2005). IFNα production correlated with IRF7 production in the lungs of mice following infection with influenza A virus. Furthermore, the levels of IFNα were significantly reduced in STAT1-deficient mice consistent with a role for IRF7-mediated positive feedback.

Analysis of MHV-68 replication *in vitro* was carried out in MEF cell lines deficient in either IFNα/β receptor or IFNβ, or in wt MEFs. A strong trend towards higher titres of cell-free virus could be detected from cell lines lacking type I IFN compared to titres of cell-free virus from the wt cell line. These studies suggest that type I IFNs play a role in the inhibition of viral particle exit from the cell. It is postulated that the differences observed between cell lines may be due to a lesser degree of ISG induction in the type I IFN deficient cell lines therefore allowing greater exit of virions from the infected cell. The IFN-stimulated ubiquitin-like protein ISG15 has been shown to be important during a number of viral infections. ISG15-deficient mice are more susceptible to influenza A, influenza B, HSV-1 and Sindbis virus infection (Lenschow *et al.*, 2007). The addition of type I IFN to HIV-1 infected cells has been shown to inhibit the assembly and release of virions from the cell. This inhibition was due to the action of ISG15 as treatment of cells with ISG15 siRNA reversed the IFN-mediated inhibition of HIV-1 release (Okumura *et al.*, 2006). ISG15-deficient mice are also more susceptible to MHV-68 infection. It may be possible that ISG15 also plays a role in type I IFN-dependent inhibition of MHV-68 virion release. Determination of the role of ISG15 and other ISGs involved in limiting MHV-68 release could be the subject of future study.

Previous studies have shown that the type I IFNs are crucial for the control of a wide range of viruses including LCMV, SFV and vaccinia virus (Van Den Broek *et al.*, 1995). The type I IFNs have been shown to be an important defence against MHV-68 infection (Barton *et al.*, 2005; Dutia *et al.*, 1999). In this study, IFNβ-deficient mice were utilised to determine a role for IFNβ specifically during MHV-68 infection. IFNβ was found to be important for the control of lytic infection. Virus titres in the lungs of IFNβ$^{-/-}$ mice were significantly higher during the peak of acute infection (day 5 when infected with 4 x 10^5 pfu and day 7 when infected with 4 x 10^3 pfu) in comparison to the viral titres in wt lungs. These data are supported by the results observed in IFNα/β R$^{-/-}$ mice where lung titres were significantly higher than in wt mice during acute infection (Dutia *et al.*, 1999). However, at times other than the

peak of acute infection, virus was cleared from the lung to a similar degree in both IFNβ$^{-/-}$ and wt mice suggesting that other immune components, such as IFNα, can compensate for the lack of IFNβ. There appeared to be a trend for higher viral titres in the spleens of IFNβ$^{-/-}$ mice compared to those of wt mice when groups were infected with 4 x 10^3 pfu of MHV-68. However, due to an outbreak of MHV infection within the IFNβ$^{-/-}$ stock, no further experiments could be carried out during the course of this study. Therefore, future work is necessary to confirm differences in the degree of latent MHV-68 infection established within the spleens of IFNβ$^{-/-}$ or wt mice. It was expected that the lack of IFNβ expression in these mice would have had a greater effect on the titres of MHV-68 observed in the lung during the early stages of infection. For example, IFNβ$^{-/-}$ mice infected with influenza A virus have enhanced virus replication in the respiratory tract at 72 hours post-infection and show more severe disease symptoms compared to wild type mice (Koerner *et al.*, 2007). Similarly, the importance of IFNβ in the lung was shown during vaccinia virus infection. IFNβ$^{-/-}$ mice infected intranasally with vaccinia virus have significantly elevated viral titres in the lung at day 5 post-infection and succumb to doses of virus that are sublethal to wild type mice (Deonarain *et al.*, 2000). On the other hand, in mice surviving past day 5 post-infection, there was no significant difference in vaccinia virus titres found between the spleens of IFNβ$^{-/-}$ and wild type mice (Deonarain *et al.*, 2000) suggesting that the adaptive immune response has compensated for the lack of IFNβ by this stage of infection. This may also be the case for MHV-68 if no significant difference is found between the splenic titres of IFNβ$^{-/-}$ and wild type mice in future repeats of this experiment. It is evident that IFNβ has a protective role during some but not all virus infections. For example, there was no difference in the course of vesicular stomatits virus infection between IFNβ-deficient and wild type mice. The absence of IFN-ß made no difference to the level of IFNα produced within the first 6 hours of infection (Barchet et al., 2002). Such observations correlate with the hypothesis that IFNα can compensate for the lack of IFNβ during some virus infections. MHV-68 infection is likely an example of this hypothesis.

The functions of particular ISGs during viral infection are currently being elucidated. This study focused on the role of ISG12a following MHV-68 infection. A MEF cell line was established from an ISG12a knockout mouse to investigate ISG12a function *in vitro*. One step growth curves were carried out in ISG12a knockout and wt cell lines as it was hypothesised that the nuclear localisation of ISG12a may be important for the regulation of MHV-68 particle release during replication. A lack of ISG12a would possibly lead to increased release of virus particles and therefore elevated viral titres. However, there was no consistent trend observed in cell-free, cell-associated or combined virus titres between the ISG12a knockout and wt MEFs at any time point investigated. These results indicate that ISG12a is not playing a major role in the regulation of MHV-68 release so is not having a major effect on the resultant viral titres *in vitro*. Mice lacking ISG12a were utilised to study the role of ISG12a *in vivo*. No difference in viral titres was observed in the lungs or MLNs between ISG12a knockout and wt mice. MHV-68 titres and the degree of splenomegaly were increased in the spleens of ISG12a knockout mice compared to wt spleens showing that ISG12a plays a role in the early stages of the establishment of latency following MHV-68 infection. Further characterisation of ISG12a expression is required to determine the mechanism by which the establishment of latency is affected. In addition to playing a role during MHV-68 infection of the spleen, ISG12 has also been shown to play a protective role during neurotropic viral infection. Upregulation of ISG12 expression in the brains of Sindbis virus infected neonatal mice correlated with increased survival times (Labrada *et al.*, 2002). It may be that ISG12 plays an important protective role against a diverse range of viruses but this is yet to be studied.

The third aim of this study was to determine the role of NK cells during the early stages of a gammaherpesvirus infection. This study used FACS analysis and intracellular staining to show that the NK cell population in the MLN was expanded at day 2 compared to day 4 post-infection and was able to produce IFNγ in response to MHV-68 infection during the early stages of infection. The early production of IFNγ from NK cells, prior to the activation of T cells, is important for the early

control of infection. For example, mice are more susceptible to HSV-1 infection when the IFNγ-producing capacity of NK cells is impaired (Liu *et al.*, 2004). Cytotoxicity assays were used to show that MLN-derived NK cells, which are activated in response to MHV-68 infection, were capable of killing susceptible targets. The cytotoxic activity of NK cells is vital for the control of many viral infections. For example, higher numbers of NK cells expressing cytotoxic markers during acute Dengue virus infection correlate with milder disease symptoms (Azeredo *et al.*, 2006). Perforin-mediated cytotoxicity was shown to be important for controlling MCMV replication in the livers and spleens of MCMV-infected mice thus demonstrating the importance of cytotoxicity for controlling certain viral infections (Loh *et al.*, 2005). However, perforin-mediated cytotoxicity does not appear to be crucial for the control of MHV-68. Perforin-deficient mice could control MHV-68 infection to the same extent as wild type mice (Usherwood *et al.*, 1997). This correlates with the relatively low level of cytotoxic response observed from MHV-68-activated NK cells in this study. Similarly, a lack of NK cell-mediated cytotoxicity did not affect the control of HSV-1 infection (Halford *et al.*, 2005).

Given the fact that the NK cell population is expanded and activated during MHV-68 infection, the role of NK cells was investigated *in vivo*. As there is no strain of transgenic mice in which NK cell activities are specifically and selectively deficient, NK cells were depleted by administration of an anti-NK cell antibody. It was found that a lack of NK cells *in vivo* did not result in significantly elevated virus titres in the lung, MLN or spleen, suggesting that NK cells are not essential for the control of MHV-68 infection. Such a result was surprising given the important role for NK cells in other virus infections such as CMV. Depletion of NK cells expressing the activatory receptor Ly49H results in up to 1000-fold higher MCMV titres in the spleens, but only 5-fold higher titres in the livers, of depleted mice compared to non-depleted mice (Daniels *et al.*, 2001). However, no difference in virus titres between NK cell-depleted and non-depleted animals was observed in any tissue investigated. Infection of IL-18-deficient mice displayed a reduced level of IFNγ production and low NK cell cytotoxicity in the lung during the first few days of influenza A virus

infection. The reduced NK cell responses in the lungs of these mice resulted in increased mortality rates (Liu *et al.*, 2004). It was expected that depletion of NK cells would result in higher MHV-68 titres in the lung at early time points during acute infection. Such is true for other herpesvirus infections. Following intranasal infection of mice with HSV-1, NK cell numbers increase in the lung and produce IFNγ. Furthermore, depletion of NK cells resulted in increased virus titres in the lung (Reading *et al.*, 2006). This was not the case for MHV-68 infection. A lack of a role for NK cells is supported by the findings of Usherwood *et al.*, (2005) whereby NK cell-depletion had no effect on the control of MHV-68 during the acute or latent stages of infection. A subtle role for NK cells during MHV-68 infection can not be ruled out as the NK cells are expanded, activated and are capable of killing susceptible targets post-infection. It may be that NK cells contribute more to control of MHV-68 infection in the natural host, the wood mouse, than in inbred laboratory strains of mice. Besides, the MHV-68 model may underestimate the role of NK cells during human gammaherpesvirus infections as studies have shown an important role for NK cells during acute EBV infection. The proportion of NK cells with an activated phenotype was significantly higher in patients with acute infection and increased NK cell numbers correlated with decreased EBV titres. This study therefore suggests an important role for NK cells in dictating the outcome of human gammaherpesvirus infection (Williams *et al.*, 2005).

MHV-76 is a deletion mutant of MHV-68, lacking four genes (M1-M4) and eight vtRNAs unique to MHV-68 and present at the left hand end of the genome. The left end of the genome is thought to play a role in pathogenesis as MHV-76 is attenuated *in vivo* (Macrae *et al.*, 2001). The ability of MHV-68 or MHV-76 to replicate in the absence of either IFNβ or NK cells was examined during this investigation in order to determine a possible immunoregulatory role for the left end of MHV-68 during the innate immune response. However, this study found no difference in the induction of type I IFN response *in vitro* following infection with either MHV-68 or MHV-76. Additionally, IFNβ knockout mice could control MHV-76 infection *in vivo* to the same extent as wild type mice. These results suggest that M1-M4 and the 8 vtRNAs

do not play an extensive role in the regulation of the type I IFN response. Similar conclusions can be drawn concerning the regulation NK cells. No difference was observed between MHV-68 or MHV-76 infection in the expansion or activation of NK cells in the MLN or during *in vivo* infection of NK cell-depleted and non-depleted mice. It was therefore concluded that the genes M1-M4 and the 8 vtRNAs do not play a major role in the regulation of NK cells following MHV-68 infection.

Overall, this study has shown that the innate immune system is important for the control of gammaherpesvirus infections. It does appear that innate immune components vary in their significance during the early stages of infection. For example, a lack of IFNβ results in greater viral titres in the lung at early time points post-infection in comparison to wild-type mice. However, mice lacking NK cells could control MHV-68 infection as well as wild-type mice. Given the redundancy and complexity of the immune response a subtle role for NK cells can not be ruled out. In addition, NK cells may be more important during human gammaherpesvirus infections than during murine gammaherpesvirus infections.

It would be interesting to look at the effects of a lack of IFNβ on NK cell function in the IFNβ$^{-/-}$ mouse. Type I IFN can stimulate NK cell proliferation and cytotoxicity (Nguyen *et al.*, 2002) so a lack of IFNβ may result in decreased NK cell responses and proliferation and thus illustrate the importance of IFNβ for development of downstream responses. Furthermore, depletion of NK cells in the IFNβ$^{-/-}$ mouse may reveal a more crucial role for NK cells during MHV-68 infection whereby reduced type I IFN responses cannot compensate for NK cell-depletion.

The role of ISG12(a) during the establishment of latency would be an interesting topic of future work with a number of avenues to investigate. Firstly, ISG12(a) might have a role involving interaction with latency-associated viral antigens in the spleen during latent infection. Infection of np27$^{-/-}$ mice with viruses lacking various latency-

associated genes, such as an ORF73-deletion mutant of MHV-68, or comparison of viral gene expression in np27$^{-/-}$ and wild-type mice would be useful for investigating this possibility. Alternatively, ISG12 expression in the spleen may be important for control of infection in a specific cell population such as DCs, leading to a less effective splenic DC response and therefore increased MHV-68 replication and/or increased expansion of MHV-68 infected B cells in the spleen. It would be of interest to carry out immunostaining to determine if cell populations differed between knockout and wild-type mice. Also, analysis of responses downstream of DCs such as IL-12 and type I IFN production would help to determine if DC function was significantly affected by a lack of ISG12(a) expression.

Although components of the left end of the MHV-68 genome have been suggested to be involved in immune regulation this study did not find any role for the genes M1-M4 or the vtRNAs in the modulation of either the IFNβ or NK cell response. However, further analysis of the downstream responses from IFNβ and NK cells may elucidate some immunoregulatory roles for these genes.

References

References

Abate, D. A., S. Watanabe and E. S. Mocarski (2004). "Major human cytomegalovirus structural protein pp65 (ppUL83) prevents interferon response factor 3 activation in the interferon response." *J Virol* **78**(20): 10995-1006.

Adler, H., M. Messerle, M. Wagner and U. H. Koszinowski (2000). "Cloning and mutagenesis of the murine gammaherpesvirus 68 genome as an infectious bacterial artificial chromosome." *J Virol* **74**(15): 6964-74.

Akula, S. M., N. P. Pramod, F. Z. Wang and B. Chandran (2001). "Human herpesvirus 8 envelope-associated glycoprotein B interacts with heparan sulfate-like moieties." *Virology* **284**(2): 235-49.

Alexopoulou, L., A. C. Holt, R. Medzhitov and R. A. Flavell (2001). "Recognition of double-stranded RNA and activation of NF-kappaB by Toll-like receptor 3." *Nature* **413**(6857): 732-8.

Amyes, E., C. Hatton, D. Montamat-Sicotte, N. Gudgeon, A. B. Rickinson, A. J. McMichael and M. F. Callan (2003). "Characterization of the CD4+ T cell response to Epstein-Barr virus during primary and persistent infection." *J Exp Med* **198**(6): 903-11.

Arase, H., E. S. Mocarski, A. E. Campbell, A. B. Hill and L. L. Lanier (2002). "Direct recognition of cytomegalovirus by activating and inhibitory NK cell receptors." *Science* **296**(5571): 1323-6.

Arnon, T. I., M. Lev, G. Katz, Y. Chernobrov, A. Porgador and O. Mandelboim (2001). "Recognition of viral hemagglutinins by NKp44 but not by NKp30." *Eur J Immunol* **31**(9): 2680-9.

Asselin-Paturel, C., A. Boonstra, M. Dalod, I. Durand, N. Yessaad, C. Dezutter-Dambuyant, A. Vicari, A. O'Garra, C. Biron, F. Briere and G. Trinchieri (2001). "Mouse type I IFN-producing cells are immature APCs with plasmacytoid morphology." *Nat Immunol* **2**(12): 1144-50.

Baigent, S. J., G. Zhang, M. D. Fray, H. Flick-Smith, S. Goodbourn and J. W. McCauley (2002). "Inhibition of beta interferon transcription by noncytopathogenic bovine viral diarrhea virus is through an interferon regulatory factor 3-dependent mechanism." *J Virol* **76**(18): 8979-88.

Balachandran, S., C. N. Kim, W. C. Yeh, T. W. Mak, K. Bhalla and G. N. Barber (1998). "Activation of the dsRNA-dependent protein kinase, PKR, induces apoptosis through FADD-mediated death signaling." *Embo J* **17**(23): 6888-902.

Balaji, K. N., N. Schaschke, W. Machleidt, M. Catalfamo and P. A. Henkart (2002). "Surface cathepsin B protects cytotoxic lymphocytes from self-destruction after degranulation." *J Exp Med* **196**(4): 493-503.

Barnes, B. J., P. A. Moore and P. M. Pitha (2001). "Virus-specific activation of a novel interferon regulatory factor, IRF-5, results in the induction of distinct interferon alpha genes." *J Biol Chem* **276**(26): 23382-90.

Barton, E. S., M. L. Lutzke, R. Rochford and H. W. t. Virgin (2005). "Alpha/beta interferons regulate murine gammaherpesvirus latent gene expression and reactivation from latency." *J Virol* **79**(22): 14149-60.

Bauer, S., V. Groh, J. Wu, A. Steinle, J. H. Phillips, L. L. Lanier and T. Spies (1999). "Activation of NK cells and T cells by NKG2D, a receptor for stress-inducible MICA." *Science* **285**(5428): 727-9.

Benoit, L., X. Wang, H. F. Pabst, J. Dutz and R. Tan (2000). "Defective NK cell activation in X-linked lymphoproliferative disease." *J Immunol* **165**(7): 3549-53.

Beresford, P. J., Z. Xia, A. H. Greenberg and J. Lieberman (1999). "Granzyme A loading induces rapid cytolysis and a novel form of DNA damage independently of caspase activation." *Immunity* **10**(5): 585-94.

Bertone, S., F. Schiavetti, R. Bellomo, C. Vitale, M. Ponte, L. Moretta and M. C. Mingari (1999). "Transforming growth factor-beta-induced expression of CD94/NKG2A inhibitory receptors in human T lymphocytes." *Eur J Immunol* **29**(1): 23-9.

Biron, C. A. (1997). "Activation and function of natural killer cell responses during viral infections." *Curr Opin Immunol* **9**(1): 24-34.

Biron, C. A., K. S. Byron and J. L. Sullivan (1989). "Severe herpesvirus infections in an adolescent without natural killer cells." *N Engl J Med* **320**(26): 1731-5.

Biron, C. A., K. B. Nguyen, G. C. Pien, L. P. Cousens and T. P. Salazar-Mather (1999). "Natural killer cells in antiviral defense: function and regulation by innate cytokines." *Annu Rev Immunol* **17**: 189-220.

Blasdell, K., C. McCracken, A. Morris, A. A. Nash, M. Begon, M. Bennett and J. P. Stewart (2003). "The wood mouse is a natural host for Murid herpesvirus 4." *J Gen Virol* **84**(Pt 1): 111-3.

Blaskovic, D., M. Stancekova, J. Svobodova and J. Mistrikova (1980). "Isolation of five strains of herpesviruses from two species of free living small rodents." *Acta Virol* **24**(6): 468.

Bluman, E. M., K. J. Bartynski, B. R. Avalos and M. A. Caligiuri (1996). "Human natural killer cells produce abundant macrophage inflammatory protein-1 alpha in response to monocyte-derived cytokines." *J Clin Invest* **97**(12): 2722-7.

Bowden, R. J., J. P. Simas, A. J. Davis and S. Efstathiou (1997). "Murine gammaherpesvirus 68 encodes tRNA-like sequences which are expressed during latency." *J Gen Virol* **78 (Pt 7)**: 1675-87.

Brooks, A. G., F. Borrego, P. E. Posch, A. Patamawenu, C. J. Scorzelli, M. Ulbrecht, E. H. Weiss and J. E. Coligan (1999). "Specific recognition of HLA-E, but not classical, HLA class I molecules by soluble CD94/NKG2A and NK cells." *J Immunol* **162**(1): 305-13.

Brooks, D. G., M. J. Trifilo, K. H. Edelmann, L. Teyton, D. B. McGavern and M. B. Oldstone (2006). "Interleukin-10 determines viral clearance or persistence in vivo." *Nat Med* **12**(11): 1301-9.

Brown, M. G., A. O. Dokun, J. W. Heusel, H. R. Smith, D. L. Beckman, E. A. Blattenberger, C. E. Dubbelde, L. R. Stone, A. A. Scalzo and W. M. Yokoyama (2001). "Vital involvement of a natural killer cell activation receptor in resistance to viral infection." *Science* **292**(5518): 934-7.

Browne, E. P., B. Wing, D. Coleman and T. Shenk (2001). "Altered cellular mRNA levels in human cytomegalovirus-infected fibroblasts: viral block to the accumulation of antiviral mRNAs." *J Virol* **75**(24): 12319-30.

Burysek, L. and P. M. Pitha (2001). "Latently expressed human herpesvirus 8-encoded interferon regulatory factor 2 inhibits double-stranded RNA-activated protein kinase." *J Virol* **75**(5): 2345-52.

Burysek, L., W. S. Yeow, B. Lubyova, M. Kellum, S. L. Schafer, Y. Q. Huang and P. M. Pitha (1999). "Functional analysis of human herpesvirus 8-encoded viral interferon regulatory factor 1 and its association with cellular interferon regulatory factors and p300." *J Virol* **73**(9): 7334-42.

Callan, M. F., L. Tan, N. Annels, G. S. Ogg, J. D. Wilson, C. A. O'Callaghan, N. Steven, A. J. McMichael and A. B. Rickinson (1998). "Direct visualization of antigen-specific CD8+ T cells during the primary immune response to Epstein-Barr virus In vivo." *J Exp Med* **187**(9): 1395-402.

Cantoni, C., C. Bottino, M. Vitale, A. Pessino, R. Augugliaro, A. Malaspina, S. Parolini, L. Moretta, A. Moretta and R. Biassoni (1999). "NKp44, a triggering receptor involved in tumor cell lysis by activated human natural killer cells, is a novel member of the immunoglobulin superfamily." *J Exp Med* **189**(5): 787-96.

Cardin, R. D., J. W. Brooks, S. R. Sarawar and P. C. Doherty (1996). "Progressive loss of CD8+ T cell-mediated control of a gamma-herpesvirus in the absence of CD4+ T cells." *J Exp Med* **184**(3): 863-71.

Cerwenka, A. and L. L. Lanier (2001). "Natural killer cells, viruses and cancer." *Nat Rev Immunol* **1**(1): 41-9.

Chee, A. V. and B. Roizman (2004). "Herpes simplex virus 1 gene products occlude the interferon signaling pathway at multiple sites." *J Virol* **78**(8): 4185-96.

Cheng, T. F., S. Brzostek, O. Ando, S. Van Scoy, K. P. Kumar and N. C. Reich (2006). "Differential activation of IFN regulatory factor (IRF)-3 and IRF-5 transcription factors during viral infection." *J Immunol* **176**(12): 7462-70.

Chisholm, S. E. and H. T. Reyburn (2006). "Recognition of vaccinia virus-infected cells by human natural killer cells depends on natural cytotoxicity receptors." *J Virol* **80**(5): 2225-33.

Clambey, E. T., H. W. t. Virgin and S. H. Speck (2000). "Disruption of the murine gammaherpesvirus 68 M1 open reading frame leads to enhanced reactivation from latency." *J Virol* **74**(4): 1973-84.

Colamonici, O., H. Yan, P. Domanski, R. Handa, D. Smalley, J. Mullersman, M. Witte, K. Krishnan and J. Krolewski (1994). "Direct binding to and tyrosine phosphorylation of the alpha subunit of the type I interferon receptor by p135tyk2 tyrosine kinase." *Mol Cell Biol* **14**(12): 8133-42.

Colucci, F., J. P. Di Santo and P. J. Leibson (2002). "Natural killer cell activation in mice and men: different triggers for similar weapons?" *Nat Immunol* **3**(9): 807-13.

Coscoy, L. and D. Ganem (2000). "Kaposi's sarcoma-associated herpesvirus encodes two proteins that block cell surface display of MHC class I chains by enhancing their endocytosis." *Proc Natl Acad Sci U S A* **97**(14): 8051-6.

Cosman, D., N. Fanger, L. Borges, M. Kubin, W. Chin, L. Peterson and M. L. Hsu (1997). "A novel immunoglobulin superfamily receptor for cellular and viral MHC class I molecules." *Immunity* 7(2): 273-82.

Cosman, D., J. Mullberg, C. L. Sutherland, W. Chin, R. Armitage, W. Fanslow, M. Kubin and N. J. Chalupny (2001). "ULBPs, novel MHC class I-related molecules, bind to CMV glycoprotein UL16 and stimulate NK cytotoxicity through the NKG2D receptor." *Immunity* **14**(2): 123-33.

Cousens, L. P., J. S. Orange, H. C. Su and C. A. Biron (1997). "Interferon-alpha/beta inhibition of interleukin 12 and interferon-gamma production in vitro and endogenously during viral infection." *Proc Natl Acad Sci U S A* **94**(2): 634-9.

Crawford, D. H. (2001). "Biology and disease associations of Epstein-Barr virus." *Philos Trans R Soc Lond B Biol Sci* **356**(1408): 461-73.

Dalod, M., T. Hamilton, R. Salomon, T. P. Salazar-Mather, S. C. Henry, J. D. Hamilton and C. A. Biron (2003). "Dendritic cell responses to early murine cytomegalovirus infection: subset functional specialization and differential regulation by interferon alpha/beta." *J Exp Med* **197**(7): 885-98.

Dalod, M., T. P. Salazar-Mather, L. Malmgaard, C. Lewis, C. Asselin-Paturel, F. Briere, G. Trinchieri and C. A. Biron (2002). "Interferon alpha/beta and interleukin 12 responses to viral infections: pathways regulating dendritic cell cytokine expression in vivo." *J Exp Med* **195**(4): 517-28.

Damania, B. and R. C. Desrosiers (2001). "Simian homologues of human herpesvirus 8." *Philos Trans R Soc Lond B Biol Sci* **356**(1408): 535-43.

Daniels, K. A., G. Devora, W. C. Lai, C. L. O'Donnell, M. Bennett and R. M. Welsh (2001). "Murine cytomegalovirus is regulated by a discrete subset of natural killer cells reactive with monoclonal antibody to Ly49H." *J Exp Med* **194**(1): 29-44.

DeFilippis, V. R., B. Robinson, T. M. Keck, S. G. Hansen, J. A. Nelson and K. J. Fruh (2006). "Interferon regulatory factor 3 is necessary for induction of antiviral genes during human cytomegalovirus infection." *J Virol* **80**(2): 1032-7.

Degli-Esposti, M. (1999). "To die or not to die--the quest of the TRAIL receptors." *J Leukoc Biol* **65**(5): 535-42.

Deonarain, R., A. Alcami, M. Alexiou, M. J. Dallman, D. R. Gewert and A. C. Porter (2000). "Impaired antiviral response and alpha/beta interferon induction in mice lacking beta interferon." *J Virol* **74**(7): 3404-9.

Der, S. D., A. Zhou, B. R. Williams and R. H. Silverman (1998). "Identification of genes differentially regulated by interferon alpha, beta, or gamma using oligonucleotide arrays." *Proc Natl Acad Sci U S A* **95**(26): 15623-8.

Derre, L., M. Corvaisier, M. C. Pandolfino, E. Diez, F. Jotereau and N. Gervois (2002). "Expression of CD94/NKG2-A on human T lymphocytes is induced by IL-12: implications for adoptive immunotherapy." *J Immunol* **168**(10): 4864-70.

Dittmer, D. P., C. M. Gonzalez, W. Vahrson, S. M. DeWire, R. Hines-Boykin and B. Damania (2005). "Whole-genome transcription profiling of rhesus monkey rhadinovirus." *J Virol* **79**(13): 8637-50.

Djerbi, M., V. Screpanti, A. I. Catrina, B. Bogen, P. Biberfeld and A. Grandien (1999). "The inhibitor of death receptor signaling, FLICE-inhibitory protein defines a new class of tumor progression factors." *J Exp Med* **190**(7): 1025-32.

Djeu, J. Y., K. Jiang and S. Wei (2002). "A view to a kill: signals triggering cytotoxicity." *Clin Cancer Res* **8**(3): 636-40.

Dokun, A. O., S. Kim, H. R. Smith, H. S. Kang, D. T. Chu and W. M. Yokoyama (2001). "Specific and nonspecific NK cell activation during virus infection." *Nat Immunol* **2**(10): 951-6.

Dutia, B. M., D. J. Allen, H. Dyson and A. A. Nash (1999). "Type I interferons and IRF-1 play a critical role in the control of a gammaherpesvirus infection." *Virology* **261**(2): 173-9.

Dutia, B. M., C. J. Clarke, D. J. Allen and A. A. Nash (1997). "Pathological changes in the spleens of gamma interferon receptor-deficient mice infected with murine gammaherpesvirus: a role for CD8 T cells." *J Virol* **71**(6): 4278-83.

Efstathiou, S., Y. M. Ho and A. C. Minson (1990). "Cloning and molecular characterization of the murine herpesvirus 68 genome." *J Gen Virol* **71 (Pt 6)**: 1355-64.

Ehtisham, S., N. P. Sunil-Chandra and A. A. Nash (1993). "Pathogenesis of murine gammaherpesvirus infection in mice deficient in CD4 and CD8 T cells." *J Virol* **67**(9): 5247-52.

Elia, A., K. G. Laing, A. Schofield, V. J. Tilleray and M. J. Clemens (1996). "Regulation of the double-stranded RNA-dependent protein kinase PKR by RNAs encoded by a repeated sequence in the Epstein-Barr virus genome." *Nucleic Acids Res* **24**(22): 4471-8.

Elsawa, S. F. and K. L. Bost (2004). "Murine gamma-herpesvirus-68-induced IL-12 contributes to the control of latent viral burden, but also contributes to viral-mediated leukocytosis." *J Immunol* **172**(1): 516-24.

Endo, T. A., M. Masuhara, M. Yokouchi, R. Suzuki, H. Sakamoto, K. Mitsui, A. Matsumoto, S. Tanimura, M. Ohtsubo, H. Misawa, T. Miyazaki, N. Leonor, T. Taniguchi, T. Fujita, Y. Kanakura, S. Komiya and A. Yoshimura (1997). "A new protein containing an SH2 domain that inhibits JAK kinases." *Nature* **387**(6636): 921-4.

Epstein, M. A., A. J. Morgan, S. Finerty, B. J. Randle and J. K. Kirkwood (1985). "Protection of cottontop tamarins against Epstein-Barr virus-induced malignant lymphoma by a prototype subunit vaccine." *Nature* **318**(6043): 287-9.

Falvo, J. V., B. S. Parekh, C. H. Lin, E. Fraenkel and T. Maniatis (2000). "Assembly of a functional beta interferon enhanceosome is dependent on ATF-2-c-jun heterodimer orientation." *Mol Cell Biol* **20**(13): 4814-25.

Farrell, H. E., H. Vally, D. M. Lynch, P. Fleming, G. R. Shellam, A. A. Scalzo and N. J. Davis-Poynter (1997). "Inhibition of natural killer cells by a cytomegalovirus MHC class I homologue in vivo." *Nature* **386**(6624): 510-4.

Fenner, J. E., R. Starr, A. L. Cornish, J. G. Zhang, D. Metcalf, R. D. Schreiber, K. Sheehan, D. J. Hilton, W. S. Alexander and P. J. Hertzog (2006). "Suppressor of cytokine signaling 1 regulates the immune response to infection by a unique inhibition of type I interferon activity." *Nat Immunol* **7**(1): 33-9.

Fitzgerald, K. A., S. M. McWhirter, K. L. Faia, D. C. Rowe, E. Latz, D. T. Golenbock, A. J. Coyle, S. M. Liao and T. Maniatis (2003). "IKKepsilon and TBK1 are essential components of the IRF3 signaling pathway." *Nat Immunol* **4**(5): 491-6.

Flano, E., C. L. Hardy, I. J. Kim, C. Frankling, M. A. Coppola, P. Nguyen, D. L. Woodland and M. A. Blackman (2004). "T cell reactivity during infectious mononucleosis and persistent gammaherpesvirus infection in mice." *J Immunol* **172**(5): 3078-85.

Flano, E., S. M. Husain, J. T. Sample, D. L. Woodland and M. A. Blackman (2000). "Latent murine gamma-herpesvirus infection is established in activated B cells, dendritic cells, and macrophages." *J Immunol* **165**(2): 1074-81.

Flano, E., I. J. Kim, J. Moore, D. L. Woodland and M. A. Blackman (2003). "Differential gamma-herpesvirus distribution in distinct anatomical locations and cell subsets during persistent infection in mice." *J Immunol* **170**(7): 3828-34.

French, A. R., E. B. Holroyd, L. Yang, S. Kim and W. M. Yokoyama (2006). "IL-18 acts synergistically with IL-15 in stimulating natural killer cell proliferation." *Cytokine* **35**(5-6): 229-34.

Fuld, S., C. Cunningham, K. Klucher, A. J. Davison and D. J. Blackbourn (2006). "Inhibition of interferon signaling by the Kaposi's sarcoma-associated herpesvirus full-length viral interferon regulatory factor 2 protein." *J Virol* **80**(6): 3092-7.

Geere, H. M., Y. Ligertwood, K. M. Templeton, I. Bennet, B. Gangadharan, S. M. Rhind, A. A. Nash and B. M. Dutia (2006). "The M4 gene of murine gammaherpesvirus 68 modulates latent infection." *J Gen Virol* **87**(Pt 4): 803-7.

Gerosa, F., A. Gobbi, P. Zorzi, S. Burg, F. Briere, G. Carra and G. Trinchieri (2005). "The reciprocal interaction of NK cells with plasmacytoid or myeloid dendritic cells profoundly affects innate resistance functions." *J Immunol* **174**(2): 727-34.

Gjermandsen, I. M., J. Justesen and P. M. Martensen (2000). "The interferon-induced gene ISG12 is regulated by various cytokines as the gene 6-16 in human cell lines." *Cytokine* **12**(3): 233-8.

Goodbourn, S., L. Didcock and R. E. Randall (2000). "Interferons: cell signalling, immune modulation, antiviral response and virus countermeasures." *J Gen Virol* **81**(Pt 10): 2341-64.

Hakki, M. and A. P. Geballe (2005). "Double-stranded RNA binding by human cytomegalovirus pTRS1." *J Virol* **79**(12): 7311-8.

Halford, W. P., J. L. Maender and B. M. Gebhardt (2005). "Re-evaluating the role of natural killer cells in innate resistance to herpes simplex virus type 1." *Virol J* **2**: 56.

Harle, P., V. Cull, M. P. Agbaga, R. Silverman, B. R. Williams, C. James and D. J. Carr (2002). "Differential effect of murine alpha/beta interferon transgenes on antagonization of herpes simplex virus type 1 replication." *J Virol* **76**(13): 6558-67.

Hasan, M., A. Krmpotic, Z. Ruzsics, I. Bubic, T. Lenac, A. Halenius, A. Loewendorf, M. Messerle, H. Hengel, S. Jonjic and U. H. Koszinowski (2005). "Selective down-regulation of the NKG2D ligand H60 by mouse cytomegalovirus m155 glycoprotein." *J Virol* **79**(5): 2920-30.

Hashimoto, S. I., T. Suzuki, S. Nagai, T. Yamashita, N. Toyoda and K. Matsushima (2000). "Identification of genes specifically expressed in human activated and mature dendritic cells through serial analysis of gene expression." *Blood* **96**(6): 2206-14.

He, B., M. Gross and B. Roizman (1997). "The gamma(1)34.5 protein of herpes simplex virus 1 complexes with protein phosphatase 1alpha to dephosphorylate the alpha subunit of the eukaryotic translation initiation factor 2 and preclude the shutoff of protein synthesis by double-stranded RNA-activated protein kinase." *Proc Natl Acad Sci U S A* **94**(3): 843-8.

Herskowitz, J., M. A. Jacoby and S. H. Speck (2005). "The murine gammaherpesvirus 68 M2 gene is required for efficient reactivation from latently infected B cells." *J Virol* **79**(4): 2261-73.

Hochrein, H., B. Schlatter, M. O'Keeffe, C. Wagner, F. Schmitz, M. Schiemann, S. Bauer, M. Suter and H. Wagner (2004). "Herpes simplex virus type-1 induces IFN-alpha production via Toll-like receptor 9-dependent and -independent pathways." *Proc Natl Acad Sci U S A* **101**(31): 11416-21.

Honda, K. and T. Taniguchi (2006). "IRFs: master regulators of signalling by Toll-like receptors and cytosolic pattern-recognition receptors." *Nat Rev Immunol* **6**(9): 644-58.

Husain, S. M., E. J. Usherwood, H. Dyson, C. Coleclough, M. A. Coppola, D. L. Woodland, M. A. Blackman, J. P. Stewart and J. T. Sample (1999). "Murine gammaherpesvirus M2 gene is latency-associated and its protein a target for CD8(+) T lymphocytes." *Proc Natl Acad Sci U S A* **96**(13): 7508-13.

Iordanov, M. S., J. M. Paranjape, A. Zhou, J. Wong, B. R. Williams, E. F. Meurs, R. H. Silverman and B. E. Magun (2000). "Activation of p38 mitogen-activated protein kinase and c-Jun NH(2)-terminal kinase by double-stranded RNA and encephalomyocarditis virus: involvement of RNase L, protein kinase R, and alternative pathways." *Mol Cell Biol* **20**(2): 617-27.

Isaacs, A. and J. Lindenmann (1957). "Virus interference. I. The interferon." *Proc R Soc Lond B Biol Sci* **147**(927): 258-67.

Ishido, S., J. K. Choi, B. S. Lee, C. Wang, M. DeMaria, R. P. Johnson, G. B. Cohen and J. U. Jung (2000). "Inhibition of natural killer cell-mediated cytotoxicity by Kaposi's sarcoma-associated herpesvirus K5 protein." *Immunity* **13**(3): 365-74.

Iversen, A. C., P. S. Norris, C. F. Ware and C. A. Benedict (2005). "Human NK cells inhibit cytomegalovirus replication through a noncytolytic mechanism involving lymphotoxin-dependent induction of IFN-beta." *J Immunol* **175**(11): 7568-74.

Izaguirre, A., B. J. Barnes, S. Amrute, W. S. Yeow, N. Megjugorac, J. Dai, D. Feng, E. Chung, P. M. Pitha and P. Fitzgerald-Bocarsly (2003). "Comparative analysis of IRF and IFN-alpha expression in human plasmacytoid and monocyte-derived dendritic cells." *J Leukoc Biol* **74**(6): 1125-38.

Johannessen, I. and D. H. Crawford (1999). "In vivo models for Epstein-Barr virus (EBV)-associated B cell lymphoproliferative disease (BLPD)." *Rev Med Virol* **9**(4): 263-77.

Kagi, D., B. Ledermann, K. Burki, P. Seiler, B. Odermatt, K. J. Olsen, E. R. Podack, R. M. Zinkernagel and H. Hengartner (1994). "Cytotoxicity mediated by T cells and natural killer cells is greatly impaired in perforin-deficient mice." *Nature* **369**(6475): 31-7.

Katze, M. G., M. Wambach, M. L. Wong, M. Garfinkel, E. Meurs, K. Chong, B. R. Williams, A. G. Hovanessian and G. N. Barber (1991). "Functional expression and RNA binding analysis of the interferon-induced, double-stranded RNA-activated, 68,000-Mr protein kinase in a cell-free system." *Mol Cell Biol* **11**(11): 5497-505.

Kawai, T. and S. Akira (2006). "Innate immune recognition of viral infection." *Nat Immunol* **7**(2): 131-7.

Kedes, D. H., M. Lagunoff, R. Renne and D. Ganem (1997). "Identification of the gene encoding the major latency-associated nuclear antigen of the Kaposi's sarcoma-associated herpesvirus." *J Clin Invest* **100**(10): 2606-10.

Kennedy, M. K., M. Glaccum, S. N. Brown, E. A. Butz, J. L. Viney, M. Embers, N. Matsuki, K. Charrier, L. Sedger, C. R. Willis, K. Brasel, P. J. Morrissey, K. Stocking, J. C. Schuh, S. Joyce and J. J. Peschon (2000). "Reversible defects in natural killer and memory CD8 T cell lineages in interleukin 15-deficient mice." *J Exp Med* **191**(5): 771-80.

Kielczewska, A., H. S. Kim, L. L. Lanier, N. Dimasi and S. M. Vidal (2007). "Critical Residues at the Ly49 Natural Killer Receptor's Homodimer Interface Determine Functional Recognition of m157, a Mouse Cytomegalovirus MHC Class I-Like Protein." *J Immunol* **178**(1): 369-77.

Kiessling, R., E. Klein and H. Wigzell (1975). ""Natural" killer cells in the mouse. I. Cytotoxic cells with specificity for mouse Moloney leukemia cells. Specificity and distribution according to genotype." *Eur J Immunol* **5**(2): 112-7.

Kim, I. J., E. Flano, D. L. Woodland, F. E. Lund, T. D. Randall and M. A. Blackman (2003). "Maintenance of long term gamma-herpesvirus B cell latency is dependent on CD40-mediated development of memory B cells." *J Immunol* **171**(2): 886-92.

Kim, S., K. Iizuka, H. L. Aguila, I. L. Weissman and W. M. Yokoyama (2000). "In vivo natural killer cell activities revealed by natural killer cell-deficient mice." *Proc Natl Acad Sci U S A* **97**(6): 2731-6.

Kotenko, S. V., G. Gallagher, V. V. Baurin, A. Lewis-Antes, M. Shen, N. K. Shah, J. A. Langer, F. Sheikh, H. Dickensheets and R. P. Donnelly (2003). "IFN-lambdas mediate antiviral protection through a distinct class II cytokine receptor complex." *Nat Immunol* **4**(1): 69-77.

Krishnan, H. H., P. P. Naranatt, M. S. Smith, L. Zeng, C. Bloomer and B. Chandran (2004). "Concurrent expression of latent and a limited number of lytic genes with immune modulation and antiapoptotic function by Kaposi's sarcoma-associated herpesvirus early during infection of primary endothelial and fibroblast cells and subsequent decline of lytic gene expression." *J Virol* **78**(7): 3601-20.

Kumar, A., Y. L. Yang, V. Flati, S. Der, S. Kadereit, A. Deb, J. Haque, L. Reis, C. Weissmann and B. R. Williams (1997). "Deficient cytokine signaling in mouse embryo fibroblasts with a targeted deletion in the PKR gene: role of IRF-1 and NF-kappaB." *Embo J* **16**(2): 406-16.

Kumar, H., T. Kawai, H. Kato, S. Sato, K. Takahashi, C. Coban, M. Yamamoto, S. Uematsu, K. J. Ishii, O. Takeuchi and S. Akira (2006). "Essential role of IPS-1 in innate immune responses against RNA viruses." *J Exp Med* **203**(7): 1795-803.

Labrada, L., X. H. Liang, W. Zheng, C. Johnston and B. Levine (2002). "Age-dependent resistance to lethal alphavirus encephalitis in mice: analysis of gene expression in the central nervous system and identification of a novel interferon-inducible protective gene, mouse ISG12." *J Virol* **76**(22): 11688-703.

Lanier, L. L. (2001). "On guard--activating NK cell receptors." *Nat Immunol* **2**(1): 23-7.

Lanier, L. L. (2005). "NK cell recognition." *Annu Rev Immunol* **23**: 225-74.

Lee, B. J., F. Giannoni, A. Lyon, S. Yada, B. Lu, C. Gerard and S. R. Sarawar (2005). "Role of CXCR3 in the immune response to murine gammaherpesvirus 68." *J Virol* **79**(14): 9351-5.

Lee, B. J., S. K. Reiter, M. Anderson and S. R. Sarawar (2002). "CD28(-/-) mice show defects in cellular and humoral immunity but are able to control infection with murine gammaherpesvirus 68." *J Virol* **76**(6): 3049-53.

Leib, D. A., M. A. Machalek, B. R. Williams, R. H. Silverman and H. W. Virgin (2000). "Specific phenotypic restoration of an attenuated virus by knockout of a host resistance gene." *Proc Natl Acad Sci U S A* **97**(11): 6097-101.

Lenac, T., M. Budt, J. Arapovic, M. Hasan, A. Zimmermann, H. Simic, A. Krmpotic, M. Messerle, Z. Ruzsics, U. H. Koszinowski, H. Hengel and S. Jonjic (2006). "The herpesviral Fc receptor fcr-1 down-regulates the NKG2D ligands MULT-1 and H60." *J Exp Med* **203**(8): 1843-50.

Lenschow, D. J., C. Lai, N. Frias-Staheli, N. V. Giannakopoulos, A. Lutz, T. Wolff, A. Osiak, B. Levine, R. E. Schmidt, A. Garcia-Sastre, D. A. Leib, A. Pekosz, K. P. Knobeloch, I. Horak and H. W. t. Virgin (2007). "IFN-stimulated gene 15 functions

as a critical antiviral molecule against influenza, herpes, and Sindbis viruses." *Proc Natl Acad Sci U S A.*

Liang, X., Y. C. Shin, R. E. Means and J. U. Jung (2004). "Inhibition of interferon-mediated antiviral activity by murine gammaherpesvirus 68 latency-associated M2 protein." *J Virol* **78**(22): 12416-27.

Lin, R., P. Genin, Y. Mamane, M. Sgarbanti, A. Battistini, W. J. Harrington, Jr., G. N. Barber and J. Hiscott (2001). "HHV-8 encoded vIRF-1 represses the interferon antiviral response by blocking IRF-3 recruitment of the CBP/p300 coactivators." *Oncogene* **20**(7): 800-11.

Lin, R., R. S. Noyce, S. E. Collins, R. D. Everett and K. L. Mossman (2004). "The herpes simplex virus ICP0 RING finger domain inhibits IRF3- and IRF7-mediated activation of interferon-stimulated genes." *J Virol* **78**(4): 1675-84.

Liu, B., S. Mink, K. A. Wong, N. Stein, C. Getman, P. W. Dempsey, H. Wu and K. Shuai (2004a). "PIAS1 selectively inhibits interferon-inducible genes and is important in innate immunity." *Nat Immunol* **5**(9): 891-8.

Liu, B., I. Mori, M. J. Hossain, L. Dong, K. Takeda and Y. Kimura (2004b). "Interleukin-18 improves the early defence system against influenza virus infection by augmenting natural killer cell-mediated cytotoxicity." *J Gen Virol* **85**(Pt 2): 423-8.

Lodoen, M. B., G. Abenes, S. Umamoto, J. P. Houchins, F. Liu and L. L. Lanier (2004). "The cytomegalovirus m155 gene product subverts natural killer cell antiviral protection by disruption of H60-NKG2D interactions." *J Exp Med* **200**(8): 1075-81.

Lodoen, M. B. and L. L. Lanier (2005). "Viral modulation of NK cell immunity." *Nat Rev Microbiol* **3**(1): 59-69.

Lodolce, J. P., D. L. Boone, S. Chai, R. E. Swain, T. Dassopoulos, S. Trettin and A. Ma (1998). "IL-15 receptor maintains lymphoid homeostasis by supporting lymphocyte homing and proliferation." *Immunity* **9**(5): 669-76.

Loh, J., D. T. Chu, A. K. O'Guin, W. M. Yokoyama and H. W. t. Virgin (2005). "Natural killer cells utilize both perforin and gamma interferon to regulate murine cytomegalovirus infection in the spleen and liver." *J Virol* **79**(1): 661-7.

Loh, J., D. A. Thomas, P. A. Revell, T. J. Ley and H. W. t. Virgin (2004). "Granzymes and caspase 3 play important roles in control of gammaherpesvirus latency." *J Virol* **78**(22): 12519-28.

Lohoff, M. and T. W. Mak (2005). "Roles of interferon-regulatory factors in T-helper-cell differentiation." *Nat Rev Immunol* **5**(2): 125-35.

Macpherson, I. and M. Stoker (1962). "Polyoma transformation of hamster cell clones--an investigation of genetic factors affecting cell competence." *Virology* **16**: 147-51.

Macrae, A. I., B. M. Dutia, S. Milligan, D. G. Brownstein, D. J. Allen, J. Mistrikova, A. J. Davison, A. A. Nash and J. P. Stewart (2001). "Analysis of a novel strain of

murine gammaherpesvirus reveals a genomic locus important for acute pathogenesis." *J Virol* **75**(11): 5315-27.

Macrae, A. I., E. J. Usherwood, S. M. Husain, E. Flano, I. J. Kim, D. L. Woodland, A. A. Nash, M. A. Blackman, J. T. Sample and J. P. Stewart (2003). "Murid herpesvirus 4 strain 68 M2 protein is a B-cell-associated antigen important for latency but not lymphocytosis." *J Virol* **77**(17): 9700-9.

Madureira, P. A., P. Matos, I. Soeiro, L. K. Dixon, J. P. Simas and E. W. Lam (2005). "Murine gamma-herpesvirus 68 latency protein M2 binds to Vav signaling proteins and inhibits B-cell receptor-induced cell cycle arrest and apoptosis in WEHI-231 B cells." *J Biol Chem* **280**(45): 37310-8.

Mandelboim, O., N. Lieberman, M. Lev, L. Paul, T. I. Arnon, Y. Bushkin, D. M. Davis, J. L. Strominger, J. W. Yewdell and A. Porgador (2001). "Recognition of haemagglutinins on virus-infected cells by NKp46 activates lysis by human NK cells." *Nature* **409**(6823): 1055-60.

Mansfield, K. G., S. V. Westmoreland, C. D. DeBakker, S. Czajak, A. A. Lackner and R. C. Desrosiers (1999). "Experimental infection of rhesus and pig-tailed macaques with macaque rhadinoviruses." *J Virol* **73**(12): 10320-8.

Marie, I., J. E. Durbin and D. E. Levy (1998). "Differential viral induction of distinct interferon-alpha genes by positive feedback through interferon regulatory factor-7." *Embo J* **17**(22): 6660-9.

Martensen, P. M., T. M. Sogaard, I. M. Gjermandsen, H. N. Buttenschon, A. B. Rossing, V. Bonnevie-Nielsen, C. Rosada, J. L. Simonsen and J. Justesen (2001). "The interferon alpha induced protein ISG12 is localized to the nuclear membrane." *Eur J Biochem* **268**(22): 5947-54.

Martinez-Guzman, D., T. Rickabaugh, T. T. Wu, H. Brown, S. Cole, M. J. Song, L. Tong and R. Sun (2003). "Transcription program of murine gammaherpesvirus 68." *J Virol* **77**(19): 10488-503.

Martin-Fontecha, A., L. L. Thomsen, S. Brett, C. Gerard, M. Lipp, A. Lanzavecchia and F. Sallusto (2004). "Induced recruitment of NK cells to lymph nodes provides IFN-gamma for T(H)1 priming." *Nat Immunol* **5**(12): 1260-5.

Meager, A., K. Visvalingam, P. Dilger, D. Bryan and M. Wadhwa (2005). "Biological activity of interleukins-28 and -29: comparison with type I interferons." *Cytokine* **31**(2): 109-18.

Meister, A., G. Uze, K. E. Mogensen, I. Gresser, M. G. Tovey, M. Grutter and F. Meyer (1986). "Biological activities and receptor binding of two human recombinant interferons and their hybrids." *J Gen Virol* **67 (Pt 8)**: 1633-43.

Melroe, G. T., N. A. DeLuca and D. M. Knipe (2004). "Herpes simplex virus 1 has multiple mechanisms for blocking virus-induced interferon production." *J Virol* **78**(16): 8411-20.

Merika, M. and D. Thanos (2001). "Enhanceosomes." *Curr Opin Genet Dev* **11**(2): 205-8.

Merino, F., G. O. Klein, W. Henle, P. Ramirez-Duque, M. Forsgren and C. Amesty (1983). "Elevated antibody titers to Epstein-Barr virus and low natural killer cell activity in patients with Chediak-Higashi syndrome." *Clin Immunol Immunopathol* **27**(3): 326-39.

Metkar, S. S., B. Wang, M. Aguilar-Santelises, S. M. Raja, L. Uhlin-Hansen, E. Podack, J. A. Trapani and C. J. Froelich (2002). "Cytotoxic cell granule-mediated apoptosis: perforin delivers granzyme B-serglycin complexes into target cells without plasma membrane pore formation." *Immunity* **16**(3): 417-28.

Mettenleiter, T. C. (2004). "Budding events in herpesvirus morphogenesis." *Virus Res* **106**(2): 167-80.

Meurs, E. F., Y. Watanabe, S. Kadereit, G. N. Barber, M. G. Katze, K. Chong, B. R. Williams and A. G. Hovanessian (1992). "Constitutive expression of human double-stranded RNA-activated p68 kinase in murine cells mediates phosphorylation of eukaryotic initiation factor 2 and partial resistance to encephalomyocarditis virus growth." *J Virol* **66**(10): 5805-14.

Mocarski, E. S. and C. T. Courcelle (2001). Cytomegaloviruses and Their Replication. Fields Virology. H. P. Knipe DM, Lippincott Williams and Wilkins: 2629-2673.

Moghaddam, A., M. Rosenzweig, D. Lee-Parritz, B. Annis, R. P. Johnson and F. Wang (1997). "An animal model for acute and persistent Epstein-Barr virus infection." *Science* **276**(5321): 2030-3.

Moorman, N. J., D. O. Willer and S. H. Speck (2003). "The gammaherpesvirus 68 latency-associated nuclear antigen homolog is critical for the establishment of splenic latency." *J Virol* **77**(19): 10295-303.

Mossman, K. L., P. F. Macgregor, J. J. Rozmus, A. B. Goryachev, A. M. Edwards and J. R. Smiley (2001). "Herpes simplex virus triggers and then disarms a host antiviral response." *J Virol* **75**(2): 750-8.

Nash, A. A., B. M. Dutia, J. P. Stewart and A. J. Davison (2001). "Natural history of murine gamma-herpesvirus infection." *Philos Trans R Soc Lond B Biol Sci* **356**(1408): 569-79.

Nguyen, K. B., T. P. Salazar-Mather, M. Y. Dalod, J. B. Van Deusen, X. Q. Wei, F. Y. Liew, M. A. Caligiuri, J. E. Durbin and C. A. Biron (2002). "Coordinated and distinct roles for IFN-alpha beta, IL-12, and IL-15 regulation of NK cell responses to viral infection." *J Immunol* **169**(8): 4279-87.

Nicholl, M. J., L. H. Robinson and C. M. Preston (2000). "Activation of cellular interferon-responsive genes after infection of human cells with herpes simplex virus type 1." *J Gen Virol* **81**(Pt 9): 2215-8.

Novick, D., B. Cohen and M. Rubinstein (1994). "The human interferon alpha/beta receptor: characterization and molecular cloning." *Cell* **77**(3): 391-400.

O'Connor, G. M., O. M. Hart and C. M. Gardiner (2006). "Putting the natural killer cell in its place." *Immunology* **117**(1): 1-10.

Okumura, A., G. Lu, I. Pitha-Rowe and P. M. Pitha (2006). "Innate antiviral response targets HIV-1 release by the induction of ubiquitin-like protein ISG15." *Proc Natl Acad Sci U S A* **103**(5): 1440-5.

Orange, J. S. (2002). "Human natural killer cell deficiencies and susceptibility to infection." *Microbes Infect* **4**(15): 1545-58.

Orange, J. S. and C. A. Biron (1996). "An absolute and restricted requirement for IL-12 in natural killer cell IFN-gamma production and antiviral defense. Studies of natural killer and T cell responses in contrasting viral infections." *J Immunol* **156**(3): 1138-42.

Orange, J. S., B. Wang, C. Terhorst and C. A. Biron (1995). "Requirement for natural killer cell-produced interferon gamma in defense against murine cytomegalovirus infection and enhancement of this defense pathway by interleukin 12 administration." *J Exp Med* **182**(4): 1045-56.

Ortaldo, J. R., R. Winkler-Pickett, A. T. Mason and L. H. Mason (1998). "The Ly-49 family: regulation of cytotoxicity and cytokine production in murine CD3+ cells." *J Immunol* **160**(3): 1158-65.

Osiak, A., O. Utermohlen, S. Niendorf, I. Horak and K. P. Knobeloch (2005). "ISG15, an interferon-stimulated ubiquitin-like protein, is not essential for STAT1 signaling and responses against vesicular stomatitis and lymphocytic choriomeningitis virus." *Mol Cell Biol* **25**(15): 6338-45.

Paladino, P., D. T. Cummings, R. S. Noyce and K. L. Mossman (2006). "The IFN-independent response to virus particle entry provides a first line of antiviral defense that is independent of TLRs and retinoic acid-inducible gene I." *J Immunol* **177**(11): 8008-16.

Pappworth, I. Y., E. C. Wang and M. Rowe (2007). "The switch from latent to productive infection in epstein-barr virus-infected B cells is associated with sensitization to NK cell killing." *J Virol* **81**(2): 474-82.

Parker, N. and A. C. Porter (2004). "Identification of a novel gene family that includes the interferon-inducible human genes 6-16 and ISG12." *BMC Genomics* **5**(1): 8.

Parolini, S., C. Bottino, M. Falco, R. Augugliaro, S. Giliani, R. Franceschini, H. D. Ochs, H. Wolf, J. Y. Bonnefoy, R. Biassoni, L. Moretta, L. D. Notarangelo and A. Moretta (2000). "X-linked lymphoproliferative disease. 2B4 molecules displaying inhibitory rather than activating function are responsible for the inability of natural killer cells to kill Epstein-Barr virus-infected cells." *J Exp Med* **192**(3): 337-46.

Parry, C. M., J. P. Simas, V. P. Smith, C. A. Stewart, A. C. Minson, S. Efstathiou and A. Alcami (2000). "A broad spectrum secreted chemokine binding protein encoded by a herpesvirus." *J Exp Med* **191**(3): 573-8.

Pavlovic, J., O. Haller and P. Staeheli (1992). "Human and mouse Mx proteins inhibit different steps of the influenza virus multiplication cycle." *J Virol* **66**(4): 2564-9.

Peacock, J. W. and K. L. Bost (2000). "Infection of intestinal epithelial cells and development of systemic disease following gastric instillation of murine gammaherpesvirus-68." *J Gen Virol* **81**(Pt 2): 421-9.

Pende, D., S. Parolini, A. Pessino, S. Sivori, R. Augugliaro, L. Morelli, E. Marcenaro, L. Accame, A. Malaspina, R. Biassoni, C. Bottino, L. Moretta and A. Moretta (1999). "Identification and molecular characterization of NKp30, a novel triggering receptor involved in natural cytotoxicity mediated by human natural killer cells." *J Exp Med* **190**(10): 1505-16.

Pfeffer, S., A. Sewer, M. Lagos-Quintana, R. Sheridan, C. Sander, F. A. Grasser, L. F. van Dyk, C. K. Ho, S. Shuman, M. Chien, J. J. Russo, J. Ju, G. Randall, B. D. Lindenbach, C. M. Rice, V. Simon, D. D. Ho, M. Zavolan and T. Tuschl (2005). "Identification of microRNAs of the herpesvirus family." *Nat Methods* **2**(4): 269-76.

Piriou, L., S. Chilmonczyk, N. Genetet and E. Albina (2000). "Design of a flow cytometric assay for the determination of natural killer and cytotoxic T-lymphocyte activity in human and in different animal species." *Cytometry* **41**(4): 289-97.

Pisegna, S., G. Pirozzi, M. Piccoli, L. Frati, A. Santoni and G. Palmieri (2004). "p38 MAPK activation controls the TLR3-mediated up-regulation of cytotoxicity and cytokine production in human NK cells." *Blood* **104**(13): 4157-64.

Poppers, J., M. Mulvey, D. Khoo and I. Mohr (2000). "Inhibition of PKR activation by the proline-rich RNA binding domain of the herpes simplex virus type 1 Us11 protein." *J Virol* **74**(23): 11215-21.

Prakash, A., E. Smith, C. K. Lee and D. E. Levy (2005). "Tissue-specific positive feedback requirements for production of type I interferon following virus infection." *J Biol Chem* **280**(19): 18651-7.

Preston, C. M., A. N. Harman and M. J. Nicholl (2001). "Activation of interferon response factor-3 in human cells infected with herpes simplex virus type 1 or human cytomegalovirus." *J Virol* **75**(19): 8909-16.

Quinnan, G. V., Jr., N. Kirmani, A. H. Rook, J. F. Manischewitz, L. Jackson, G. Moreschi, G. W. Santos, R. Saral and W. H. Burns (1982). "Cytotoxic t cells in cytomegalovirus infection: HLA-restricted T-lymphocyte and non-T-lymphocyte cytotoxic responses correlate with recovery from cytomegalovirus infection in bone-marrow-transplant recipients." *N Engl J Med* **307**(1): 7-13.

Ramaiah, K. V., M. V. Davies, J. J. Chen and R. J. Kaufman (1994). "Expression of mutant eukaryotic initiation factor 2 alpha subunit (eIF-2 alpha) reduces inhibition of guanine nucleotide exchange activity of eIF-2B mediated by eIF-2 alpha phosphorylation." *Mol Cell Biol* **14**(7): 4546-53.

Rasmussen, U. B., C. Wolf, M. G. Mattei, M. P. Chenard, J. P. Bellocq, P. Chambon, M. C. Rio and P. Basset (1993). "Identification of a new interferon-alpha-inducible gene (p27) on human chromosome 14q32 and its expression in breast carcinoma." *Cancer Res* **53**(17): 4096-101.

Raulet, D. H. (2003). "Roles of the NKG2D immunoreceptor and its ligands." *Nat Rev Immunol* **3**(10): 781-90.

Ravetch, J. V. and L. L. Lanier (2000). "Immune inhibitory receptors." *Science* **290**(5489): 84-9.

Reading, P. C., P. G. Whitney, D. P. Barr, M. J. Smyth and A. G. Brooks (2006). "NK cells contribute to the early clearance of HSV-1 from the lung but cannot control replication in the central nervous system following intranasal infection." *Eur J Immunol* **36**(4): 897-905.

Reddehase, M. J., J. Podlech and N. K. Grzimek (2002). "Mouse models of cytomegalovirus latency: overview." *J Clin Virol* **25 Suppl 2**: S23-36.

Rezaee, S. A., C. Cunningham, A. J. Davison and D. J. Blackbourn (2006). "Kaposi's sarcoma-associated herpesvirus immune modulation: an overview." *J Gen Virol* **87**(Pt 7): 1781-804.

Robertson, K. (1999). PhD Thesis. University of Edinburgh.

Rodrigues, L., M. Pires de Miranda, M. J. Caloca, X. R. Bustelo and J. P. Simas (2006). "Activation of Vav by the gammaherpesvirus M2 protein contributes to the establishment of viral latency in B lymphocytes." *J Virol* **80**(12): 6123-35.

Roizman, B. and Knipe DM (2001). Herpes simplex viruses and their replication. Fields Virology. H. P. Knipe DM, Lippincott Williams and Wilkins: 2399-2460.

Roizman, B. and P. E. Pellet (2001). The family Herpesviridae: A brief introduction. Fields Virology. D. M. Knipe and P. M. Howley, Lippincott Williams and Wlkins: 2381-2398.

Russell, J. H. and T. J. Ley (2002). "Lymphocyte-mediated cytotoxicity." *Annu Rev Immunol* **20**: 323-70.

Salazar-Mather, T. P., J. S. Orange and C. A. Biron (1998). "Early murine cytomegalovirus (MCMV) infection induces liver natural killer (NK) cell inflammation and protection through macrophage inflammatory protein 1alpha (MIP-1alpha)-dependent pathways." *J Exp Med* **187**(1): 1-14.

Samuel, C. E. (2001). "Antiviral actions of interferons." *Clin Microbiol Rev* **14**(4): 778-809, table of contents.

Sanchez, R. and I. Mohr (2007). "Inhibition of the Cellular 2'-5' Oligoadenylate Synthetase by the Herpes Simplex Virus-1 Us11 protein." *J Virol.*

Sangster, M. Y., D. J. Topham, S. D'Costa, R. D. Cardin, T. N. Marion, L. K. Myers and P. C. Doherty (2000). "Analysis of the virus-specific and nonspecific B cell response to a persistent B-lymphotropic gammaherpesvirus." *J Immunol* **164**(4): 1820-8.

Sarawar, S. R., J. W. Brooks, R. D. Cardin, M. Mehrpooya and P. C. Doherty (1998). "Pathogenesis of murine gammaherpesvirus-68 infection in interleukin-6-deficient mice." *Virology* **249**(2): 359-66.

Sarawar, S. R., R. D. Cardin, J. W. Brooks, M. Mehrpooya, A. M. Hamilton-Easton, X. Y. Mo and P. C. Doherty (1997). "Gamma interferon is not essential for recovery from acute infection with murine gammaherpesvirus 68." *J Virol* **71**(5): 3916-21.

Sarawar, S. R., R. D. Cardin, J. W. Brooks, M. Mehrpooya, R. A. Tripp and P. C. Doherty (1996). "Cytokine production in the immune response to murine gammaherpesvirus 68." *J Virol* **70**(5): 3264-8.

Sarawar, S. R., B. J. Lee, M. Anderson, Y. C. Teng, R. Zuberi and S. Von Gesjen (2002). "Chemokine induction and leukocyte trafficking to the lungs during murine gammaherpesvirus 68 (MHV-68) infection." *Virology* **293**(1): 54-62.

Sato, K., S. Hida, H. Takayanagi, T. Yokochi, N. Kayagaki, K. Takeda, H. Yagita, K. Okumura, N. Tanaka, T. Taniguchi and K. Ogasawara (2001). "Antiviral response by natural killer cells through TRAIL gene induction by IFN-alpha/beta." *Eur J Immunol* **31**(11): 3138-46.

Screpanti, V., R. P. Wallin, A. Grandien and H. G. Ljunggren (2005). "Impact of FASL-induced apoptosis in the elimination of tumor cells by NK cells." *Mol Immunol* **42**(4): 495-9.

Seaman, W. E., M. Sleisenger, E. Eriksson and G. C. Koo (1987). "Depletion of natural killer cells in mice by monoclonal antibody to NK-1.1. Reduction in host defense against malignancy without loss of cellular or humoral immunity." *J Immunol* **138**(12): 4539-44.

Selvarajah, S. (2001). PhD Thesis.

Seo, T., J. Park, C. Lim and J. Choe (2004). "Inhibition of nuclear factor kappaB activity by viral interferon regulatory factor 3 of Kaposi's sarcoma-associated herpesvirus." *Oncogene* **23**(36): 6146-55.

Shariatmadari, R., P. P. Sipila, I. T. Huhtaniemi and M. Poutanen (2001). "Improved technique for detection of enhanced green fluorescent protein in transgenic mice." *Biotechniques* **30**(6): 1282-5.

Sheppard, P., W. Kindsvogel, W. Xu, K. Henderson, S. Schlutsmeyer, T. E. Whitmore, R. Kuestner, U. Garrigues, C. Birks, J. Roraback, C. Ostrander, D. Dong, J. Shin, S. Presnell, B. Fox, B. Haldeman, E. Cooper, D. Taft, T. Gilbert, F. J. Grant, M. Tackett, W. Krivan, G. McKnight, C. Clegg, D. Foster and K. M. Klucher (2003). "IL-28, IL-29 and their class II cytokine receptor IL-28R." *Nat Immunol* **4**(1): 63-8.

Shigematsu, H., B. Reizis, H. Iwasaki, S. Mizuno, D. Hu, D. Traver, P. Leder, N. Sakaguchi and K. Akashi (2004). "Plasmacytoid dendritic cells activate lymphoid-specific genetic programs irrespective of their cellular origin." *Immunity* **21**(1): 43-53.

Siegal, F. P., N. Kadowaki, M. Shodell, P. A. Fitzgerald-Bocarsly, K. Shah, S. Ho, S. Antonenko and Y. J. Liu (1999). "The nature of the principal type 1 interferon-producing cells in human blood." *Science* **284**(5421): 1835-7.

Simas, J. P., R. J. Bowden, V. Paige and S. Efstathiou (1998). "Four tRNA-like sequences and a serpin homologue encoded by murine gammaherpesvirus 68 are dispensable for lytic replication in vitro and latency in vivo." *J Gen Virol* **79 (Pt 1)**: 149-53.

Simas, J. P., D. Swann, R. Bowden and S. Efstathiou (1999). "Analysis of murine gammaherpesvirus-68 transcription during lytic and latent infection." *J Gen Virol* **80 (Pt 1)**: 75-82.

Sivori, S., S. Parolini, M. Falco, E. Marcenaro, R. Biassoni, C. Bottino, L. Moretta and A. Moretta (2000). "2B4 functions as a co-receptor in human NK cell activation." *Eur J Immunol* **30**(3): 787-93.

Sivori, S., D. Pende, C. Bottino, E. Marcenaro, A. Pessino, R. Biassoni, L. Moretta and A. Moretta (1999). "NKp46 is the major triggering receptor involved in the natural cytotoxicity of fresh or cultured human NK cells. Correlation between surface density of NKp46 and natural cytotoxicity against autologous, allogeneic or xenogeneic target cells." *Eur J Immunol* **29**(5): 1656-66.

Smyth, M. J., E. Cretney, J. M. Kelly, J. A. Westwood, S. E. Street, H. Yagita, K. Takeda, S. L. van Dommelen, M. A. Degli-Esposti and Y. Hayakawa (2005). "Activation of NK cell cytotoxicity." *Mol Immunol* **42**(4): 501-10.

Sparks-Thissen, R. L., D. C. Braaten, K. Hildner, T. L. Murphy, K. M. Murphy and H. W. t. Virgin (2005). "CD4 T cell control of acute and latent murine gammaherpesvirus infection requires IFNgamma." *Virology* **338**(2): 201-8.

Spear, P. G. and R. Longnecker (2003). "Herpesvirus entry: an update." *J Virol* **77**(19): 10179-85.

Steed, A. L., E. S. Barton, S. A. Tibbetts, D. L. Popkin, M. L. Lutzke, R. Rochford and H. W. t. Virgin (2006). "Gamma interferon blocks gammaherpesvirus reactivation from latency." *J Virol* **80**(1): 192-200.

Stevenson, P. G. and P. C. Doherty (1998). "Kinetic analysis of the specific host response to a murine gammaherpesvirus." *J Virol* **72**(2): 943-9.

Stevenson, P. G., J. S. May, X. G. Smith, S. Marques, H. Adler, U. H. Koszinowski, J. P. Simas and S. Efstathiou (2002). "K3-mediated evasion of CD8(+) T cells aids amplification of a latent gamma-herpesvirus." *Nat Immunol* **3**(8): 733-40.

Stewart, J. P., E. J. Usherwood, A. Ross, H. Dyson and T. Nash (1998). "Lung epithelial cells are a major site of murine gammaherpesvirus persistence." *J Exp Med* **187**(12): 1941-51.

Sunil-Chandra, N. P., S. Efstathiou, J. Arno and A. A. Nash (1992). "Virological and pathological features of mice infected with murine gamma-herpesvirus 68." *J Gen Virol* **73 (Pt 9)**: 2347-56.

Tabeta, K., P. Georgel, E. Janssen, X. Du, K. Hoebe, K. Crozat, S. Mudd, L. Shamel, S. Sovath, J. Goode, L. Alexopoulou, R. A. Flavell and B. Beutler (2004). "Toll-like receptors 9 and 3 as essential components of innate immune defense against mouse cytomegalovirus infection." *Proc Natl Acad Sci U S A* **101**(10): 3516-21.

Takaoka, A., H. Yanai, S. Kondo, G. Duncan, H. Negishi, T. Mizutani, S. Kano, K. Honda, Y. Ohba, T. W. Mak and T. Taniguchi (2005). "Integral role of IRF-5 in the gene induction programme activated by Toll-like receptors." *Nature* **434**(7030): 243-9.

Tan, L. C., N. Gudgeon, N. E. Annels, P. Hansasuta, C. A. O'Callaghan, S. Rowland-Jones, A. J. McMichael, A. B. Rickinson and M. F. Callan (1999). "A re-evaluation of the frequency of CD8+ T cells specific for EBV in healthy virus carriers." *J Immunol* **162**(3): 1827-35.

Tanaka, N., M. Sato, M. S. Lamphier, H. Nozawa, E. Oda, S. Noguchi, R. D. Schreiber, Y. Tsujimoto and T. Taniguchi (1998). "Type I interferons are essential mediators of apoptotic death in virally infected cells." *Genes Cells* **3**(1): 29-37.

Tanaka, S. S., Y. L. Yamaguchi, B. Tsoi, H. Lickert and P. P. Tam (2005). "IFITM/Mil/fragilis family proteins IFITM1 and IFITM3 play distinct roles in mouse primordial germ cell homing and repulsion." *Dev Cell* **9**(6): 745-56.

Tomasec, P., V. M. Braud, C. Rickards, M. B. Powell, B. P. McSharry, S. Gadola, V. Cerundolo, L. K. Borysiewicz, A. J. McMichael and G. W. Wilkinson (2000). "Surface expression of HLA-E, an inhibitor of natural killer cells, enhanced by human cytomegalovirus gpUL40." *Science* **287**(5455): 1031.

Townsley, A. C. (2004). PhD Thesis, University of Edinburgh.

Townsley, A. C., B. M. Dutia and A. A. Nash (2004). "The m4 gene of murine gammaherpesvirus modulates productive and latent infection in vivo." *J Virol* **78**(2): 758-67.

Trapani, J. A. and M. J. Smyth (2002). "Functional significance of the perforin/granzyme cell death pathway." *Nat Rev Immunol* **2**(10): 735-47.

Tripp, R. A., A. M. Hamilton-Easton, R. D. Cardin, P. Nguyen, F. G. Behm, D. L. Woodland, P. C. Doherty and M. A. Blackman (1997). "Pathogenesis of an infectious mononucleosis-like disease induced by a murine gamma-herpesvirus: role for a viral superantigen?" *J Exp Med* **185**(9): 1641-50.

Tseng, C. T. and G. R. Klimpel (2002). "Binding of the hepatitis C virus envelope protein E2 to CD81 inhibits natural killer cell functions." *J Exp Med* **195**(1): 43-9.

Uematsu, S., S. Sato, M. Yamamoto, T. Hirotani, H. Kato, F. Takeshita, M. Matsuda, C. Coban, K. J. Ishii, T. Kawai, O. Takeuchi and S. Akira (2005). "Interleukin-1 receptor-associated kinase-1 plays an essential role for Toll-like receptor (TLR)7- and TLR9-mediated interferon-{alpha} induction." *J Exp Med* **201**(6): 915-23.

Usherwood, E. J., J. W. Brooks, S. R. Sarawar, R. D. Cardin, W. D. Young, D. J. Allen, P. C. Doherty and A. A. Nash (1997). "Immunological control of murine gammaherpesvirus infection is independent of perforin." *J Gen Virol* **78 (Pt 8)**: 2025-30.

Usherwood, E. J., S. K. Meadows, S. G. Crist, S. C. Bellfy and C. L. Sentman (2005). "Control of murine gammaherpesvirus infection is independent of NK cells." *Eur J Immunol* **35**(10): 2956-61.

Usherwood, E. J., A. J. Ross, D. J. Allen and A. A. Nash (1996a). "Murine gammaherpesvirus-induced splenomegaly: a critical role for CD4 T cells." *J Gen Virol* **77 (Pt 4)**: 627-30.

Usherwood, E. J., J. P. Stewart, K. Robertson, D. J. Allen and A. A. Nash (1996b). "Absence of splenic latency in murine gammaherpesvirus 68-infected B cell-deficient mice." *J Gen Virol* **77 (Pt 11)**: 2819-25.

van Berkel, V., J. Barrett, H. L. Tiffany, D. H. Fremont, P. M. Murphy, G. McFadden, S. H. Speck and H. I. Virgin (2000). "Identification of a gammaherpesvirus selective chemokine binding protein that inhibits chemokine action." *J Virol* **74**(15): 6741-7.

van Berkel, V., B. Levine, S. B. Kapadia, J. E. Goldman, S. H. Speck and H. W. t. Virgin (2002). "Critical role for a high-affinity chemokine-binding protein in gamma-herpesvirus-induced lethal meningitis." *J Clin Invest* **109**(7): 905-14.

van den Broek, M. F., U. Muller, S. Huang, R. M. Zinkernagel and M. Aguet (1995). "Immune defence in mice lacking type I and/or type II interferon receptors." *Immunol Rev* **148**: 5-18.

van Dommelen, S. L., N. Sumaria, R. D. Schreiber, A. A. Scalzo, M. J. Smyth and M. A. Degli-Esposti (2006). "Perforin and granzymes have distinct roles in defensive immunity and immunopathology." *Immunity* **25**(5): 835-48.

van Pesch, V., H. Lanaya, J. C. Renauld and T. Michiels (2004). "Characterization of the murine alpha interferon gene family." *J Virol* **78**(15): 8219-28.

Vance, R. E., J. R. Kraft, J. D. Altman, P. E. Jensen and D. H. Raulet (1998). "Mouse CD94/NKG2A is a natural killer cell receptor for the nonclassical major histocompatibility complex (MHC) class I molecule Qa-1(b)." *J Exp Med* **188**(10): 1841-8.

Veals, S. A., C. Schindler, D. Leonard, X. Y. Fu, R. Aebersold, J. E. Darnell, Jr. and D. E. Levy (1992). "Subunit of an alpha-interferon-responsive transcription factor is related to interferon regulatory factor and Myb families of DNA-binding proteins." *Mol Cell Biol* **12**(8): 3315-24.

Virgin, H. W. t., P. Latreille, P. Wamsley, K. Hallsworth, K. E. Weck, A. J. Dal Canto and S. H. Speck (1997). "Complete sequence and genomic analysis of murine gammaherpesvirus 68." *J Virol* **71**(8): 5894-904.

Wang, F., P. Rivailler, P. Rao and Y. Cho (2001). "Simian homologues of Epstein-Barr virus." *Philos Trans R Soc Lond B Biol Sci* **356**(1408): 489-97.

Wathelet, M. G., C. H. Lin, B. S. Parekh, L. V. Ronco, P. M. Howley and T. Maniatis (1998). "Virus infection induces the assembly of coordinately activated transcription factors on the IFN-beta enhancer in vivo." *Mol Cell* **1**(4): 507-18.

Weber, F., G. Kochs and O. Haller (2004). "Inverse interference: how viruses fight the interferon system." *Viral Immunol* **17**(4): 498-515.

Weck, K. E., M. L. Barkon, L. I. Yoo, S. H. Speck and H. I. Virgin (1996). "Mature B cells are required for acute splenic infection, but not for establishment of latency, by murine gammaherpesvirus 68." *J Virol* **70**(10): 6775-80.

Wei, S., A. M. Gamero, J. H. Liu, A. A. Daulton, N. I. Valkov, J. A. Trapani, A. C. Larner, M. J. Weber and J. Y. Djeu (1998). "Control of lytic function by mitogen-

activated protein kinase/extracellular regulatory kinase 2 (ERK2) in a human natural killer cell line: identification of perforin and granzyme B mobilization by functional ERK2." *J Exp Med* **187**(11): 1753-65.

Willer, D. O. and S. H. Speck (2003). "Long-term latent murine Gammaherpesvirus 68 infection is preferentially found within the surface immunoglobulin D-negative subset of splenic B cells in vivo." *J Virol* **77**(15): 8310-21.

Williams, H., K. McAulay, K. F. Macsween, N. J. Gallacher, C. D. Higgins, N. Harrison, A. J. Swerdlow and D. H. Crawford (2005). "The immune response to primary EBV infection: a role for natural killer cells." *Br J Haematol* **129**(2): 266-74.

Wu, J., Y. Song, A. B. Bakker, S. Bauer, T. Spies, L. L. Lanier and J. H. Phillips (1999). "An activating immunoreceptor complex formed by NKG2D and DAP10." *Science* **285**(5428): 730-2.

Yie, J., M. Merika, N. Munshi, G. Chen and D. Thanos (1999). "The role of HMG I(Y) in the assembly and function of the IFN-beta enhanceosome." *Embo J* **18**(11): 3074-89.

Yokota, S., N. Yokosawa, T. Okabayashi, T. Suzutani, S. Miura, K. Jimbow and N. Fujii (2004). "Induction of suppressor of cytokine signaling-3 by herpes simplex virus type 1 contributes to inhibition of the interferon signaling pathway." *J Virol* **78**(12): 6282-6.

Yoneyama, M., M. Kikuchi, T. Natsukawa, N. Shinobu, T. Imaizumi, M. Miyagishi, K. Taira, S. Akira and T. Fujita (2004). "The RNA helicase RIG-I has an essential function in double-stranded RNA-induced innate antiviral responses." *Nat Immunol* **5**(7): 730-7.

Yu, M., J. H. Tong, M. Mao, L. X. Kan, M. M. Liu, Y. W. Sun, G. Fu, Y. K. Jing, L. Yu, D. Lepaslier, M. Lanotte, Z. Y. Wang, Z. Chen, S. Waxman, Y. X. Wang, J. Z. Tan and S. J. Chen (1997). "Cloning of a gene (RIG-G) associated with retinoic acid-induced differentiation of acute promyelocytic leukemia cells and representing a new member of a family of interferon-stimulated genes." *Proc Natl Acad Sci U S A* **94**(14): 7406-11.

Yuan, W. and R. M. Krug (2001). "Influenza B virus NS1 protein inhibits conjugation of the interferon (IFN)-induced ubiquitin-like ISG15 protein." *Embo J* **20**(3): 362-71.

Zamanian-Daryoush, M., T. H. Mogensen, J. A. DiDonato and B. R. Williams (2000). "NF-kappaB activation by double-stranded-RNA-activated protein kinase (PKR) is mediated through NF-kappaB-inducing kinase and IkappaB kinase." *Mol Cell Biol* **20**(4): 1278-90.

Zarember, K. A. and P. J. Godowski (2002). "Tissue expression of human Toll-like receptors and differential regulation of Toll-like receptor mRNAs in leukocytes in response to microbes, their products, and cytokines." *J Immunol* **168**(2): 554-61.

Zhou, A., J. M. Paranjape, S. D. Der, B. R. Williams and R. H. Silverman (1999). "Interferon action in triply deficient mice reveals the existence of alternative antiviral pathways." *Virology* **258**(2): 435-40.

Zhu, F. X., S. M. King, E. J. Smith, D. E. Levy and Y. Yuan (2002). "A Kaposi's sarcoma-associated herpesviral protein inhibits virus-mediated induction of type I interferon by blocking IRF-7 phosphorylation and nuclear accumulation." *Proc Natl Acad Sci U S A* **99**(8): 5573-8.

Zhu, H., J. P. Cong, G. Mamtora, T. Gingeras and T. Shenk (1998). "Cellular gene expression altered by human cytomegalovirus: global monitoring with oligonucleotide arrays." *Proc Natl Acad Sci U S A* **95**(24): 14470-5.

Zimmermann, A., M. Trilling, M. Wagner, M. Wilborn, I. Bubic, S. Jonjic, U. Koszinowski and H. Hengel (2005). "A cytomegaloviral protein reveals a dual role for STAT2 in IFN-{gamma} signaling and antiviral responses." *J Exp Med* **201**(10): 1543-53.